Hypercholesteremia as a regulator in Haematopoiesis and Leukaemic Stem Cells in Acute Myeloid Leukaemia

Sarab Nabil A Taha

Thesis submitted in fulfilment of the requirement for

The Degree of Doctor of Philosophy

At
Cardiff University
College of Biomedical and Life Sciences
School of Bioscience – Biomedicine

January 2023

Acknowledgment

In the name of Allah, Most Gracious, Most Merciful
Praise be to Allah, The Cherisher and Sustainer of the Worlds
and
Peace and Blessings be upon the last Prophet and Messenger
Mohammad to whom I dedicate this humble thesis.

Despite the fact that there usually turns out to be only one name on the cover, every thesis is a collaborative effort, and this is monumentally true for this one. It owes its existence to many people whose expert guidance, great encouragement, unfailing financial and moral support made it achievable.

I am profoundly indebted to His Majesty King Salman bin Abdul Aziz Al-Saud for believing in the potentials of Saudi women and granting me a generous scholarship in the challenging academic world of United Kingdom.

Also, I want to express my deepest and most sincere gratitude to my mentors at King Fahad Medical City: Dr. Ismail Bakhsh and Dr. Suha Tashkandi, my supervisor: Dr. Neil Rodrigues, my advisors: Dr. Dipak Ramji and Dr. Tim Hughes at Cardiff University for their constant support, precious time, and invaluable assistance.

I like to offer my appreciation and respect to the employees and members of School of Biosciences European Cancer stem cells research institute (ESCRI) team at Cardiff University for their kind assistance and inviting environment. I also wish to extend my thanks and regards to the government of Saudi Arabia, namely the Ministry of Education - King Fahad Medical City (KFMC), I am profoundly grateful for the opportunity to pursue my postgraduate education overseas.

Needless to say, I am greatly obliged to my family back home for their tolerance in sharing my heart and mind for so long. My parents Maha Hashim and Nabil Taha have always encouraged me to set high goals for myself and sustained me through difficult times. Her maternal love, constant prayers and unfailing support have been crucial to

my success beyond measure. Similarly, my father's expectations and trust paved every step of the way. A word of appreciation should also go to my sister Basma and brothers Khalid and Hatim for always cheering me up.

I also thank everyone who helped me in any way, especially all my friends who were with me in this journey. Alphabetically listed: Dr. Alaa Ismail, Dr. Alaa Al-Ahmadi, Dr. Hind Al Qahtani, Dr.Nouf Al-Shehri, Dr. Reem Al-Otaibi and Dr. Reem Madani. Without these terrific people, I couldn't have survived this experience.

Moreover, I would like to exhibit my thank and respect to all staff and members of School of Biosciences European Cancer stem cells research institute (ESCRI) staff, at Cardiff University for their kind assistance and welcoming atmosphere especially my colleagues Dr. Badi Al-Otaibi, Dr. Alhomaidi Al-Mutairi and Dr.Ali Abdulfattah and Dr.Hamed al Zahrani.

Last but not least, I owe special thanks to my husband Amr Maqnas and children Yousef, Yasmeen, Bayan and Abdullah. Their love and patience have heartened me day in day out. My children’s sweet words and naughtiness helped me stay in balance. I will fondly recall them. My family was beyond doubt the greatest support abroad. Also, an acknowledgment for Maria Anna, the child minder, who without her kind gesture with my children in the past four and a half year, this project will not be possible.

Abstract

Accumulating evidence suggests an emerging association between perturbed haematopoiesis, development of leukaemia and cardiovascular disease in the context of a high-fat western diet. To explore this subject, I investigated the role of atherosclerosis prone low-density lipid receptor (*Ldlr*) in normal and leukaemic haematopoiesis and the impact of a high-fat diet (HFD) or normal chow diet (ND) in this setting. In steady-state, under normal dietary conditions, mice engineered to be deficient in the LDL receptor (*Ldlr*$^{-/-}$) had increased numbers of haematopoietic stem cells (HSCs), which was associated with increased cell cycling and an increase in inflammatory cytokines and chemokines. In *Ldlr*$^{-/-}$ mice bone marrow differentiation, as assessed by the CFC assay, was decreased while paradoxically white blood cells were increased which mapped to CD4+ T cell and monocyte increases in the peripheral blood. To induce hypercholesteremia and atherosclerosis, *Ldlr*$^{-/-}$ mice were fed a HFD and the attendant impact on haematopoiesis was evaluated. A significant increase in HSCs and associated early progenitor compartments (HSPCs) was noted in *Ldlr*$^{-/-}$ mice fed HFD alongside an increase in committed progenitor cells of both the myeloid and lymphoid lineage. As expected, inflammatory immune cell subsets were increased together with increases in platelets and alterations in regulatory immune cells in *Ldlr*$^{-/-}$ mice fed HFD. HSCs from *Ldlr*$^{-/-}$ mice fed HFD performed poorly in functional analysis, as judged by competitive transplantation, displaying significant multi-lineage differentiation defects. Underpinning these defects, RNA-seq analysis revealed altered apoptosis, inflammation, lipid metabolism pathways, RNA biology, and AML enriched gene pathways in HSCs from *Ldlr*$^{-/-}$ mice fed a HFD. These molecular pathways mapped not only to haematological disease, like AML, and cardiovascular disease, but also nephrotoxicity and hepatoxicity, highlighting the widespread impact of perturbed haematopoiesis induced by HFD and atherosclerosis. Unexpectedly, we found that MLL-AF9 transformed HSPCs from *Ldlr*$^{-/-}$ mice fed a HFD developed AML later than their ND counterparts, but this was likely reflected by a delayed migration of leukaemic blast cells from BM to PB. This argument was supported by altered adhesion protein expression in human MLL-AF9 AML cell lines exposed to atherogenic lipoproteins *in vitro*. Decreased markers of immune recognition were also observed in human MLL-AF9 AML cell lines exposed to atherogenic lipoproteins *in vitro*. The data provided in this thesis provide mechanistic

insights into how HFD epigenetically disrupts HSC function and haematopoiesis in the setting of atherosclerosis, and it provides a starting point to further explore relationship between HFD, atherosclerosis and how perturbed haematopoiesis can lead to AML.

Table of Contents

List of Figures

List of tables

List of Abbreviation

ABCA1	ATP binding cassette transporter
ABCG1	ATB binding cassette transporter subfamily G member
AGM.	Aorta gonad mesonephros
ALL	Acute lymphoblastic leukaemia
AMKL	Acute megakaryoblastic leukaemia
AML	Acute myeloid leukaemia
AMPK	Activated protein kinase
ApoE	Apolipoprotein E
ASXL1	Additional sex combs protein 1
Bcl-2	B-cell lymphoma
BM	Bone marrow
Bmi1	Polycomb group RING finger protein
Bp	Base pair
C/EBPs	CCAAT/enhancer-binding protein alpha
cAMP.	Cyclic adenosine monophosphate
CBC	Complete blood count
CD	Cluster of differentiation
CFC- Mix	Colony forming cells granulocyte, erythrocyte, macrophage, megakaryocyte
CFC	Colony forming assay
CFU-M	Colony forming cells Monocyte
CFU-E	Colony Forming Unit Erythrocyte
CFU-G	Colony Forming Unit Granulocyte
CFU-GEMM	Granulocyte/Erythroid/Macrophage/Megakaryocyte
CFU-GM	Colony Forming Unit Granulocyte/Macrophage
CFU-M	Colony Forming Unit Macrophage
CH	Clonal haematopoiesis
CHIP	Clonal haematopoiesis of intermediate potential
CLPs	Common lymphoid progenitors
CLL	Chronic Lymphocytic Leukaemia

CML	Chronic myeloid leukaemia
CMPs	Common myeloid progenitors
CO2	Carbon dioxide
CSF	Colony stimulating factors
CVD	Cardiovascular diseases
CXCL12	C-X-C motif chemokine 12
CXCR 4	Chemokine receptor type 4
DNA	Deoxyribonucleic acid
DNMTA3	DNA methyltransferase
E	Embryonic day
ECM	Extra Cellular Matrix
EDTA	Ethylenediaminetetraacetic acid
EVI1	Ecotropic pro-Viral Integration site 1
E-MK cells	Erythrocyte / Megakaryocyte cells
EMPs	primitive megakaryocyte and macrophage progenitors
ERK	The extracellular-signal-regulated kinase
ETP	Earliest thymic progenitors
FAB	French American British
FACs	Fluorescent activating cell sorting
FBS	Foetal Bovine Serum
FDR	False Discovery Rate
Flk1	Foetal liver kinase 1
FLT3	Fms-like tyrosine kinase 3
g	Gram
GATA	GATA binding protein
G-CSF	Granulocyte colony-stimulating factor
GFP+	Green fluorescent protein +
GFI1	Growth Factor Independent-1
GMP	Granulocyte/Macrophage Progenitor
GM-CSF	Granulocyte macrophage colony, stimulating factor receptors
GMPs	Granulocyte and monocyte progenitors

GSEA	Gene Set Enrichment Analysis
HDL	High-density lipoprotein
HFD	High fat diet
HGB	Haemoglobin
HPCs	Haematopoietic progenitor cells
HSCs	Haematopoietic stem cells
HSPCs	Haematopoietic stem and progenitor cells
HOX	Homeobox
ICAM1	Intracellular adhesion molecule 1
ICP	Ingenuity Canonical Pathway
IDL	Intermediate density lipoprotein
IGF-1	Insulin/insulin-like growth factor
IHD 1	Isocitrate dehydrogenases 1
IHD 2	Isocitrate dehydrogenases 2
IL	Interleukin
IMDM	Iscove's Modified Dulbecco's Medium
inv	Inversion
IPA	Ingenuity Pathway Analysis
IPSS	International Prognostic Scoring System
JAK2	Janus kinase 2
Ko	Knockout
KSL	C-kit+ sca-1 + lineage
LDL	Low density lipoprotein
LDLR	Low-density lipoprotein receptor
Lin-	lineage negative
LK	Lineage - C-kit+
LMPP	Lymphoid primed multipotent progenitor
LMO2	LIM Domain Only-2
LRP	Low density lipoprotein receptor-related protein
LSCs	Leukaemia stem cells
LSK	Lineage - sca-1 + C-kit+
LT	Long term
Ly6	Lymphocyte antigen 6

MACS	Magnetic Activated Cell Sorting
MCP-1	Monocyte chemoattractant protein-1
MDS	Myelodysplastic syndrome
MDSC-M	Myeloid derived suppressor cells – monocytes
MDSC-G	Myeloid derived suppressor cells-Granulocytes
MEPs	Megakaryocyte/erythroid progenitors
MEIS	Myeloid Ectropic Insertion Site
MFI	Mean fluorescence intensity
Mg	Milligram
µg	Microgram
mL	Millilitre
µL	Microliter
MLL-AF:	Mix lineage leukaemia -AF9
mM	Millimolar
MPN	Myeloproliferative neoplasm
MPPs	Multi-potent progenitor cells
mRNA	Messenger Ribo Nucleic Acid
MSC	Mesenchymal Stem Cell
MLP	Multi lymphoid progenitors
mTOR	Mechanistic target of rapamycin
MyD88	Myeloid differentiation primary response 88
ND	Normal chow diet
NF-κB	Nuclear factor kappa-light-chain-enhancer of activated B cells
NH4Cl	Ammonium Chloride
NGS	Next generation sequencing
NK	Nature killer
NMP1	Nucleophosmin-1
NO	Nitric oxide
NOD/SCID	Non-obese diabetic/severe combined immunodeficiency
O_2	Oxygen
OCT	Optimum temperature formulation
ORO	Oil -Red-O
Ox-LDL	Oxidized low-density lipoprotein

P 53	Protein 53
Pb	Peripheral blood
PBS	Phosphate-buffered saline
PCR	Polymerase chain reaction
PL	Platelets
PML-RARα	Promyelocytic leukaemia - retinoic acid receptor
PU.1	Purine Rich sequence 1
RBCs	Red blood cells
rcf	Relative centrifugal force
rpm	Revolutions per minute
RT	Room Temperature
RNA	Ribo Nucleic Acid
ROS	Reactive oxygen species
RUNX1	Runt-related transcription factor 1
Sca-1	Stem cells antigen
SCF	Stem Cell Factor
SDF-1	Stromal cell derived factor-1
SCFR/c-Kit	Stem Cell Growth Factor Receptor
SCL/TAL1	Stem Cell Leukaemia /T-cell Acute Lymphocytic Leukaemia-1
SEM	Standard error of mean
SFK	Src family kinases
Shh	Sonic hedgehog
SLAM	Single lymphocyte activating molecule
SMCs	Smooth muscle cells
SR-BI	Scavenger receptor reporter type BI expression
SRSF2	Serine/arginine-rich splicing factor 2
ST	Short term
STAT	Signal transducer and activator of transcription
t	Translocation
TAM	Tumour associated macrophage
TET2	Ten Eleven Translocation gene 2
TFs	Transcription Factors
TGF- β	Transforming Growth Factor-β

TCGA	The Cancer Genome Atlas
TET	Ten-eleven translocation
Thy1.1	Thymus cell antigen
TLR	Toll like receptor
TPO	Thrombopoietin
VCAM1	Vascular cell adhesion protein 1
VLDL	Very low-density lipoprotein
WBCs	White blood cells
WHO	World Health Organisation
WT	Wild Type

Chapter 1: Introduction

1.1 Hàematopoiesis

1.1.1. Haematopoietic stem cells: an overview and experimental definitions

The blood system is comprised of several cell types with distinct functions, including white blood cells responsible for innate and acquired immunity, megakaryocytes that produce platelets required for blood haemostasis and erythrocytes that transport /export oxygen (O_2) and Carbon dioxide (CO_2) (Rieger and Schroeder 2012). All these cell types descend from haematopoietic stem cells (HSCs) residing in the bone marrow (BM), the major location of adult haematopoiesis (Bernitz et al. 2016). Blood cells turnover and are replaced actively during lifetime, as every day new cells are produced to replace those that have reached the end of their lifespan (Chao et al. 2008). The lifespan of mature blood cells varies depending on their function or type, they vary from hours to years. Lymphocytes live the longest, around 200 days while granulocytes live hardly mere 14 days maximum (Perry et al. 1959). Blood cell production is increased in a lineage specific manner when required under conditions of pathologic stress, for example, anaemia or during infection. This complex, continuous process producing blood products in humans and animals is called haematopoiesis, derived from the Greek for blood (haem) and to generate (poiesis) (Rieger and Schroeder 2012).

Initially researchers noted the wide diversity of cells, with different differentiation (or specialisation) stages, when examining components of mature bone marrow. They proposed the likelihood that those cells are derived from one common precursor cell, the haematopoietic stem cell (HSC). The term “stem cell” was coined in the middle of nineteenth century by Ernst Haeckel (Ramalho-Santos and Willenbring 2007). After World War II concluded, the study of radiation sickness was very relevant and researchers investigating this found that in lethally irradiated mice receiving intravenously injected normal bone marrow from genetically identical mice, death due to irradiation was averted and blood production was restored (Rekers et al. 1950).

However, it was unclear whether these cells were single (i.e. clonal) multipotent or multiple restricted HSC populations, until seminal work from James Till and Ernest McCulloch showed that putative HSCs are multipotential using the mouse CFU-S assay (Till and McCulloch 1961). This led investigators to hypothesize that a cellular component of the bone marrow was responsible for restoring blood cell production, that also retained a lymphoid capability (Haeckel 1868; Wu et al. 1968).

HSC characterisation can now been defined by their antigenicity, as judged by flow cytometry, and prospectively isolated HSCs and their progenitor cells can be grown in cultured *in vitro* to cells with functional blood forming potential in certain lineages (Morrison and Weissman 1994) (Osawa et al. 1996) (Kondo et al. 1997; Akashi et al. 2000) (Kiel et al. 2005). However, only *in vivo* testing in bone marrow transplantation can determine the true multi-lineage differentiation capability. In an extension of bone marrow transplantation experiments, serial transplantation can specifically determine HSC self-renewal capacity – one of the principal features of HSCs (Morrison and Weissman 1994). To self-renew, HSCs must be able to generate more HSCs and also differentiate on division. Due to the relatively short lifespan of mature blood cells, HSC constantly replenish the HSC pool with new self-renewing cells and differentiated progenitors, all while keeping the HSC pool at an optimal size (Seita and Weissman 2010). HSCs are also relatively quiescent (Kunisaki et al. 2013) and all these HSC fates are tightly control by bone marrow local microenvironment (the niche)(Morrison and Scadden 2014).

1.1.2. Embryonic and adult haematopoiesis

During embryogenesis, distinct waves of embryonic haematopoiesis have been described. However, there is continued debate about whether each wave results from a separate blood cell or a continuation of a previous haematopoiesis stream due to the overlap between the different waves of haematopoiesis (Rieger and Schroeder 2012). Haematopoietic production occurs in a first of which occurs in the embryonic yolk sac (megaloblastic haematopoiesis). In the second wave, which begins in the embryonic aorta-gonad-mesonephros (AGM) area and gives rise to adult haematopoiesis (normoblastic haematopoiesis), that generates the HSCs (Clements

and Traver 2013) and MSCs (Mendes et al. 2005) that sustain the body's constant production of blood cells.

Haematopoiesis starts when epiblast cells migrate into ectoderm and endoderm intermediate space. Afterward, they migrate into extraembryonic yolk sac at around day 7 post conception, forming blood foci, a development site of initiation cells containing Flk1+ VE cadherin+ CD41− endothelial cells along with CD41+ blood cells. This stage is termed ‘primitive’ haematopoiesis, with its primary function being red blood cell production to facilitate tissue oxygenation and these cells are not involved into adult haematopoiesis (Palis et al. 1999). Primitive erythroblasts, which in mice express embryonic globins, enter the circulation when the heart begins to beat and begin to enucleate at E12.5. These erythroblasts then create the erythrocytes that transiently circulate in pups after birth (Fraser et al. 2007). Moreover, at embryonic day 7.25 (E7.25), the mouse yolk sac also produces primitive megakaryocyte and macrophage progenitors (EMPs) (Xu et al. 2001; Hoeffel and Ginhoux 2018). At E8.25, the yolk sac contains a variety of myeloid progenitors (including granulocyte-macrophage progenitors, mast cell progenitors, and high proliferative potential colony-forming cells), which later colonize the fetal liver and give rise to mature cells onwards at E10.5 (Palis et al. 1999).

The second wave is called ‘definitive’ haematopoiesis, which starts around day 8 post conception, when heartbeat initiates (Ottersbach et al. 2010). In this stage, erythroid progenitors (burst-forming unit erythroid or BFU-E) generate then colonized in fetal liver, which then produces first definitive erythrocytes (McGrath et al. 2011). Also, at embryonic day 8, yolk sac EMPs begin to give rise to the definitive erythrocytes, granulocytes, and macrophages that will be generated in the fetal liver (Bertrand et al. 2007). Collectively, yolk sac haematopoietic waves aid the embryo development and survival without HSCs (Palis 2016). The first HSCs develop on the dorsal aorta or aorta-gonads-mesonephros (AGM) during this time. Nevertheless, pro-HSCs expressing (Lin–VE cadherin+ cKit+ CD41+ CD43– CD45–) are detected at E9.5 while at E10.5-11.5 AGM comprise both Type I (VE- cadherin+CD45-CD41^{low}) and Type II (VE- cadherin+CD45+) pre-HSCs (Rybtsov et al. 2011; Rybtsov et al. 2014).

Soon after they develop in the AGM, they migrate to the placenta starting E10.5-E11 (Gekas et al. 2005) and foetal liver to expand at E12 (Kumaravelu et al. 2002). Thus, foetal placenta and liver are considered essential HSC transient reservoirs before bone marrow colonization at E17 (Christensen et al. 2004). Isolated cells from bone marrow stage can fully reconstitute the haematopoietic compartment in transplantation experiments; they express MHC class I, CD45, CD150 and Sca-1 (Golub and Cumano 2013) Just prior to birth, HSCs migrate and seed the spleen and to bone marrow, where they remain resident for a lifetime (Figure 1.1).

Subsequently, blood production takes place in the bone marrow of all major bones, within the body and, when growing into adulthood, it is confined to the central skeleton and proximal ends (Estefa et al. 2021). However, the liver and spleen can recommence their haematopoiesis role whenever needed in times of pathological and physiological need, which is termed extramedullary haematopoiesis (Jagannathan-Bogdan and Zon 2013) (Kieusseian et al. 2012). It is accepted that most of adult HSC compartments are generated during embryonic development (Golub and Cumano 2013). However, it is worth mentioning that the fundamental properties of HSCs in each organ site differ during development, ranging from rapid cycling HSCs in the foetal liver to relative quiescence in adult bone marrow (Seita and Weissman 2010). Within a brief window of time after birth, HSCs in mice make the transition from their foetal to adult state (Bowie et al. 2007). A summary of HSCs when they generated in the embryo where it starts producing in the fetal liver and continue in the bone marrow is presented in Table 1.1. This highly regulated process is tightly regulated with a network of signalling pathways and haematopoietic factors such as the runt-domain transcription factor RUNX1 , also known as CBFα and AML1, which is considered one of the earliest markers for HSCs specification and it start expressing in the dorsal aorta (North et al. 1999). Also, Nodals and bone morphogenetic proteins (BMPs) , related to transforming growth factor-β (TGFβ) family of signalling molecules (Dutko and Mullins 2011) are involved in HSC ontogenesis. Other pathways involved in HSC ontogenesis include Fibroblast growth factor (FGF) signalling, which binds to their FGF receptor (FGFR) or receptor-like genes. This dimer activate several downstream intracellular signalling pathways including phosphoinositide 3-kinase (PI3K)-AKT and mitogen-activated protein kinase pathways (Turner and Grose 2010). The Notch pathway plays an important role in cellular signalling and embryonic patterning (Kopan

and Ilagan 2009). Notch signalling regulates many stages of T-cell development and is crucial for the creation of definitive embryonic haematopoietic stem cells (Schwanbeck and Just 2011). Notch main role is to determine arterial program. In Notch mutant murine and zebrafish models , lack artery development and certainly lack of haematopoiesis (Bigas and Espinosa 2012).

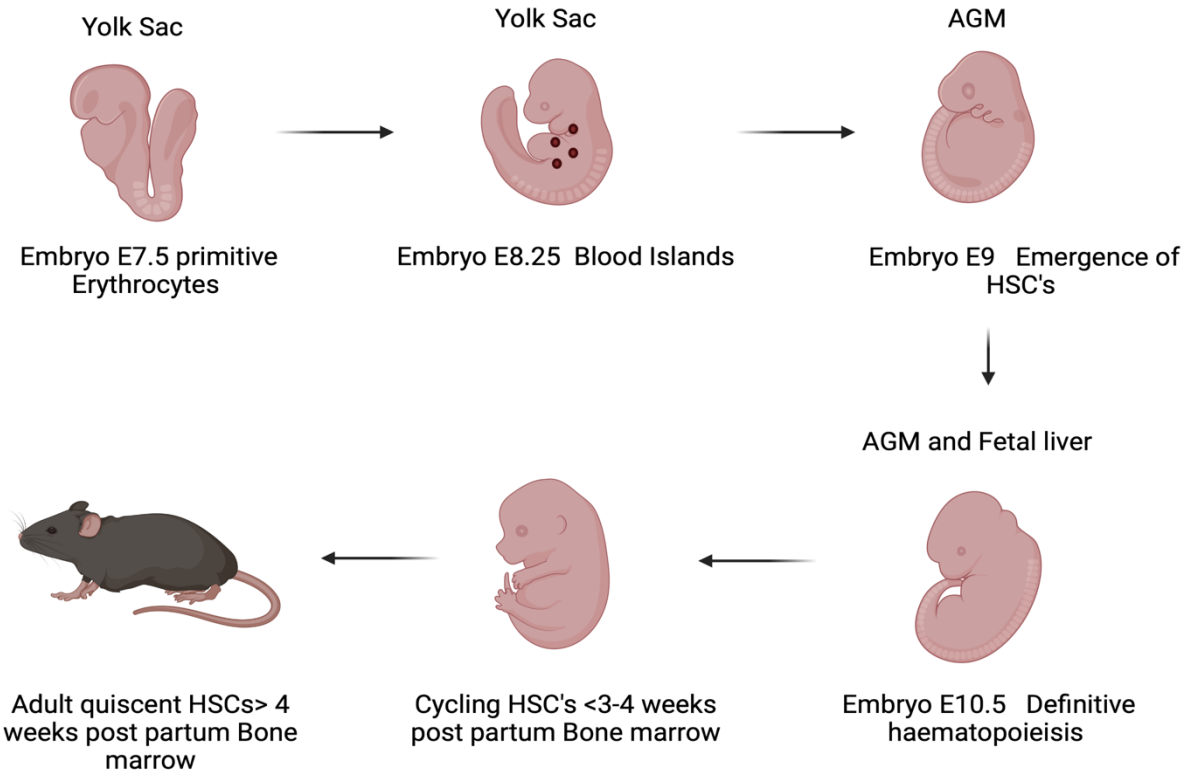

Figure 1.1 Embryonic Developmental Regulation of Haematopoiesis in the Mouse. Haematopoiesis start form embryonic day 7 as primitive phase in yolk sac and then definitive stage representing in aorta-gonads-mesonephros (AGM), Placenta and liver.

Table 1. 1 Immunophenotypic markers of murine haematopoietic cells and HSCs during development.

Day of conception	site	Cell type	Possible immunophenotype	Stage	Reference
E 7.5	Yolk Sac	Haemangioblasts	-	Primitive Haemopoiesis	(Golub and Cumano 2013)
E 7.5	Yolk Sac	Macrophages	-	Primitive Haemopoiesis	(Hoeffel and Ginhoux 2018)
E7.5-E8	Yolk Sac	Megakaryocyte	-	Primitive Haemopoiesis	(Xu et al. 2001)
E 9.5	Aorta – gonads-mesonephros (AGM)	Pro-HSCs	VE-cadhrin+ CD45-CD41^{low} CD43-	Definitive Haematopoiesis	(Rybtsov et al. 2014)
E10.5–E11.5	Aorta – gonads-mesonephros (AGM)	Pre-HSCs	VE-cadherin+ CD41+ CD43+ Tie-2 CD45-	Definitive Haematopoiesis	(Rybtsov et al. 2011)
E11-E12.5	Foetal placenta	HSCs	c-kit+ CD34±	Definitive Haematopoiesis	(Gekas et al. 2005)
E 12	Foetal Liver	HSCs	C-kit + CD150+ CD48- HLA Class I	Definitive Haematopoiesis	(Kieusseian et al. 2012)
4 weeks post-partum	Spleen and bone marrow	Cycling HSCs	C-kit + Sca-1+ CD150 + CD48-	Adult Haematopoiesis	(Kiel et al. 2005)

1.1.3. Cell cycle regulation for HSCs quiescence, self-renewal, and differentiation

HSCs are distinguished from other stem cells by their ability to self-renew and specialize into any type of adult blood cell. Because HSCs preserve a steady supply of lineage cells throughout life, self-renewal of HSCs is essential for preventing the HSC pool from depletion (Seita and Weissman 2010). HSC cell-cycle activity mirrors the needs of the developing organism. It has been found that in the murine foetal liver, HSCs divide extensively to meet growth demands, and that around 100% of HSCs are activated during the cycle (Nygren et al. 2006). In contrast, throughout adulthood, around 75% of HSCs remain in quiescence and about 25% enter the cell cycle to maintain blood homeostasis for a long duration (Cheshier et al. 1999). A wide variety of intracellular and extracellular systems work together to keep cells in a stable state of either quiescence or proliferation depending on physiologic demand. Interphase and mitosis are the two stages that make up the cell cycle. There are three stages within the interphase, and they are referred to as G1, S, and G2. At G1 checkpoint, cells decide whether to continue growing in the S phase or enter a resting phase (G0-phase, also known as quiescent phase) (Pardee 1974). During the S-phase, cells continue to develop and get ready to divide by synthesizing new DNA. Mitosis (M phase) is the cell division phase, and the M-checkpoint is where the success of mitosis is evaluated. Cell cycle division produces offspring HSCs and/or committed progenitor cells from HSCs, which can be either symmetric or asymmetric divisions (Nakamura-Ishizu et al. 2014). The cell cycle regulatory proteins such as cyclin-dependent protein kinases (CDKs) prompt HSCs to induce the cell cycle phases, whereas cyclin-dependent kinase inhibitors (CKIs) are required to retain HSCs in a quiescent state (Morgan 1997). Scientists investigating G1 checkpoint regulator, cyclin-dependent kinase inhibitor, p21 utilizing $p21^{cip1/waf1}$ (p21) knock out mice found an increase in haematopoietic stem cell proliferation and absolute number under steady state haematopoiesis(Cheng et al. 2000b). The same group report that the CDKI $p27^{kip1}$ (p27) significantly affects progenitor proliferation and pool size, but has no effect on stem cell quantity, cell cycle, or self-renewal (Cheng et al. 2000a).

CDKs assemble an active complex with their cyclin partner at each phase of the cell cycle. Retinoblastoma family of transcriptional proteins (RB, p107, and p130) is a group of cell cycle repressors that act on E2*f* TFs to prevent cells from entering the cell cycle (Ho and Dowdy 2002; Giacinti and Giordano 2006). By forming the cyclin-D CDK4/6 complex, CDK4 and CDK6 signal cyclin-D to phosphorylate retinoblastoma proteins (RBPs), which in turn activates E2*f* TFs and drives cells into the G1 phase. Additional phosphorylation of RBPs is carried out by a cyclin-E CDK2 complex near the end of G1-phase, and this is necessary for progression into S-phase, when DNA synthesis may begin. The passage through S and G2 phases are maintained by the cyclin-A CDK2 and cyclin-A CDK1 complexes, respectively. The cyclin-B CDK1 complex stimulates entry into the M phase and subsequent cell division at the end of the cell cycle (Ho and Dowdy 2002; Giacinti and Giordano 2006). After being deleted in adult mice, RBPs caused a rise in HSC proliferation and a decline in HSC quiescence (Viatour et al. 2008). Also, the self-renewal ability of HSCs is maintained by the B-lymphoma Mo-MLV insertion region 1 (BMI1), which suppresses the production of p16/p19 proteins. Mice lacking Bmi1 had elevated p16/p19 expression, a dramatic drop in cycling HSCs, and a disruption in the ability of mature HSCs to self-renew (Park et al. 2003). In addition, reports found an increase in cycling HSCs numbers in the CDKI p18 knockout mice while preserving self-renewal ability (Yuan et al. 2004). The p57 protein, which controls HSC dormancy, triggers the production of p21, which, as alluded to above, has been implicated in HSC quiescence (Cheng et al. 2000b). In serial transplantation tests, CDKI p57-null adult mice showed a reduction in quiescent HSCs and defects in HSCs capacity for self-renewal (Matsumoto et al. 2011). Collectively, these data show the complex requirement of various aspects of the cell cycle machinery in maintaining HSC quiescence. However, other regulatory proteins have an impact on the quiescence HSCs; numerous cytokines and signalling pathways are also involved. For example, TGFβ and Notch ligands produced from BM stromal cells regulate HSC quiescence and self-renewal respectively (Ezoe et al. 2014).

1.1.4. Other mechanisms of intrinsic and extrinsic regulation of adult haematopoiesis

HSC function is under 'master' control through a series of nuclear regulators, namely transcription factors, which covers all classes of DNA-binding proteins that regulate gene transcription and therefore HSPC behaviour and fate (Huilgol et al. 2019). Within the haematopoietic system, key HSC transcription factors identified include MLL, Gata2, Runx1, TEL/ETV6, SCL / TAL1 and LMO; their function has been primarily uncovered in experiments with knock-out mice (Rossi et al. 2012) (Table 1.2).

Table 1. 2 Critical intrinsic and extrinsic regulators of HSC function.

	Function	**References**
Growth Factor or chemical modulator		
NOTCH Ligand	Instructing communication between HSCs and their niche, as it requires cell- to-cell contact for activation.	(Lampreia et al. 2017)
WNT proteins (β-catenin, T-cells Factors (TCF) and Lymphoid enhancer binding factor	Embryonic HSC development	(Richter et al. 2017)
Bone morphogenetic protein (BMPs)& (SMADs)	Early haematopoietic development, BMP4 directly regulates Integrin-α4 expression through SMAD-independent p38 MAPK-mediated signalling.	(Dutko and Mullins 2011)
Angiopoietin-like factors	HSC maintenance.	(Kadomatsu and Oike 2019)
Thrombopoietin	Self-renewal and homing	(Kovtonyuk et al. 2016)
Kit ligand or SCF (stem cell factor)	Embryonic HSC development	(Azzoni et al. 2018)
Retinoic acid, Homeobox (HOX proteins)	Haematopoietic stem cell self-renewal as well as the	(Collins 2008) (Alharbi et al. 2013)

	production and differentiation of regulatory T cells and myeloid cells. Early development, with lineage and differentiation stage-restricted patterns	
Prostaglandin E2 (PGE2)	Expands a subset of HSPCs with limited self-renewal	(Porter et al. 2013)
Cell-cycle regulators		
INK4A (also known as p16)	HSC Self-Renewal	(Perez-Campo et al. 2014)
INK4C (also known as p18)	Increases HSC quiescence	(Yuan et al. 2004)
Pten (phosphatase and tensin homolog	Maintaining HSCs in quiescent state	(Li et al. 2016)
p53 pathway	Cell cycle control, senescence, and apoptosis	(Pant et al. 2012)
Proto-oncogene c-myc	Regulation of proliferation, differentiation, and apoptosis	(Hoffman et al. 2002)
WAF1 (also known as p21)	Apoptosis inhibition	(Peterson et al. 2007)
CDX and HOX proteins		
Hoxa7, Hoxa9, Hoxa10 and Hoxb4	Differentiation and proliferation	(Argiropoulos and Humphries 2007)
caudal-related homeobox transcription factor (CDX2)	Embryogenesis and early developmental haematopoiesis	(Vu et al. 2020)
MEIS1	Adult HSC maintenance and expansion ,provide new evidence that highlights key roles of Meis1 in both	(Miller et al. 2016)

	megakaryopoiesis and erythropoiesis.	
Blood transcription factors		
GATA2	Essential for Maintenance of adult HSC	(Menendez-Gonzalez et al. 2019)
Growth factor independence 1 (Gfi1)	Development and function of haematopoietic stem cells (HSCs), B and T cells, dendritic cells, granulocytes and macrophages.	(van der Meer et al. 2010)
Tel/Etv6	Maintain haematopoiesis Embryonic Haematopoiesis Erythroid and megakaryocytic development	(Hock and Shimamura 2017)
JUNB	Controls LT-HSC proliferation and limits their rate of production of myeloid progenitors by maintaining appropriate responsiveness to Notch and TGF-β signalling,	(Santaguida et al. 2009)
SOX17	Foetal haematopoiesis in the yolk sac and fetal liver, especially in the maintenance of fetal and neonatal HSCs, but not adult HSCs	(Nakajima-Takagi et al. 2013)
PU.1	A direct regulator of myeloid, dendritic-cell, and	(Rothenberg et al. 2019)

	B cell functional programs, antagonist of terminal erythroid cell differentiation, also expressed in the earliest stages of T-cell development	
Myb	Erythroid cellular proliferation/differentiation balance, sustains proliferation, and a low MYB environment favours accelerated differentiation	(Wang et al. 2018b)
CREB (cyclic-AMP-responsive-element-binding protein) CBP	Adult HSC maintenance	(Chan et al. 2011)
ZFX	Self-renewal in embryonic and adult HSC's.	(Galan-Caridad et al. 2007)
Runt-related transcription factors (RUNX1)	Definitive haematopoietic stem cell (HSC)	(Lam and Zhang 2012)
SCL/TAL1, T-cell acute leukaemia protein 1	Haematopoietic cell development during embryo-genesis.	(Vagapova et al. 2018)
Chromatin-associated factors		
Enhancer of zeste homolog 2 (EZH2)	Regulates normal haematopoietic stem cell self-renewal and differentiation. EZH2 also controls normal B cell differentiation.	(Herviou et al. 2016)
Mixed Lineage Leukaemia *(MLL)*	Embryonic haematopoietic stem cell (HSC) development and	(Jude et al. 2007)

	maintenance of adult HSCs and progenitors	
RAE28	Regulating the proliferation, self-renewal, and differentiation of stem cells.	(Ohta et al. 2002)

1.1.5. Control of haematopoietic lineage commitment and differentiation

Differentiation of HSCs into different lineages requires precise regulation to produce the correct type of specific lineage when needed (Rieger and Schroeder 2012). A widespread shift in gene expression is required for HSPC differentiation to a particular lineage. Choosing and committing to a lineage is followed by the induction and maintenance of genetic programs that are exclusive to that lineage, which is regulated overall by transcription factors. Key to this process is the silencing of genes from other lineages while simultaneously encouraging the expression of lineage-specific transcription factors. This, for example, can be accomplished through positive autoregulation of a lineage-specific transcription factor while inhibiting opposing transcription factors in processes referred to as transcriptional antagonism (Orkin 2000)(Kerenyi and Orkin 2010). While transcription factors are the master regulators of haematopoiesis, cofactors, chromatin modifiers, microRNAs, and other regulatory RNAs all work together in intricate networks to maintain steady gene expression to achieve lineage specification (Davidson 2010). For example, induction and propagation in erythroid requires GATA2, GATA1 and FOG1, while B -lymphoid requires PU.1, IKAROS, E2A, EBF1 and PAX5 and IL-7Ra. Moreover, T cells needs Notch, TCF1, BCL1 1b, GATA3 while myeloid and erythroid lineages are controlled mainly by PU.1 and GATA1 respectively (Rieger et al. 2009). I will detail some critical blood transcription factors in the subsequent paragraphs and outline their importance in lineage commitment (summarised in Table 1.2).

The member of the basic helix-loop-helix (bHLH) transcription family known as stem cell leukaemia/T-cell acute lymphocytic leukemia1 (SCL/TAL1) is required for the development of HSCs. Germline Scl/Tal1 knockout (KO) mice do not survive past

embryonic day 9.5 and die due to haematopoietic defects, indicating that *scl* is crucial in early haematopoietic development. Also, they show severe deficiencies in blood development at the yolk sac stage (Robb et al. 1995). Deletion of Scl/Tal1 in the adult BM mice demonstrated that Scl/Tal1 is not important for adult HSCs maintenance, but hinders the ultimate differentiation of erythroid/megakaryocyte lineages (Mikkola et al. 2003).

Runt-related transcription factor1 (RUNX1, also known as acute myeloid leukemia-1) plays a crucial role in the differentiation of endothelial cells into haematopoietic cells and is required for HSC development in the aortic gonad-mesonephros area (Chen et al. 2009). *Runx1* KO mice are incompetent to produce haematopoietic clusters in the AGM region, representing *Runx1* functions throughout early stages of blood cell development. Conversely, conditional deletion of *Runx1* after the definitive haematopoiesis revealed that *Runx1* is dispensable for the HSC maintenance (Chen et al. 2009). Further, a deficiency in haematopoiesis results in the death of double Runx1 and Gata2 heterozygote mice towards the middle of their pregnancies, whereas single heterozygote *Runx1* or *Gata2* animals survive (Wilson et al. 2010). Runx1 has a crucial role in controlling haematopoiesis, particularly megakaryocyte and platelet development (Huang and Cantor 2009). *Runx1*$^{-/-}$ engineered murine models fail to live between E12.5 to E13.5 due to failure of definitive haematopoiesis and central nervous system haemorrhage (Wang et al. 1996).

Both primitive and definitive haematopoiesis depend on LIM domain protein 2 (LMO2). Lmo2 KO mice display abnormality in erythropoiesis in the yolk sac which causes foetal life at E10.5 (Warren et al. 1994). Oligomeric complexes are formed when the LMO2 protein binds to and interacts with other proteins such SCL/TAL1, E2A, LDB1, and GATA1. Erythroid differentiation cannot occur without this complex (Wadman et al. 1997).

In order to control haematopoiesis, Friend leukaemia integration1 (FLI1), a member of the Ets-family of TFs, must first bind to the target gene sequence GGA (A/T). At E12.5, Fli1-null embryos are fatal due to extensive haemorrhaging in the anterior dorsal aorta region (AGM)(Spyropoulos et al. 2000) . The formation of the HSCs requires a delicate trio composed of Fli1, Scl/Tall, and Gata2 (Pimanda et al. 2007) and in progenitors, Fli1 promotes megakaryocyte differentiation. Mice deficient in Fli1 have anaemia and a

dramatic decrease in megakaryocyte progenitors, resulting in thrombocytopenia (Spyropoulos et al. 2000).

In the process of generating committed myeloid/lymphoid progenitors from lymphoid-primed multipotential progenitors (LMPPs), a member of the Ets family called purine box-binding protein-1 (PU.1) is the main player (Iwasaki et al. 2005; Arinobu et al. 2007). Pu.1 and Gata1 TFs regulate the differentiation of HSCs into myeloid/lymphoid or erythroid/megakaryocyte lineages. The relationship between Pu.1 and Gata1 is antagonistic so that Gata1 downregulates Pu.1 and promotes the formation of megakaryocyte/erythrocyte progenitors, whereas conversely Pu.1 inhibits Gata1 and directs the process toward myeloid/lymphoid populations (Nerlov et al. 2000). In support of this, a mouse engineered with Fluorescent reporter protein (GFP) knock-in of the Pu.1 locus demonstrated that Pu.1 is substantially expressed in LMPPs and that Pu.1-GFP+ LMPPs differentiate to myeloid/lymphoid lineages with minimal potential towards erythroid/megakaryocyte cells (Arinobu et al. 2007). Furthermore, repopulating capability of HSCs was severely compromised and early myeloid and lymphoid precursors were not produced normally in Pu.1 KO mice (Iwasaki et al. 2005). Knock-in mice expressing GFP under the control of the Gata1 promoter showed, however, that Gata1 GFP+ is most abundant in primitive common myeloid progenitors (CMPs) that lose their lymphoid potency and instead give rise to erythroid, megakaryocyte, and myeloid compartments (Miyawaki et al. 2015). For proper erythrocyte development, GATA1 is essential both throughout embryonic and adult stages (Fujiwara et al. 1996) . Gata1, Gata2, Kruppel Like Factor-1 (Eklf1), and friend of GATA1 (Fog1), stem cell leukaemia SCL TFs all act together to control erythropoiesis. Crucial for megakaryopoiesis is the expression of the genes Gata1, Gata2, Fli1, and Runx1 (Orkin and Zon 2008).

The CCAAT/enhancer-binding protein alpha (C/EBP) is required for the maturation of granulocytes and directs multipotent progenitors towards myeloid lineages (Radomska et al. 1998). Inactivation of Cebp in adult animals prevented GMPs from forming and accumulated myeloblasts, suggesting that Cebp governs the differentiation of CMPs into GMPs (Zhang et al. 2004). The expression of C/EBP and PU.1 is antagonistic to one another, which helps to identify the different types of mature blood cells. Overexpression of Cebp represses monocytes and promotes granulocyte differentiation, whereas upregulation of Pu.1 drives monocyte differentiation and suppresses granulocytes' maturation (Radomska et al. 1998).

In terms of transcription factors that are required for lymphoid commitment, IKAROS promotes the differentiation of HSCs into lymphoid cells and is crucial for the early commitment of lymphoid progenitors (Yoshida and Georgopoulos 2014). A precipitous reduction in B-cells, T-cells, and natural killer cells was seen in BM mice with germline deletion of Ikaros, whereas erythroid and myeloid cell frequencies were unaffected (Georgopoulos et al. 1994). Lymphoid cells with low Ikaros expression also express less Flt3 and IL7R signalling receptors (Yoshida et al. 2006).

T-cell development is orchestrated by Notch1 signalling and GATA3. Lymphoid cell fate is controlled by Notch1 signalling (Golub 2021). When Notch1 was overexpressed in BM mice, they saw an increase in T-cells and a decrease in B-cells. In contrast, Pax5 promotes B-cells development by inhibiting Notch1 signalling receptors (Pui et al. 1999; Delogu et al. 2006). While erythroid, myeloid, and B-cell frequencies were unaffected in Gata3-null embryonic stem cells, mature T-cells were lacking due to a lack of double-negative thymocyte development (Ting et al. 1996)

1.1.6. Haematopoiesis and ageing

The ability of HSCs to regenerate is diminished with age. Reduced self-renewal, poor homing and engraftment after transplantation, and myeloid-biased differentiation are all hallmarks of HSCs aging (Dykstra et al. 2011). The number of HSCs is said to rise paradoxically with age in both mice and humans (Morrison et al. 1996). However, evidence to support the concept that an increase in HSC numbers compensates for age-related abnormalities is lacking from current models of HSC (Geiger et al. 2013) and functional decline of HSCs has been noted during aging (Abdelfattah et al. 2021). Notably, substantial DNA damage in form of strand breaks during aging in HSC has been associated with widespread DNA repair pathways activation during HSC quiescence (Beerman et al. 2014). A recent study showed and monitored the collective dividing activity of slow-cycling HSCs during adult hood. They identified a proportion of seldom dividing HSCs that contained all the long-term HSC (LT-HSC) action inside the aging HSC fraction. They simultaneously accomplish four detectable symmetrical self-renewal divisions to expand its size before entering a state of dormancy. This study demonstrates that the mechanism of HSC expansion involves successively

longer periods between cell divisions, with long-term regeneration capacity lost with a fifth division (Bernitz et al. 2016).

1.1.7. Haematopoietic niche

HSCs reside in the bone marrow microenvironment or (the haematopoietic stem cell niche). BM comprises a heterogeneous mixture of cell types including blood cells, perivascular mesenchymal cells, osteoblasts, macrophages, osteoclasts, endothelial cells, sympathetic nerve fibres and fat cells. These cells provide guidance for haematopoietic development (Calvi and Link 2014). A multitude of signalling pathways have been shown to be activated in HSCs by the niche (e.g., the cytokine receptors c-Kit and Mpl, Wnt, Notch, Sonic hedgehog, and integrin signalling) (Ehninger and Trumpp 2011). Imaging and genetic modification in mice models have recently permitted the discovery of discrete vascular niches that have been demonstrated to govern the balance between quiescence, proliferation, and regeneration of the bone marrow following damage (Rieger and Schroeder 2012).

Quiescent HSCs predominantly inhabit the endosteal (bone) niche, which is hypoxic and the vascular arteriolar niche, whereas actively cycling HSCs are found in sinusoidal sites (Mendelson and Frenette 2014). The endosteal zone contains a disproportionately high number of HSCs; only around 20% of HSCs are located within half the distance to the central vein, whereas 80% are located within half the distance to the bone surface (Kunisaki et al. 2013). Consequently, HSCs depend on their environment for self-renewal and differentiation regulation factors cues, which are generated from various niches and cell types within the niche. For example, HSCs maintain a quiescent state under the influence of thrombopoietin produced from osteoblasts. Moreover, HSCs migration from the inner bone marrow niche to the vascular niche is regulated by the chemokine CXCL12 secreted from stromal nestin-expressing mesenchymal stem cells (MSCs) (Yoshihara et al. 2007). CXCL12 acts on CXCR4 receptor on the HSCs and its one of the important niche retention signals (Ehninger and Trumpp 2011).

Oxygen tension, shear stress, contractile forces, and temperature are all examples of physical cues that can operate as regulatory signals inside the bone marrow niche(Lander et al. 2012). In addition to bound or released chemicals from neighbouring cells (Wang and Wagers 2011). One of the cells are perivascular stromal cells in mice. They express Platelet-derived growth factor receptor- (PDGFR- α), CD51 (also called ITGAV), and nestin. These cells highly express stem cell factor (SCF) and chemokine (C-X-C motif) ligand 12 (CXCL12) that play important roles in HSC maintenance and retention (Pinho et al. 2013). Thrombopoietin (TPO), angiopoietin-1 (Ang1), stem cell factor (SCF), and stromal-derived factor-1 (SDF1, also known as C-X-C chemokine-12 [CXCL12]) are all soluble growth factors and cytokines produced by HSC niches that promote HSCs maintenance. Myeloproliferative leukaemia protein (c-MPL) is a receptor expressed on HSCs that TPO interacts to. TPO/c-MPL signalling is required for both HSC self-renewal and megakaryocyte maturation (Kimura et al. 1998). HSCs from c-Mpl-null mice employed in the serial transplantation experiments revealed a diminished quantity and self-renewal capacity (Kimura et al. 1998). The tyrosine kinase receptor TIE2 mediates the interaction between Ang1 and HSCs, helping to keep HSCs in a quiescent state by ensuring they stay adhered to bone (Arai et al. 2004). SCF, which is secreted by both osteoblast and vascular endothelial cells, provides growth and survival to HSCs via interacting to the tyrosine kinase receptor c-kit. Scf knock-in mice investigations demonstrated that vascular endothelial cells were a key source of SCF in BM niches, while a considerable reduction in the HSC numbers was detected in Scf-vascular endothelial cells null mice (Ding et al. 2012). HSCs react to SDF1 via the CXC-chemokine-4 receptor (CXCR4), which is primarily expressed by perivascular stromal cells but also by endothelial and osteoblast cells to a lesser extent (Ding and Morrison 2013). In the perivascular area of the bone marrow (BM), there are cells called CXCL12 abundant reticular (CAR) cells that release a lot of this chemokine. CAR cells are the predominant component in BM niches and play a crucial role in the quiescence of HSCs by binding to them via CXCR4 in both the endosteal osteoblastic and perivascular endothelial niches(Sugiyama et al. 2006) (Figure 1.2). Nevertheless, Bone marrow's low-oxygenic niche protects HSCs from the damaging effects of ROS for the long term (Jang and Sharkis 2007). Cell ageing, numerous diseases, and cancer are all accelerated by high concentrations of both endogenous and exogenous active oxygen, as well as by an excess of reactive oxygen species (ROS) (Chen et al. 2017). Stem cells have a protective metabolic phenotype that

allows them to generate less reactive oxygen through oxidative metabolism and better scavenge free radicals through glycolysis and the pentose phosphate pathway (Perales-Clemente et al. 2014)

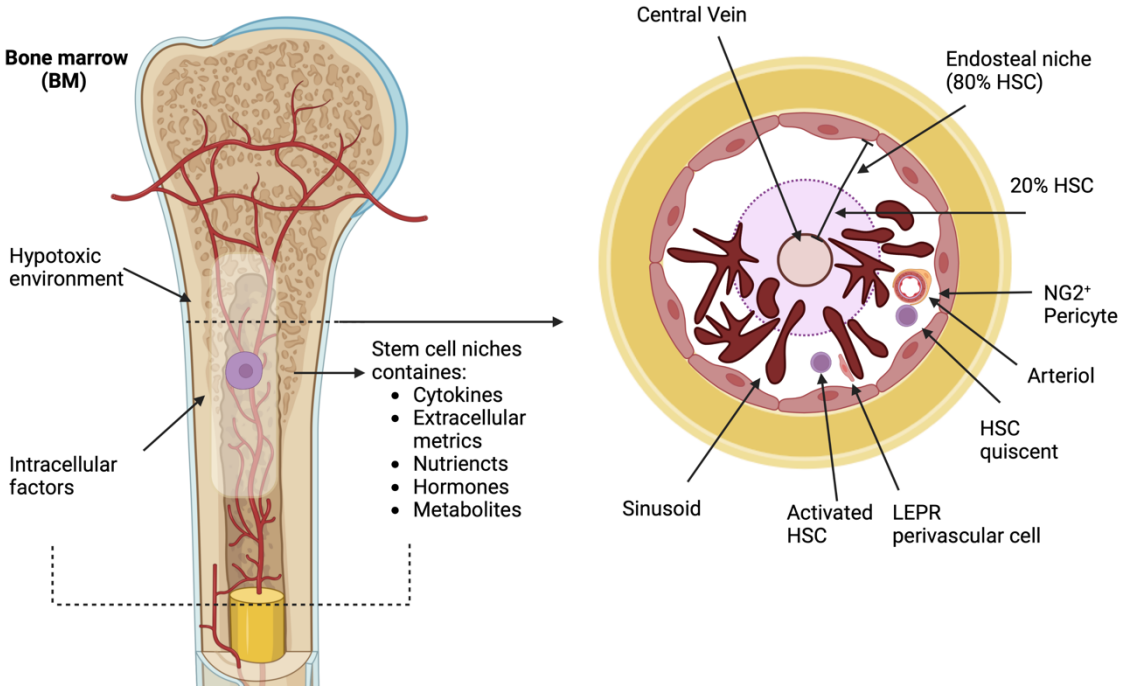

Figure 1.2 Haematopoietic niche located in bone marrow.

HSCs live in hypoxic microenvironment which sustains dormant HSCs with low intracellular reactive oxygen species (ROS). The bone marrow accommodates HSCs with all essential requirements for lifelong span. Quiescent HSCs are located around NG2+ pericyte, endothelial cells encapsulating small arterioles. 80% of HSC inhabit the endosteal area near the bone surface.

1.1.8. Murine haematopoietic hierarchy and immunophenotypic characterisation

A considerable amount of literature has been published on murine haematopoiesis and the expression of cell surface markers that correlate with the functional capacity of HSCs (Parekh and Crooks 2013). Since 1988, when fluorescence-activated cell sorting (FACS) technology allowed for the purification of HSCs from mouse bone marrow based on cell surface marker or phenotypes (Spangrude et al. 1988) . This study characterised HSCs as negative cells for mature lineage antigens: T-cells, CD3; B-cells, B220; T- helper, CD4; T-cytotoxic, CD8; RBCs, Ter119; Monocytes, Mac1; and Neutrophils, Gr1 and positive for Sca-1 (Ly6A), Thy-1 and c-kit (Spangrude et al. 1988). Sca-1 and Thy-1 are Glycosylphosphatidylinositol-linked immunoglobulin (Holmes and Stanford 2007; Bradley et al. 2013) and the c-kit is a tyrosine kinase receptor (Abbaspour Babaei et al. 2016). All multipotent blood cells can thus be isolated in Lineage - Sca-1+ C-kit+ (LSK) population from the bone marrow of adult mice. Those LSK cells have been redefined over the last 30 years and can be sub-classified further into three populations: 1. Multipotent long-term HSCs (LT-HSCs), which can self-renew and differentiate to 2. Short-term HSCs (ST-HSCs) and 3. Multipotent Progenitors (MPPs). These populations are separated according to differences in SLAM family markers CD150 (also known as Slamf1) and CD48 (Slamf2) expression (Mayle et al. 2013). Utilizing CD150 and CD48 in immunophenotyping can subdivide the heterogeneous LSK compartment into four distinct subpopulations: HSCs, LSK+CD150+CD48-; MPPs, LSK+CD150-CD48-; HSPC1, LSK+CD150-CD48+; and HSPC2, LSK+CD150+CD48+ (Kiel et al. 2005). HSPC1 and HSPC2 cells are heterogeneous committed progenitors with the ability to develop into lymphoid and myeloid progenitors at the expense of megakaryocytes/erythrocytes, while HPC2 cells give rise to all limited haematopoietic progenitors with reduced T-lymphoid potential(Brown et al. 2018). Since HSPC1 cells are largely positive for CD135 (about 75%) (Oguro et al. 2013) and both HSPC1 and LMPPs have lymphoid/myeloid reconstitution potential, HSPC1 are there quite similar to LMPPs (Yang et al. 2005) (lymphoid-myeloid primed progenitors) which are LSK+CD34+ $CD135^{High}$ (Adolfsson et al. 2005).

The capacity of HSCs to self-renew is determined by CD150 expression in LSK CD34- compartments, which also sheds light on whether these cells are myeloid or lymphoid biased (Beerman et al. 2010; Morita et al. 2010). Myeloid-biased HSCs (LSK+CD34-CD150^{high}), lymphoid-biased HSCs (LSK+CD34-CD150$^{-/low}$), and balanced-biased HSCs (LSK CD34 CD150^{intermediate}) are the three distinct subpopulations that may be identified based on CD150 expression. The CD150^{high} HSCs have the greatest potential for self-renewal and can efficiently reconstitute all CD150 fractions in successive transplantation trials.

Previous models of the haematopoietic hierarchy failed to discriminate between primitive myeloid/lymphoid/erythroid/megakaryocyte progenitors; however, Pietras et al. have proposed an alternative model that does so (Pietras et al. 2015). The Flt3 marker is used in conjunction with the slam markers to subdivide HSPCs into five distinct groups: LT-HSCs, LSK Flt3- CD150+ CD48-; ST-HSCs (MPP1), LSK Flt3- CD150- CD48-; MPP2, LSK Flt3- CD150+ CD48+; MPP3, LSK Flt3- CD150-CD48+; and MPP4, LSK Flt+CD150-CD48+. MPP 2 and 3 in this paradigm are myeloid-biased MPPs that have limited capacity to generate lymphoid cells, whereas MPP4 progenitors are lymphoid-biased MPPs that maintain GMP potential.

Multipotent Progenitors (MPPs) generate oligopotent progenitors that are characterised lineage restricted differentiated capability and self-renewal inability. These are common myeloid progenitors (CMP) (Akashi et al. 2000) or common lymphoid progenitors (CLP) (Kondo et al. 1997). CLP population can be characterised within Lin-Sca-1^{low} c-Kit^{low} with additional interleukin 7 receptor α chain (IL-7R α; CD127). It differentiates into restricted, committed, precursors of lymphoid cells B cells, T cells and Natural killer cells. which will differentiate future into mature cells (Kondo et al. 1997). Additionally, CD135 were proposed to prove that CLPs give rise to T cells and B cells equivalently. CLPs can be identified as Lin-Sca-1^{low} c-Kit^{low}CD127+ CD135+. (Karsunky et al. 2008). CMP are derived from Lin-Sca-1-c-Kit+ population (Akashi et al. 2000). They give rise to CMPs; LK CD34+CD16/32- which in turn differentiate into megakaryocyte/erythrocyte progenitors MEP; LK CD34-CD16/32- to give committed to megakaryocytes-erythrocytes progenies or granulocyte /macrophage progenitors GMP; LK+CD34+CD16/32+ that is responsible for development of granulocytes-macrophages (monocytes, neutrophils, eosinophils,

and basophils) mature blood cells (Akashi et al. 2000). Moreover, Miyawaki and Akashi 2015, included CD41 to specify a new CMP with robust differentiation potency toward myeloid/erythroid lineages making the new CMP defined as LSK+CD34+CD41^{high} (Miyawaki et al. 2015).

Another group Pronk et al., 2007 utilized CD150, Integrin subunit alpha-2b (CD41), and Endoglin (CD105) markers to characterise myeloid precursors in murine models to refine the definitions of provided by the Akashi and Weissman labs (Pronk et al. 2007). In this model, myeloid-lineages directed from CMPs is divided into pre-granulocyte/macrophage precursors (Pre-GM; LK+CD150-CD41-CD16/32-CD105-) and then advance to GMPs (LKCD150-CD41-CD16/32+). While erythroid-megakaryocyte lineages are directed from CMPs which differentiate into erythroid/megakaryocyte progenitors (Pre-MegE; LK CD150+CD41-CD16/32-CD105) that eventually generate either megakaryocyte-progenitors (MkP; LK+CD150+CD41+) or erythroid-precursors (Pre CFU-E; LK+CD150+CD41-CD16/32-CD105+). Nevertheless, an alternate concept of haematopoietic lineage commitment was shown by Adolfsson et al. They found that the MEP is directly produced from the ST-HSC/MPP compartments, whereas a subset known as lymphoid-primed multipotential progenitors (LMPPs) has the potential to create both CLPs and GMPs but loses the ability to develop into megakaryocytes and erythrocytes. CMPs are not a part of the hierarchy and are simply a mixture of myeloid cells. Moreover, since CMPs have previously been recognized as LK CD34+ CD16/32-, the traditional and alternative models meld into the composite model (Adolfsson et al. 2005; Iwasaki and Akashi 2007). ST-HSCs in this model progress to CMPs and LMPPs and it is possible for both CMPs and LMPPs to develop into GMPs. Figure 1.3 and Figure 1.4 summarize and detail the complexity of the murine haematopoietic differentiation hierarchy, as it currently stands.

Altogether, these finding indicate that HSCs are responsible for the generation of all haematopoietic lineages and the maintenance of long-term haematopoiesis over life. However, evolving research suggests that haematopoietic clones of MPPs rather than LT-HSCs govern the haematopoiesis hierarchy. While transplantation experiments shed light on the functional characterization of BM compartments including repopulation potential under stress conditions and BM homing, our understanding of

haematopoietic populations in steady state is still limited (Sun et al. 2014; Rodriguez-Fraticelli et al. 2018). To address this, by monitoring mouse adult haematopoietic compartments within situ transposon labelling techniques, Sun et al. studied the development of native blood cells (Sun et al. 2014). About 5% of LT-HSCs were shown to have clonal beginnings with MPPs, myeloid progenitors, and mature cells, whereas about 50% of MPPs and myeloid progenitors had comparable clonal roots with adult blood cells, as determined by in vivo monitoring of haematopoietic lineages. These results suggest that in steady-state haematopoiesis, multipotent progenitor clones are responsible for the majority of the haematopoietic lineage differentiation, with a smaller contribution from LT-HSCs. In steady-state haematopoiesis, LT-HSC/MPP2 cells are the specific primary source of megakaryocyte progenitors, whereas multipotent clones have the capacity to sustain production of myeloid, lymphoid, and erythroid lineages(Cabezas-Wallscheid et al. 2014). Carrelha et al. studies agree with megakaryocyte specific HSCs conclusion independently by employing a completely different strategy based on single cell transplantation (Carrelha et al. 2018). In light of these findings, it may be concluded that MPP clones are accountable for the maintenance of most native long-term blood formation rather LT-HSCs. Based on these studies together, the mouse haematopoietic hierarchy is still controversial and hierarchy models presented here will undoubtedly undergo multiple revisions and iterations in the future.

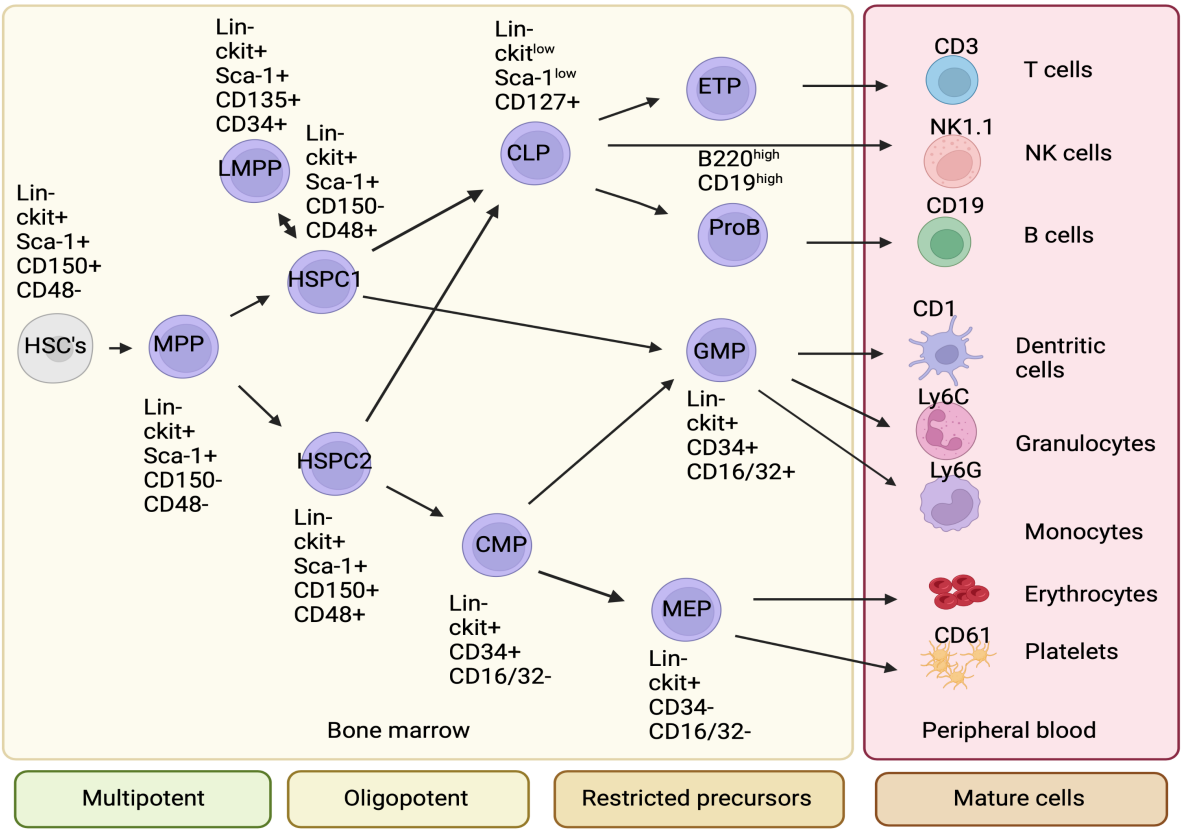

Figure 1.3 Oguro et al. model of murine haematopoietic hierarchy.

As HSCs differentiate into progenitors, they lose their self-renewal potential and form more specialised haematopoietic cell progeny. Cells can then be classified according to surface phenotype. HSC: Haematopoietic stem cell; HSPC: Haematopoietic stem and progenitor; MPP: Multi-Potent Progenitor; LMPP: lymphoid-primed multipotent progenitors; CLP: Common Lymphoid progenitor; CMP: Common Myeloid Progenitor; GMP: Granulocyte/Macrophages Progenitor; MEP: Megakaryocyte-Erythroid Progenitor. Adopted from (Oguro et al. 2013)

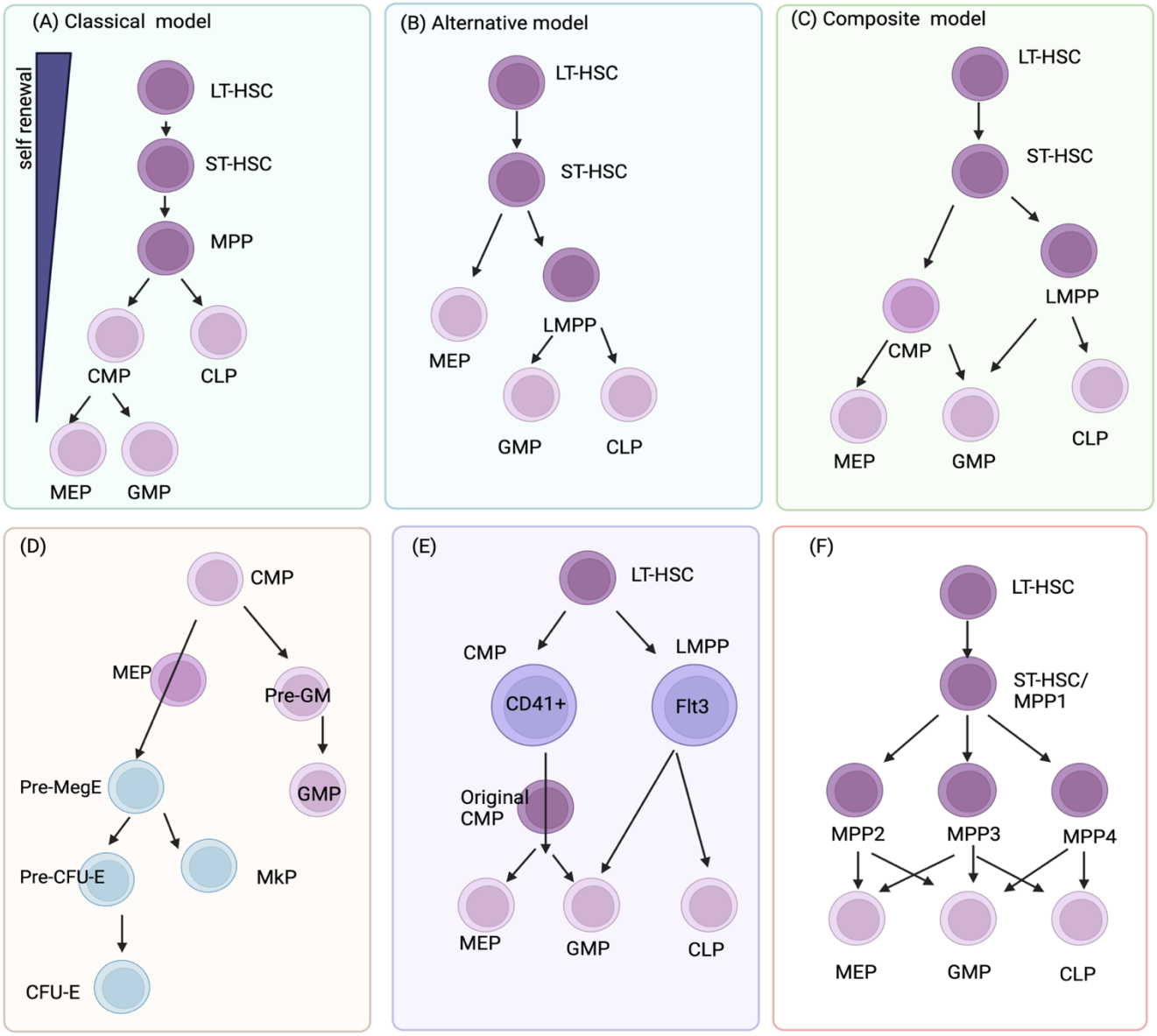

Figure 1.4 Proposed hierarchical structure to describe haematopoietic (A) Classical model. (B) Alternative model. (C) composite paradigm. (D) Differentiated scheme of myeloid/erythroid/megakaryocyte progenitors. (E) revised paradigm based on CD41-CMP and Flt3-LMPP. (F) Pietras et al. model.

1.1.9. Immunophenotypic characterizations and the human haematopoietic hierarchy

Purification methods for human HSCs, such as cell-surface expression analyses and transplantation procedures to measure HSC function, are comparable to those utilized for mouse HSCs, though they are less well characterised overall. Human bone marrow (BM) cells have been engrafted into immunodeficient mouse models (NOD/SCID/IL2Rγ ^{null}; NSG mice) to lessen the xenogeneic rejection that normally occurs (Notta et al. 2011). Human HSPCs are 0.5-5% of bone marrow and cord blood cells and are concentrated in lin-CD34+CD38-, which is not the case for mouse HSPCs (Larochelle et al. 1996; Notta et al. 2011). Differentiation from HSCs (Lin-CD34+ CD38- CD45RA- CD90+ CD49f+) results in multipotent progenitors with restricted self-renewal (MPPs; Lin- CD34+ CD38- CD45RA- CD90-CD49f-) that proceed to generate CMPs (Lin- CD34+ CD38+CD45RA- CD135+ CD10-CD7-) and multi-lymphoid progenitors, (MLPs; Lin-CD34+CD38-CD45RA+CD90CD135+CD10+ CD7-) (Manz et al. 2002; Doulatov et al. 2010; Notta et al. 2011). Later, MLPs generate macrophage precursors and CLPs (Lin-CD34+ CD38+ CD45RA+ CD10+), whereas CMPs divide into GMPs (Lin-CD34+ CD38+ CD45RA+ CD135+ CD10- CD7-) and MEPs (Lin-CD34+CD38+CD135- CD10- CD7-) (Galy et al. 1995; Manz et al. 2002). Recently, a two-tier model has been proposed to represent human blood cell commitment, which challenges earlier hierarchical models that fail to account for oligopotent progenitors (Notta et al. 2016). The multipotent HSCs/MPPs dwell at the top of this hierarchy, generating the subsequent unipotent progenitors that give rise to all the different types of adult blood cells. Recently, single cell RNA signature analysis of around 200,000 BM cells allowed the identification of 26 different cell groups in healthy individuals, allowing for the creation of a comprehensive atlas of these populations for haematopoietic reference (Qin et al. 2021).

1.2 Haematological malignancies

Haematological malignancies are a group of diseases that are characterised by the accumulation of malignant blood cells in haematopoietic organs or the lymphatic system(Khoury et al. 2022). These malignant cells result in symptoms anaemia and

neutropenia as a result of malignant cells infiltration into haematopoietic organs suppressing normal haematopoietic production (Hoffbrand and Moss 2011). Leukaemias are the most studied example of haematological malignancy, and they are classified into either acute or chronic according to the aggressiveness of their disease. Each can also subdivided into myeloid or lymphoid according to cell of origin (Reta et al. 2010). Leukaemia is characterised by accumulated genetic alteration in HSPC clones which can lead to changes in proliferation rate, decreased apoptosis or differentiation arrest (Zjablovskaja and Florian 2019).

1.2.1 Acute myeloid leukaemia

Acute myeloid leukaemia is a clonal disease characterised by differentiation arrest of myeloid cells at various stages and uncontrolled division which causes malignant cell accumulation (Ferrara and Schiffer 2013). AML incidences increase with ageing; 8.8 cases /100,000 are reported in general population in comparison to 17.9/100,000 in 65 and older aged population (Estey and Dohner 2006; Khaled et al. 2016). Several attempts have been made to understand, characterise, and classify such a heterogeneous disease into subgroups to help in diagnosis, treatment and follow up (Bawazir et al. 2019). Scientists and clinicians have sub-grouped AML according to differences of phenotype, cell morphology, cytogenetic translocation and cellular cytochemical features (Konoplev and Bueso-Ramos 2006). The French American-British FAB system to classify AML based on available technologies at that time, morphology and cytochemistry has also been proposed (Bain and Estcourt 2013). Nevertheless, pathologist nowadays do not use this classification. A recent WHO 2016 classification adapted FAB classification and further added molecular modification, genetic mutation and recurrent genetic abnormalities for more accurate diagnosis (Kansal 2016). Upon diagnosis prognosis prediction is very important to tailor patient treatments the strongest disease-specific risk factors are chromosomal abnormalities, whereas age is the most important patient-specific risk factor (Mosquera Orgueira et al. 2021). Patients with cytogenetically normal AML might have their prognosis defined by the mutational status of the genes NPM1, FLT3, and CEBPA (Liersch et al. 2014).

However, the WHO categorization leaves a significant portion of AML in ill-defined and hazy subgroups. According to WHO classifications, patients of AML coupled with post-chemotherapy and Myelodysplastic syndrome (MDS) are known to have poor prognosis and be resistant to treatment (Long et al. 2022). Genetic profiling oof 1540 patients which included cytogenetic analyses and 111 gene sequencing identifies distinctive molecular groupings that represent different AML evolution pathways with a total of 5234 driver mutation involving 76 gene (Papaemmanuil et al. 2016). New WHO classification relied mainly on biologic features such as gene fusions e.g. BCR::ABL1 , rearrangements such as t(9;22)(q34;q11) , and mutations e.g. NUP98 (Khoury et al. 2022). Lagunas-Rangel et. al. 2017 classified AML mutations into: class I mutation with proliferative and survival advantages (FLT3, KIT, RAS, PNPN11, JAK2, CBL), class II mutations with alteration of cellular differentiation (PML-RARA, RUNX!-RUNX1T1, CBFB-MYH11,MLL,CEBPA, NPM1) and without classification or with epigenetic modification (DNMT3a,TET2,IDH1,IDH2,ASXL1,WT1) (Lagunas-Rangel et al. 2017).

1.2.2 Leukaemia stem cells

It has been hypothesised that malignant transformation happens in HSPCs because of the accumulation of recurrent genetic mutations in key regulatory genes, like transcription factors, where they gain the ability of unlimited self-renewal with differentiation block. Moreover, microenvironmental influences can also play a role in epigenetic alteration (Lane et al. 2009). Thus, deregulation of the mechanisms regulating HSPC fates (i.e., quiescence, apoptosis, self-renewal and differentiation) can lead to the development of a mutated HSPC pool that could lead to leukaemia. For example, HSCs are quiescent and have a lower protein synthesis rate(van Velthoven and Rando 2019). Under stress conditions, HSCs increase protein synthesis which could exceed quality control, leading to accumulation of unfolded or misfolded proteins(Walter and Ron 2011). This in turn will stress the endoplasmic reticulum (ER) in-order to compensate for the unfolded protein response UPR. This is very crucial for HSCs to maintain the haematopoietic system and when UPR in ER is over stressed haematological malignancies occurs (Sigurdsson and Miharada 2018). Moreover, repeated cell divisions induced by chronic stress along with ageing leads to accumulation of DNA damage which affect HSCs function (Nijnik et al. 2007). There

is evidence that apoptosis plays a role in controlling HSC integrity, since the number of HSCs increases when the oncogene bcl-2 is overexpressed to inhibit apoptosis (Zhou et al. 2019). When these signalling pathways are aberrantly activated, tumorigenesis occurs, indicating that HSPCs are a prime target for altering mutations in cancer (Sever and Brugge 2015).

AML is driven by a subset of leukemic cells derived from HSPC compartments termed leukemic stem cells or leukemic initiating cells (LSCs) (Jordan 2007). It is generally acknowledged that these cells are resistant to eradication, they eventually cause relapse and, importantly, they need to be therapeutically targeted to effect cure (Long et al. 2022). Inducing growth arrest, apoptosis and/or differentiation of LSCs are attractive targets for therapy, as they would eliminate the origin source of leukaemic cell growth and accumulation. It is thus crucial to examine LSC in AML in prognosis, monitoring, and drug screening processes. Therapeutically, antigens selectively expressed by LSCs (e.g., CD123, CLL-1) might be targets for very successful therapies (Testa et al. 2019). It has also been shown that AML cells and LSCs may be eradicated by targeting the mitochondrial protein and biogenesis of LSCs (Skrtic et al. 2011).

1.3 Hypercholesteremia

As alluded to earlier, intrinsic, or extrinsic factors can trigger HSC activation and these include, but are not limited to, chronic bacterial infection, stress, injury and/or hypercholesterolemia (Baldridge et al. 2010; Heidt et al. 2014; Dutta et al. 2015). Hypercholesteremia is a common disorder characterised by imbalance in the two major cholesterol transport blood lipoproteins: low-density lipoprotein (LDL) and high-density lipoprotein (HDL). Constantly elevated LDL with a reduction in HDL is the main risk factor in atherosclerosis (Ma and Feng 2016). The WHO has reported double the percentage of hypercholesteremia in high income countries in comparison to low-income countries (Organization 2011). They correlated death from coronary heart disease with Western-type, calorically rich, high cholesterol consumption (Christ et al. 2018). Cholesterol is a sterol that is essential to the plasma membrane of cells by creating “rafts” that facilitate molecule signalling, insulation, control cell/environment

fluidity (Pike 2009). It is also used by steroid hormones, bile acid (Schade et al. 2020) and myelin sheath assembly (Saher et al. 2005) and has further been implicated in cell cycle induction (Singh et al. 2013) and mitochondrial functions (Martin et al. 2014).

Cholesterol is synthesised in the endoplasmic reticulum, starting from acetate in a series of consecutive enzymic reactions. The most complicated and time-consuming process is the reaction catalysed by 3-hydroxy-3-methylgluttaryle-Co-A to mevalonate (Friesen and Rodwell 2004). Synthesised cholesterol is transported to the liver or peripheral tissues as water soluble lipoprotein particles. There are numerous types of lipoproteins, such as very low-density lipoprotein (VLDL), intermediate density lipoprotein (IDL), low-density lipoprotein (LDL) and high-density lipoprotein (HDL). The Dominant lipoprotein is LDL, which carries cholesterol from the liver to the intercellular store in the peripheral tissue. In contrast to HDL, which transports cholesterol from the peripheral tissues toward the liver, to be ultimately converted to bile salt and excreted (McLaren et al. 2011). One LDL particle contains >1600 cholesterol molecules with apolipoprotein (apoB100) along with phospholipids (Goldstein and Brown 2009). LDL is transported into the cells through LDL receptors (LDLr) by receptor-mediated endocytosis, where it is degraded into amino acids and cholesterol. LDL has a physiological role in cell cycle induction(Fernandez et al. 2004), protein glycosylation (Loaeza-Reyes et al. 2021) and mitochondrial metabolism (Martin et al. 2014). However, the main physiologic aim of LDLr is to keep the LDL concentration in the blood low to avoid a build-up of vascular fatty streaks (Goldstein and Brown 2009).

1.4 LDL Receptor gene, Structure, Function and Metabolism

LDLr function was discovered when studying the consequence of an LDL receptor mutation that manifested as profound familial hypercholesteremia FH homozygotes and less severe familial hypercholesteremia heterozygotes (Nordestgaard et al. 2013). FH heterozygotes individuals have a two-fold increase in Plasma LDL and are prone to heart attacks in their early thirties. These mutations affect 1/500 individuals (Varret et al. 2008). FH homozygotes, which accounts for about one in 1 million often have heart attacks in childhood (if not treated) (Goldstein and Brown 2015).

The LDLr gene is responsible for manufacturing LDL receptors in different cells. In humans, it is located on 19p13.2, which is the short (p) arm of chromosome 19 at position 13.2. It is composed of 18 exons, separated by 17 introns (Gent and Braakman 2004) (Figure 1.5).

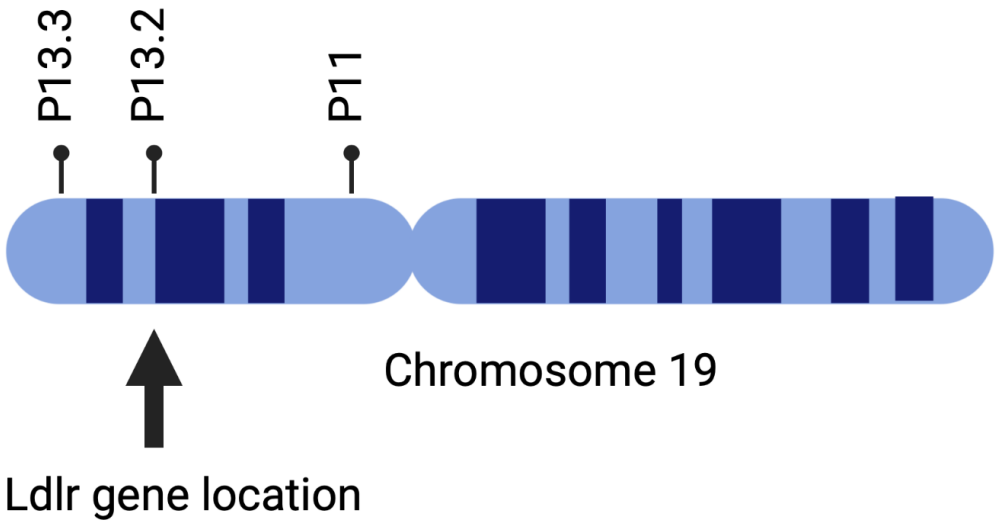

Figure 1.5 LDLr gene location in human.
Location of the LDLR gene, the short (p) arm of chromosome 19 at position 13.2.

The LDL receptor is a multi-domain protein. The first domain consists of the NH2 terminal 292 amino acids, composed of 40 amino acids repeated with minor variants. This domain is negatively charged at multiple sites in order to bind to a positively charged a-helix in apoE molecules. The second domain consists of approximately 400 amino acids. The third domain lies immediately external to the membrane-bridging domain and consists of 58 amino acids that comprises 18 serine or threonine residues. This region also contains the clustered O-linked sugar chains. The fourth domain involves 22 hydrophobic amino acids that reside along the plasma membrane. The fifth domain is the cytoplasmic tail, which contains COOH-terminal fragments of 50 amino acids projecting in the cytoplasm (Esser et al. 1988; Gent and Braakman 2004; Huang et al. 2010). This domain plays an important role in clustering coated pits (explained in detail later) (Figure 1.6).

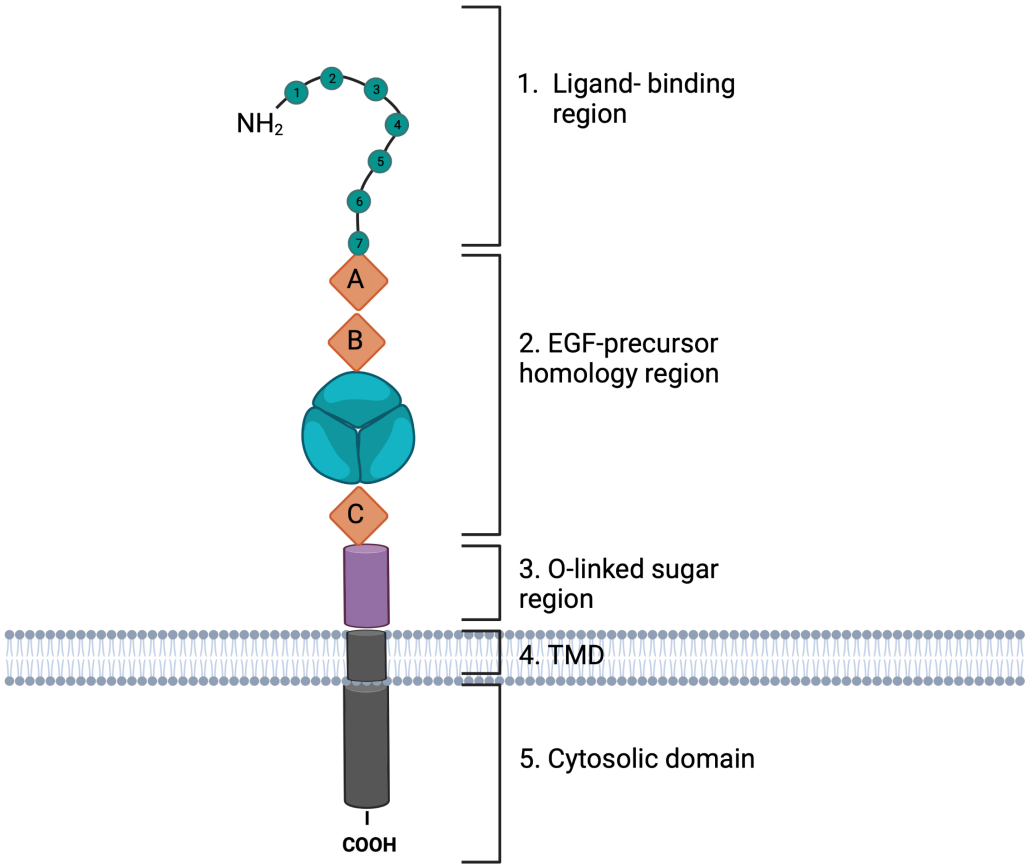

Figure 1.6 Low density lipoprotein receptor consisting of five domains.

First: Ligand binding region consists of seven cysteine- rich repeats (R1 – R7) with cysteine residues. Second: Ectodomain contains amino acid stretches with homology to the epidermal growth factor or EGF-precursor protein. The third region in the LDLR ectodomain is enriched in serine and threonine residues that function as receptor sites for O-linked sugars. Fourth: Transmembrane domain TMD, a hydrophobic domain of 24 amino acids anchors the LDLR in cellular lipid bilayer. Fifth: Cytosolic domain which regulate endocytosis and intracellular transport of the LDLR (Gent and Braakman 2004).

As alluded to above, the major function of the LDLr is to control plasma cholesterol levels, firstly limiting LDL production by the removal of the precursor and, secondly, enhancing LDL degradation by facilitating cellular uptake of circulating LDL (Goldstein and Brown 1985). LDLr regulation is facilitated by sterol regulatory element binding proteins (SREBPs). SREBPs are identified in inactive forms in the endoplasmic reticulum (ER). When cellular cholesterol quantity rises after cholesterol uptake by the LDL receptor, increased ER sterol levels triggers cholesterol to associate to the SREBP cleavage activating protein (SCAP), a protein that stimulate the migration of SREBPs from the ER to Golgi. In the Golgi, SREBPs undergo proteolytic transformation to active forms that transport to the nucleus and ultimately stimulate the transcription of genes engaged in cholesterol synthesis. However, when intracellular cholesterol levels are high, the SCAP/SREBP complex does not move to the Golgi, SREBPs are not processed, and cholesterol synthesis discontinues (Yang et al. 2020a).

Collectively, LDL is carried into cells using LDLr by receptor-mediated endocytosis. Once LDL-derived cholesterol enters the cell, it acts on several processes to stabilize cholesterol content. This is done by suppressing the 3-hydroxy-3-methyl-glutaryl-coenzyme A reductase (HMG-CoA reductase gene) along with its enzyme protein, downregulating the LDL receptor gene by inhibiting sterol regulated membrane-bound transcription factors (the SREBP pathway) and also activating the cholesterol storage enzyme (acyl CoA: cholesterol acyl-transferase ACAT) (Brown and Goldstein 1997). Nevertheless, modified LDL are ingested in specialised cells by a different receptors , mainly scavenger receptors, as SR-A, SR-BI, and CD36 (Poznyak et al. 2020) (Figure 1.7).

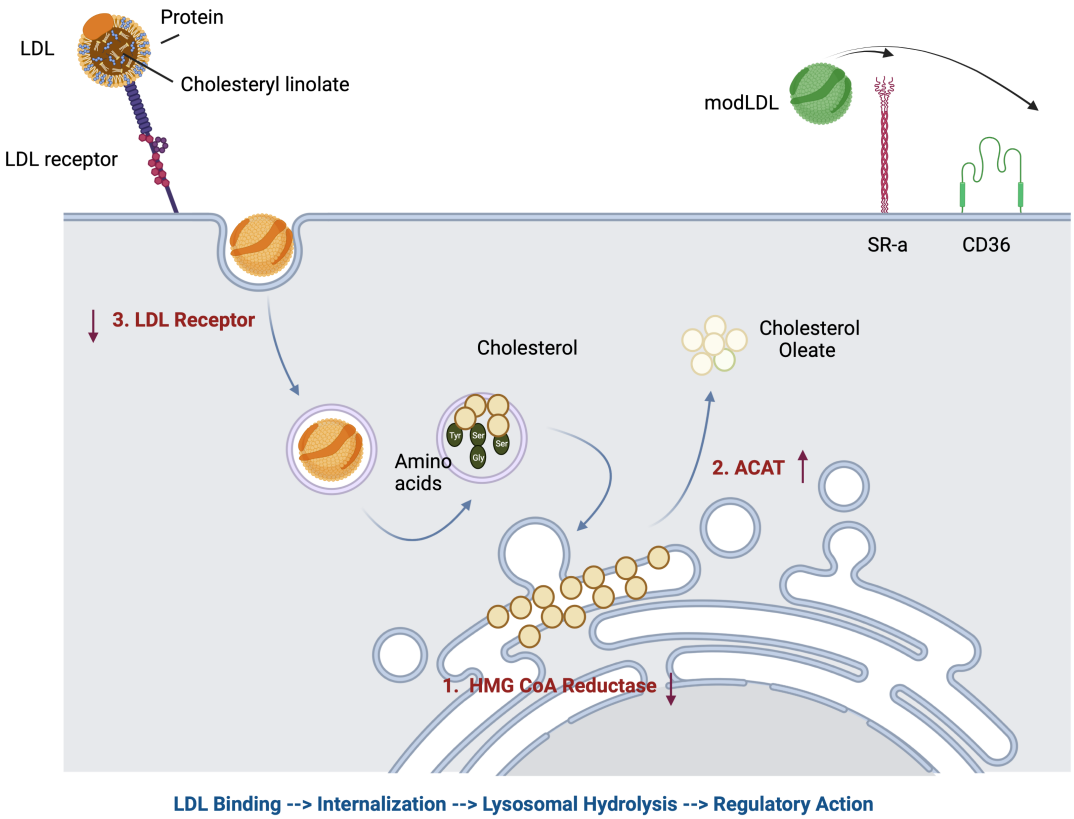

Figure 1.7 Sequential steps in the LDL receptor pathway of mammalian cells. cholesterol-carrying LDL particles bind to transmembrane LDL receptors and are internalized into cells via receptor-mediated endocytosis. The endocytosed LDL particles are delivered to lysosomes where the LDL cholesterol is hydrolysed into cholesterol and amino acids. Released cholesterol is transferred from the partical membrane to the endoplasmic reticulum, the site at which cellular cholesterol content is tightly regulated by HMG-CoA reductase gene. Then Acyl-CoA:cholesterol acyltransferase ACAT catalyzes the formation of cholesteryl esters from cholesterol and long-chain fatty-acyl-coenzyme A. when cholesterol content is enough LDLR is downregulated.

Post LDL delivery, the LDL receptors detach from their ligands by lowering the pH at the endosomes and move to the cell surface again. The LDL receptors, along with their metabolites, are expressed primarily in the liver (70% of total LDL uptake)(Bilheimer et al. 1984). The remaining 30% of total LDL uptake includes all bone marrow derived cells (leukocytes), involving macrophages in all tissue organs (Fazio et al. 1997).

As mentioned above, LDL receptor production is regulated by the SREBP pathway and is crucial for the action of statin drugs in lowering LDL levels. This drug is taken by individuals with hereditary or diet-induced hypercholesteremia. When statins are consumed, they are digested in the liver where they inhibit HMG-CoA reductase pathways to reduce cholesterol synthesis. Simultaneously, low liver cholesterol activates SREBP pathways, thus increasing the LDL receptors in liver cells. This, in turn, removes LDL from the blood and releases cholesterol to be used in different metabolic routes. Likewise, activated SREBPs stimulate HMG-CoA reductase production, but not cholesterol. The net effect of the statin drug is a low LDL level with a balanced level of cholesterol (Schonewille et al. 2016).

1.5 Atherosclerosis

LDL increase is dependent of several genetic component such as familial hypercholesteremia and environmental factors such as high fat diet and lack of exercise and aging (Glass and Witztum 2001). These factors will lead to an increase in plasma LDL, predisposing it for oxidation by oxygen radicals (Steinberg 2002). The term "oxidative stress" refers to a state in which the body's natural anti-oxidant defences are overwhelmed by the body's increased production of reactive oxygen species (ROS) (Peluso et al. 2012). The oxidation of LDL-cholesterol by reactive oxygen species (ROS) is considered to have a larger role than native-LDL in atherogenesis, in addition to its roles in inflammatory responses, apoptosis, cell proliferation, and alterations in vascular tone (Zhang and Gutterman 2007). In the context of atherosclerosis, endothelium, smooth muscle, and adventitia all contribute to ROS production in the vascular wall. ROS sources include xanthine oxidase, cyclooxygenase, lipoxygenase, cytochrome P450, uncoupled nitric oxide synthases,

and NAD(P)H oxidase depending on cell type and activation (Lakshmi et al. 2009). Oxidised LDL will not only be picked up by escaped monocytes, but also by circulating macrophages, which are the main component of atheroma in atherosclerosis (Steinberg 2002).

Atherosclerosis is a progressive complicated process where both lipids (e.g. apolipoprotein-B) and inflammatory cells are retained in arterial walls to produce atherosclerotic plaque (Libby 2012). Lipoprotein first triggers an innate immune response, mainly monocytes and macrophages, and then the adaptive system is dominated by T cells. At arterial branching points, sheer force, along with some genetic elements such as arterial thickening and metabolic factors such as increased ROS, activate and increase the permeability of the arterial endothelial cells (Zhou et al. 2014). While that happens, LDL particles accumulate under the subendothelial space and interact with extracellular matrix (ECM) compounds by apoB – LDL - proteoglycans interaction. When oxygen radicals perform chemical modification and produce oxidized LDL, this leads to adhesion marker upregulation, increase of ECM proteins and secretions of chemokines, such as monocyte chemotactic protein-1 (MCP-1), inflammatory cytokines and growth factors to recruit circulating monocytes and T cells to the site of activation (Buckley and Ramji 2015).

Recruited monocytes roll and adhere to activated endothelium via integrin β2 (CD18) on monocytes and endothelial adhesion markers P-selectins and E-selectins. Activated endothelial cells, in turn, express vascular cell-adhesion molecule-1 (VCAM-1) and intercellular adhesion molecule-1 (ICAM-1) to initiate binding with integrins, very late antigen-4 and lymphocyte function-associated antigen-1 in order to enhance adhesion and facilitate monocyte migration through the endothelium (Libby 2002). Monocyte migration is promoted further by additional secretion of chemokines from the following cells: 1. Endothelial cells such as MCP-1, macrophages colony stimulating factor (MCSF), Interleukin-8 (IL-8) and tumour necrosis factor - α (TNF- α). 2. Platelets endothelial cell adhesion molecule-1 and junction adhesion molecule-A. Once the monocytes reach the subendothelial, they ingest LDL and, moreover, differentiate into macrophages that pick up oxidised LDL and turn into foam cells (Li and Glass 2002). Macrophages foam cells are characterised by massive accumulation of oxidative LDL recognised by scavenger receptors (Linton and Fazio 2001).

Nowadays lipid–laden foam cells is considered a hallmark of atheroma (Libby 2012). Oxidised LDL will stimulate an inflammatory response via toll-like receptor (TLR-4) and enhance lipoprotein accumulation in macrophages (Bekkering et al. 2014). Then chemokines released by activated endothelial cells and smooth muscle cells bound to G protein-coupled receptors (present on leukocytes) induce immune cell recruitment. These cells include neutrophils, T cells, B cells, mast cells and additional monocytes (Libby 2002). Combined inflammatory cells (primarily activated macrophages and dendritic cells) will trigger the adaptive immune system by employing effector T cells and B cells. This mechanism goes together with vascular smooth muscle cells (VSMCs) activation reaction, which causes ongoing vascular injury by accumulating myofibroblasts in the intima (Tabas and Lichtman 2017). Inflammatory cells and/or activated vascular cells also secrete inflammatory chemokines such as monocyte chemoattractant protein-1 (MCP-1) and macrophages inflammatory protein (MIP-2α), cytokines such as tumour necrosis factor α (TNF- α), interferon γ (IFN- γ) (Moss and Ramji 2016) , and growth factors such as granulocyte macrophage colony-stimulating factor (GM-CSF) and monocyte CSF (M-CSF) (Gencer et al. 2021), which contribute to the persistence the inflammation processes (Figure 1.8)

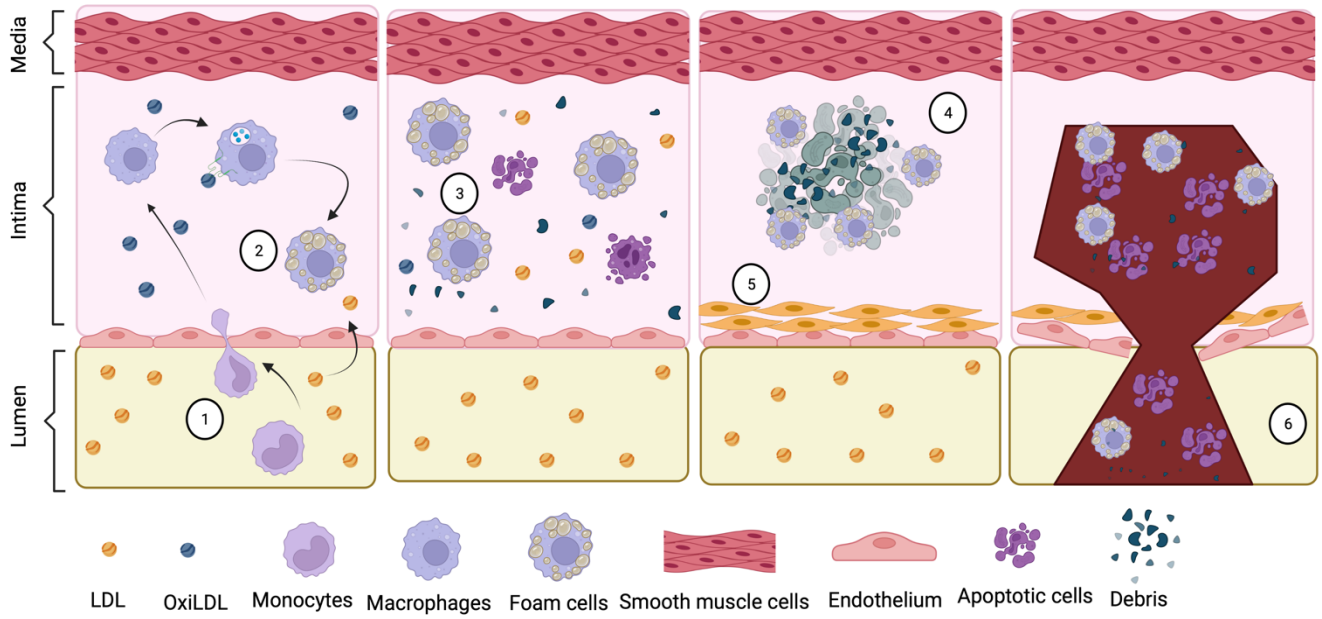

Figure 1.8 An outline of the progression of the atherosclerosis disease.

1. The endothelium is activated, and an inflammatory response is initiated when circulating LDL becomes lodged in the artery intima. There are several adhesion

molecules and chemokines that are expressed by activated endothelial cells, and they help to draw circulating monocytes to the location. Transmigration of monocytes into the intima, where they undergo differentiation into macrophages, occurs via adhesion and rolling. **2.** LDL uptake by LDL receptor is highly regulated (explained earlier). However, oxidative LDL via scavenger receptors expressed by macrophages is an autonomous unregulated process. When combined with disturbed metabolism, it results in the formation of Foam cells – the hallmark of atherosclerosis. **3.** In addition to decreased efferocytosis, the build-up of apoptotic cells and necrotic debris is a result of cholesterol-induced cytotoxicity, which causes an increase in these types of cell death. **4.** As the atherosclerotic plaque progresses, a lipid-rich necrotic core is formed as a result of secondary necrosis and a protracted inflammatory response, as well as the build-up of apoptotic cells and debris, pro-atherogenic lipoproteins, and lipoprotein remnants. **5.** To stabilize the plaque, VSMCs go from the media to the intima, where they help remodel the extracellular matrix (ECM) and form a protective fibrous cap between the necrotic core and the lumen. **6.** Protease activity destroys the ECM, undermining the integrity of the protective cap, in advanced illness and under an elevated inflammatory environment. Clinical issues arise from plaque susceptibility and rupture, which causes plaque contents to leak into the lumen and cause thrombosis.

1.6 Atherosclerosis and Altered Haematopoiesis

Since innate and adaptive immune cells involved in atherosclerosis are manufactured in the bone marrow through haematopoiesis, continuous recruitment of these immune cell types in atherosclerosis will cause an increase in HSC and progenitor production in order to recover the demand for haematopoietic derived cells. As evidence of this, the main risk factor for atherosclerosis is persistent high LDL in peripheral blood and researchers have observed increased LDL with amplified HSPCs proliferation with myeloid lineage skewing (van der Valk et al. 2017).

Researchers have observed an abundance of monocytes in pre-atherosclerotic subjects, mainly CD14++ in humans and LY6C^{hi} in mice. Part of the monocyte population, immunophenotypically isolated as LY6C^{hi} in mice, differentiate into macrophages, which, in turn, causes an inflammatory phenotypes (Yang et al. 2014). Constant recruitment of monocytes from the bone marrow in atherosclerosis lead to HSCs seeding in the spleen, which results in elevated extramedullary haematopoiesis (Fernandez-Garcia et al. 2020). Feng et al, 2012 elegantly showed that LDL causes the proliferation and mobilization of HSPC in in *Ldlr* knockout mice (*Ldlr*$^{-/-}$) mice, which have impaired LDL clearance and, thus, a high plasma level of LDL cholesterol (Ishibashi et al. 1994), correlating with elevated monocytes and granulocytes in *Ldlr*$^{-/-}$ mice. In this study the frequency of HSPCs in peripheral blood and bone marrow of both *Ldlr*$^{-/-}$ and wild type mice consuming both normal and high fat diets was measured and HSPC enriched Lin-Sca-1+cKit+ (LSK) cells were increased in *Ldlr*$^{-/-}$ and wild type mice consuming a high fat diet (Feng et al. 2012). Mechanistically, hypercholesteremia promotes bone marrow HSPC mobilization to peripheral blood by disturbing the SDF-1: CXCR4 axis (Gomes et al. 2010; Murphy and Tall 2016). High cholesterol amplifies C-X-C motif chemokine ligand 12/ stromal cell-derived factor 1 (CXCL12/SDF1) in the plasma, a chemokine that is antagonist to HSCs chemokine receptor 4 (CXCR4) which attract HSCs form BM to peripheral blood. CXC12/SDF1 is stimulated by GM-CSF, IL-17 and IL-23 (Oguro 2019). Feng et al. also showed that LDL partially induced extracellular signal regulated kinase (ERK) phosphorylation in LSK cells and causes at least partial differentiation into granulocytes. Additionally, hypercholesteremia affects HSPCs cellular membrane and causes upregulation in IL-3 and granulocyte-

monocyte colony stimulating factors (GM-CSF) receptors (Yvan-Charvet et al. 2010a). Thus, increases in frequency and mobility in LSK populations in hypercholesteraemic mice resemble pre-bone marrow transplantation, where growth factors are given to enhance HSPC production from the BM in the donor but more likely reflect pre-malignant clonal states (Heyde et al. 2021).

1.7 Clonal haematopoiesis of indeterminate potential CHIP

HSCs in the aged population show reduced regenerative potential along with a decline in self-renewal ability, impaired engraftment, and myeloid biased differentiation. Hypercholesteremia and cardiovascular disease and AML are most prevalent in the ageing population (beyond age 50) (Bernitz et al. 2016; Khatri et al. 2016). In ageing, HSPCs tend to naturally acquire genetic/epigenetic leukaemia causing mutations in a phenomena known as clonal haematopoiesis of indeterminate potential CHIP (Jaiswal and Ebert 2019). CHIP is characterised by an increased HSC clone caused by a somatic mutation without the presence of overt haematologic malignancy, dysplasia, or cytopenia. With time, these HSC clones compete with normal / healthy HSCs and undergo clonal expansion over normal white blood cells (WBCs) with the total number of WBCs remaining constant in most cases where leukaemia doesn't develop. However, CHIP is associated with a 0.5–1.0% risk of leukaemia annually and it increases cardiovascular disease risk caused by atherosclerosis by two-fold (Jaiswal et al. 2017). Prevalent mutations associated in CHIP include epigenetic regulators DNMT3A, TET2, ASXL1, DNA damage repair genes PPM1D and TP53, the regulatory tyrosine kinase JAK2, or mRNA spliceosome components SF3B1 and SRSF2 which are found in 80% of CHIP patients (Marnell et al. 2021) (Figure 1.9).

CHIP mutations will affect the HSCs from the apex haematopoietic hierarchy and these mutation bearing HSCs continue to differentiate and lead to aberrant activation of pathways in terminally differentiated cells, such as macrophage which are the main player in hypercholesteremia-associated inflammation (Papa et al. 2020). Reports showed that these transformed innate immune cells in CHIP have an impact on cardiovascular disease by increasing inflammation. For instance, in a Competitive BM transplant with *Tet2*$^{-/-}$ cells in irradiated *Ldlr*$^{-/-}$ mice experiment done by (Jaiswal et al.

2017) Tet2-deficient macrophages exhibit elevated NLRP3 inflammasome-mediated IL-1 production in response to a high-fat diet-induced atherosclerosis. Also, irradiated *Ldlr*$^{-/-}$ mice transplanted with Jak2 -expressing BM cells and given HFD showed increases in early and advanced atherosclerosis, manifested by neutrophil infiltration and plaque instability. Moreover, Jak2 macrophages show increased secretions of pro-inflammatory mediators (Wang et al. 2018a). Together, the identification of CHIP links haematological disease with cardiovascular disease.

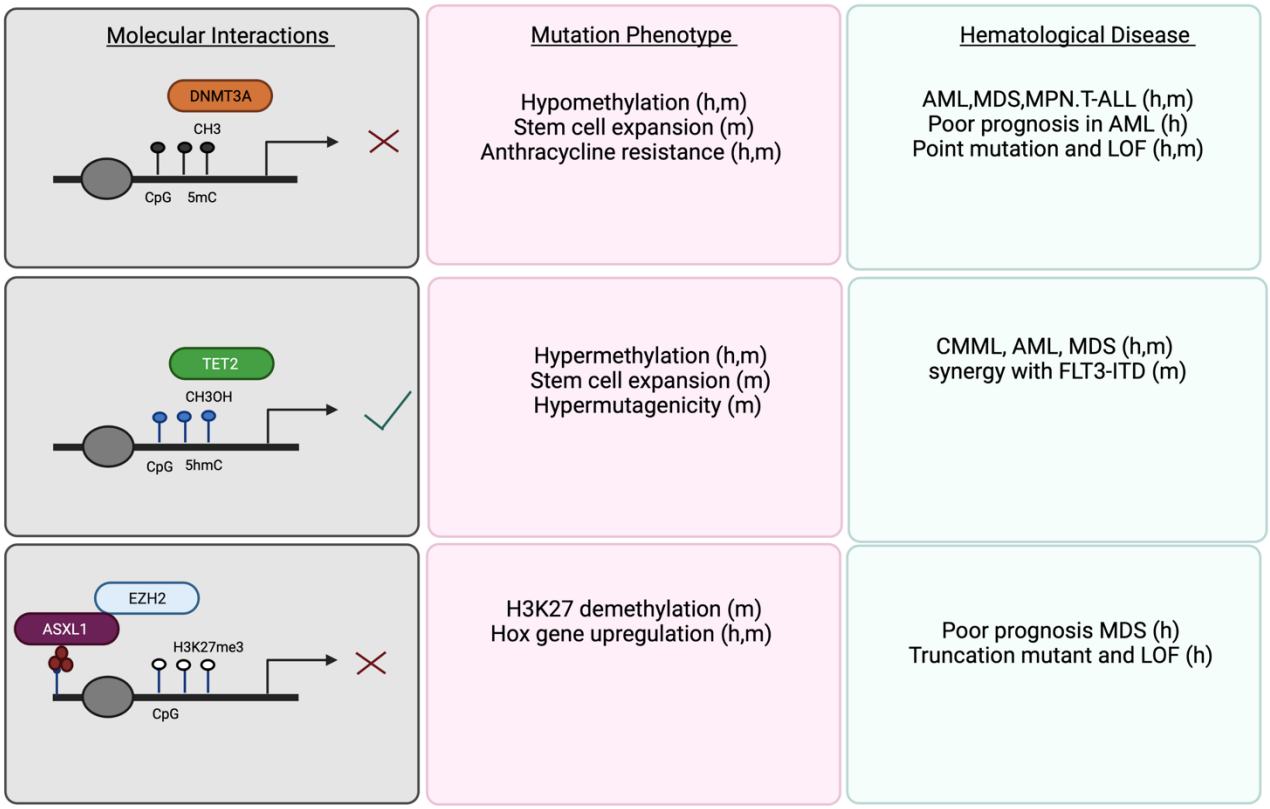

Figure 1.9 Epigenetic Regulators of Clonal Haematopoiesis.

Diagram showing how DNMT3A catalyzes CpG methylation (black circles), TET2 produces 5hmC (blue circles), and ASXL1 produces H3K27 trimethylation by enlisting the help of PRC2 complex member EZH2. The links with haematological disorders and functional decline are given to the right side. The letters "m" and "h" indicate conclusions that are supported by mouse and human evidence (Bowman et al. 2018).

1.8 Inflammation driven by hypercholesteremia and atherosclerosis and the association with acute myeloid leukaemia

When pre-malignant cells arise due to aging/recurrent hits, they are usually removed by the surveying immune system in a process termed immunosurveillance. However, an impaired immune systems caused by inflammation (associated with hypercholesteremia and atherosclerosis for example) will allow pre-malignant cells to escape and expand (Mantovani and Sica 2010). Moreover, inflammation indirectly activates different classes of oncogenes and promotes cancer development by awakening or suppressing key components of the immune system including macrophages, immature monocyte, regulatory B cells and regulatory T cells, as well as checkpoints that control T cell differentiation (Grivennikov et al. 2010). Once the balance between positive immunity and the regulatory mechanisms controlling it are disturbed by inflammation, neoplastic cells could escape immunosurveillance (Naik et al. 2018). This has led to the rise of the elimination, equilibrium and escape theory of cancer immunosurveillance (Dunn et al. 2004).

Specifically, the relationship between the hypercholesteremia and development of haematopoietic malignancy could be multifactorial and includes several stressors such as age and hypercholesteremia associated inflammation. The link between hypercholesteremia and acute myeloid leukaemia was established when Buchwald et al. 1992 proposed that LDL can serves as a protective agent from cellular damage post chemotherapy and/or radiation when treating AML patients (Buchwald 1992). More direct evidence for a link between hypercholesteremia and acute myeloid leukaemia was attained when another group observed that leukemic cells isolated from AML patients contain high LDL content when compared to normal cells and AML patients exhibit hypocholesteraemia (Bhuiyan et al. 2017). Furthermore, it was shown that AML cells secrete factors to encourage cellular LDL uptake. Finally, hypercholesteremia treatment with statins, which lower LDL, yield encouraging results in AML treatment/prognosis by inducing apoptosis (Burke and Kukoly 2008). Statin therapy has been shown to reduce untoward inflammatory activity, including changes in C-reactive protein (CRP), serum amyloid A, tumour necrosis factor alpha (TNF-α),

interleukin-6 and brain natriuretic peptide levels (Hindler et al. 2006). Moreover, researchers made efforts to target LSCs in AML. By utilising high-throughput screening systems that mirror the complicated physiology of LSCs and supportive associations with the bone marrow niche, they found that in an *in vivo* bone marrow transplantation model and *in vitro* testing, lovastatin demonstrated anti-LSC efficacy which involved the inhibition of HMG-CoA reductase (Hartwell et al. 2013).

1.9 Project aims and objectives

In order to study hypocholesteraemia and atherosclerosis-related inflammation and its impact on haematopoiesis and leukaemia, animal models that resemble human anatomy and pathophysiology and generate results that can extrapolate to human medicine are needed. The mouse model used in this project is *Ldlr*$^{-/-}$ shares the topography of human atherosclerotic disease. L*dlr*$^{-/-}$ mice have moderate steady-state cholesterol levels of 200-300 mg/dl on normal chow diet and > 1500- 2000 mg/dl on a high fat diet (Getz and Reardon 2006). Once a mouse reaches 8 weeks the expectant level of lipid profile is as follows: moderately high VLDL, very high LDL and normal HDL levels. This model resembles the human lipid profile (LDL) (Emini Veseli et al. 2017). Moreover, preliminary evidence suggests disruption of *Ldlr* appears to have minimal adverse effect on inflammation in steady state, which will permit a clear understanding of inflammation generated by elevated LDL (Emini Veseli et al. 2017).

The overall aim of this thesis is to provide insights into the impact of severe hypercholesteremia and atherosclerosis on haematopoiesis and the development of leukaemia using a germline *Ldlr* knock-out murine model in the context of a high-fat diet (HFD) and normal diet (ND) with the following specific aims:

1. To investigate the requirement for *Ldlr* in steady-state haematopoiesis using *Ldlr*$^{-/-}$ mice fed a ND for 8-12 weeks.

2. To evaluate the impact of severe hypercholesteremia and atherosclerosis on haematopoiesis using *Ldlr*$^{-/-}$ mice ingesting HFD or ND for 12 weeks using sophisticated immunophenotypic panels to assess haematopoietic potential in the

context of hypercholesteremia and to investigate the molecular programming impacting HSC function.

3. To explore functionally and immunophenotypically the impact of severe hypercholesteremia and atherosclerosis on leukemogenesis using a retroviral mouse model of AML driven by the MLL-AF9 oncogene. And to mimic this in a human setting by using human AML cells bearing the MLL-AF9 oncogene cultured high doses (non-toxic) of atherogenic lipids.

Chapter 2: Material and Methods

2.1 Materials

Table 2.1 and Table 2.2 contains a list of the materials, reagents and antibodies employed in this investigation.

Table 2. 1 Compounds and reagents used in the study.

Material or Reagent	**Supplier**
Agarose	Fisher Scientific, UK
Foetal bovine serum (FBS)	Life technologies, UK
multiplex immunoassays based on electrochemiluminescence absolute quantification of INF-γ, TNF-α, MCP-1, MIP1-α, IL1-β, IL-6, IL-10	Meso Scale Discovery QuickPlex SQ120, USA
Isolate II genomic DNA kit, BIOLINE	Qiagen, UK
mangoMix^{TM}	Bioline
LDL receptor DNA primers sequences	Sigma
High fat diet [21% (w/w) pork lard and 0.15% (w/w) cholesterol]	Special Diets Services, UK
Ambion ^{TM} nuclease -free water	Thermo-scientific, UK
Cryoprotectant tissue freezing reagents (Legras et al.)	Thermo-scientific, UK
Hanks's balanced salt solution (HBSS)	Thermo-scientific, UK
16% Paraformaldehyde (Pfaller et al.)	Thermo-scientific, UK
RPMI 1640 with L-glutamine medium	Thermofisher, UK
Dulbecco's phosphate-buffered saline (DPBS)	Thermofisher, UK
Corning syringe filters polyethersulfone membrane pore size 0.22 µm	Merck

Corning syringe filters polyethersulfone membrane pore size 0.4 µm	Merck
Chemometec, Via1-Cassette	Chemometec
MitoSOX™ Red mitochondrial superoxide indicator	Molecular Probes™
Human low-density lipoprotein	Generon, Kelen Biomedical, UK
Human high oxidized low-density lipoprotein	Generon, Kelen Biomedical, UK
75 cm^2 TC treated flask with filter cap	Greiner

Table 2. 2 Antibodies used in flow cytometry analysis of in vivo and in vitro assays.

Target cell population	Antibody	Conjugate	Conc. And dilution	Supplier
BM HSPCs and committed progenitors $1X10^7$ cells/ml for steady state analysis $2X10^7$ cells/ml for	c-Kit (CD117)	APC	0.2 mg/mL, 1/100	Biolegend
	CD150	PE-Cy7	0.2 mg/mL, 1/100	
	Sca-1	PE, APC-CY7	0.2 mg/mL, 1/25	
	CD48	FITC	0.5 mg/mL, 1/50	
	CD16/32	PEcy7	0.2 mg/mL, 1/25	
	CD127 (IL-7rα)	BV650, PE	0.2 mg/mL, 1/50	
	CD135 (Flt3)	PE	0.2 mg/mL, 1/50	
	FC Block	NA	0.2 mg/mL, 1/25	
	CD34	FITC	0.2 mg/mL, 1/25	eBiosceinces
Lineage positive cells $2X10^5$ cells/ml	MAC-1	Biotin	0.2 mg/mL, 1/50	Biolegend
	Gr-1	Biotin	0.2 mg/mL, 1/50	
	Ter119	Biotin	0.2 mg/mL, 1/50	
	CD3	Biotin	0.2 mg/mL, 1/50	
	CD4	Biotin	0.2 mg/mL, 1/50	

	CD8	Biotin	0.2 mg/mL, 1/50	
Biotin binding molecule	streptavidin	Pacific Blue, PerCP	0.2 mg/mL, 1/100	eBiosceinces
Myeloid cells (non-specific)	Mac-1 (CD11b)	APC	0.2 mg/mL, 1/1000	Biolegend
	Gr-1	PEcy7, FITC	0.2 mg/mL, 1/1000	
Granulocytes	Ly6G	FITC, PerCP	0.2 mg/mL, 1/1000	
Monocyte	Ly6C	PEcy7	0.2 mg/mL, 1/1000	
	CD115	APCCy7	0.2 mg/mL, 1/1000	
Macrophages	F4/80	PE	0.2 mg/mL, 1/1000	
Erythroid markers	CD71	PE	0.2 mg/mL, 1/1000	
	Ter119	APCCy7	0.2 mg/mL, 1/1000	
Megakaryocytes	CD41	FITC	0.2 mg/mL, 1/1000	
T cells, TCR	CD3	FITC, PE, APC	0.2 mg/mL, 1/1000	
T helper	CD4	PEcy7	0.2 mg/mL, 1/1000	
T cytotoxic	CD8	PE, APC cy7	0.2 mg/mL, 1/1000	
NK cells	NK1.1	FITC	0.2 mg/mL, 1/1000	
Activated NK cells	NKP46	PerCP	0.2 mg/mL, 1/1000	

B cells	CD19	APC Cy7	0.2 mg/mL, 1/1000	
Apoptosis marker	Annexin V	PE	0.2 mg/mL, 1/50	
Proliferation marker	KI67	PE	0.2 mg/mL, 1/50	
THP-1 and NOMO-1	Human IL-1β	PerCP	0.2 mg/mL, 1/1000	R&D Systems
	Human LDLR	APC	0.2 mg/mL, 1/1000	
	Human CD11b	APC	0.2 mg/mL, 1/1000	Biolegend
	Human CD13	APCCy7	0.2 mg/mL, 1/1000	
	Human CD33	BV510	0.2 mg/mL, 1/1000	
	Human MPO	FITC	0.2 mg/mL, 1/1000	
	Human HLADR	APCCy7	0.2 mg/mL, 1/1000	
	Human CD47	PECy7	0.2 mg/mL, 1/1000	
	Human CD64	PerCP	0.2 mg/mL, 1/1000	
	Human CD44	BV510	0.2 mg/mL, 1/1000	
	Human CD11c	PEcy7	0.2 mg/mL, 1/1000	

2.2 *In Vivo* Methods

2.2.1 Animals and Feeding

2.2.1.1 Ldlr$^{-/-}$ Mice

C57BL/6 male *Ldlr*$^{-/-}$ mice were obtained from Prof. Dipak Ramji Group (Cardiff University, Cardiff, UK) (Al-Ahmadi et al. 2021). *Ldlr*$^{-/-}$ mice were originally created by Dr. Shun Ishibashi, Dr. Michael Brown and Dr. Joseph Goldstein at Howard Hughes Medical Institute, University of Texas Southwestern Medical Centre, Texas, USA(Ishibashi et al. 1993). The mutation was achieved by gene targeting of the LDL receptor locus in C57BL/6 mice (Ishibashi et al. 1993).

2.2.1.2 Confirmation of Ldlr knockout status using genomic DNA PCR

DNA extraction was carried out in accordance with the manufacturer's instructions (ISOLATE II Genomic DNA Kit, BIOLINE). For at least 2-3 hours at 56°C, ear punch specimens were treated in Proteinase K and lysis buffer (GL). Following that, the samples were treated for 10 minutes at 70°C in lysis buffer (G3). The samples were then placed into the ISOLATE II Genomic DNA spin column with ethanol (97%) to enhance the DNA binding. Following centrifugation and washing with wash buffers (GW1) and (GW2), the samples were eluted in 70°C warmed elusion buffer. Then, 12.5μl of mango mix (Bioline), 0.10μl of each primer, 4μl of each DNA sample, and 8.30μl of nuclease-free water was added to achieve a total reaction volume of 25μl as indicated by manufacturer's procedure (Mangomix™, BIOLINE. PCR was carried out according to the manufacturer's procedure (Mangomix™, BIOLINE) and was amplified using a Bio-Rad T100™ Thermal Cycler. Table 2.3 contains the PCR conditions and DNA primers sequences (Sigma). Then, the PCR reaction was visualised using in house made 3% agarose gel containing a 1:30000 dilution of Saferview (Biolegend) and the bands on the gels were detected, viewed, and annotated using Bio-Rad Gel Doc XR and ImageLab software (Figure 2.1).

Table 2.3 Primer sequence and PCR reaction cycle protocol.

Primer Type	Sequence 5'→3'	PCR Reaction Cycle
Common	TAT GCA TCC CCA GTC TTT GG	94°C for 2 min 94°C for 30 sec 60°C for 30 sec 72°C for 40 sec Repeat steps 2-4 for 10 cycles 94°C for 15 sec 60°C for 15 sec 72°C for 10 sec Repeat steps 6-8 for 28 cycles 72 °C for 2 min
Wild Type Reverse	CTA CCC AAC CAG CCC CTT AC	
Mutant Reverse	ATA GAT TCG CCC TTG TGT CC	

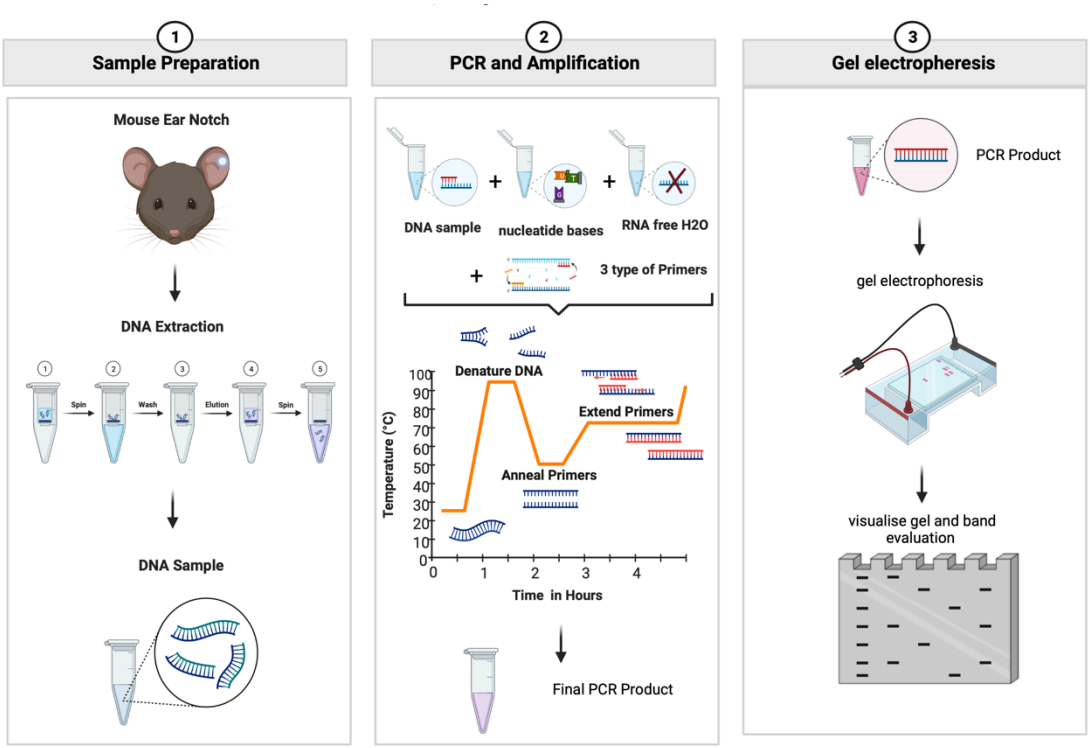

Figure 2.1 Schematic of Ldlr knockout gene detection.

This was achieved in three steps: First, DNA extraction from ear notch tissue. Second, preparation of PCR master mix using mango mix (Bioline), primers, DNA sample, and nuclease-free water and the PCR reaction. Finally, PCR products were run in 3% agarose gel, then visualised for band detection.

Genomic PCR of ear notches collected from each genotype demonstrated full deletion of the Ldlr gene in Ldlr $^{-/-}$ mice (Figure 2.2)

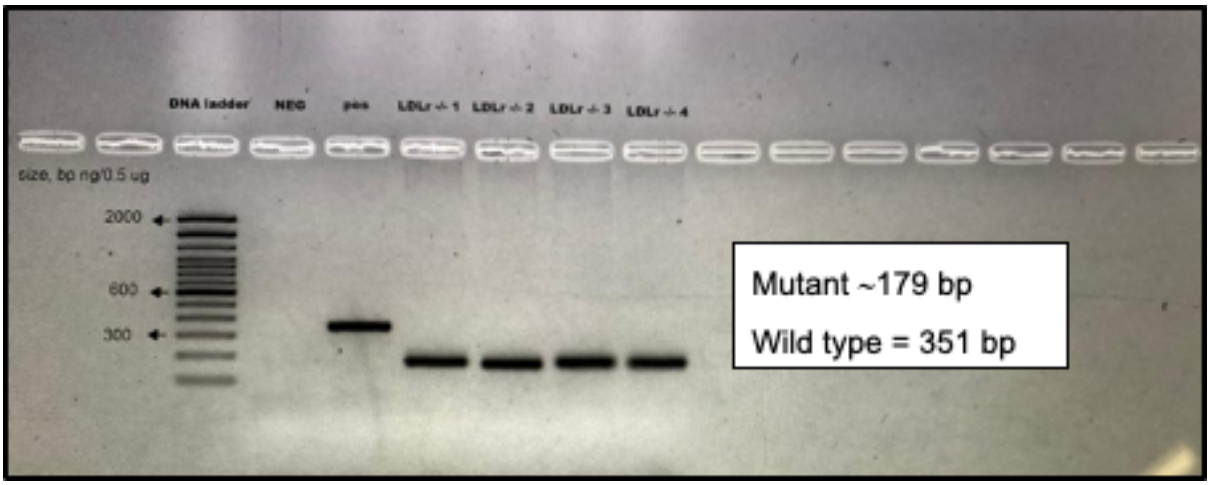

Figure 2.2 Gel band showing genomic PCR results for Ldlr gene deletion in experimental mice.

2.2.1.3 Animal care and High Fat Diet feeding

The Cardiff University Institutional Ethics Review Committee and the United Kingdom Home Office approved all studies and protocols, and experiments were conducted in accordance with the National Institutes of Health's Guide for the Care and Use of Laboratory Animals (NIH Publication No. 85–23, revised 1996; Experimental licences 30/3380 and 30/3365 and personal license I5A9F964D).

8-12-week-old male *Ldlr$^{-/-}$* mice were kept in a vented cage in a light- and temperature-controlled environment (12-hour light/dark cycle, 22°C) with unrestricted access to food and water. For 12 weeks, the mice were randomly assigned to one of two groups and fed either a high fat diet (HFD) [21% (w/w) pork lard and 0.15 percent (w/w) cholesterol] or Normal Chow Diet (19% protein extruded rodent diet) Envigo^{TM}. At the end of the study, all mice were sacrificed by increasing the levels of CO_2 and death was confirmed by cervical dislocation.

2.2.2 Sample collection and preparation

2.2.2.1 Peripheral blood analysis for complete blood count and immunophenotyping

Blood was obtained in Ethylenediaminetetraacetic acid EDTA microtubes (Mirovette CB 300, Cat 16.444, SARSTEDT) through tail bleeding technique with the aid of animal holder, ensuring not to exceed 20μl for animal well-being purposes. For Complete blood count (CBC), extracted peripheral blood were analysed on a 19-parameter haematology analyser (Celltac Alpha MEK-6500K, Nihon Kohden).

2.2.2.2 Heart blood collection and heart sections

Mice were euthanized by gradual increase in CO_2 level. Then, palpitation was used to confirm death. Next, whole blood was taken in heparinised tube from the heart by cardiac puncture. Briefly, a 26-gauge needle was inserted bevel up at a 30-40° angle through the diaphragm. Keeping the syringe parallel to the mouse's midline, a needle was inserted slightly to the left of and behind the sternum. Then, plunger was retracted slightly to create a vacuum within the syringe and advance the needle slowly until a flash of blood emerged in the needle hub. Whole blood from cardiac puncture was collected into Eppendorf tubes containing heparin (5000 U/mL) to prevent clotting and the animal was immediately euthanized upon completion of blood collection by cervical dislocation. Plasma was obtained by centrifugation whole blood for 10 minutes at 12,000g. The heart was then collected, washed with phosphate buffer saline (PBS) (Gibco™), put in a Shandon base model, and instantly coated with optimal temperature formulation (Legras et al.) (Thermo Fisher Scientific), and snap frozen in dry ice. Samples were transferred into -80°C freezer.

2.1.2.3 Plasma cytokines processing and analysis

Whole blood from cardiac puncture was collected into Eppendorf tubes containing heparin (5000 U/mL) to prevent clotting. Plasma was obtained by centrifugation for 10 minutes at 12,000g. Then supernatant was transferred into a new Eppendorf tube and

shipped in dry ice to Central biotechnology services (CBS), Cardiff University for murine inflammatory Cytokines and chemokines (INF-γ, TNF-α, MCP-1, MIP1-α, IL1-β, IL-6, IL-10) measurements. Cytokines and chemokines were quantified using electrochemiluminescence immunoassays principle using Meso Scale Discovery QuickPlex SQ120, USA (Han et al. 2021).

2.1.2.4 Heart sectioning

Cryosections of OCT-implanted hearts were obtained using a microtome cryostat sectioning at –20 ˚C ± 3˚C. Following that, serially cut 10μM slices from the aortic roots were used to see all three leaflets of the aortic valves. Finally, slices were collected on polylysine-coated slides and air dried for 1 hour prior to storage at – 80ºC.

2.1.2.5 Heart sections staining using Haematoxylin & Eosin

Haematoxylin and eosin (H&E) staining is a widely used histological staining method. Haematoxylin is a dark blue/purple stain that stains basophilic substances such as DNA in nuclei, resulting in blue/purple stained nuclei. The red stain eosin, which is employed as a counterstain, is acidic in nature, which results in a contrasting red staining of positive structures such as cytoplasmic proteins. For 5 minutes, thawed sections were washed in distilled water and then stained with 5 percent (w/v) Gill's haematoxylin (0.1 percent (w/v) haematoxylin, 0.02 percent (v/v) sodium iodate, and 2% (v/v) glacial acetic acid). After that, the slides were washed in running tap water until clear (approximately 10 minutes). For 10 minutes, slides were counterstained with Eosin and then dehydrated in 80%, 95%, and 100 % ethanol for 5 minutes each. Finally, the slides were incubated for 5 minutes in xylene before being mounted with D.P.X. At a magnification of X40, images were acquired using a Leica DMRB brightfield microscope and ProgRes® CapturePro 2.8.8 software (X4 objective).

2.1.2.6 Bone marrow, Spleen and Thymus Collection and Processing

After heart collection, hip, femur, and tibia bones were harvested to obtain bone marrow cells. Bones were crushed in a pestle and mortar in 10 ml 1X PBS (Gibco™)

supplemented with 2% Heat inactivated Foetal Bovine Serum (Gibco™) or FBS (v/v), referred to as 2% PBS-FBS from here on. Obtained medium containing single cells was filtered in a 70µm strainer (Miltenyi Biotec) into 50 ml Falcone tube. This step was repeated three times until a 30 ml Bone marrow cell suspension was acquired. Spleen and thymus were formerly collected, weighted using analytical scales and measurements were obtained. Spleen and Thymus were placed in a 70µm strainer within a 6-cm petri plate containing 2% FBS/PBS and mashed using a 5 ml syringe plunger. This technique was performed three times to get a 7 ml and 4 ml cell suspensions for spleen and thymus samples respectively. Cell counting was carried out using two different platforms, BD Accuri™ C6 Plus Flow Cytometer (BD™, USA). then, cell counting cassette (Chemometec,USA) ran in Automated cell counter (NucleoCounter® NC-200) (Figure 2.3).

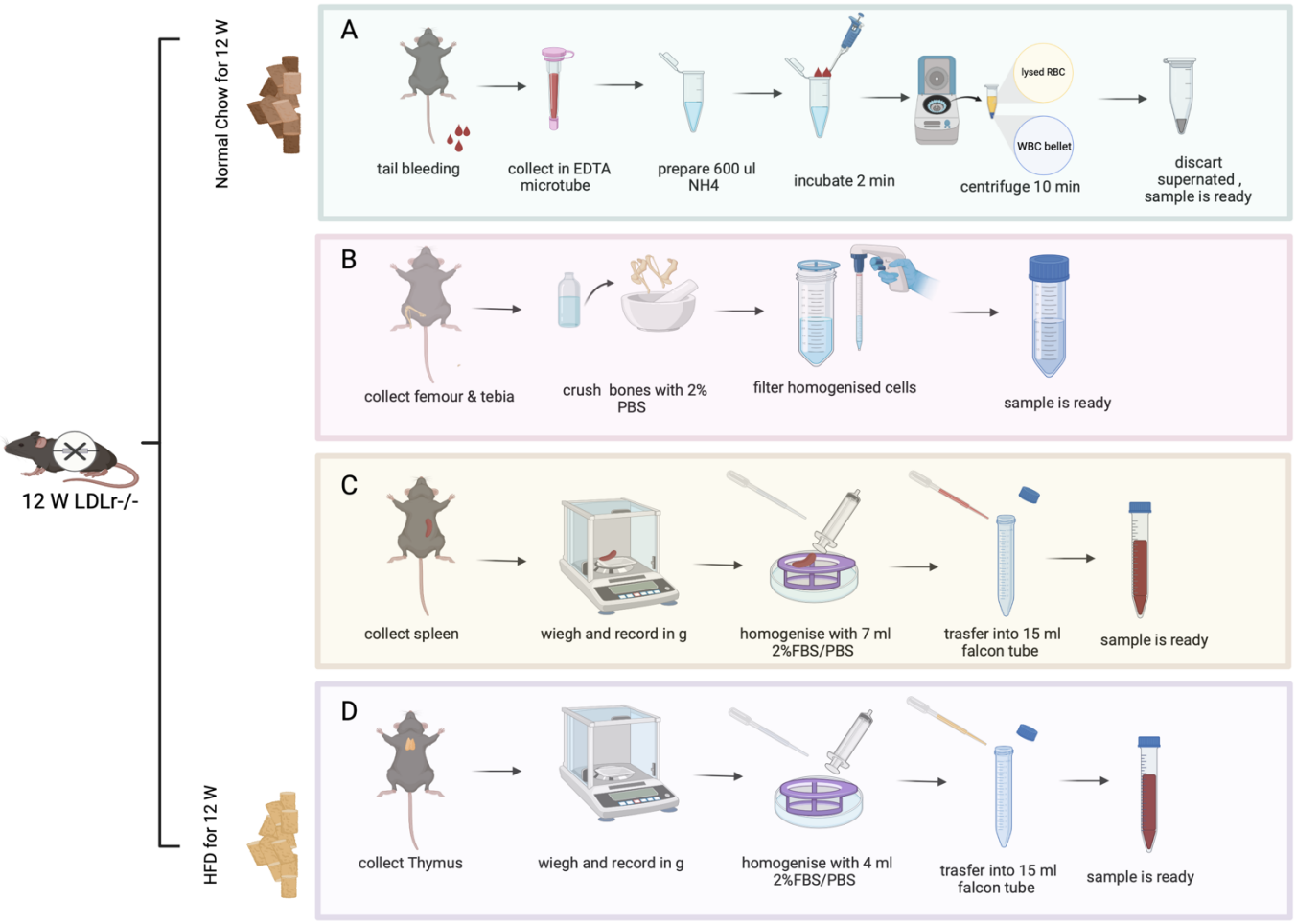

Figure 2.3 Ldlr-/- mice sample processing.

(A) Peripheral blood from the tail vein was dropped into EDTA microtube, red blood cells were lysed, and blood centrifuged to obtain the WBC pellet. B) Post-CO_2 euthanization, bones were collected, crushed, and then filtered. C) Spleen was collected, weighed, and then homogenised in 7 ml 2% FBS/PBS using a 70μM filter and a syringe plunger. D) Thymus was processed using the same spleen method, except for using 4 ml 2% FBS/PBS instead.

2.2.3 Immunophenotyping of immature and mature blood cells

2.2.3.1 Bone marrow samples

To analyse the signalling lymphocytic activation molecule (SLAM) and progenitor cell populations, 10 million cells were transferred from the cell suspension to fresh 5 ml Falcon tubes and pelleted at 500 x g, 4°C for 5 minutes. Unless otherwise specified, all centrifugation processes were performed at this setting. Cells were subsequently resuspended in 50 µl (1% v/v) FC block then 50 µl of a mixture of antibody cocktail including biotin antibodies CD3, CD4, CD8, B220, MAC-1, Gr.1, and Ter119 and fluorochrome-conjugated antibodies specific for HSCs and other immature cells found in the SLAM and progenitor populations, as described in Table 2.4, and incubated at 4°C for 30 minutes. Cells were then washed with 2% PBS-FCS, pelleted, and resuspended for an additional 30 minutes at 4°C in PerCP-Cy5.5 conjugated streptavidin (2%; v/v). Post incubation cells were washed again in 2% PBS-FCS, pelleted, and resuspended in fresh 2% PBS-FCS for analysis. Analysis of SLAM bone marrow cell populations was carried out using a method described in (Mayle et al. 2013; Oguro et al. 2013). Briefly, the earliest haematopoietic progenitors in the bone marrow lack differentiation markers (**L**ineage negative) and express stem cell markers stem cell antigen 1 (**S**ca-1) and c-**K**it (CD117); they are hence referred to as **LSK** cells. This heterogeneous LSK cell population has been further defined using CD150 and CD48. The CD150+ CD48- subset of LSK progenitors contains long-lived self-renewing haematopoietic stem cells (HSCs), whereas more mature CD150- CD48- LSK cells lack self-renewal capacity but retain the ability to differentiate into all blood cell types and are thus referred to as multipotent progenitors (MPPs) (Oguro et al. 2013) (Figure 2.4).

To label committed progenitor cells, 10 million BM cells were treated in 100µl of an antibody cocktail including biotin antibodies CD3, CD4, CD8, B220, MAC-1, Gr.1, and Ter119. Following that, c-kit, Sca-1, CD127, CD34, CD135 (Flt3) and CD16/32 were added to examine the CMP, GMP, CLP, and LMPP populations. Following 30 minutes of incubation at 4°C, cells were washed with 2% FBS/PBS and centrifuged for 5 minutes at 500g. The pellet was then resuspended in 100µl Streptavidin-Percp

solution. After 30 minutes, the cells were washed and resuspended in 2% FBS/PBS (Figure 2.5). Analysis of committed progenitors in bone marrow cell populations was carried out using a method described in (Challen et al. 2009; Mooney et al. 2017). In short, progenitor cells in the bone marrow lack differentiation markers (**L**ineage negative) and only express c-**K**it (CD117); they are hence referred to as **LK** cells. This heterogeneous LK cell population has been further defined using CD16/32 and CD34 markers. CMP are gated using CD34+ CD16/32^{low}. CMP in turn generate megakaryocyte/erythrocyte (MEP) gated using CD16/32 - CD34- and granulocyte/macrophage progenitor cells (GMP) CD16/32+CD34+. Moreover, common lymphoid progenitors are found beneath LSK and LK populations: c-kit^{low} Sca-1^{low} and exclusively express CD127. Lymphoid-primed multipotent progenitors (LMPP) are identified using CD34+CD135+ (Flt3) (Will and Steidl 2010)(Figure 2.5).
After completing the SLAM, progenitor, lineage, and single cell fluorochrome preparations, stained cell suspensions were filtered onto sterile 40μM pore filters and kept at 4°C. Flow cytometry analysis of the samples was performed using a BD FACS Fortessa^{TM} flow cytometer. 20μg/mL 6-Diamidino-2-Phenylindole, Dihydrochloride DAPI nuclear stain with a final concentration of 0.2 μg/mL was applied immediately prior to analysis to detect live cells, and the cells were vortexed. Samples were acquired until they reached minimum three million cells; this is important to detect statistically correct number of rare HSPC populations. To eliminate cross-spill over across fluorochromes, each sample was compensated using single cell fluorochrome staining. Following that, cell populations were gated using cell-specific markers, as indicated in Table 2.2. To verify the accuracy of gating, a back gating approach was used, in which the final gated populations were superimposed over their parent populations. Cell population analysis was performed using the FlowJo v.10 program (Tree star INC, USA). The gating method is depicted schematically in Figures 2.4 and 2.5.

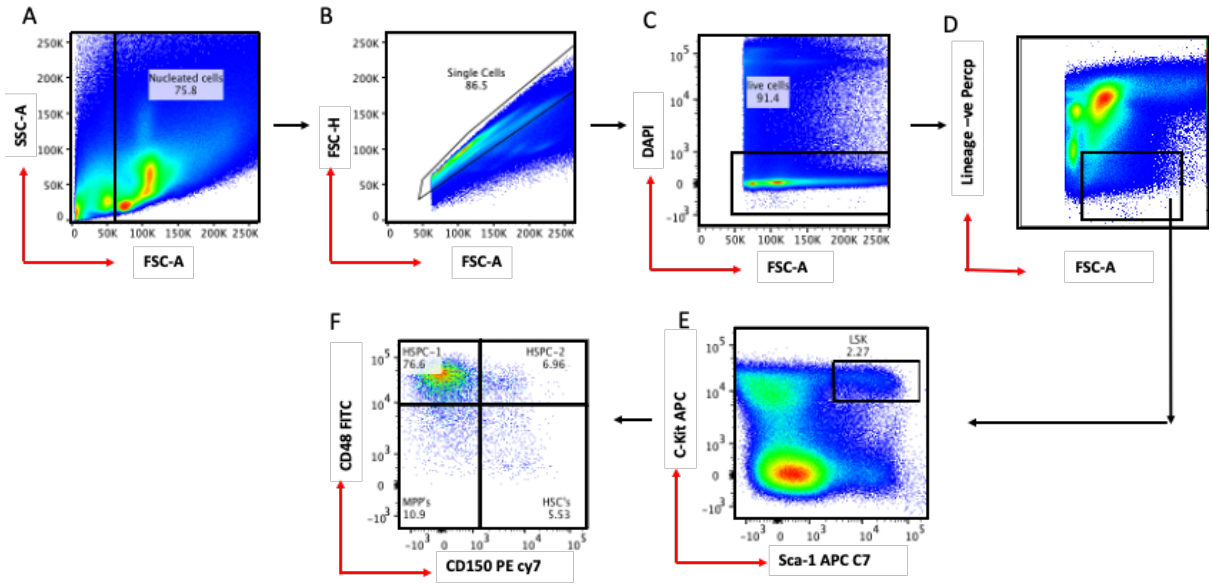

Figure 2.4 Flow cytometry Pseudocolor plots demonstrating the gating approach utilised to distinguish HSPCs from bone marrow.

A) Debris and dead cells were omitted to allow for the detection of nucleated cells. B) To eliminate clumps and doublets, single cells were gated from WBCs. C) Live cells were then gated as DAPI negative. D) Lineage negative population were gated. E) LSK population were selected as lineage negative, Sca-1+, c-kit+. F) LSK comprises the most primitive cells: HPC1, HPC2, HSC, MPP. The frequency and cell count of each HSPCs were calculated using percentages of each cell type in the BM cells and total bone marrow count.

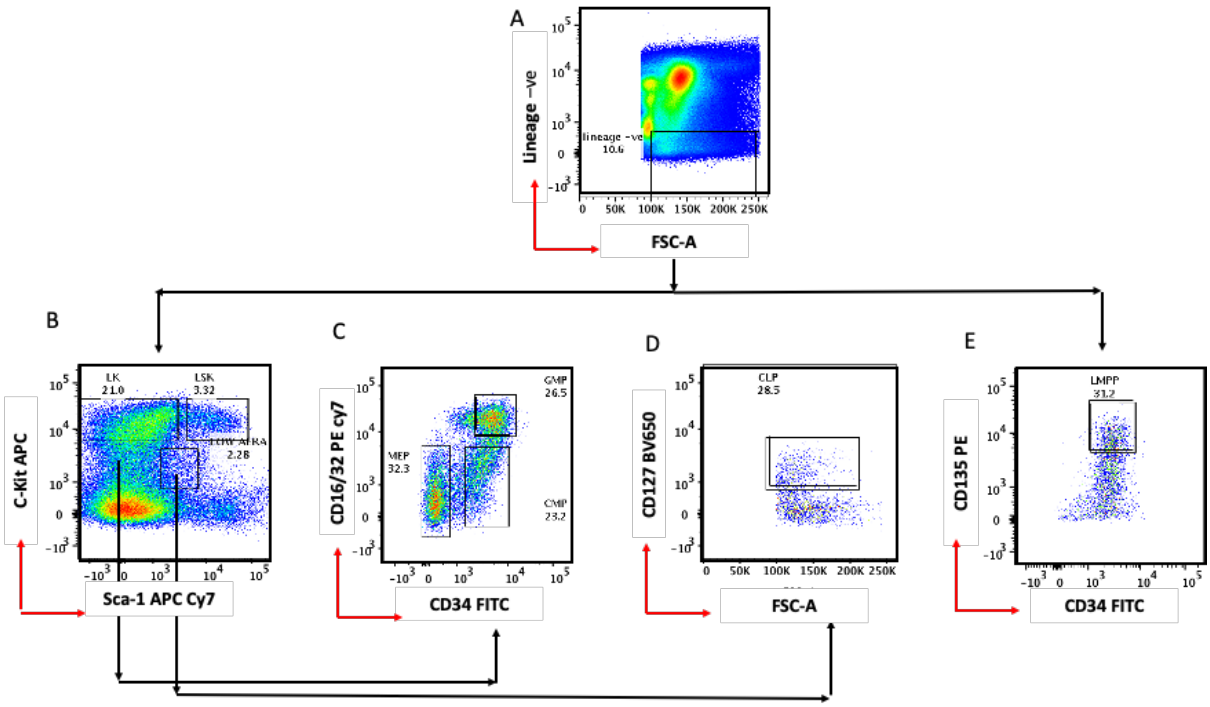

Figure 2.5 Flow cytometry plots demonstrating the gating approach utilised to identify committed progenitors from bone marrow.

A) Lineage negative populations were isolated. B) c-kit+ were gated to enrich the LK population. C) differential expression of CD16/32 and CD34 comprises lineage-specific progenitors GMP, CMP, and MEP.D) CLP populations were created by separating them from c-kit^{low} Sca-1^{low} populations. E) LMPP are identified using CD135 (Flt3) Vs.CD34. The frequency and cell count of HSPCs were calculated using the percentages of each cell type and total cell count.

2.2.3.2 Bone marrow lineage positive cells

To label lineage positive cells, 200,000 bone marrow cells were treated for 30 minutes at 4^{o}C with a cocktail of antibodies including myeloid markers (CD11b, Gr-1), an erythroid marker (Ter119, CD71), a megakaryocyte (CD41), a T lymphoid cell markers (CD3, CD4, CD8a), and a B lymphoid cell marker (CD19). Following that, cells were washed with 2% FBS/PBS and centrifuged for 5 minutes at 500g. The pellet was resuspended in a 2% FBS/PBS solution. 20μg/mL DAPI nuclear stain with a final concentration of 0.2μg/mL was applied immediately prior to analysis to detect live cells, and the cells were vortexed. Samples were acquired until they reached 20,000 events. To eliminate cross-contamination across fluorochromes, each sample was

compensated using single cell fluorochrome staining. Following that, cell populations were gated using cell-specific markers, as indicated in Table 2.4. To verify the accuracy of gating, a back gating approach was used, in which the final gated populations were overlaid over their parent populations. Cell population analysis was performed using the FlowJo v.10 program (Tree star INC, USA). The gating method is depicted schematically in Figures 2.6 and Figure 2.7.

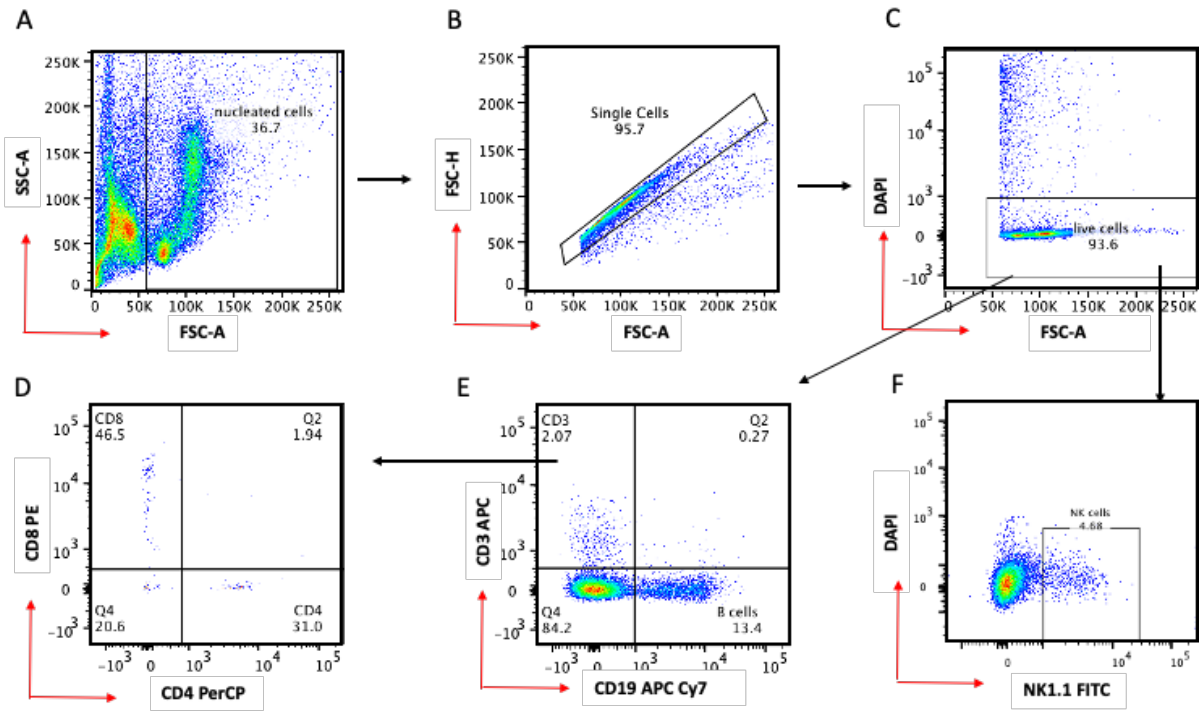

Figure 2.6 Flow cytometry plots demonstrating the gating scheme for lymphoid lineage positive cells.

A) SCC and FSC are employed to eliminate dead cells and Debris. B) Singlets are gated using FSC-H Vs. FSC-A. C) Live cells are DAPI negative. E) B cells were gated using CD19 and Lymphoid Differentiated cells type T were gated using TCR CD3. D) T cells are further characterised into T helper using CD4 and T cytotoxic using CD8. F) NK cells were gated using NK1.1 marker.

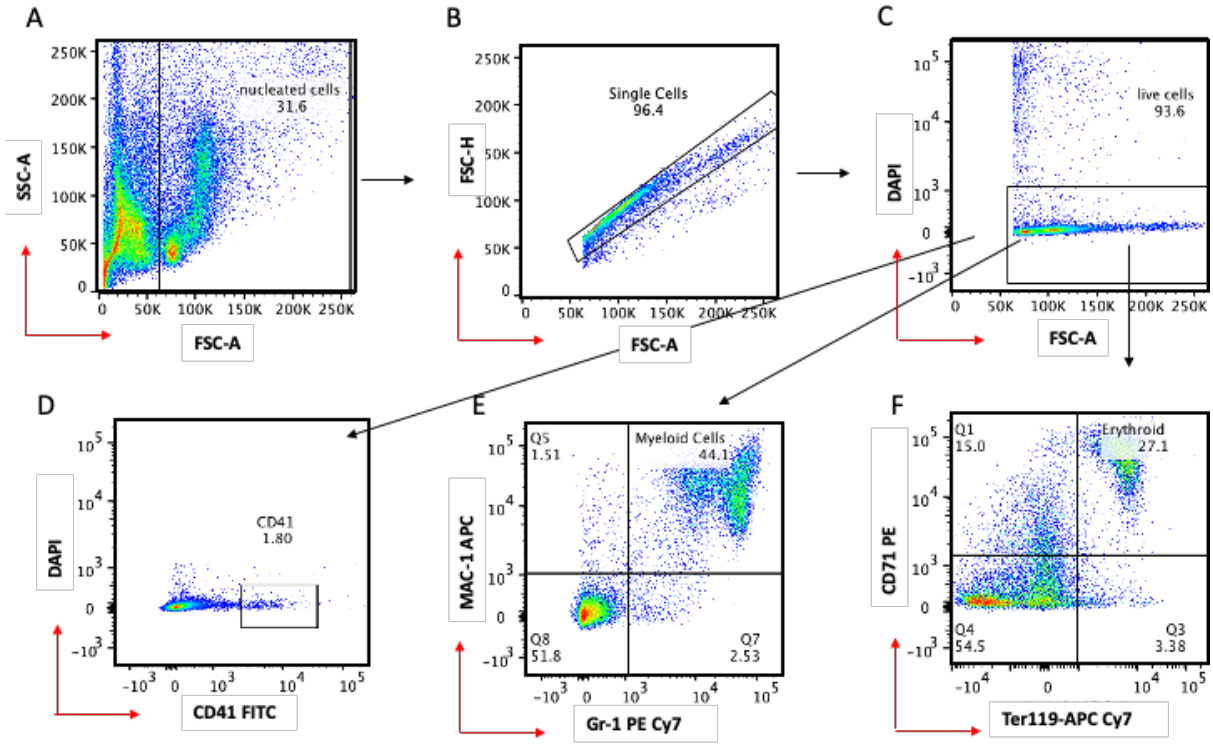

Figure 2.7 Flow cytometry plots demonstrating the gating scheme for myeloid lineage positive cells.

(A-C) After excluding nucleated cells and singlets, Live cells (DAPI negative). D) megakaryocytes are gated using CD41, E) Myeloid cells are Mac-1/Gr-1 Positive cells, F) Ter119 and CD71 are used to distinguish Erythroid cells.

2.2.3.3 Annexin V assay

As previously discussed, 10 million BM cells were stained for SLAM and progenitor markers (section 2.2.3.1). Following that, cells were rinsed with cold 2% FBS/PBS. The BM cells were treated with an annexin-binding buffer containing an Annexin V – PE fluorochrome conjugate and incubated for 30 minutes at room temperature in the dark. 6µl of 20µg/ml DAPI with a final concentration of 0.2µg/mL was added to the samples and maintained on ice until flow cytometry analysis (Figure 2.8). Analysis was applied as described in (Vignon et al. 2013)

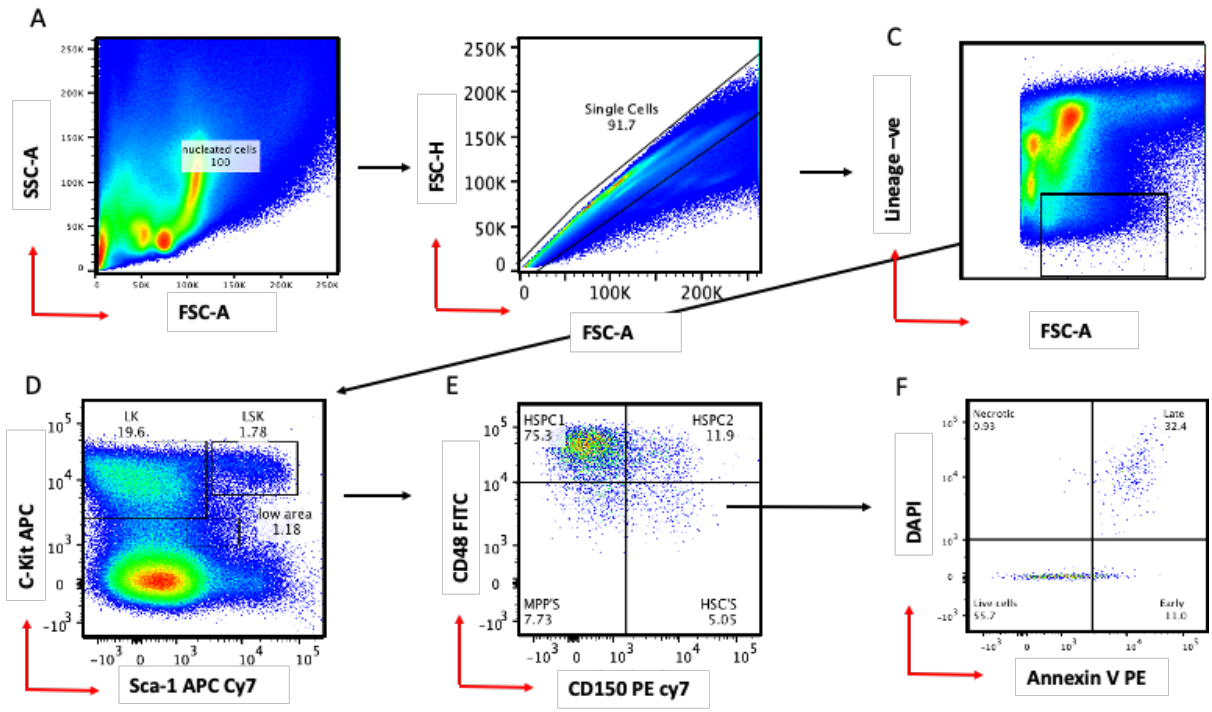

Figure 2.8 Flow cytometry plots demonstrating the gating approach applied to identify apoptotic cells.

A) Debris and dead cells were included to identify all nucleated cells. B) To eliminate clumps and doublets, single cells were gated from WBCs. C) The lineage negative population was then gated for analysis. D) which was then gated for analysis of the LSK population. E) CD48 Vs. CD150 are employed to define the LSK subpopulations. F) Annexin V–PE fluorochrome conjugate/DAPI staining was used to detect the phases of apoptosis: living cells (Annexin V- DAPI-), early apoptosis (Annexin V+ DAPI-), late apoptosis (Annexin V+ DAPI+), and Necrosis (Annexin V- DAPI+). The

frequency of various phases of apoptosis was calculated using the percentage of each gate and total nucleated cells count in the bone marrow sample.

2.2.3.4 Cell Cycle analysis using Proliferation marker Ki-67 assay

As previously stated, 10 million BM cells were stained for SLAM and progenitor markers (section 2.2.3.1). Following that, cells were rinsed with cold phosphate-buffered saline (PBS) and fixed for 10 minutes in 2% paraformaldehyde at room temperature. After washing the cells with cold PBS, the samples were permeabilised for 24 hours at 4ºC with 0.1% saponin containing Ki-67 PE fluorochrome conjugate (10μl/10 million cells). After incubation cells were washed with cold PBS then resuspended in 2% FBS/PBS. Following that, the samples were treated with DAPI at a final concentration of 5 μg/ml for 10 min and filtered through 30 μm Nylon filter prior flow cytometry analysis (Figure 2.9). Analysis protocol were adopted from (Vignon et al. 2013) utilizing an isotype control tube.

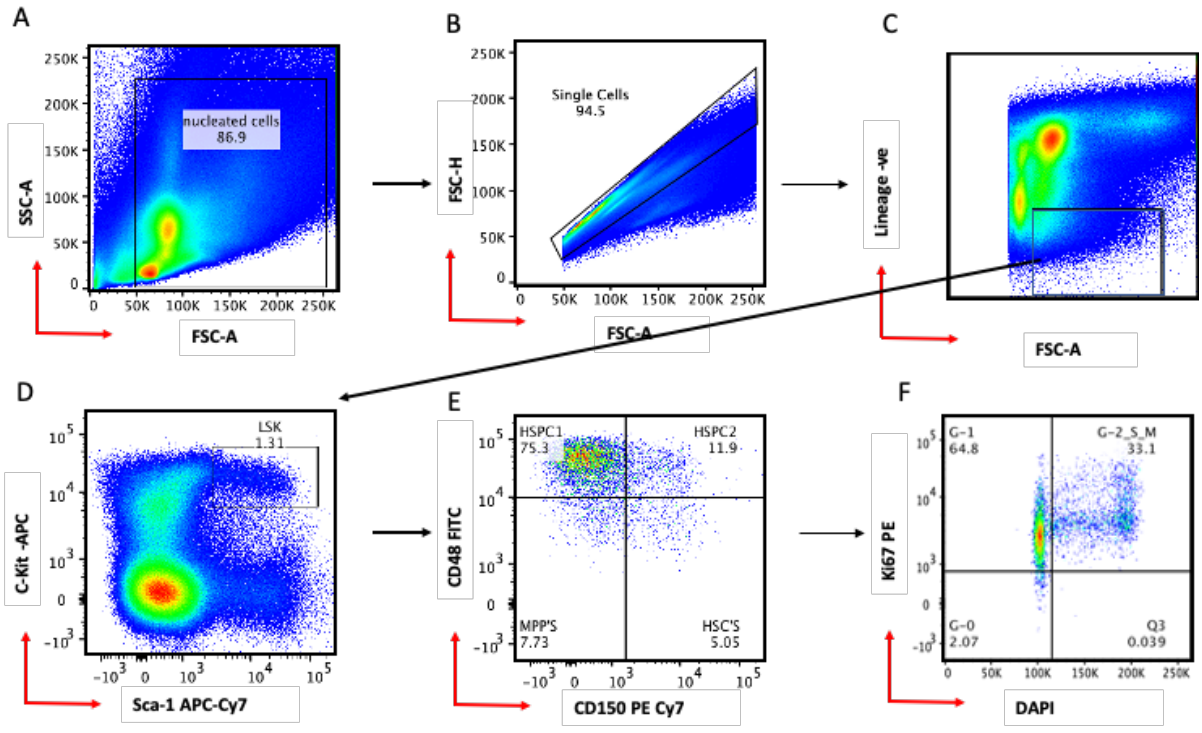

Figure 2.9 Flow cytometry plots demonstrating the cell cycle gating method used to identify cell cycle phases.

A) Debris and dead cells were omitted to allow better detection of WBCs. B) To eliminate clumps and doublets, single cells were gated from WBCs. C) lineage

negatives were then gated. D) Which served as the gate for the LSK population. E) LSK compartments were then identified using a CD48 and SLAM marker CD150. F) G_0 (KI67- DAPI-), G_1 (KI67+ DAPI-), and S/G_2/M (KI67+ DAPI+) were used to define the cell cycle phases, DAPI are gated using linear scale. Calculations of the frequency of various phases of the cell cycle were made using the percentage of each gate and total bone marrow cell count.

2.2.4 Peripheral blood staining

12µl of peripheral blood was added to 600 ml NH_4CL (prepared in-house**:** 90g NH_4CL (o.155M), 10g $KHCo_3$ (0.01M), 370 mg EDTA (0.1 mM), dissolved in one litre of ddH2O, filter to sterilize through 0.22 μM pore filter) and incubated for 2 min. Next, the sample was centrifuged at 400g for 10 minutes at room temperature. The supernatant containing lysed red blood cells was then aspirated carefully to obtain the pellet. Then, mixed antibodies were added to the pellet, incubation took place at 4°C in dark. The antibody panels contain extended lymphoid panel (CD3, CD4, CD8, NK1.1, NKP46 and CD19) and extended Myeloid panels (Mac-1, Gr-1, Ly6C, Ly6G, F4/80, CD115) see (Table 2.2). The pellet was washed to avoid nonspecific background in data acquisition step. Finally, 3 µl of 20 μg/ml DAPI with a final concentration of 0.2µg/mL was added to the samples and maintained on ice until flow cytometry analysis. Every sample were acquired until 20,000 events from nucleated cells are achieved. To ensure that no fluorochrome cross-contamination occurred, each sample was compensated using single cell fluorochrome staining. Cell populations were then gated using cell-specific markers, as stated in Table 2.2. To validate the gating techniques, a back gating strategy was adopted, in which the final gated populations were placed on their parent populations. The FlowJo v.10 software was used to conduct cell population analysis (Tree star INC, USA). In Figures 2.10 and 2.11, the gating approach is illustrated schematically. Analysis was adopted from the following references (Yang et al. 2014; Bronte et al. 2016).

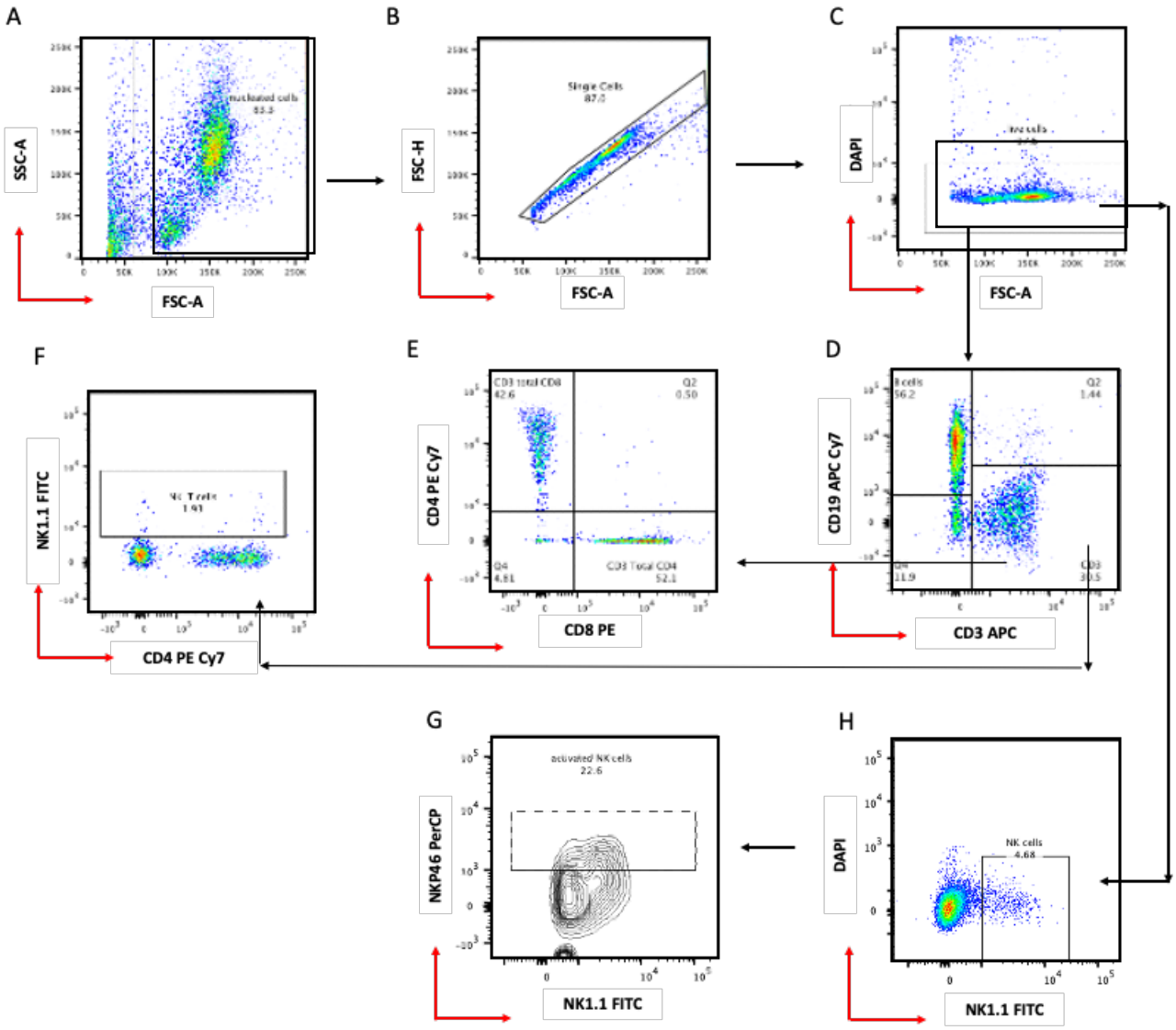

Figure 2.10 Flow cytometry plots showing the sequential gating strategy applied to identify main peripheral blood lymphoid cell populations: T cells (T helper, T Cytotoxic), B cells, and NK cells.

A) Debris and nucleated RBCs were excluded to gate for nucleated cells only. B) Singlets were gated from nucleated cells to exclude doublets. C) Live cells were then gated to exclude dead cells. D) B cells (CD19) and T cells (CD3) were gated. F) From T cells, NKT cells were gated using NK1.1 Vs CD4. E) from T cells, T helper (CD4) and T cytotoxic (CD8). H) from live cells NK cells were gated using NK1.1. G) Activated NK cells were identified using NK1.1 Vs. NKP46.

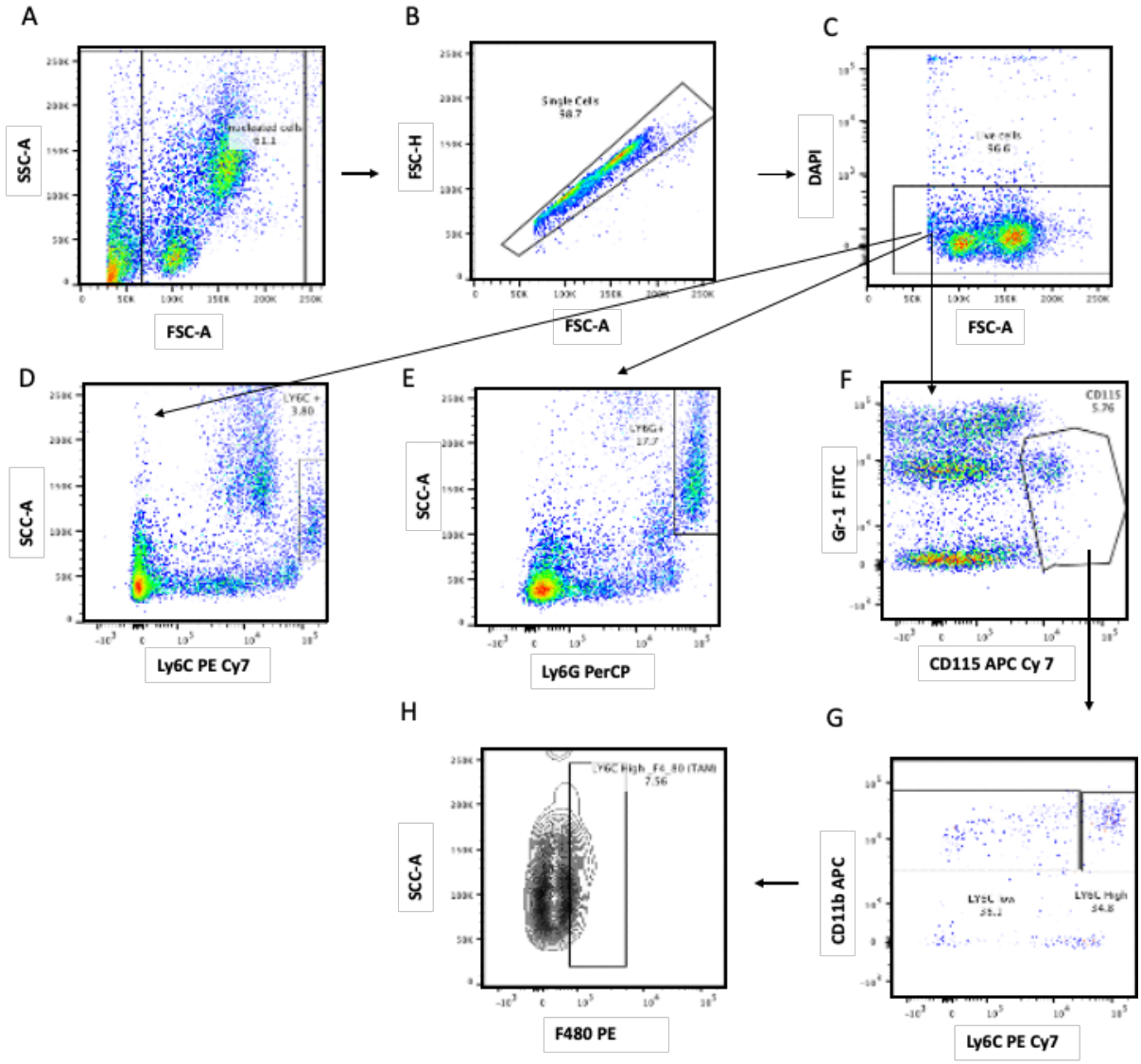

Figure 2.11 Flow cytometry plots showing the sequential gating strategy applied to identify the main peripheral blood myeloid populations: Monocytes or MDCS-M, Granulocytes or MDCS-G.

A) Debris and nucleated RBCs was excluded to gate for nucleated cells. B) Singlets were gated from nucleated cells to exclude doublets. C) Live cells were then gated to exclude dead cells. D) monocytes or MDSC-M are marked by LY6C+ Ly6G-, E) Granulocytes or MDSC-G are marked by Ly6C- Ly6G+. F) from live cells specific monocyte markers CD115+ was gated for further monocyte characterization. G) MAC-1 vs. LY6C^{bright} or LY6C^{dim} are used to distinguish classical or inflammatory monocytes. H) LY6C+F4/80+ are used to gate Tumour Associated Macrophages(Bronte et al. 2016).

2.2.5 Spleen immunophenotyping characterization

200,000 spleen cells were treated for 30 minutes at 4°C with a cocktail of antibodies including myeloid marker (CD11b, Gr-1), a T lymphoid cell markers (CD3, CD4, CD8a), and a B lymphoid cell marker (CD19). Following that, cells were washed with 2% FBS/PBS and centrifuged for 5 minutes at 500g. The pellet was resuspended in a 2% FBS/PBS solution. 20μg/mL DAPI nuclear stain at a final concentration of 0.2μg was applied immediately prior to analysis to detect live cells, and the cells were vortexed. Samples were acquired until they reached 20,000 events. To eliminate cross-contamination across fluorochromes, each sample was compensated using single cell fluorochrome staining. Following that, cell populations were gated using cell-specific markers, as indicated in Table 2.4. To verify the accuracy of gating, a back gating approach was used, in which the final gated populations were overlaid over their parent populations. Cell population analysis was performed using the FlowJo v.10 program (Tree star INC, USA). The gating method is depicted schematically in Figures 2.12.

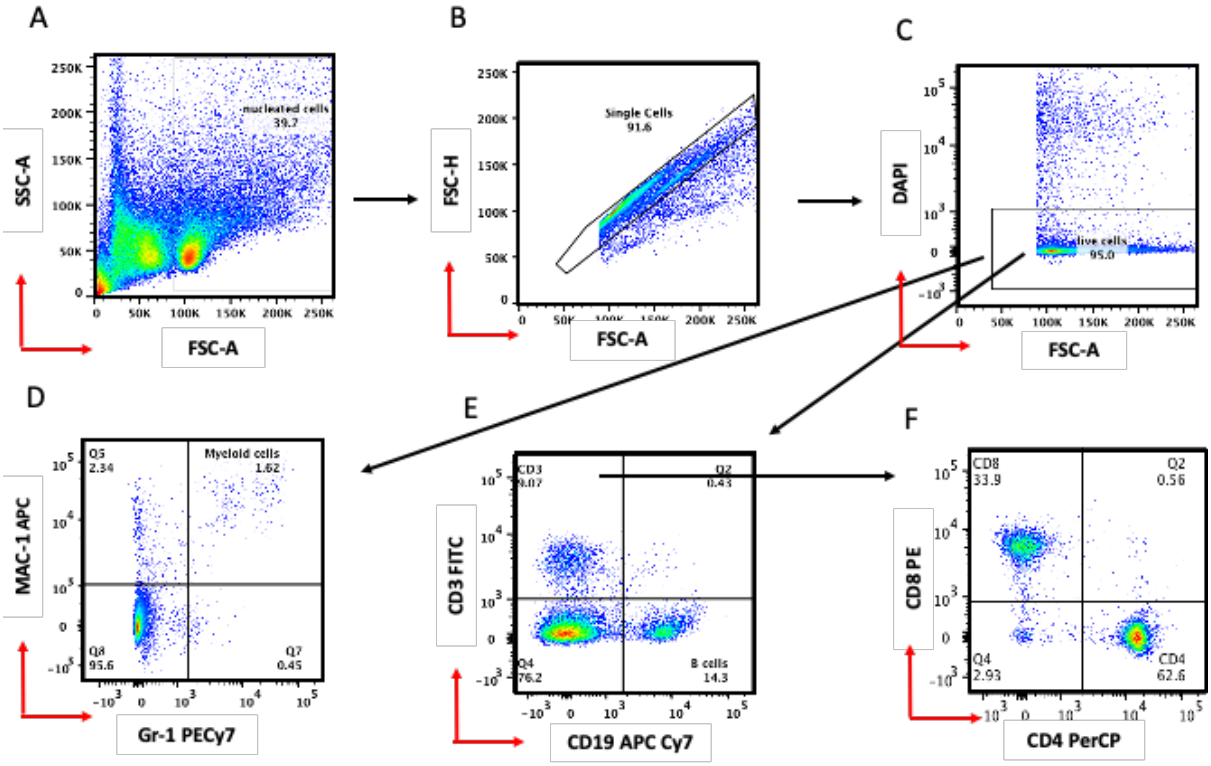

Figure 2.12 Flow cytometry plots showing (Lymphoid + myeloid) gating strategy for spleen analysis.

A) In the first plot, debris and nucleated RBCs were excluded. B) Then single cells were gated from WBCs to exclude doublets. C) DAPI negative population are defined as Live cells. D) Myeloid compartments defined are Mac-1 + Gr-1+. E) T cells are defined as CD3+ and B cells are defined by CD19. F) T helper and T cytotoxic defined as CD4 and CD8 respectively**.** Percentages of each cell type are plotted within each gate.

2.2.6 Thymus immunophenotyping

200,000 thymus cells were treated for 30 minutes at 4ºC with a cocktail of Lymphoid related antibodies including (CD3, CD4, CD8a), and a B lymphoid cell marker (CD19). Following that, cells were washed with 2% FBS/PBS and centrifuged for 5 minutes at 500g. The pellet was resuspended in a 2% FBS/PBS solution. 20 μg/mL DAPI nuclear stain at a final concentration of 0.2μg was applied immediately prior to analysis to detect live cells, and the cells were vortexed. Samples were acquired until they reach 20,000 events. To eliminate cross-contamination across fluorochromes, each sample was compensated using single cell fluorochrome staining. Following that, cell populations were gated using cell-specific markers, as indicated in Table 2.4. To verify the accuracy of gating, a back gating approach was used, in which the final gated populations were overlaid over their parent populations. Cell population analysis was performed using the FlowJo v.10 program (Tree star INC, USA). The gating method is depicted schematically in Figures 2.13.

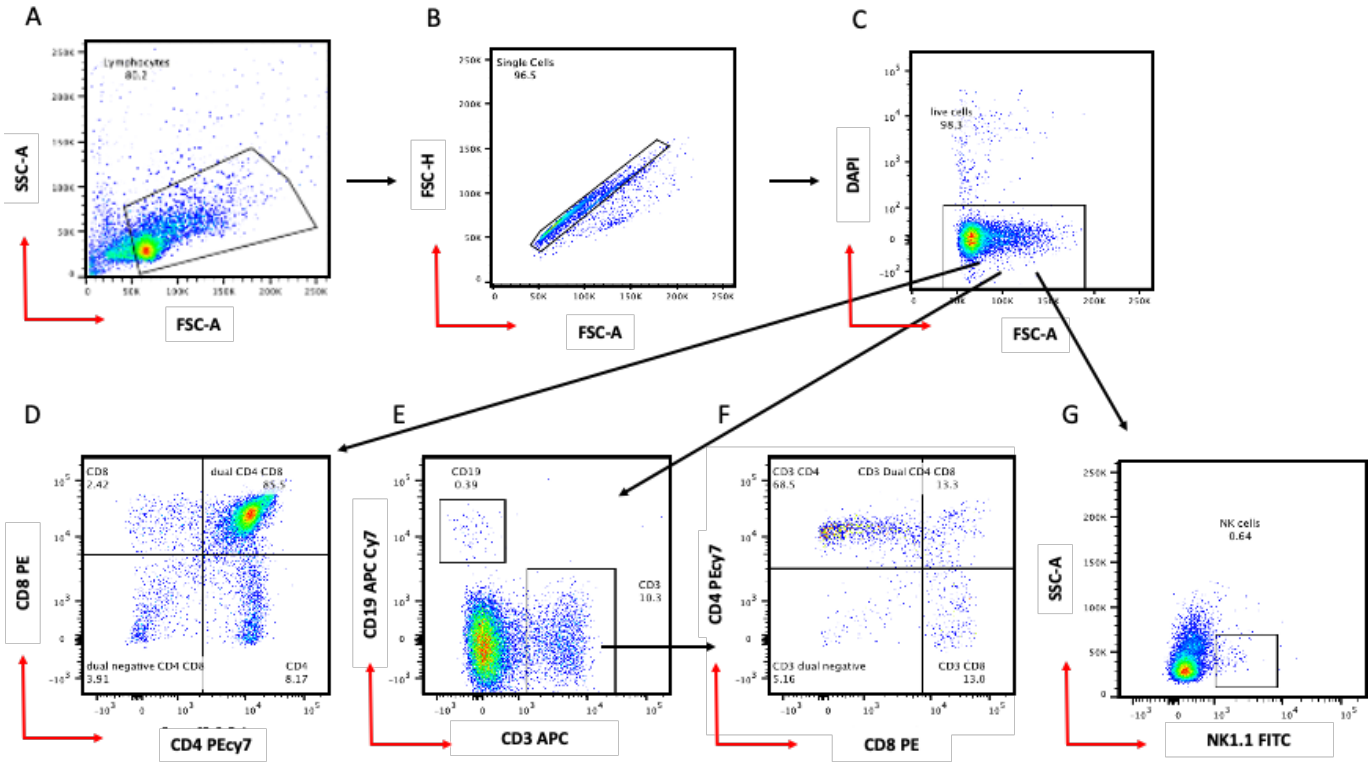

Figure 2.13 Flow cytometry plots showing gating strategy for lymphoid cell analysis of thymus.

A) In the first plot, debris and nucleated RBCs were excluded. B) Then single cells were gated from WBCs to exclude doublets. C) DAPI negative population are defined as Live cells. D) Immature T cells do not express the pan T cells marker (CD3), profound dual positive CD4/CD8 DP with less CD4 and CD8 cells respectively also DN are cells not expressing CD4/CD8. E) mature T cells are defined as CD3 +, B cells as CD19+. F) T helper and T cytotoxic defined as CD4 and CD8 respectively**.** G) NK cells are defined as NK1.1 positive**.** Percentages of each cell type are plotted within each gate.

2.2.7 *In vitro* clonogenic assay

Bone marrow was processed using sterile practice and bone marrow cells were counted. Then 20,000 cells live cells were inoculated in Methocult ™ 3434 media (Stem Cell Technologies) and plated using a 5 ml syringe attached to a 19G blunted needle. Cells were incubated in a humidified incubator at 37°C and 5%CO_2. The colonies were enumerated and scored using an inverted microscope (Leica) at day 10 (Figure 2.14).

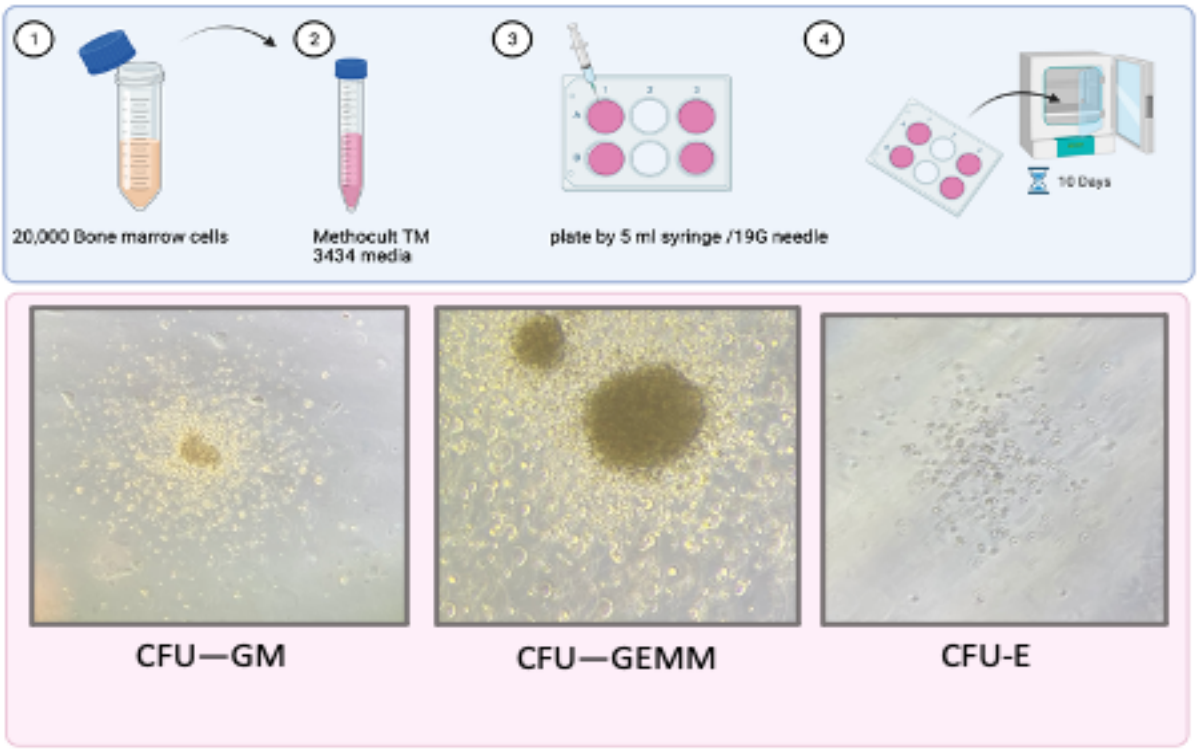

Figure 2.14 Identification of colonies derived from mouse haematopoietic progenitors from bone marrow.

Key: CFU-GM, Colony-Forming Unit Granulocytes, Macrophages. CFU-GEMM, Colony-Forming Unit Granulocytes, Erythroid, Macrophages, Megakaryocytes. CFU-E, Colony-Forming unit Erythroid.

Table 2. 4 Antibody panels used in immunophenotyping.

Class	Antibody	Conjugates	Targeted population/ function	Markers
SLAM	Ly-6A/E (Sca-1) CD48 CD150 CD117 (c-Kit) Lineage cocktail (biotinCD3, CD4, CD8a, Gr-1, Mac-1, B220,Ter119)	APC Cy7 FITC PECy7 APC PerCP	HSC's HSPC-1 HSPC-2 MPP's	Lineage - c-Kit+ Sca-1+ CD150+ CD48- Lineage - c-Kit+ Sca-1+ CD150 - CD48+ Lineage - c-Kit+ Sca-1+CD150+CD48+ Lineage - c-Kit+ Sca-1+ CD150- CD48-
Progenitors	Ly-6A/E (Sca-1) CD117 (c-Kit) CD127 CD34 CD16/32 Lineage cocktail (biotinCD3, CD4, CD8a, Gr-1, Mac-1, B220, Ter119)	APC Cy7 APC BV650 FITC PECy7 PerCP	GMP CMP MEP CLP LMPP	Lineage - c-Kit+ CD34+CD16/32+ Lineage - c-Kit+ CD34+ CD16/32- Lineage - c-Kit+ CD34- CD16/32- Lineage - c-Kit^{low} Sca-1^{low} CD127+ Lineage - c-Kit+ Sca-1+ CD34+ CD135+
Myeloid	Ly-6G/Ly-6C (Gr-1) CD11b (Mac-1) TER-119 CD41 CD71 Ly6C Ly6G CD115	PECy7 APC APC Cy7 FITC PE	Myeloid Erythroid Megakaryocytes MDSC-M MDSC-G Macrophages	Gr-1+ Mac-1+ CD71+ TER-119+ CD41+ Ly6G -Ly6C+ CD115+ Ly6G+ Ly6C- CD115- Ly6G- Ly6C- F4/80+

	F4/80			
Lymphoid	CD3 CD4 CD8 NK1.1 NKP46	FITC PECy7 APCCy7 FITC PerCP	TCR T helper T cytotoxic NK cells Activated NK cell TNK cells DN T cells	CD3+ NK1.1 – CD3+CD4+CD8- CD3+CD4-CD8+ CD3- NK1.1+ CD3- NK1.1+NKp46+ CD3+NK1.1+ CD3+CD4-CD8-
Transplanted Recipient marker	CD45.2 alleles specific	PE BV510	All cell lineages	/
Transplanted Donor marker	CD45.1 alleles specific	PE	All cell lineages	/

2.2.8 Murine Haematopoietic stem cell transplantation assay

In irradiated transplant recipient mice, haematopoietic stem cells (HSCs) are capable of self-renewal and multi-lineage restoration of haematopoiesis. As such, bone marrow transplantation (BMT) is a critical test for determining the functional activity of murine HSCs (Eich et al. 2019).

2.2.8.1 HSC staining

To obtain pure HSCs from the bone marrow, CD45.2 bone marrow cells suspension was obtained as explained in section 2.1.2.6 and illustrated in figure 2.3/B. All procedure steps were performed under Class III biological safety cabinet to ensure sterile procedure conditions. Whole bone marrow samples were pelleted by centrifugation for 5 min at 500g, supernatant was decanted, and nucleated red blood

cells were lysed by NH_4CL for 2 minutes. Then lysed red blood cells were washed by adding sterile 2% FBS/PBS. Cells were then ready for c-kit enrichment.

2.2.8.2 c-kit enrichment using AutoMACS™ magnetic cell separation and HSC's sorting

Pelleted bone marrow cells were re-suspended in 300μl sterile 2% FBS/PBS containing 20μl of c-kit (CD117) magnetic microbeads (Milteny Biotec, Germany). Cells are then placed on a blood sample rotator (15 RPM) to avoid cells/magnet clumping and ensure homogenous staining and incubated for 20 minutes in dark. Then, cells are washed using 2% FBS/PBS and filtered by 40μl strainer (cells Trics) and then transferred into AutoMACS (Milteny Biotec, Germany) for c-kit enrichment procedure utilizing Possleds programme. Next, the enriched c-kit sample underwent SLAM staining explained in section 2.2.3.1. Following that, Lineage -ve CD48-CD150+, HSCs were sorted into 200μl sterile 2% FBS/PBS using a BD FACSAria™ fusion (BD Biosciences) gating strategy illustrated in Figure 2.4.

2.2.8.3 Bone marrow c-kit enriched sample cryopreservation

To carry out the leukaemia experiment, a small volume of BM c-kit frozen murine BM cells (around 2,000,000) was used. First, 10% DMSO and 90% FBS solution are prepared and refrigerated prior of sample processing. Then, the c-kit enriched sample was spun for 5 minutes at 500g at 4°C. After removal of supernatant, cells are resuspended in cold freezing media and promptly dispensed into a 2ml cryovial (Camlab limited) and stored at -80°C for less than one month or transferred into liquid nitrogen (-175 °C) for long term storage.

2.2.8.4 HSC transplantation

Primary transplantation was performed with the use of donor 150 HSCs (CD45.2) isolated from *Ldlr*$^{-/-}$ mice fed a HFD or ND and 200,000 whole bone marrow cells BL6.SJL (CD45.1) mice (competitor/support cells). Recipient CD45.1 mice were irradiated with a dosage of 9Gy (a split dose separated by 4 hours). 200,000 CD45.1 BM cells (competitor/support cells) were transplanted intravenously with 150 HSCs

into lethally irradiated CD45.1 recipient mice. Cells in 2%FBS/PBS were injected into recipient mice in amounts of up to 200µl per animal via tail vein. The mice were bled every four weeks until they were 16 weeks old to assess HSCs function and multi-lineage haematopoietic reconstitution capacity. For the total engraftment assay, the mice were dissected after 16 weeks for the bone marrow, spleen, and thymus immunophenotypic assessment Figure 2.15.

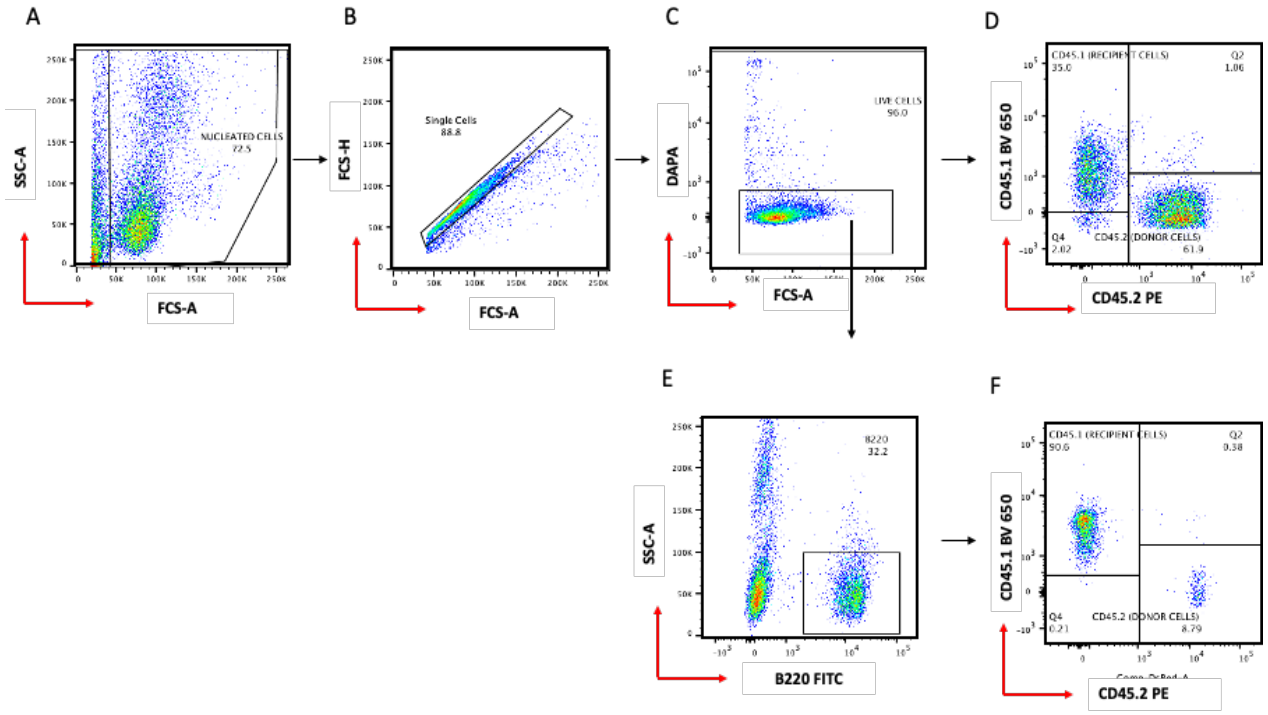

Figure 2.15 Gating strategy for donor contribution analysis in peripheral blood samples.

A) Nucleated cells were gated excluding debris and nucleated RBC. B) Singlets were gated from FSC-H vs. FCS-A.C) DAPI negative are live cells and should exceed 90%. D) From live cells, CD45.2 (donor cells) Vs. CD45.1(recipient cells) were plotted to determine total donor contribution across the two main cohorts *Ldlr*$^{-/-}$ on ND and *Ldlr* $^{-/-}$ on HFD. E) Mature cells are also gated from live cells. F) From each mature cell populations, here B cells (B220) are the example, CD45.1 vs. CD45.2 were assessed to donor contribution measurements.

2.2.9 MLL/AF9 Leukemogenesis assay

MLL/AF9 is a fusion gene generated by the t (9;11) translocation. It is responsible for producing many subtypes of acute leukaemias and one of them is human acute monocytic leukaemia. HSPC cells transduced with MLL/AF9 possess the potential to initiate leukaemia and differentiate into mature progenies in vivo. Also, they expand without limit in vitro. thus, enabling to transfer clonal leukemic cells into large number of experimental mice (Hasegawa et al. 2015).

2.2.9.1 c-kit enrichment and cryopreservation

Ldlr$^{-/-}$ bone marrow cells from HFD and ND groups were obtained using the c-kit enrichment procedure explained in section 2.2.3.1 and section 2.2.8.2. Frozen samples are then defrosted in 37^{o}C water bath until only a small piece of ice remains and were immediately spun for 5 minutes at 500g, the supernatant was decanted and washed again using 2% FBS/PBS to reduce the cytotoxic effect of DMSO on fragile frozen cells. The cells were then ready for retrovirus transduction.

2.2.9.2 Retrovirus production

2.2.9.2.1 DNA generation and plasmids

Thanks to Dr. Daniela Krause from Goethe University Frankfurt, who generously donated murine cell virus construct (MSCV-MLLAF9-GFP). pCMV-VSV-G plasmid was generously donated by Prof. Kamil Kranc (University of Edinburgh). StbI3 bacteria (Sigma) were used to copy DNA plasmids. Bacteria taken from glycerol stock were cultured into agar plate, then one colony was grown into 250 ml of LB- broth medium with 100 µg/ml of ampicillin (Gibco) on a shaker overnight. Next day, using EndoFree plasmid Maxi kit manufacturer's instructions (Qiagen), DNA was extracted and purified from the liquid culture. To elute the DNA, DNAase-free water (a molecular probe) was utilised. The optimal DNA concentration was > 1 µg/ml. The DNA aliquots were preserved in the freezer at –20 °C (Figure 2.16).

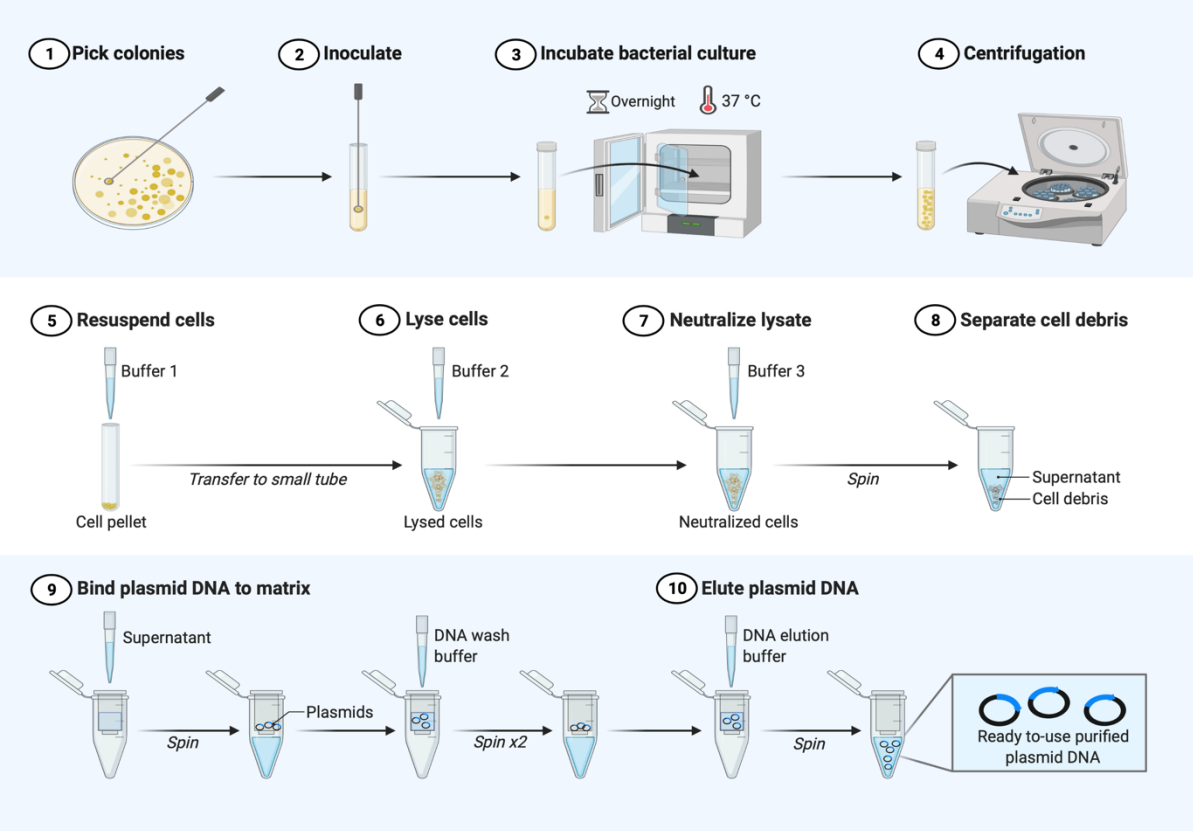

Figure 2.16 Plasmid Purification using EndoFree plasmid Maxi kit.

2.2.9.2.2 Packaging cell lines

To yield retroviral stocks, transient transfection of retroviral vectors into the Platinum-E packaging cell line was employed. Platinum E cells (Cells biolabs) were derived from the HEK293T cell line. Platinum E cells were preserved in DMEM (Gibco, UK) supplemented with 2 mM L-glutamine (Gibco) and sterile 10% heat-activated FBS, which was incubated in a humidified 5% CO_2 at 37°C. As soon as the cells reached 70-90% confluency, HEK293T cells were passaged.

2.2.9.2.3 Retrovirus packaging and generation

To produce retroviruses, a calcium phosphate method was employed. This method is based on formulating calcium phosphate-DNA precipitate to facilitate binding of the DNA to the cell surface. Initially, in a sterile 5 ml Falcon tube, 62.5µl of calcium chloride (Sigma) was agitated with 437.5µl of dd H_2O containing 11.5µg of MLL-AF9 retroviral

vector and retroviral envelop. Then, the mixture was transferred into another 5 ml Falcon tube containing 2X HEBES buffer saline (Sigma) drop by drop to introduce air, the retrovirus mixture was incubated for 12 minutes. Following that, transfection buffer was prepared using chloroquine and DEMEM (ThermoFisher). Then, 70% confluent Platinum E 10 cm dish plate was removed. Media was aspirated without disturbing the adherent Platinum E cells. Subsequently, freshly made transfection buffer was added and immediately the retrovirus mixture was gently mixed by swirling. The dish was incubated again in 5% CO_2 at 37 ^{o}C for 8 to 14 hours. Following that, transfection media was renewed, incubated for another 24 hours before harvesting the virus containing supernatant. Virus harvest was done post 24 hours and 48 hours and filtered through a 0.45 μm filter (Merk), and frozen at -80^{o}C (Guo et al. 2017a) (Figure 2.17).

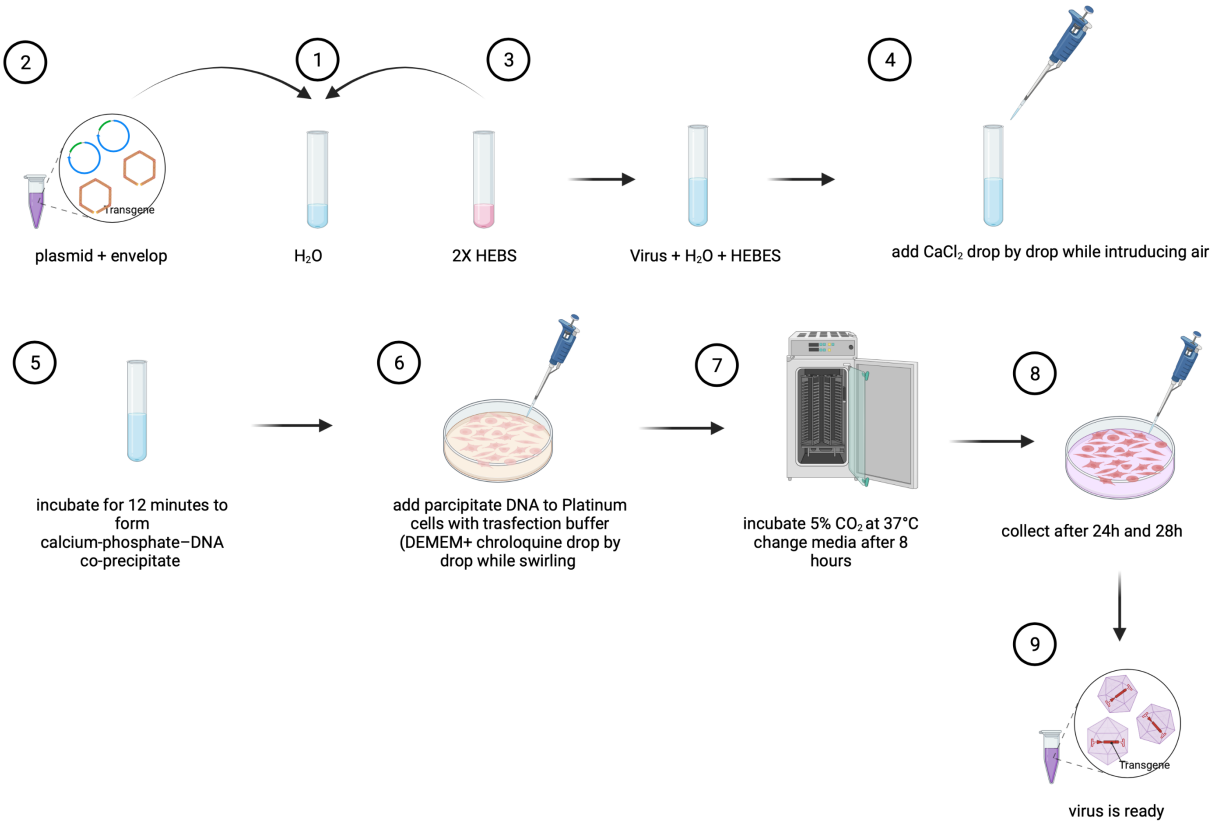

Figure 2.17 Retrovirus virus production using the calcium phosphate transient transfection method.

Briefly, a volume of $CaCl_2$ was added gradually to plasmid, envelop, dd H_2O and 2X phosphate-based buffer to form calcium phosphate precipitate. Then virus/DNA precipitate are incubated with the producer cell line (Plat E) in the transfection buffer. Generated viruses were collected 24- and 48-hours post-media change.

2.2.9.2.4 Retrovirus transduction of HSPCs

1 million c-kit+ bone marrow cells were cultured overnight in IMDM supplemented with 10% fetal calf serum, 40 ng/ml SCF, 20 ng/ml IL-3, and 20 ng/ml IL-6 (Pepro Tech, Rocky Hill, NJ, USA) along with 1% antibiotics. Following that, retrovirus encoding the oncogene MLL-AF9 were centrifuged for 2 hours at 2100g in a ready retronectin-coated plate. Afterwards, supernatant was removed, pre-stimulated c-kit cells were added, and the plate was centrifuged again for 5 min at 500g. The plate was incubated 5% CO_2 at 37°C, 8 to 12 hours. after the initial transduction, media was changed. MLL-

AF9 transduced cells were then maintained for 72 hours prior to sorting live cells for GFP+ fluorescence.

2.2.9.2.5 Pre-leukemic colony forming unit and leukemic mice peripheral blood immunophenotyping

2500 live, GFP+ transduced cells were plated using a 5 ml syringe attached to a 19 G blunted needle in methylcellulose medium (Stem Cell Technologies, Vancouver, Canada). The culturing media is Methocult™ 3232 media contains 400 ng/ml SCF, 200 ng/ml IL-6, 200 ng/ml, GM-CSF, 200 ng/ml IL-3, and 400 μg/ml Penicillin-Streptomycin (Thermo-fisher). Post 5 days of culture, colonies were counted, examined using an inverted microscope (Leica) and were immunophenotyped by flow cytometry. after the third round of replating and colonies recording, cells were counted. 100,000 cells c-kit positive cells (GFP+ cells) together with 200,000 CD45.2 BM cells (support cells) were transplanted into lethally irradiated primary CD45.1 recipients to generate pre-LSCs. Recipient mice were injected with cells in 2% FBS/PBS with up to 200 μL per mouse. After transplantation, recipient mice are kept in ventilated scantainers. Mice were monitored daily for leukaemia clinical signs and bled weekly for pre-leukaemic cells quantification (Figure 2.18).

In each CFC round, 20,000 cells were washed/ stained using a mixture of immature and mature myeloid antibodies (MAC-1, Gr-1 and c-kit), cells were first washed with 2% FBS/PBS, then stained with diluted antibodies, incubated for 30 min at 4^{o}C. Afterword, cells were washed using 2% FBS/PBS and centrifuged for 5 min at 500g. after decanting the supernatant, cells were resuspended in 2% FBS/PBS. Cells were acquired BD LSR Fortessa™ (BD Biosciences) and myeloid markers expression where quantified (Virtaneva et al.) using FlowJo software (Tree star INC, USA). For peripheral blood pre leukaemia cells quantification, peripheral blood was obtained and processed as described earlier in Section 2.2.4. GFP+ cells % were analysed in FITC channel after acquisition on the BD LSR Fortessa™ (BD Biosciences) and analysed using FlowJo software (Tree star INC, USA).

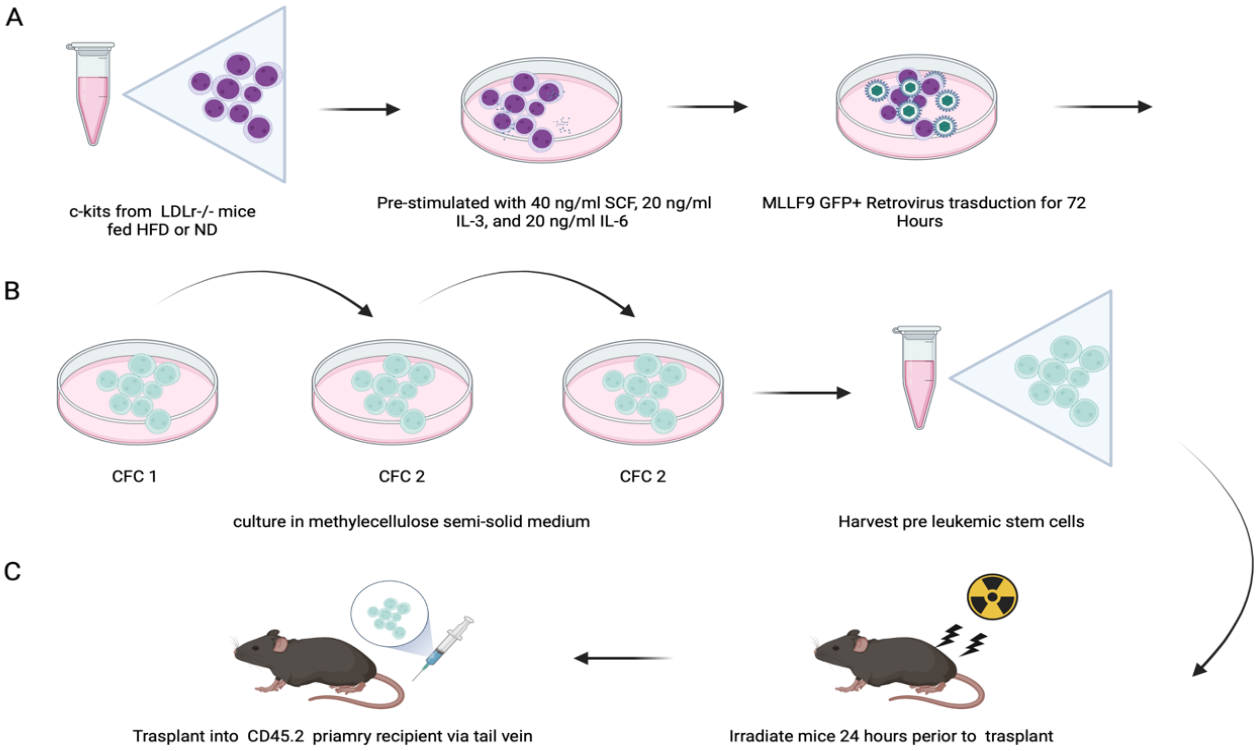

Figure 2.18 Retrovirus transduction of MLL-AF9 into c-kit+ cells from Ldlr-/- mice fed on HFD or ND and the pre-leukaemic assay design

A) c-kit+ cells are pre-stimulated with growth factors. B) They were plated for three rounds in Methocult^{TM} 3232 media. C) Transfected 100,000 MLLF9 GFP+ c-kit+ cells in 2% FBS/PBS along with 200,000 support cells were injected via tail vein into lethally irradiated recipient mice.

2.3 *In Vitro* methods

2.3.1 Cells line maintenance and culture

2.3.1.1 THP-1 and NOMO-1

THP-1 and NOMO-1 are both non-adherent human monocytic leukaemia cell lines.

THP-1 cells were derived from the bone marrow of a 1-year-old child with acute myeloid leukaemia (AML FAB M5) during his second relapse; the patient reported to have a high level of lysozyme activity in the cytoplasm, phagocytic activity, and cells responded to TPA-induced differentiation; cells carry the t(9;11) that leads the expression of MLL-AF9 fusion gene (Tsuchiya et al. 1980; Traore et al. 2005). They are considered an appropriate model for immune-toxicity experiments as they resemble the structural and functional characteristics of human monocytes. They are large, circular-shape and around 18 μm to 21 μm diameter (Prajitha and Mohanan 2021).

NOMO-1 was generated from the bone marrow of a 31-year-old woman with acute myeloid leukaemia (AML FAB M5a) During her second relapse, the cells were described as having significant lysozyme activity in the cytoplasm, phagocytic activity, and sensitivity to differentiation stimulation with TPA; they also had the t(9;11) with mutation (q23;p22) and carry MLL-AF9 fusion gene (Kato et al. 1986; Drexler et al. 2004; Quentmeier et al. 2004).

THP-1 cell line was obtained from Professor Dipak Ramji (Cardiff University) while NOMO-1 cell line was a kind gift from Professor Richard Darley (Cardiff University). They were grown and maintained at 37°C in a humidified 5% CO_2 incubator in RPMI1640 media with L-glutamine, supplemented with 10% (v/v) FBS and penicillin-streptomycin (100 units/mL and 100g/mL, respectively). Cells were doubled to 60% confluency in 75 cm^3 tissue culture flasks before being pelleted (5 minutes, 250 x g) and resuspended in new fresh culture medium at a 1:3 ratio.

2.3.1.2 Cell line establishment, cryopreservation, and storage in liquid nitrogen

Upon retrieving stock cells from liquid nitrogen storage, cells were defrosted promptly in a water bath. After pelleting (5 minutes, 250 x g), cells were resuspended in 5 mL fresh RPMI1640 media with L-glutamine, supplemented with 10% (v/v) FBS. Then transferred to a 25 cm3 tissue culture flask, and incubated at 37°C, 5% (v/v) CO_2. Culture media were changed on a regular basis until cell cultures were formed, and then maintained and sub-cultured according to the procedures outlined in Section 2.3.1.1. To generate frozen stocks, cells of passage 3 or fewer were grown to 80% confluency, pelleted, and resuspended in cell 70% DMSO/FBS freezing medium. Cells were then transferred to 1 mL precisely labelled cryotubes and frozen overnight at -80°C in a Nalgene™ Cryo 1°C freezing container. For long-term storage, cryotubes were moved to liquid nitrogen.

2.3.1.3 Cell counting and viability assessment

To determine the correct number of cells necessary for the experiment, the concentration of cells in suspension was determined using a glass haemocytometer equipped with a 5 × 5 grid (Helena Biosciences, UK). Cells were pelleted and reconstituted in 1 ml fresh RPMI1640 media with L-glutamine, supplemented with 10% (v/v) FBS. Following that, 20μL of cell suspension was diluted in 20μL trypan blue, 7μl was added to a haemocytometer and covered with a cover slip. The average cell count (live and dead) per square of the 5 x 5 grid was determined and multiplied by 10^4 and 2 (dilution factor) to produce the cell count per ml. Then live cell count was divided by the total cell count to calculate the viability percentage. Only viability with > 98% are used in further assays. 3 different passages were used to form both THP-1 and NOMO-1 cells in 3 independent experiments.

2.3.2 Cell-based assays

2.3.2.1 LDL and Oxi-LDL Cytotoxicity analysis

300,000 cells of the human monocytic leukaemia cells lines THP-1 and NOMO-1 were incubated in 1 ml fresh RPMI1640 media with L-glutamine, supplemented with 10% (v/v) FBS. 50 μg/ml of LDL (Generon, Kelen Biomedical, UK) and 15 μg/ml of oxi-LDL (Generon, Kelen Biomedical, UK) were added. For the control well, similar volume of vehicle was added. Cells were incubated in 5% CO_2 at 37°C. After 3 days in culture, cellular morphology was assessed, then cells were harvested, counted and 300,000 cells were re-cultured again in 1 ml fresh RPMI1640 media with L-glutamine, supplemented with 10% (v/v) FBS and the same volume of LDL and oxi-LDL respectively. Cells were replated up to 6 times. The remaining cells were immunophenotypically assessed by employing a wide range of myeloid markers, adhesion molecules and inflammatory receptors at day 22. Also, at the end of the experiment ROS studies were conducted (Pfaller et al. 2001) (Figure 2.19).

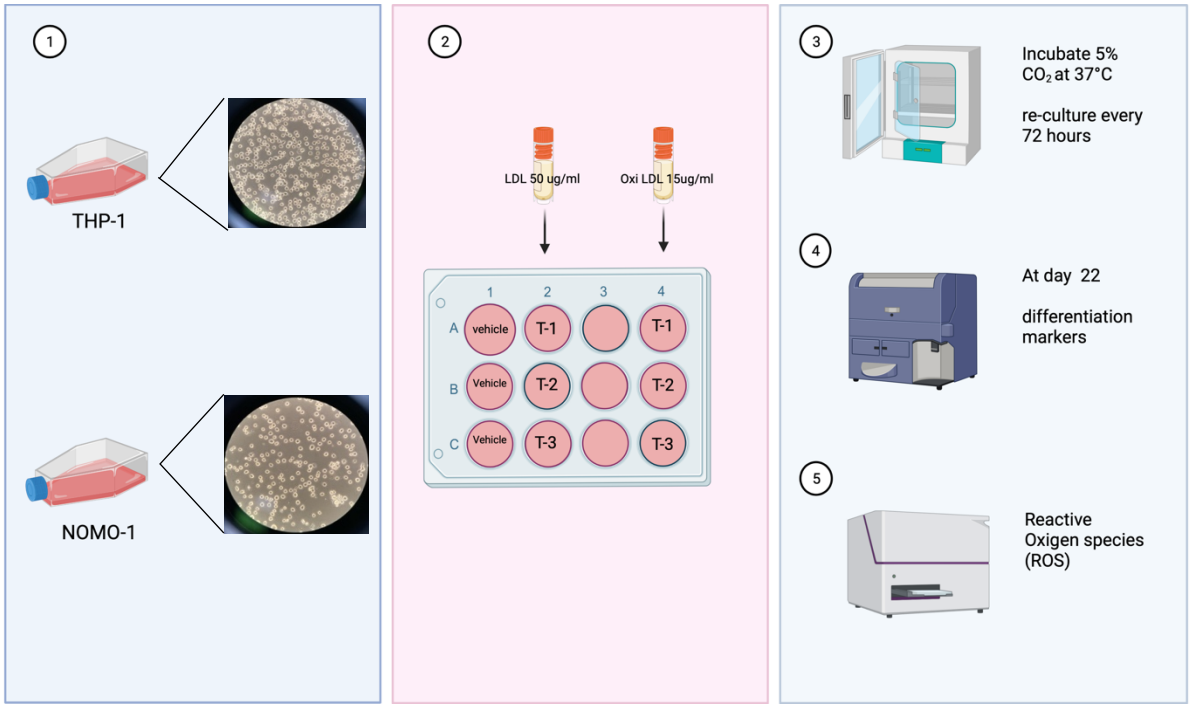

Figure 2.19 In vitro method to assess impact of LDL and Oxi LDL on AML cells. Maintained myeloid leukaemia cells lines were treated with LDL and re-cultured every 3 days. Cultured cells were characterised immunophenotypically, and reactive oxygen species were measured in three independent experiments.

2.3.2.2 Immunophenotyping

THP-1 and NOMO-1 cells were treated separately. 20,000 were washed with 2% FBS/PBS and centrifuged 5 min at 500g. then Cells were then split between master-mixes of antibody and isotype panels (Table 2.2) and incubated at 4^{o} C in dark for 30 minutes. Afterward, unbound antibodies were removed by washing the cells with 2% FBS/PBS and centrifuged 5 min at 500g. after decanting the supernatant, cells were repopulated in 2% FBS/PBS. Cells were acquired in BD LSR Fortessa^{TM} (BD Biosciences) and all markers expression percentages are recorded and median fluorescence intensity where quantified (Virtaneva et al.) using FlowJo software (Tree star INC, USA). MPO cytoplasmic staining was done using Intracellular Staining Permeabilization Wash Buffer (Biolegend).

2.3.2.3 Pre-analytical and post-analytical quality control

Quality control steps were implemented to ensure accurate, precise, and reliable immunophenotypic results in these assays. For pre-analytical quality control measurements, LDL and Oxi LDL were filtered using 0.22 μm filter (Merk) to avoid cultural contamination. Moreover, antibodies were pre-mixed in 1% bovine serum albumin/ 0.1% sodium azide to minimize human pipetting error. Then a portion was pre-tested using normal human blood. Culture wells were inspected for any bacterial growth or aberrant morphology or adherences every three days. also, supernatant was inspected for turbidity. Moreover, a negative control was employed containing the working solution solvent salts (vehicle) to assess antigenic changes precisely. THP-1 and NOMO-1 cells were only used when viability exceeded 97%. For post analytical quality control human peripheral blood sample (intra-control) was stained at the experiment day to test pre-mix antibodies efficiency. Moreover, peripheral blood results have also been used in fluorochrome compensation step. Furthermore, three negative controls levels were used. Negative tube with no antibodies added to set the dot plot negative quadrant, vehicle control tube for various markers baseline and cytoplasmic isotype negative tube.

2.3.2.4 Reactive oxygen species detection

The effect of LDL and Oxi LDL induced ROS production was evaluated using the MitoSOX™ Red Mitochondrial Superoxide Indicator Kit according to manufacturer's guidelines (Thermo Fisher). The kit employs a novel fluorogenic dye for highly selective detection of super- oxide in the mitochondria of live cells. The dye is cell permeable and selectively targeted to mitochondria. Once in the mitochondria, MitoSOX™ Red reagent is oxidized by superoxide and exhibits red fluorescence. Briefly, 80,000 cells were washed with 1X HBSS (Gibco™), then 100μl of 5μM Mitosox™ working solution were added to all vehicle and treated wells except for blank well. Cells were incubated for 30 minutes at humid 37°C, 5% (v/v) CO_2. Afterward, cells were seeded in 96 -well plated. Fluorescence was measured in microplate reader CLARIOstar^{Plus} at excitation/emission (Ex/Em) 510/580 nm.

2.3.3 RNA Sequencing

2.3.3.1 RNA sample processing

Bone marrow were processed as described previously in Section 2.1.3.5 and7000 HSC's (LSK+CD48-CD150+) were sorted on FACS-Aria™ into 350µl of 1%-ß-mercaptoethanol RLT-buffer. Samples were kept at -80° C until shipment.

2.3.3.2 RNA library preparation and sequencing

Library construction and RNA-sequencing were carried out by Novogene Company Limited (Cambridge, UK). Post RNA extraction, data's validity through quality control (QC) was carried out at each stage of the process. Samples passed through three steps of QC. Nanodrop for preliminary quantification, agarose gel electrophoresis to test the extent of RNA degradation and to detect possible contamination, and RNA integrity/quantification were checked by Agilent 2100™ Bioanalyser. After passing the QC, RNA was enriched using oligo(dT) beads. Then they were fragmented randomly using a fragmentation buffer. Subsequently, cDNA was synthesised using random hexamer and reverse transcriptase. Following that, second-strand synthesis buffer (Illumina) was added with dNTPs, RNase H and Escherichia coli polymerase I. cDNA library underwent purification, terminal repair, A-tailing, ligation of sequencing adapters, size selection, and PCR enrichment to create the final cDNA product. Library concentrations were quantified using Qubit 2.0 fluorometer (Life Technologies) to be normalised to 1 ng/µl. DNA sizes were assessed using Agilent 2100™, then for better yield insert size was quantified by quantitative PCR (Q-PCR). Lastly, DNA libraries were pooled together and normalised to 4nM and sequenced using a 75-base-paired-end (2x75bp PE) dual-index-read-format on the Illumina® HiSeq™ sequencer as per the manufacturer's guidelines.

2.3.3.3 RNA sequencing bioinformatic analysis

Raw data from Illumina HiSeq™ were recorded in a FASTQ file. To analyse clean reads, data quality control was assessed using Phred score. Then raw data was

filtered to remove low quality reads or adapters containing reads by performing paired-end mode. Only filtered reads are used to map status of RNA-sequenced data to the GRCm38.mm10 mouse-genome. TopHat2 software are used for mapping sequences and to calculate reads counting for both exons and transcripts. generated raw data, including the number of reads that corresponded to each gene were assembled by cufflinks (Trapnell et al. 2010). To identify differentially expressed genes, DEseq2 Bioconductor package in the R-scripts statistical computing programme was used (Anders and Huber 2010). p-values and adjusted p-values (False Discovery Rate, FDR values) were calculated to minimise false discovery risks. Novogene carried out the analyses described above.

Once data sets were generated, biological replicates went through RNA-Seq pearson correlation between samples, where the closer the correlation coefficient is to 1, the greater the similarity of the samples. Then differential gene expression was analysed and reported by Volcano plots, cluster analysis and Venn Diagram. Following that, deferentially expressed genes were presented by Gene Ontology (GO, http://www.geneontology.org/) in a form of a list, chart and directed Acyclic graph (DAG). To explore multiple genes interactions KEGG (Kyoto Encyclopedia of Genes and Genomes) enrichment list, enrichment scattered plot and enrichment pathway were utilised. Gene Set Enrichment Analysis (GSEA) was also used to identify significantly enriched pathways with FDR values < 0.05 using KEGG in the GSEA Molecular Signatures Database (MSigDB, V4.0.2). Also, input data for differential expressed genes with adjusted p-value <0.05 were analysed using The Ingenuity Pathway Analysis (IPA, Qiagen-Bioinformatics) programme, to investigate the gene ontology and common canonical pathways. Finally, the Broad Institute's Morpheus online tool was used to generate heat maps for gene expression profiles and Prism™ were utilised to generate specific conditions heatmaps.

2.3.4 Statistical analysis

Statistical analysis and graphs were conducted using GraphPad Prism 9.4.1 software (GraphPad Software). Data were identified by the mean and error bars are displayed in standard error of the mean (SEM). Prior to analysis, all data were subjected to Anderson and Pearson tests for normality. Statistical significance was determined using an unpaired 2-tailed t-test, Mann-Whitney U test or One-Way ANOVA- Tukey's multiple comparisons test unless mentioned otherwise. Differences between samples were considered significant based on the p-value: *, $P < 0.05$; **, $P < 0.01$; ***, $P < 0.001$; ****, $P < 0.0001$.

Chapter 3: Examining the requirement for *Ldlr* in steady-state haematopoiesis.

3.1 Introduction

Haematopoiesis is a process of maintenance and maturation of all blood cells, including leukocytes (Alomari et al. 2019; Harslof et al. 2021). The founding unit of leukocytes is the Haematopoietic Stem Cell (HSC), which sustains blood production through life. HSCs, which reside in the bone marrow, comprise approximately 0.01% of total bone marrow cells (Mayle et al. 2013). They are predominantly quiescent and are classified as either long-term self-renewing or transiently self-renewing short-term HSCs (Trumpp et al. 2010). The HSC pool is maintained in steady-state settings by asymmetrical division, in which one descendent remains as an HSC and the other differentiates into a progenitor cell, which then differentiates into mature blood cells. This process is tightly controlled by a spectrum of intrinsic and extrinsic haematopoietic regulatory factors and cytokines (Oguro et al. 2013) (Wilson et al. 2008; Copley et al. 2012; Alomari et al. 2019).

HSC functions are directly influenced by and respond to a variety of physiological stressors with the potential to disrupt normal haematopoiesis, including DNA damage, inflammation, infections, metabolic stress, obesity, and psychosocial stress (Oguro 2019) (Poller et al. 2020). One of these haematopoietic stressors, chronic inflammation, is triggered by hypercholesterolemia that causes atherosclerosis (Murphy et al. 2014). Atherosclerosis begins when lipoprotein-rich cholesterol builds on the artery wall, and a state of chronic inflammation is sustained through the recruitment of innate immune cells as well as adaptive immune cells to the site of atherosclerotic plaque development (Libby 2002). Innate immune cells, that is monocytes, macrophages and granulocytes, are well-known for their roles in the progression of atherosclerosis (Murphy et al. 2008). Granulocytes are proposed to be the first cells to be drawn to the developing plaque, where they release elastase and metalloproteinase, which causes extracellular matrix disintegration and inflammatory cell adhesion (Drechsler et al. 2010; Cain et al. 2011). Monocytes, that are attracted later, absorb lipids and differentiate into foam cells, which are characteristic of

atherosclerosis (Swirski et al. 2007). Inflammatory and/or activated vascular cells also generate inflammatory cytokines like tumour necrosis factor (TNF)- α interferon (IFN)-γ, granulocyte macrophage colony-stimulating factor (GM-CSF), and monocyte CSF (M-CSF), which exacerbate inflammation (Rafieian-Kopaei et al. 2014). As a result, hypercholesterolemia-related leucocytosis, and monocyte-to-macrophage conversion aid atherosclerosis progression (Rafieian-Kopaei et al. 2014). Thus, haematopoietic cells have been identified as critical participants in the origin, progression, and continuance of atherosclerotic plaques (Libby 2002). Indeed, a link between cardiovascular diseases, hypercholesteremia and leucocytosis is now well established, with most patients with cardiovascular disease displaying neutrophilia and monocytosis (Soehnlein and Swirski 2013).

3.2 Aims

Hypercholesteremia is defined by increase in low density lipids (LDLs) and decrease in high-density lipids (HDLs) (Mehu et al. 2022). LDL is delivered into cells via LDL receptors (LDLr) and digested into amino acids and cholesterol via receptor-mediated endocytosis (Yang et al. 2020a). Thus, a major regulatory goal of the LDLr pathway is to keep LDL levels in the blood low to avoid the formation of vascular fatty streaks (Huszar et al. 2000). LDLr also aids the uptake of apolipoprotein B and E-containing lipoproteins into the cell (Yang et al. 2020a). LDL receptor deficiency, as well as mutations in the LDL receptor gene, are responsible for the phenotypic cardiovascular events seen in familial hypercholesterolemia (Mosig et al. 2008). Mice lacking *Ldlr*, when fed a typical diet, have slightly higher plasma cholesterol levels than wild-type mice and develop no or only very moderate atherosclerosis (Venegas-Pino et al. 2013). In terms of lipoprotein particles, the rise is more pronounced in IDL (intermediate density lipoprotein) and LDL particles, but HDL and triglycerides remain unaltered (Emini Veseli et al. 2017). Preliminary analysis of blood and bone marrow of *Ldlr* $^{-/-}$ mice fed a high-fat diet have revealed increased HSPC proliferation and differentiation with myeloid bias as well as increased BM cell mobilization (Feng et al. 2012). Subclasses of lipoproteins appear to regulate HSC proliferation differently, with LDLs promoting and HDLs inhibiting HSC numbers (Feng et al. 2012; Seijkens et al.

2014) (Kaperonis et al. 2006). However, the impact of *Ldlr* absence on steady-state haematopoiesis in the setting of a normal diet has not been defined comprehensively.

Thus, in this chapter, a germline defective *Ldlr* mouse model was employed to assess steady-state haematopoiesis, specifically assessing HSPC compartment, lineage committed progenitors and fully differentiated cells in *Ldlr*$^{-/-}$ mice aged 8–12 weeks and their wild-type control counterparts. In these *Ldlr* loss of function mice, immunophenotypic investigation of haematopoietic cell compartments and functional potential of haematopoietic progenitors was conducted in CFC assays (Figure 3.1).

This overarching goal of this chapter is to investigate the role of *Ldlr*$^{-/-}$ in comparison to wild-type controls in steady-state haematopoiesis, with the following specific aims:
1. Assess LDL receptor expression on haematopoietic stem and progenitor cells (HSPCs) and lineage committed cells in the bone marrow using bioinformatics and flow cytometry.
2. Evaluate the abundance of haematopoietic stem and progenitor cells (HSPCs) and lineage committed cells in the bone marrow by immunophenotyping.
3. Characterise lineage committed cells in the peripheral blood, spleen, and thymus by immunophenotyping and complete blood count (CBC) analysis
4. Determine the functional capacity of haematopoietic progenitors by use of the colony forming cell (CFC) assay.
6. Evaluate levels of plasma cytokines and chemokines to discern levels of inflammation.

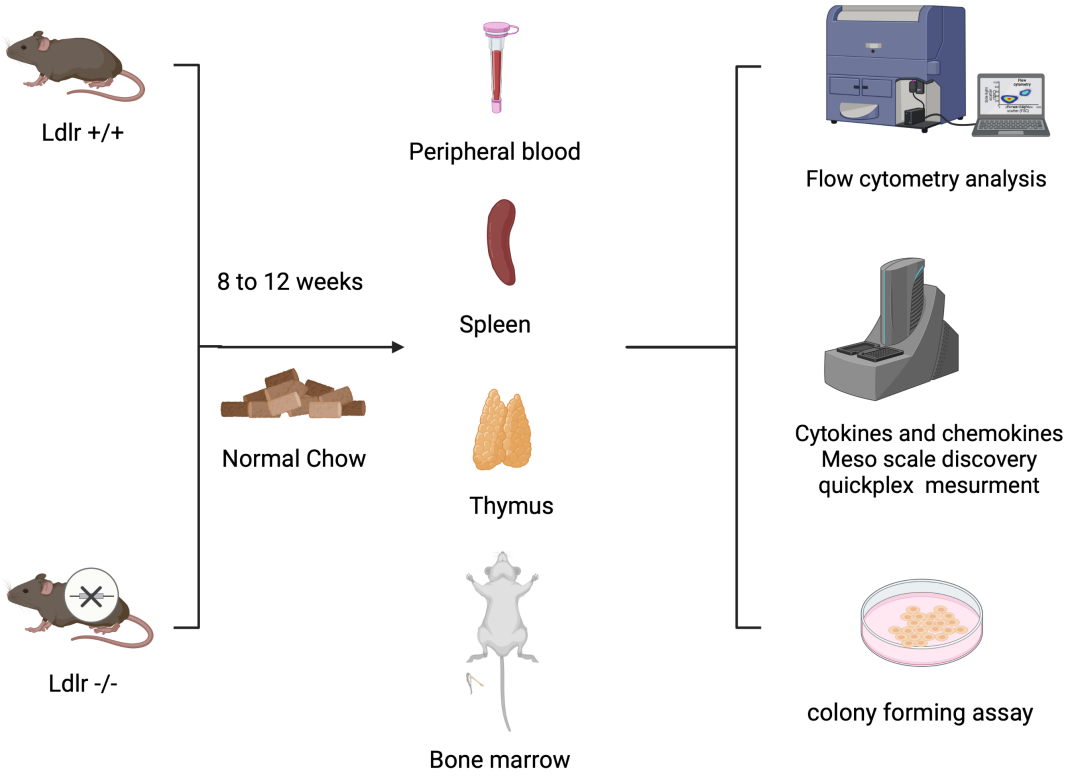

Figure 3.1 Experimental method for determining the role of Ldlr in haematopoiesis. Ldlr-/-: Ldlr knock-out mice, Ldlr+/+: wild—type mice.

3.3 Results

3.3.1 LDLR expression on normal mouse haematopoietic cells

In 2019, Bagger et al. in Bloodspot generated a database of mRNA expression across all humans and murine haematopoietic cell types. Interrogation of single cell expression data for *Ldlr* in this database revealed that *Ldlr* expression is expressed in HSC sub-populations, and myeloid and dendritic cell progenitors but at a comparatively lower level in lymphoid progenitors (Figure 3.2). However, murine LDLR protein expression in steady-state haematopoiesis and more mature myeloid and lymphoid populations has not been established. Using LDLR antibody, we therefore measured LDLR surface protein levels by flow cytometry of 8–12-week-old wild-type mice to assess its presence on immature and mature murine blood cell types (Figure 3.3). LDLR was expressed on HSC containing LSK, and its sub-populations (HSPC-1, HSPC-2, HSCs and MPP), accounting for 1% -16% of these populations, and myeloid progenitors, lymphoid progenitors and mature lymphoid and myeloid blood cells expressed LDLR at a similar level to LSK. In contrast, MEP displayed the most abundant LDLR expression, with approximately 50% of this population expressing LDLR.

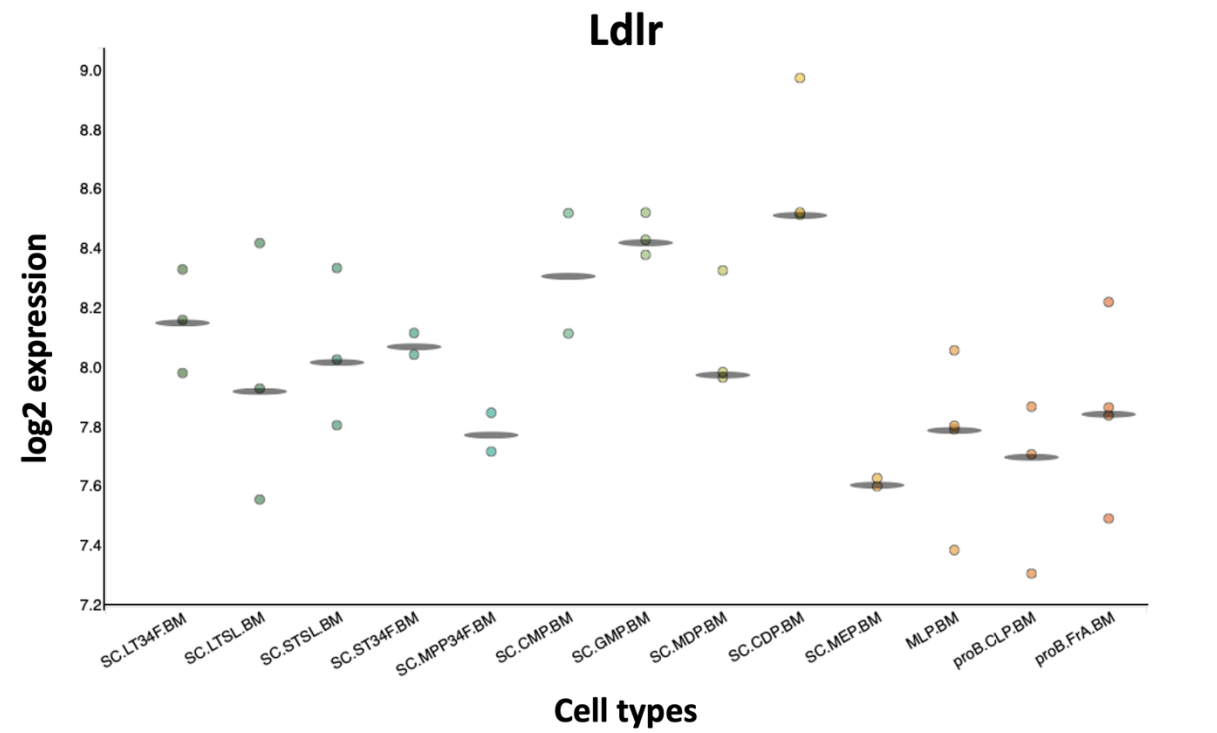

Figure 3.2 Ldlr gene expression database of mouse haematopoietic cells provided by BloodSpot (https://servers.binf.ku.dk/bloodspot/).

This database incorporates single cell RNA-seq and bulk sequencing of highly purified FACS sorted cells to visualize the expression (in log2 expression, to reduce the data variability at high intensities while increasing variability at low intensities) of genes or signatures across haematopoietic cells. Bloodspot generates a plot of gene expression in haematopoietic cells at various stages of development. Gene aliases and gene signature names are extracted from the MSigDB database. Data are displayed as a default figure. The plot is a strip chart of gene expression after normalisation, showing increased *Ldlr* gene expression in highly proliferative HSPCs starting from common dendritic precursors but not primitive haematopoietic cells (Bagger et al. 2019).

Key: SC.LT34F.BM:Long-Term Reconstituting Stem Cell (LT-HSC), SC.LTSL.BM: Long-Term Reconstituting Stem Cell, SC.STSL.BM: Short-Term Reconstituting Stem Cell, SC.ST34F.BM: Multipotent Progenitor (ST-HSC), SC.MPP34F.BM: Multipotent Orogenitor (MPP), SC.CMP.BM: Common Myeloid Progenitor, SC.GMP.BM: Granulocyte-Monocyte Progenitor, SC.MDP.BM: Monocyte DC Precursors (MDP), SC.CDP.BM: Common DC Precursors (CDP), SC.MEP.BM: Megakaryocyte-Erythroid

Progenitor, MLP.BM: Multilineage Progenitor, proB.CLP.BM: Common Lymphoid Progenitor, proB.FrA.BM: Fr. A (pre-pro-B).

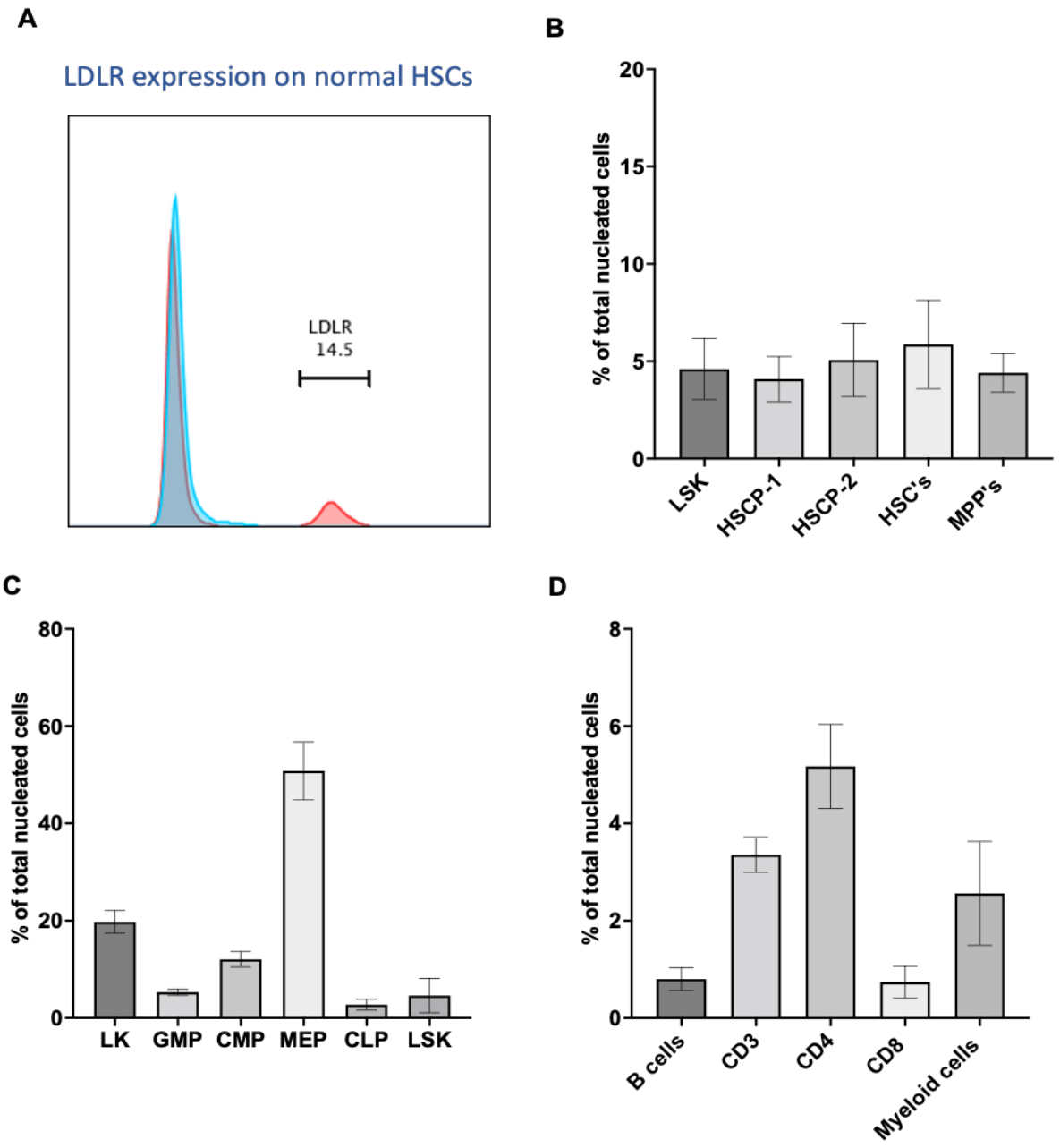

Figure 3.3 LDLR protein expression on mature and immature blood cells from 8-12 week old wild- type mice.

A. Representative FACS histogram of LDLR expression on normal BM HSCs. B. LDLR expression on LSK, HSC's HSCP-1, HSCP-2 and MPP's. B. LDLR expression on MEP and LK populations of haematopoietic progenitors. C. LDLR presence of blood cells in BM. D. LDLR expression in PB cells. Error bars represent the mean ±

SEM of the individual experiments using 4-5 wild mice. LSK: lin$^-$ Sca-1$^+$ C-kit$^+$, LK: lin$^-$ c-kit$^+$, HPC1: haematopoietic progenitor 1, HPC2: haematopoietic progenitor 2, HSCs: haematopoietic stem cells, MPP: multiple progenitors, GMP: granulocyte monocyte progenitor, CMP: common myeloid progenitor, CLP: common lymphoid progenitor.

3.3.2 Bone marrow cellularity is unaffected by the absence of Ldlr.

Having established expression of LDLR in the mouse haematopoietic system, we next turned to analyse the haematopoietic potential of *Ldlr*$^{-/-}$ mice. First, the BM cellularity of control (wild-type Thy1.1) and *Ldlr*$^{-/-}$ mice was evaluated, and no significant statistical differences were seen between the two genotypes (Figure 3.4).

3.3.3 *Ldlr*$^{-/-}$ mice have a significant increase impact on immunophenotypic HSC frequency.

Following that, different HSPC sub-populations were immunophenotyped from each genotype using flow cytometry. This experiment showed the distribution of the HSPC-enriched LSK compartments, which is a heterogeneous population enriched for HSCs, is similar in *Ldlr*$^{-/-}$ population in comparison to control (Thy1.1) mice. There were significant increases in HSCs in frequency in *Ldlr*$^{-/-}$ mice but no variation in the frequency and absolute number of MPP, HSPC1, and HSPC2 LK compartments was observed. Similarly, lineage-specific progenitors (GMP, CMP, MEP, and CLPs) were examined, and equivalence in the frequency and absolute numbers of each population within LK was observed in each genotype. Except for the increase in the frequency of HSCs, it can be concluded that *Ldlr* loss has minimal effect on HSPC content in steady-state haematopoiesis (Figure 3.5 and Figure 3.6).

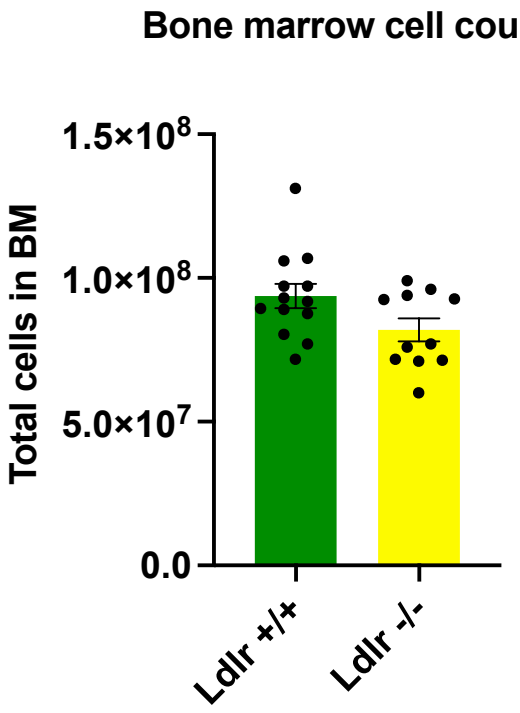

Figure 3.4 Ldlr deficiency has no effect on BM cellularity.

The numbers displayed represent the total number of cells in the BM extracted from both tibias and femur. Mann Whitney test was used for statistical analysis (GraphPad prism). For each genotype, the error bars indicate the mean SEM of the different tests utilising Control: 13 animals KO: 11 mice.

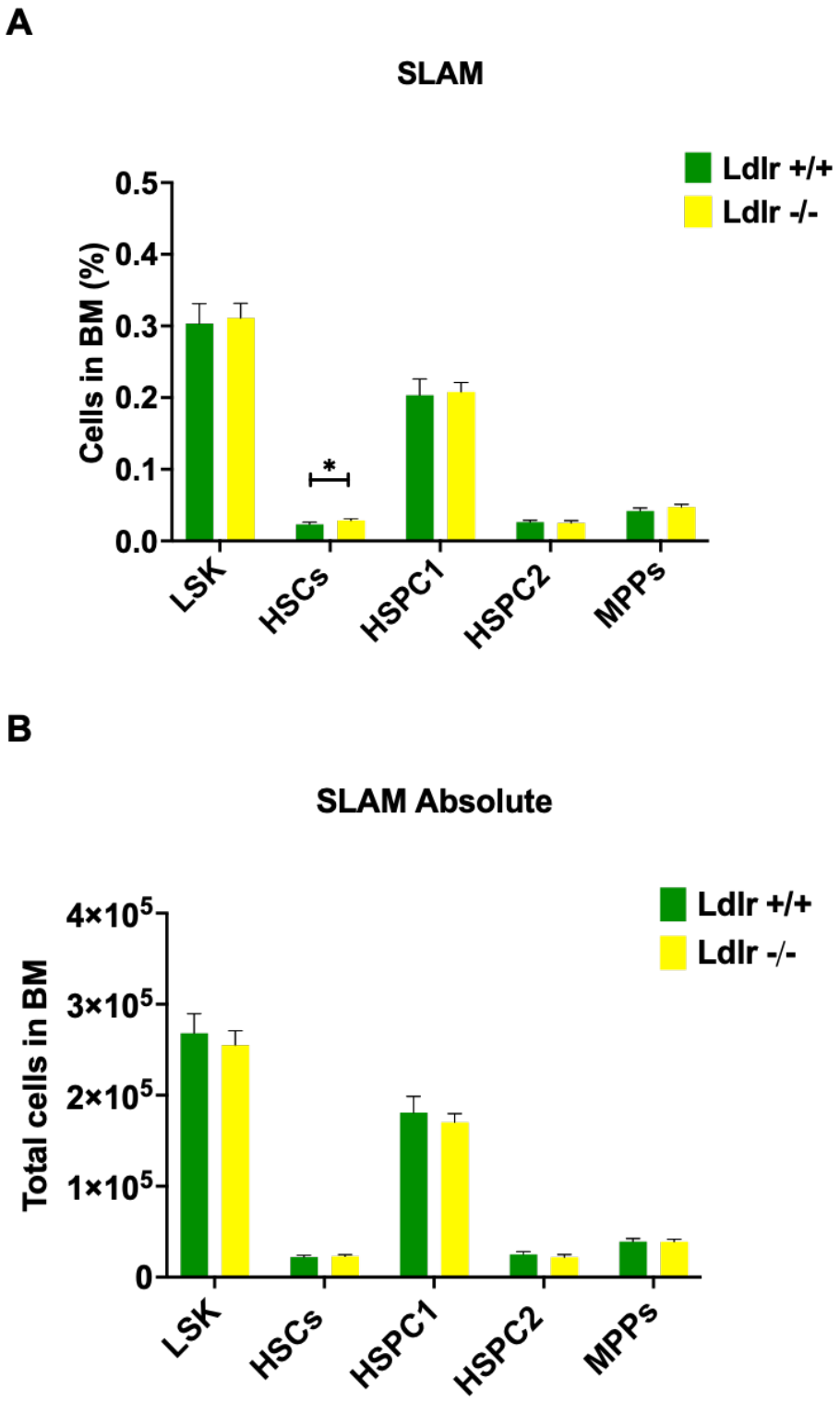

Figure 3.5 Loss of Ldlr has minimal effect on abundance of immunophenotypic HSPCs.

Flow cytometry analysis was used to label bone marrow cells from both tibia and femur for LSK compartments (HSCs, HSPC-1, HSPC-2 and MPPs). The percentages (frequencies) of each cell type were multiplied by the total number of cells in the BM

to get absolute counts of each cell type. The frequency (A) and total cell number (B) of distinct compartments from the total BM are presented here. The Mann Whitney test was used for statistical analysis (GraphPad prism); *P≤ 0.05. For each genotype, the error bars indicate the mean SEM of analysis utilising 9 wild-type mice and 9 *Ldlr* $^{-/-}$ mice.

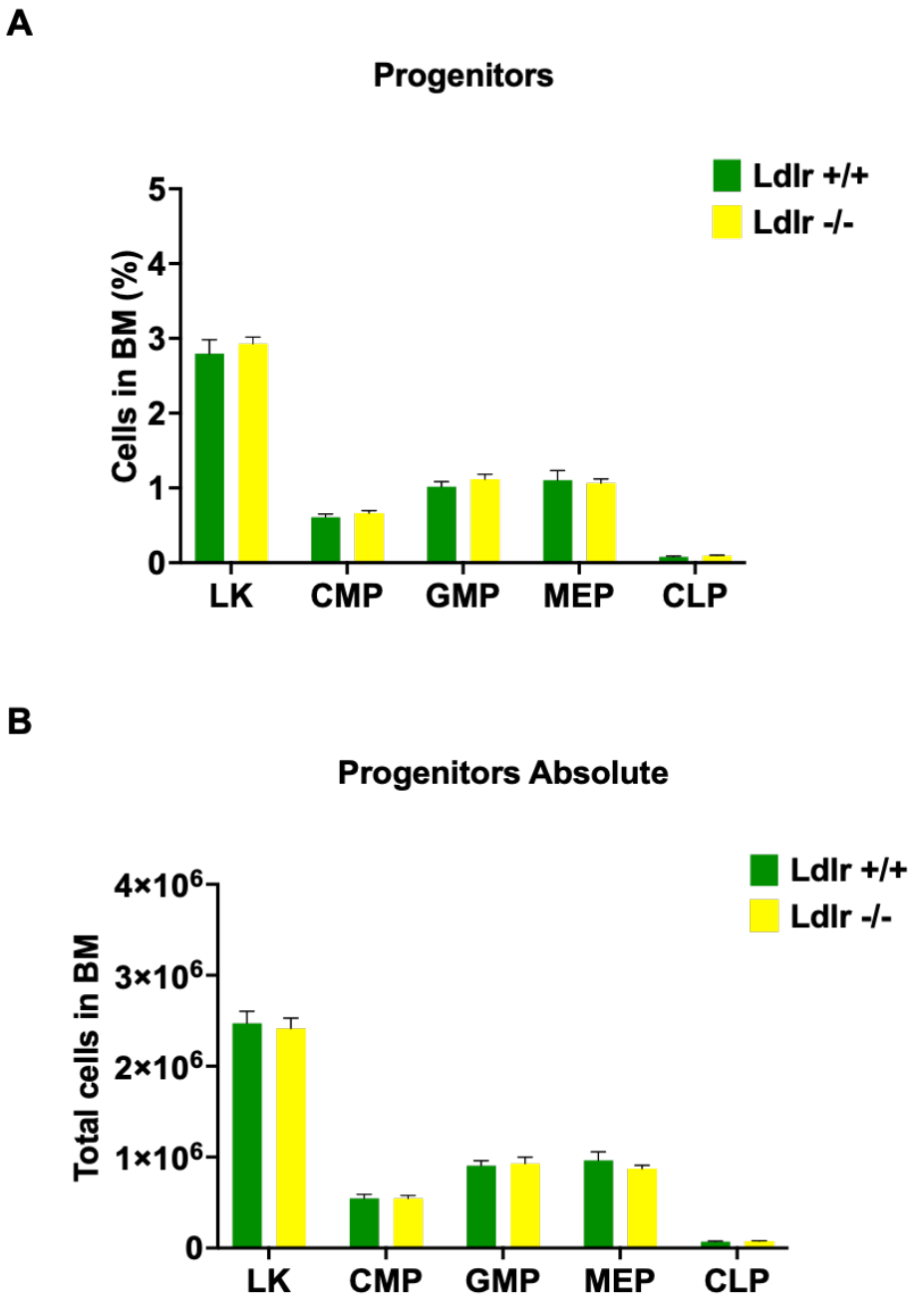

Figure 3.6 No impact of Ldlr gene deletion on haematopoietic progenitors.

Tibia and femur from both genotypes were collected and bone marrow cells harvested. Immunophenotypic staining was performed for LK and its compartments (GMP, CMP, MPPs) in addition to CLP. The percentages (frequencies) of each cell type were multiplied by the total number of cells in the BM to get absolute counts of each progenitor cell type. The frequency (A) and total cell number (B) of distinct compartments from the total BM are presented here. The Mann Whitney test was used for statistical analysis (GraphPad prism). For each genotype, the error bars indicate the mean SEM of the different analysis utilising 9 wild-type animals and 9 *Ldlr*$^{-/-}$ animals.

3.3.4 *Ldlr* loss had no effect on bone marrow lymphocytes.

Having examined the *Ldlr* in HSPCs, I next turned to analyse the impact of *Ldlr* on lineage-specific mature blood cells in the BM. It was observed that T lymphocytes (T helper or CD4, and T cytotoxic or CD8) and B lymphocytes frequency and absolute number the bone marrow were similar for each genotype (Figure 3.7).

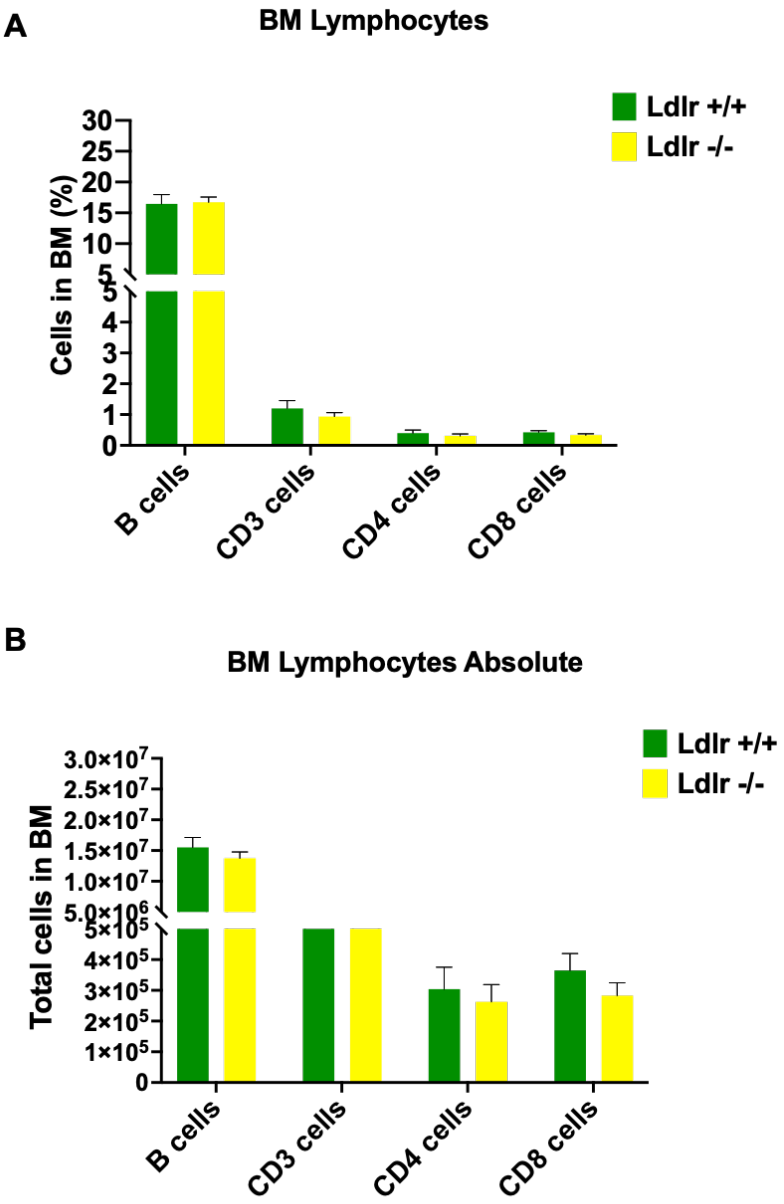

Figure 3.7 Ldlr deficiency has no impact on bone marrow cells.

The frequency and absolute cell count of major lymphoid cells are depicted in bar graphs (A and B). The Mann Whitney test was used for statistical analysis (GraphPad prism). The error bars show the mean SEM of individual studies using Control: 14 mice and KO: 11 mice.

3.3.5 *Ldlr* deficiency causes a significant increase in frequency of myelopoiesis and decrease in mature erythropoiesis.

Bone marrow mature myeloid and mature erythroid cells were immunophenotypically analysed in *Ldlr*$^{-/-}$ mice in comparison to control mice. Mature myeloid cells (Gr-1/ Mac-1) were significantly increased while Erythroid cells (Ter119/CD71) showed significant decrease in the relative percentage in the *Ldlr*$^{-/-}$ genotype. However, following absolute count analysis, only mature erythroid decrease remains significant. In addition, megakaryocytic cells (CD41) showed no significant change in both percentages and absolute numbers in the *Ldlr*$^{-/-}$ genotype (Figure 3.8).

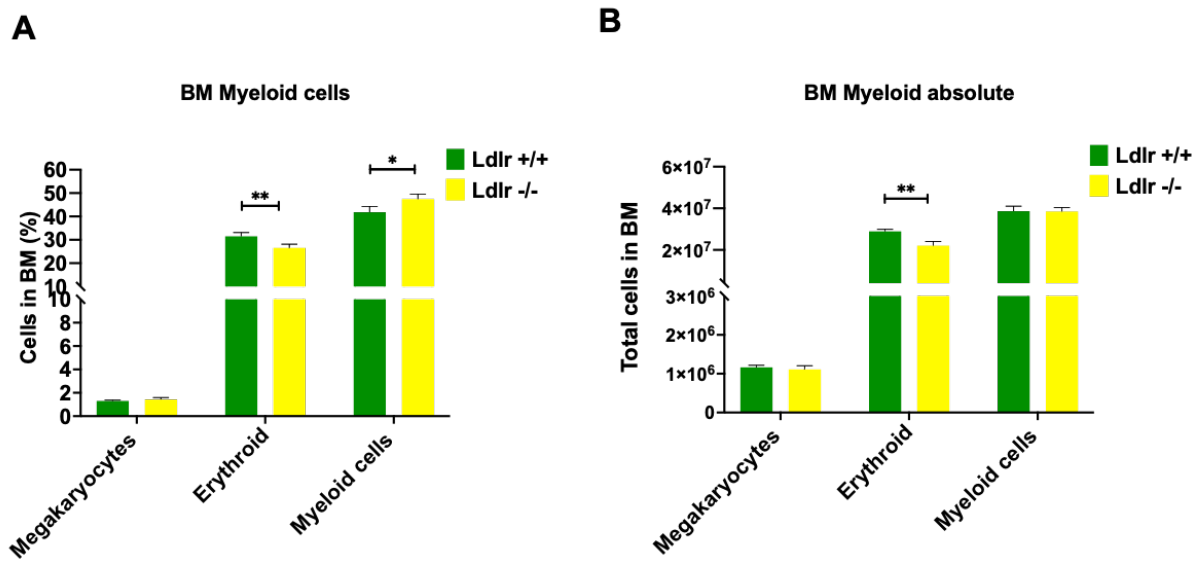

Figure 3.8 Ldlr deficiency enhances myelopoiesis and supresses erythropoiesis in steady-state bone marrow.

The frequency and absolute cell count of megakaryocyte, erythroid and myeloid compartments are depicted in bar graphs (A and B). The Mann Whitney test was used for statistical analysis (GraphPad prism); * P≤0.05, ** P≤ 0.01. The error bars show the mean SEM of individual studies using 13 wild-type mice and 10 *Ldlr*$^{-/-}$ mice.

3.3.6 *Ldlr* loss cause significant monocytosis and T helper cell lymphocytosis in peripheral blood.

To confirm bone marrow analysis results mirrored results in the peripheral blood system, we conducted detailed immunophenotypic analysis of peripheral blood, including T cells (T helper, T cytotoxic), B cells, granulocytes, and monocytes in *Ldlr*$^{-/-}$ mice. There was substantial increase in the myeloid population, particularly monocytes (bright MAC-1, dim Gr-1) in the *Ldlr*$^{-/-}$ genotype. Moreover, T helper (CD4) lymphocytosis was also observed in *Ldlr*$^{-/-}$ mice (Figure 3.9). Furthermore, complete blood count testing was performed and showed an increased WBC count in *Ldlr*$^{-/-}$ mice consistent with monocytosis and mild lymphocytosis observed by immunophenotypic analysis (Figure 3.9 and 3.10)

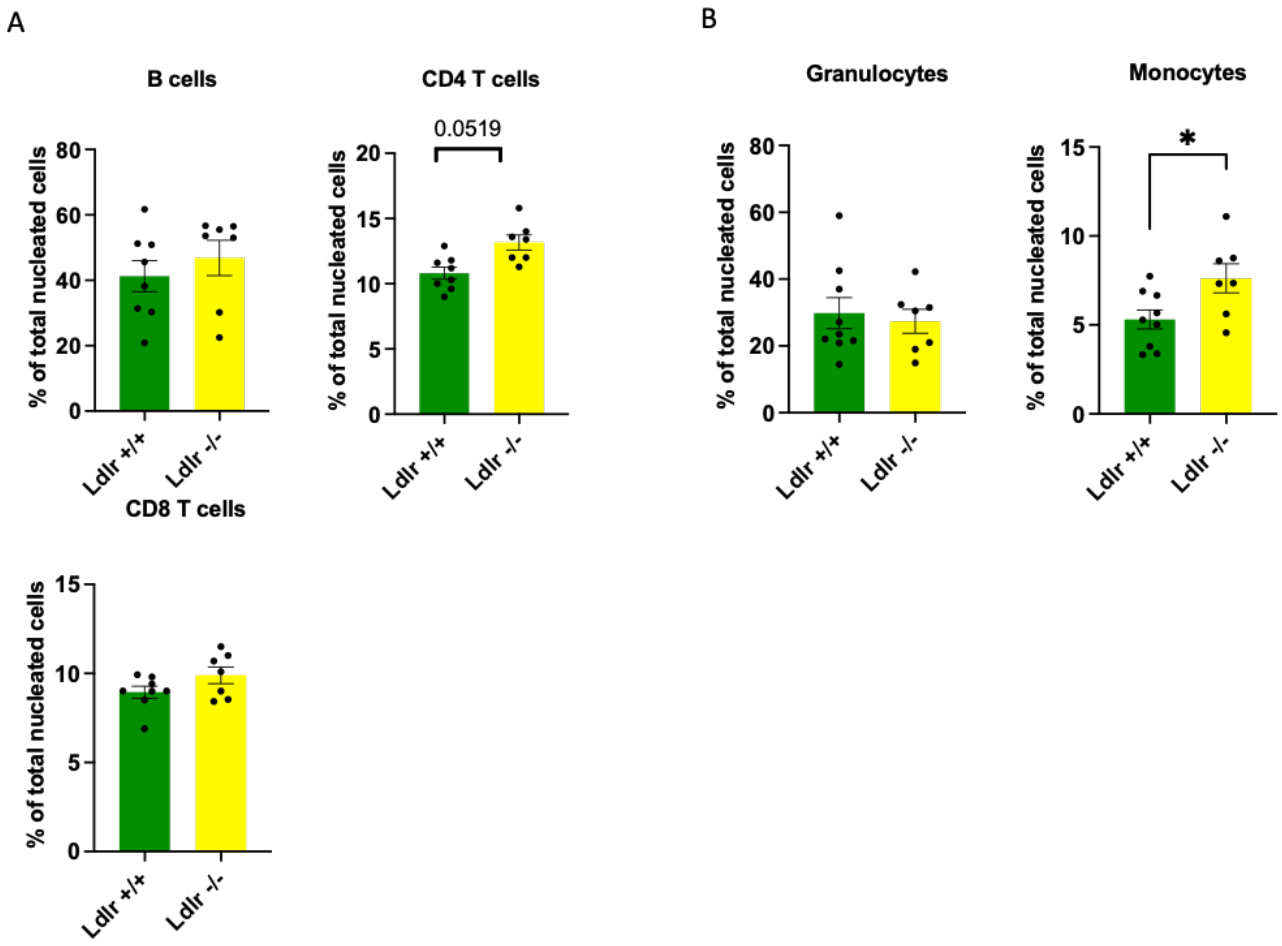

Figure 3.9 The frequency of monocyte cells in the peripheral blood is increased by Ldlr deficiency.

The frequency of myeloid and lymphoid cells in peripheral blood is represented by a bar graph for (A) Lymphoid cells and (B) Myeloid cells. The Mann Whitney test was used for statistical analysis (GraphPad prism); * P≤ 0.05, error bars indicate the mean SEM of individual studies employing 9 wild-type mice and 7 *Ldlr*$^{-/-}$ mice.

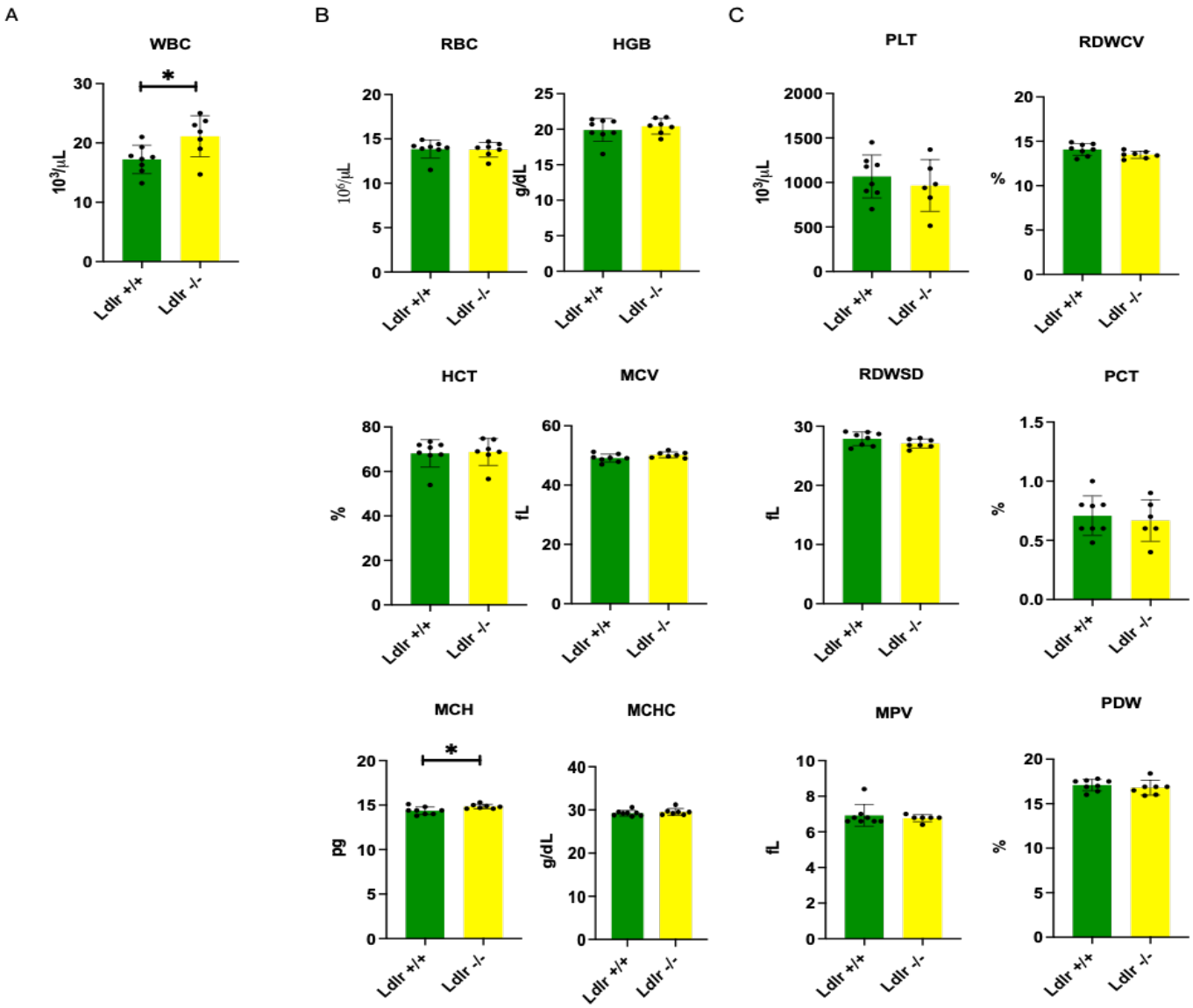

Figure 3.10 Complete blood count (CBC) analysis indicates a significant increase in white blood cell (WBC) and mean corpuscular haemoglobin (MCH) in Ldlr-/- mice.

CBC results are shown on bar graphs. Total white blood cells (A); red blood cells studies (B); platelets (C). Key: WBC: White blood cells, RBC: Red blood cells, HGB: Haemoglobin, HCT: Haematocrit, MCV: Mean corpuscular volume, MCH: Mean corpuscular haemoglobin, MCHC: Mean corpuscular haemoglobin concentration, PLT: Platelets, PCT: Platelet-crit, MPV: platelets distribution volume, PDW: platelets distribution width. The Mann Whitney test was used for statistical analysis (GraphPad prism); *P <0.05. The error bars indicate the mean SEM of individual studies employing 7 and 8 mice per genotype as controls.

3.3.7 Spleens from *Ldlr-/-* mice display enhanced extra-medullary myelopoiesis

We next analysed spleens of *Ldlr*$^{-/-}$ mice, as they are the main organ of extramedullary haematopoiesis (Cenariu et al. 2021) and production of blood cells outside the bone marrow happens when normal production is compromised due to various metabolic, genetic or other physiologic disorders (Fernandez-Garcia et al. 2020). In contrast to the control cohort, *Ldlr*$^{-/-}$ mice spleens showed a significant absolute count decline, even though there was no reduction in spleen weights between the two groups. I am speculating that the primary cause of this was because cell counts were performed using two different platforms during this thesis. Further cellular analysis for B cells (CD19), T cells (CD3) and myeloid cells (MAC-1, Gr-1), showed prominent myeloid cell accumulation in *Ldlr*$^{-/-}$ mice, mirroring data obtained in the bone marrow. On the other hand, there were no effect on total cell count of the myeloid and lymphoid populations in the spleen of *Ldlr*$^{-/-}$ mice due to the decrease in cellularity (Figure 3.11).

3.3.8 Moderate thymocyte-specific differentiation block in *Ldlr*$^{-/-}$ mice at the Double Negative to Double Positive transition.

Having observed T helper (CD4) lymphocytosis in *Ldlr*$^{-/-}$ mice, we next elected to assess T-cell precursors residing in the thymus. In the *Ldlr*$^{-/-}$ genotype, thymuses weight and total cell counts were comparable to wild type (Thy1.1) thymii. However, the frequency of double positive (dual CD4/CD8 positive was significantly increased. Consequently, double negative (dual CD4/CD8 negative), mature CD4 and mature CD8 were markedly decreased, indicating disrupted T-cell maturation in *Ldlr*$^{-/-}$ mice. These data suggest a block of thymocyte-specific differentiation block in *Ldlr*$^{-/-}$ mice at the DN to DP transition. In contrast, B cell frequency or counts remained unaffected between the genotypes (Figure 3.12).

3.3.9 Functional haematopoietic differentiation impairment in granulocyte-macrophage lineage in bone marrow of *Ldlr*$^{-/-}$ mice

So far, I have shown that *Ldlr* deficiency causes disruption to HSPC numbers and appears to impact haematopoietic differentiation, as judged by immunophenotyping, yet the functional capacity of *Ldlr*$^{-/-}$ bone marrow remains unclear. Thus, we used the methylcellulose CFC assay to functionally assess the haematopoietic differentiation capacity of *Ldlr*$^{-/-}$ bone marrow. Here, *Ldlr*$^{-/-}$ or wild type (Thy1.1) bone marrow cells were plated in cytokine enriched methylcellulose to facilitate HSPC differentiation. Total CFCs from *Ldlr*$^{-/-}$ BM demonstrated lower overall ability to differentiate. This defect mapped to the CFU-GM sub-class of haematopoietic progenitor, which was found to be significantly decreased in *Ldlr*$^{-/-}$ mice (Figure 3.13).

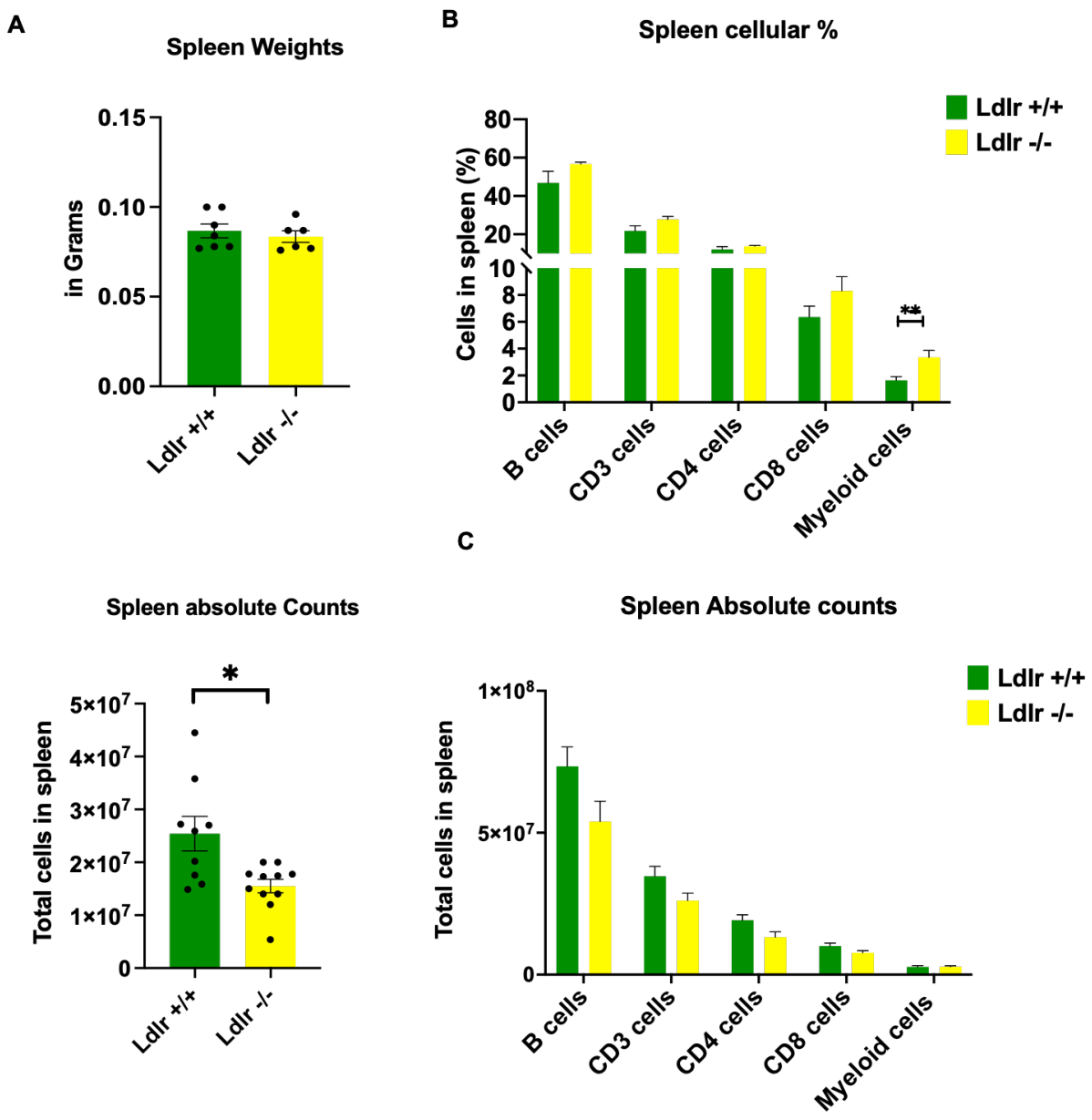

Figure 3.11 The absence of Ldlr has no influence on the frequency or cell count of B cells or T cells but increases frequency of myeloid cells in the spleen.

(A) total cell count and spleen weight. (B) B cells, T cells and myeloid cells frequencies were assessed immunophenotypically from *Ldlr*$^{+/+}$ and *Ldlr*$^{-/-}$ spleens. (C) B cells, T cells and myeloid cells total cell counts were calculated by multiplying total cell counts by specific cell percentages from *Ldlr*$^{+/+}$ and *Ldlr*$^{-/-}$ spleens. The Mann Whitney test was used for statistical analysis (GraphPad prism); *P≤ 0.05, ** P≤ 0.01. Error bars indicate the mean SEM of individual studies employing 9 wild-type mice and 10 *Ldlr*$^{-/-}$ mice.

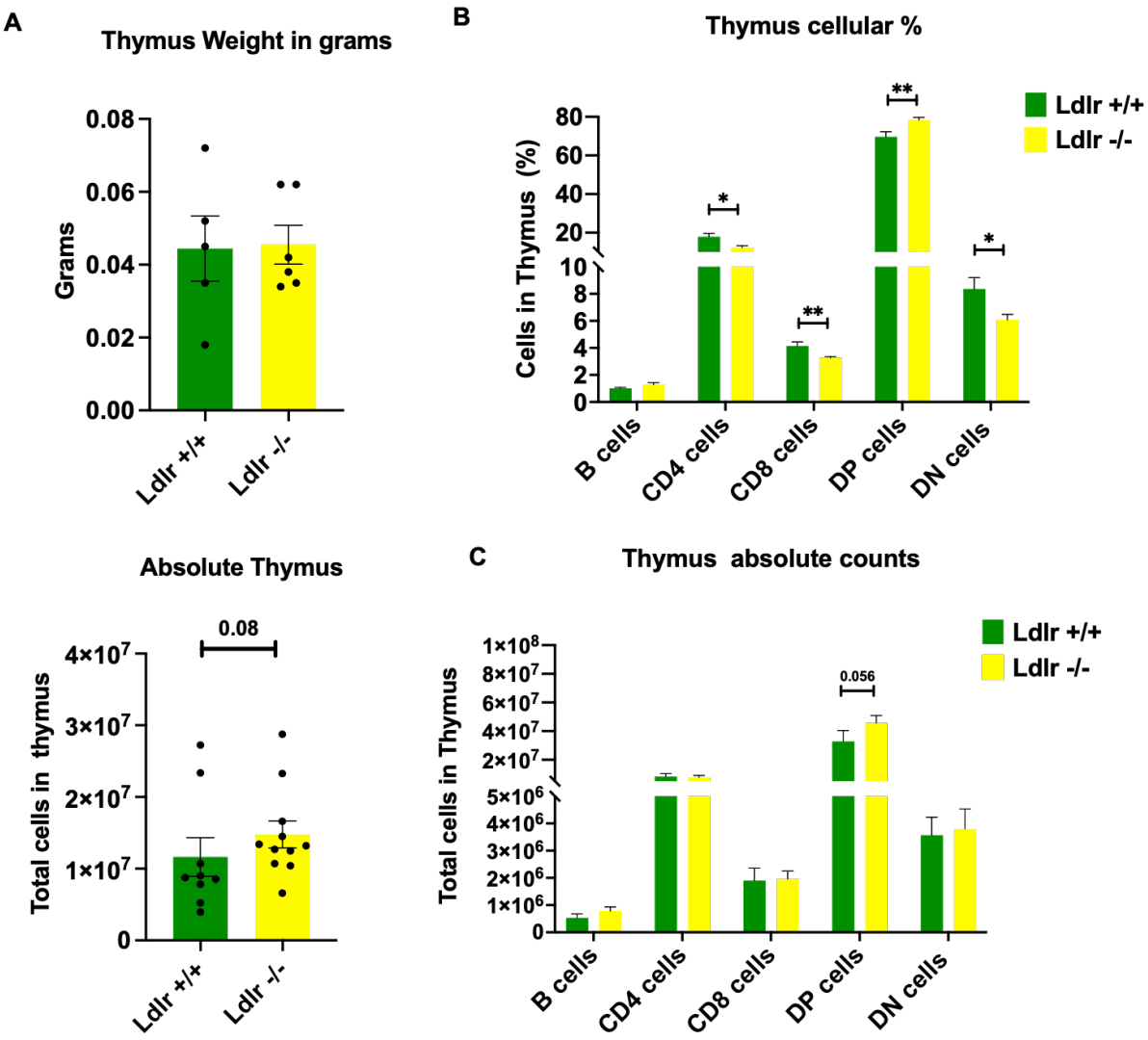

Figure 3.12 Disrupted T cell maturation in thymus of Ldlr-/- mice.

(A) Thymus wights were measured post harvesting, organs were smashed and filtered, and then total cell counts were evaluated. (B), B cells and T cells positive and negative selection cells were assessed and compared to wildtype mutual cell type. (C) subsequently B cells and mature and immature T cell sub-types were calculated by multiplying specific cell type by total cell counts. Statistical analysis was performed using a Mann Whitney test (GraphPad prism); ** P≤ 0.01, *P≤ 0.05. Error bars indicate the mean SEM of individual studies employing 9 wild-type mice and 10 *Ldlr*$^{-/-}$ mice.

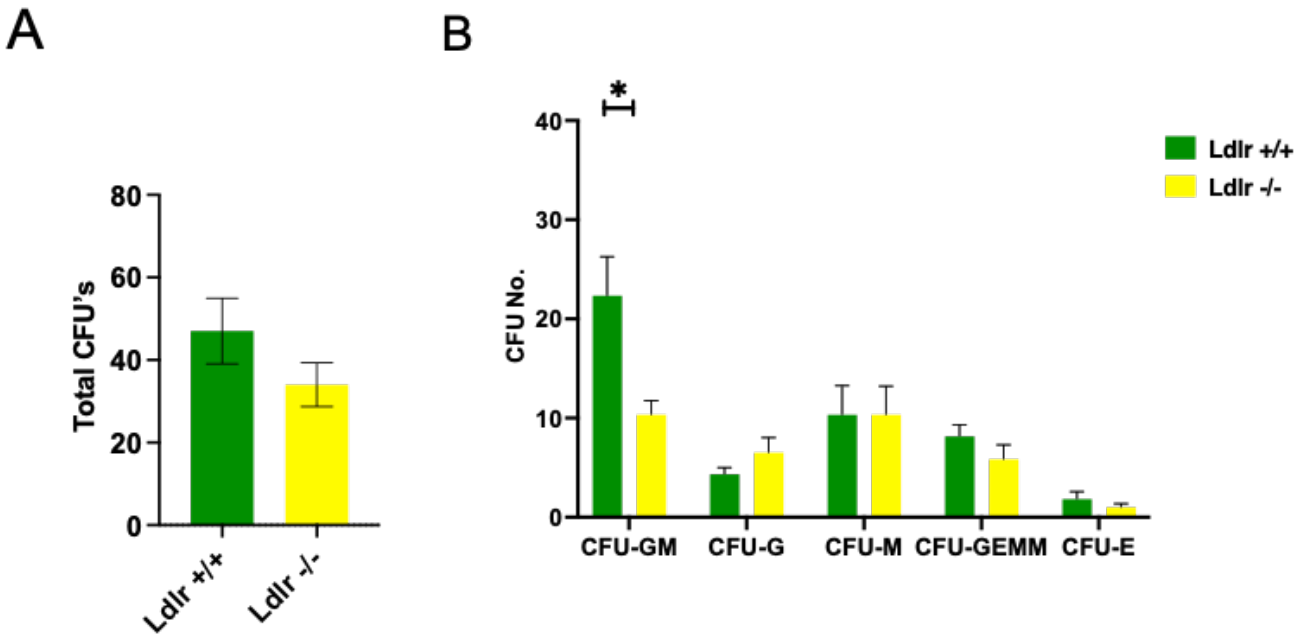

Figure 3.13 Bone marrow from Ldlr-/- mice displayed reduced granulocyte-macrophage lineage-restricted hematopoietic differentiation ability.

The total number of microscopically examined colonies is represented by a bar graph (A). CFU-GM (macrophage granulocyte), CFU-M (monocyte), CFU-GEMM (mixed) and CFU-E (erythroid) are the types of colonies mostly found in functional assays (B). The total cell number of mentioned units from the total BM are presented here (B). The Mann Whitney test was used for statistical analysis (GraphPad prism); *P≤ 0.05. The error bars reflect the mean SEM of the individual studies, which were conducted with six mice per genotype.

3.3.10 Haematopoietic stem cells from *Ldlr*$^{-/-}$ mice show an increase in proliferation

To investigate the mechanistic basis for increased HSC frequency in *Ldlr*$^{-/-}$ mice, we first investigated the cell cycle kinetics of HSPC populations by conducting the Ki67/DAPI proliferation assay. This assay discriminates quiescent cell population (G0 cell) and measure cell cycle distribution (G1, S, G2/M). Results indicated an increase in HSC cycling in the G2/S/M phase from *Ldlr*$^{-/-}$ mice, explaining the significant increase in frequency of HSCs observed from *Ldlr*$^{-/-}$ mice. However, there were no significant differences in frequencies of remaining haematopoietic stem/progenitor populations (HSPC-1, HSPC-2 and MPPs) (Figure 3.14). Additionally, no differences in cell cycling activity of committed haematopoietic progenitors was noted (Figure 3.15).

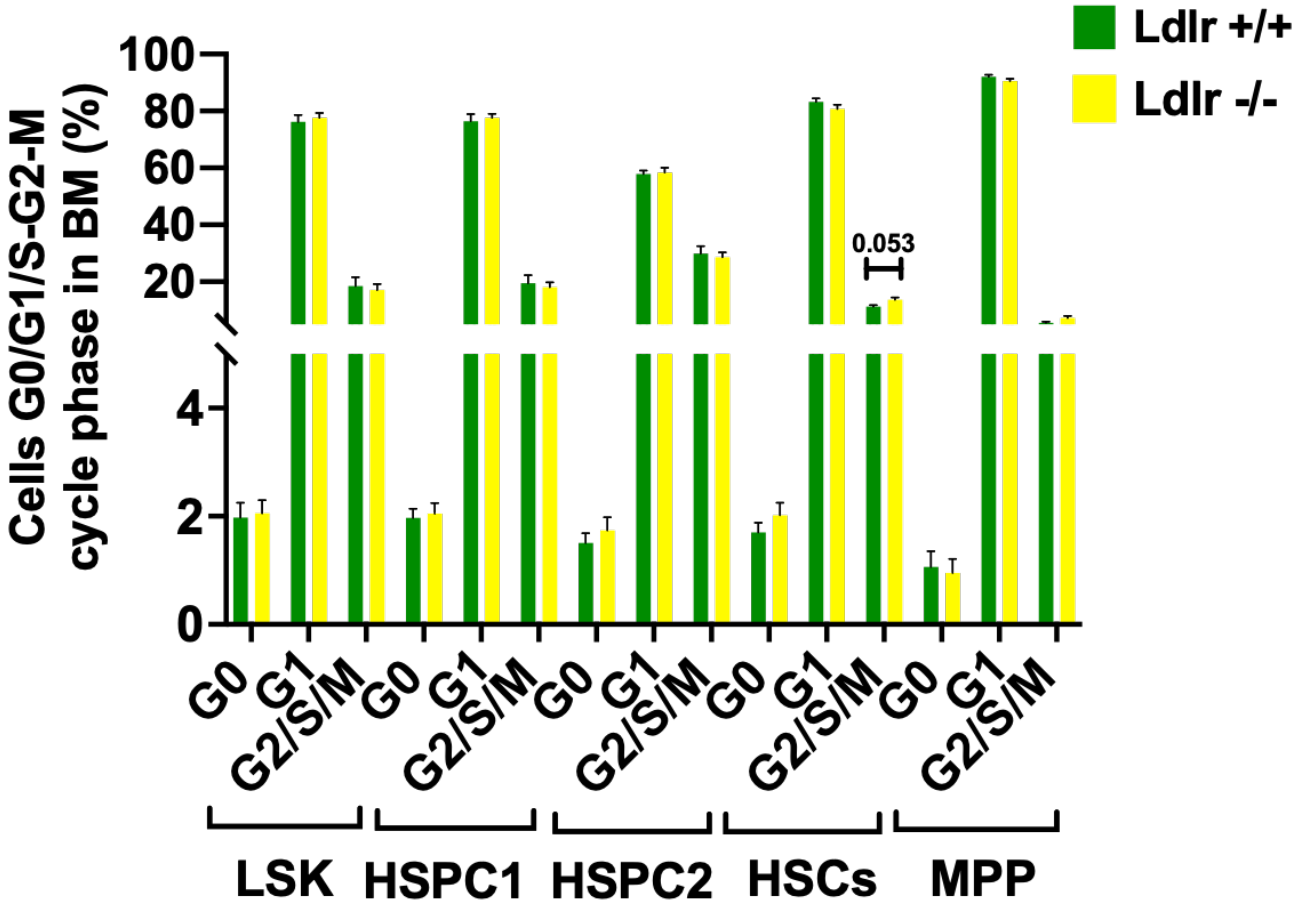

Figure 3.14 Ldlr-/- HSCs show increased proliferation.

Bar graph shows the frequency of G0, G1 and G2-S-M phases of cell cycle in haematopoietic stem LSK, HSCs, HSPC-2, HSPC-1 and MPPs. Statistical analysis was performed using a Mann Whitney test (GraphPad prism). Error bars represent the mean ± SEM of the individual experiments using 9 mice from each group.

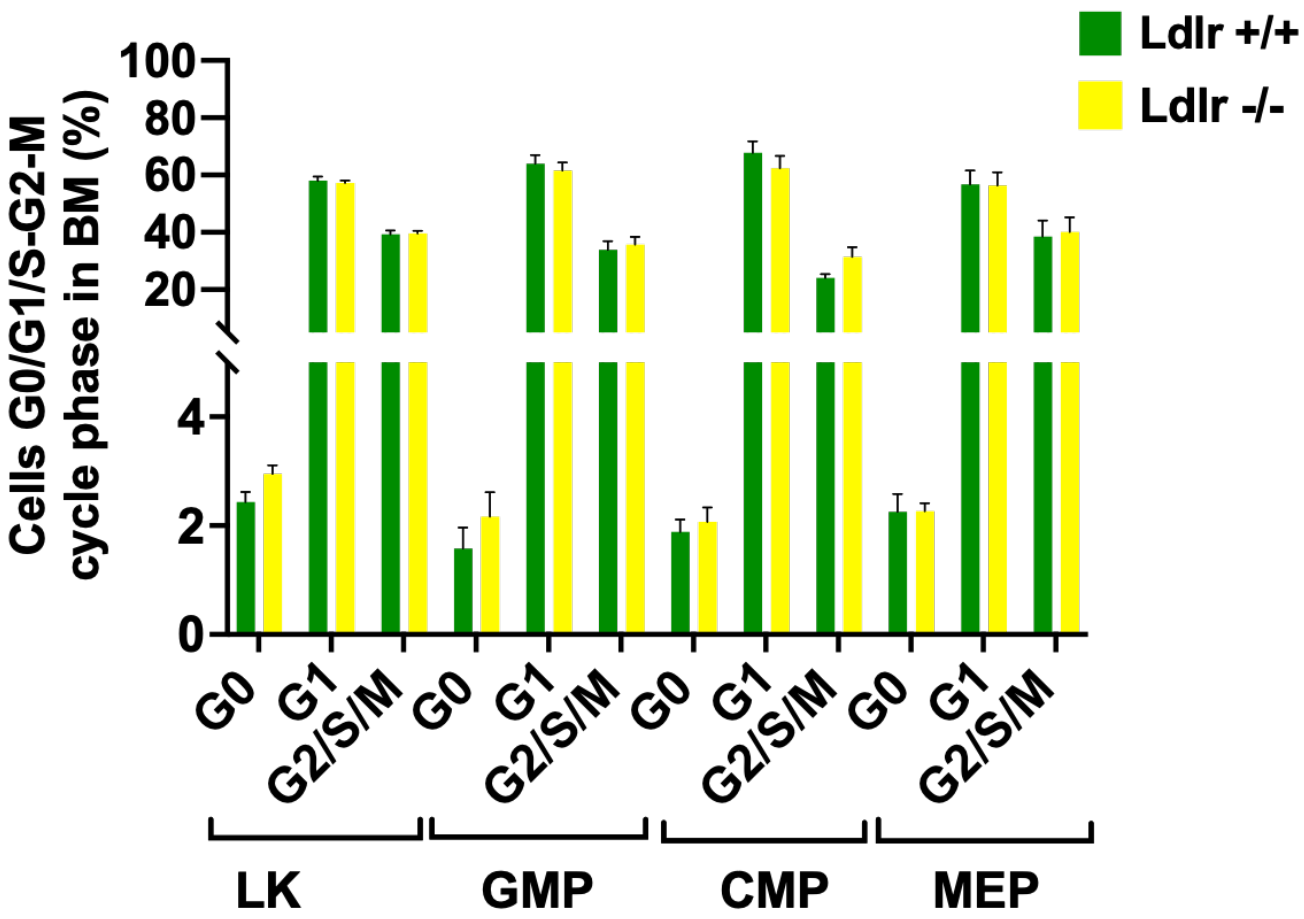

Figure 3.15 Ldlr deficiency has no impact on committed haematopoietic progenitor cell cycling.

Bar graph shows the frequency of quiescent G0 and proliferating G1, G2-S-M cell cycle stages in LK (A) and LK subpopulations GMP (B), CMP (C) and MEP (D). Statistical analysis was performed using a Mann Whitney test (GraphPad prism). Error bars represent the mean ± SEM of the individual experiments using 9 mice from each genotype.

3.3.11 Plasma from *Ldlr*$^{-/-}$ display enhanced inflammatory cytokines and chemokines

Since HSCs in *Ldlr*$^{-/-}$ mice were more proliferative, we next asked whether these mice had an enhanced inflammatory status, perhaps due to moderate hypocholesteraemia observed in these animals (Moore et al. 2003; Mukhopadhyay 2013), which may, in turn, explain the enhanced proliferative kinetics of HSCs. Cytokines are a group of low-molecular-weight proteins, they are important in cell signalling and immune system regulation and can be classed as either pro- or anti-atherogenic (Moss and Ramji 2016). Major cytokines are Interleukins (IL), colony-stimulating factors (CSF), tumour necrosis factors (TNF) and interferons (IFN). Chemokines Monocyte chemoattractant Protein -1 (MCP-1) and Macrophage inflammatory protein (MIP-1) are chemoattracting cytokines, its function is to recruit immune cells through intracellular signalling pathways. Using commercially available kits from Meso Scale Discovery (Rockville, MD), we assessed plasma from *Ldlr*$^{-/-}$ or control mice for IL-1β, IL-6, IL-10, IFN-λ, TNF-α, MIP-1α and MCP-1 expression. Illustrating the heightened inflammatory environment in *Ldlr*$^{-/-}$ mice, IL-1β, IL-6, IL-10, TNF-α and MCP-1 chemokine were all increased, providing a plausible mechanism for increased HSC proliferation in *Ldlr*$^{-/-}$ mice (Figure 3.16).

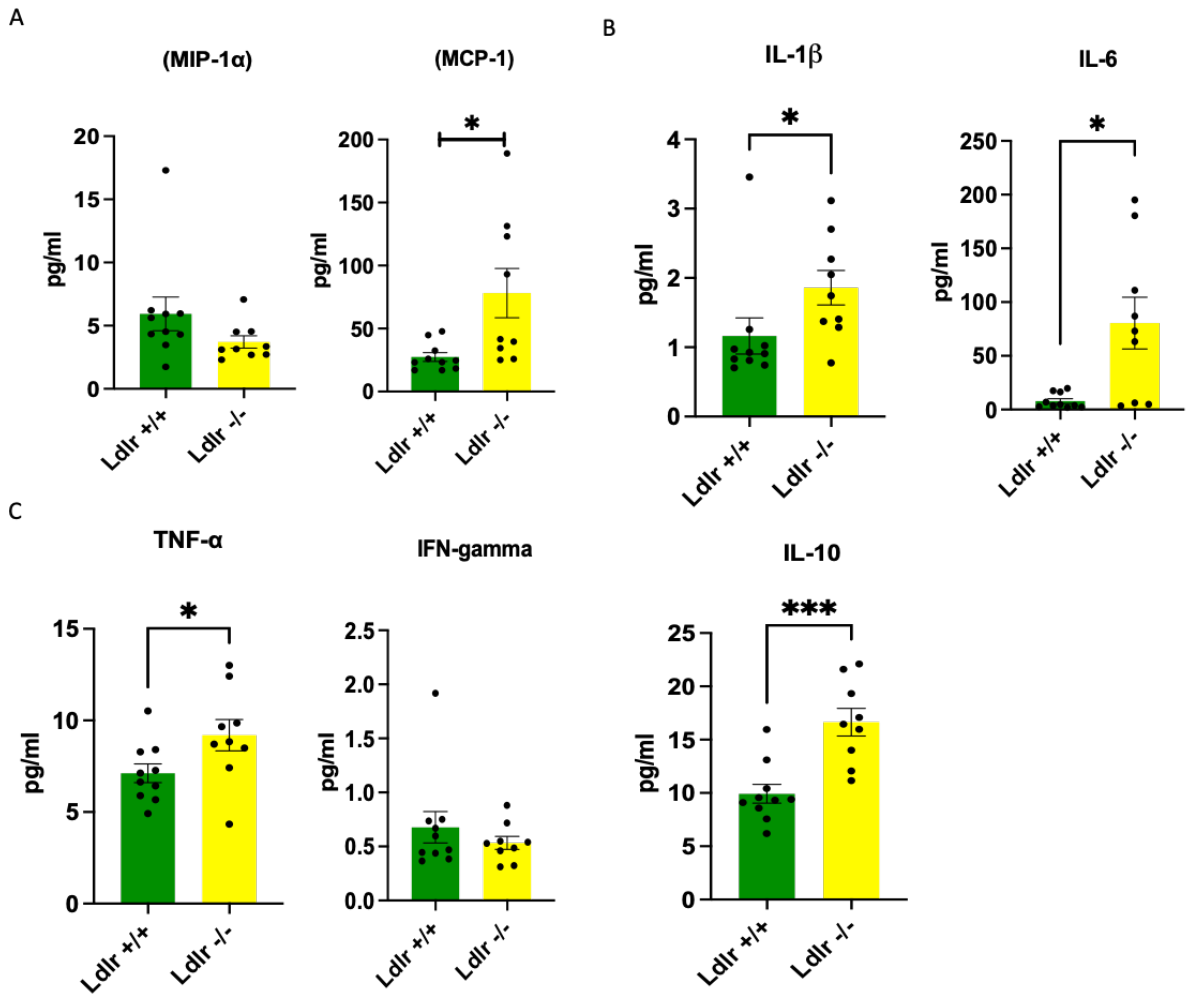

Figure 3.16 Quantitative assessment of Ldlr-/- mice plasma shows escalation of inflammatory chemokines/cytokines in plasma.

A) Chemotactic chemokine macrophage inflammatory protein-1 alpha MIP-1α/CCL3 and MCP-1 levels and monocyte chemoattractant protein-1 MCP-1/CCL2 levels in *Ldlr* $^{+/+}$ and *Ldlr* $^{-/-}$ mice B) pro-inflammatory Cytokines: IL-1β, IL-6 and anti-inflammatory cytokines IL-10 plasma levels in atherogenic model versus control. C) proinflammatory signals TNF-α IFN-γ levels in *Ldlr*$^{+/+}$ and *Ldlr* $^{-/-}$ mice. Statistical analysis was performed using a Mann Whitney test (GraphPad prism); * P≤0.05 and *** P ≤ 0.001. Error bars indicate the mean SEM of individual studies analysing 10 wild-type mice and 9 *Ldlr*$^{-/-}$ mice.

3.3.12 Apoptosis among haematopoietic stem/progenitor cells (HSPC) populations remains unchanged in *Ldlr-/-* mice

Enhanced cell survival may also explain the increase in immunophenotypic HSCs observed in *Ldlr-/-* mice. I therefore used the Annexin V/DAPI to assess variations in apoptosis within the HSPC compartments of *Ldlr-/-* mice. It was found that *Ldlr* deficiency had no effect on early apoptosis in most HSPCs/progenitors, except for MEP, which surprisingly showed a considerably lower frequency of early apoptosis in the *Ldlr*$^{-/-}$ group compared to the control group (Figure 3.17 and Figure 3.18).

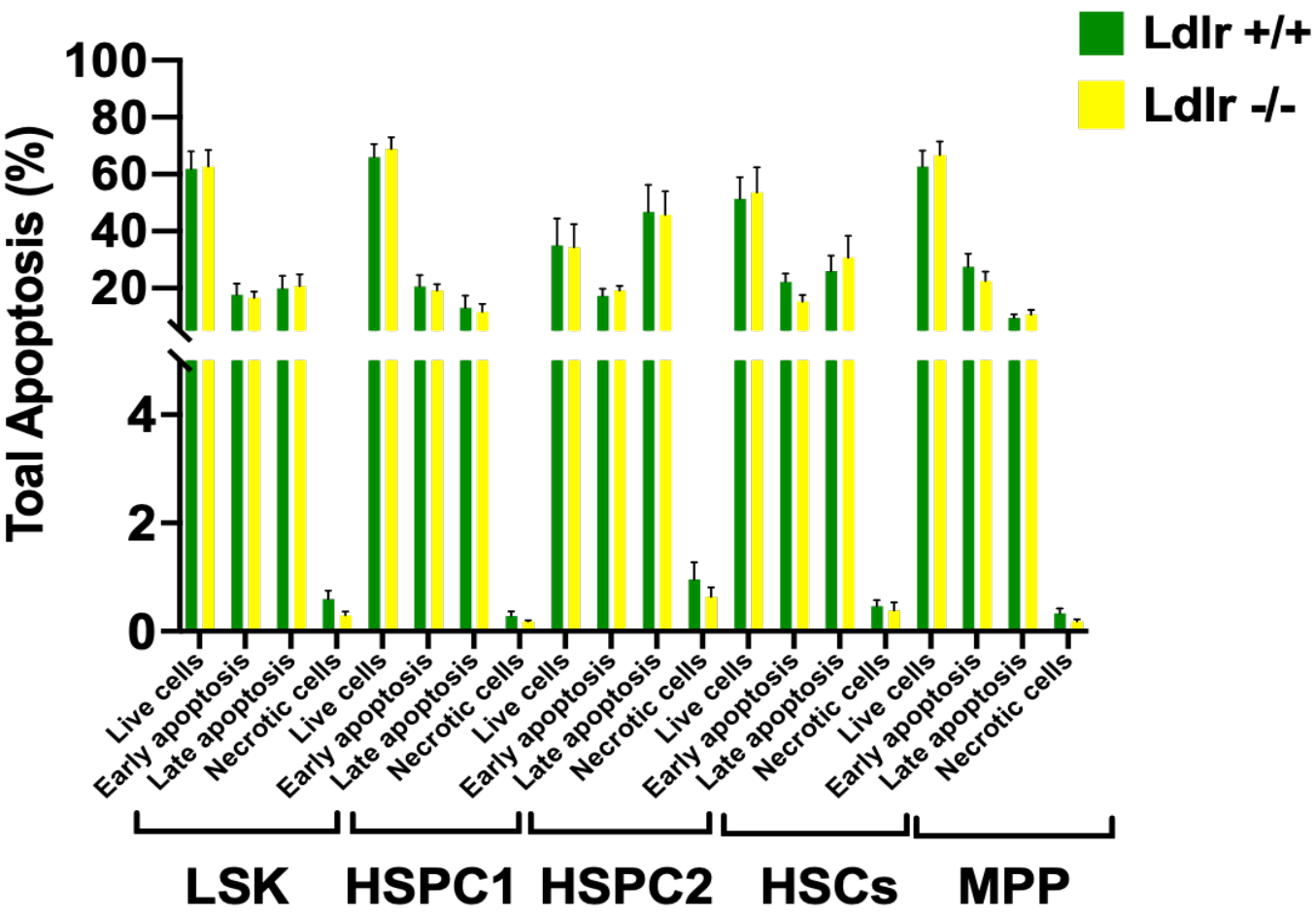

Figure 3.17 Ldlr deficiency has no impact on haematopoietic stem/progenitor cell survival.

The frequency of viable (Annexin V- DAPI-), early apoptotic (Annexin V+ DAPI-), and late apoptotic (Annexin V+ DAPI+) and Necrotic (Annexin V- DAPI+) LSK and their compartment sub-populations in wild-type and *Ldlr-/-* mice. Statistical analysis was performed using a Mann Whitney test (GraphPad prism). Error bars represent the mean ± SEM of the individual experiments using 9 mice from each genotype.

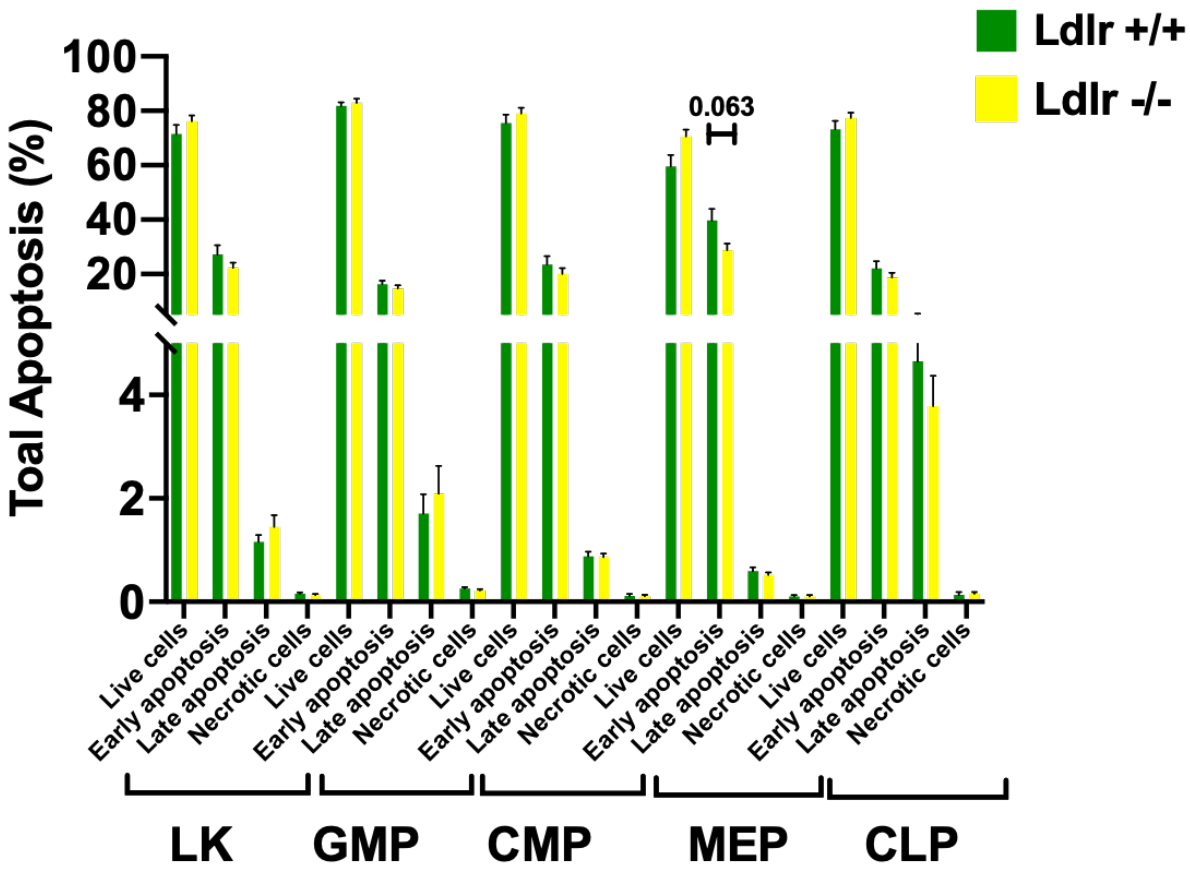

Figure 3.18 Meg/Erythroid Progenitor Cell Survival Enhanced in Ldlr-/- mice.

The frequency of viable (Annexin V- DAPI-), early apoptotic (Annexin V+ DAPI-), and late apoptotic (Annexin V+ DAPI+) and Necrotic (Annexin V- DAPI+) LK and their compartment cells in WT and *Ldlr-/-* mice in (A) LK cells, (B) GMPs, (C) CMP, (D) MEP and (E) CLP. Statistical analysis was performed using a Mann Whitney test (GraphPad prism). Error bars represent the mean ± SEM of the individual experiments using 9 mice from each group.

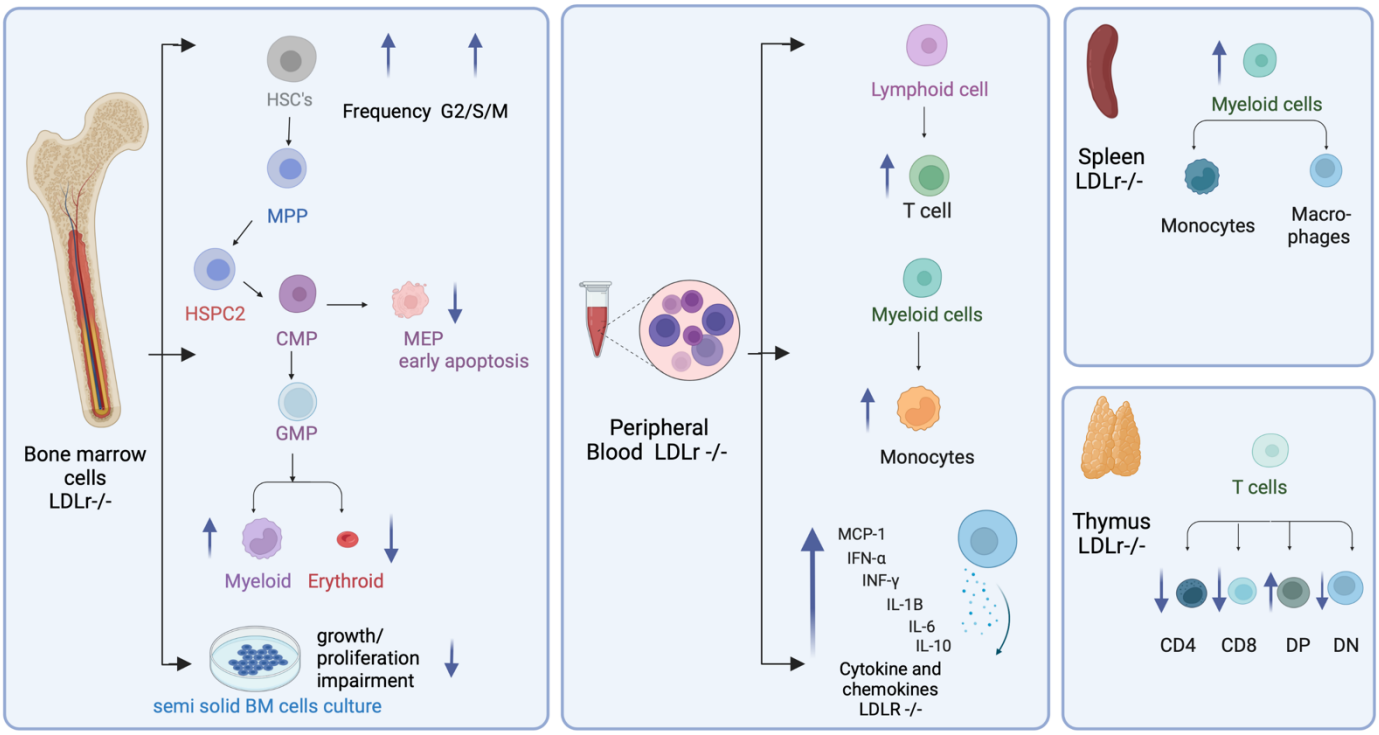

Figure 3.19 A summary diagram of the role of Ldlr in normal haematopoiesis.

Adult *Ldlr*$^{-/-}$ mice on a normal diet showed enhanced primitive haematopoietic activity in the bone marrow reflected by the rise in the G2/S/M fraction on HSCs and the reduction in MEP early apoptosis. Cytokine measurements showed an increase in inflammatory cytokines and chemokines, perhaps explaining the increased proliferative status of HSCs from *Ldlr*$^{-/-}$ mice. Moreover, there were increased production of bone marrow monocytes, yet BM differentiation was impaired. These findings were replicated in both peripheral blood and spleen. In examination of the thymus, the development and differentiation of T cells due to a potential block in double negative cells differentiating to double positive cells.

3.4 Discussion

The low-density lipoprotein (LDL) receptor (LDLR) is a protein with 860 amino acids that regulates cholesterol-rich LDL endocytosis (Südhof et al. 1985; Goldstein and Brown 2009). Genetic mutation in this gene causes a defect in LDL clearance from the body, consequently, increasing LDL cholesterol; this causes a mild inflammatory event (Ma and Feng 2016) and, in the context of normal diet, causes mild hypercholesteremia (Seijkens et al. 2014). Previously, LDL receptor expression on mature blood cells and HSPCs was reported to be high (Lara et al. 1997; Bagger et al. 2019) and *Ldlr* deficiency was linked to HSPC proliferation, innate and adaptive cells proliferation, and accumulation in atherosclerotic lesions in the setting of a high-fat diet (Fazio et al. 1997; Libby 2002). However, the requirement for *Ldlr* in normal steady state haematopoiesis has not been fully elucidated. In this chapter, a germline defective *Ldlr* mouse model (*Ldlr*$^{-/-}$) was therefore employed to study haematopoietic cell compartments in the bone marrow, peripheral blood, spleen, and thymus in young mice fed a normal diet. Immunophenotypic examination of the bone marrow, spleen, thymus, and peripheral blood, as well as functional study of BM progenitors *in vitro*, were used to assess the influence of *Ldlr* deficiency on steady state haematopoiesis. Colony forming assays using whole BM cells were used to investigate the functional differentiation and proliferation potential of haematopoietic progenitor cells from knockout mice. Finally, inflammatory cytokine/chemokine, cell cycle assessment and apoptosis studies were employed to evaluate HSPC cellular kinetics (Figure 3.19).

A recent article presented a curated gene expression database, which assessed *Ldlr* expression in haematopoietic cells at various maturation phases in the haematopoietic hierarchy. As a complementary experiment to the published gene expression data, we also measured LDLR protein expression on HSPC and lineage specific cells in bone marrow along with mature peripheral blood cells by flow cytometry. We found that our protein LDLR expression data were broadly consistent, with expression throughout the haematopoietic hierarchy, though slight differences were found between our gene expression and protein data (e.g. in CLP compartment), which may be ascribed to the lack of correlation, on occasion, between mRNA and protein ratios (Silva and Vogel 2016).

HSC number was enhanced in *Ldlr*$^{-/-}$ mice which was associated with an increase in cell cycle activity in the G2/S/M fraction specifically. Other studies have also shown that the hypercholesterolemic BM microenvironment promotes HSPC expansion (Seijkens et al. 2014). Thus, the mild hypercholesterolemic environment observed under steady-state in *Ldlr-/-* mice may contribute to the enhanced proliferative status of HSCs (Ishibashi et al. 1994). Mechanistically enhanced HSC proliferation could be explained, in part, by the increased inflammatory tone observed in *Ldlr*$^{-/-}$ mice. Atherosclerosis was originally described as atherosclerotic lesions develop in consequence of sheer force injury to the arterial endothelium walls, subsequently, immune cells and platelets adhere and aggregate to the site of injury, followed by cytokines and chemokine production (interferons, tumour necrosis factors, interleukins, colony stimulating factors, chemokines, growth factors and tumour necrosis factors) by stressed cells and tissues to orchestrate effector cells. Thus, this condition is considered as an immunoinflammatory disease (Ross 1986; Medzhitov 2008). Indeed, in this chapter we confirmed a significant increase in select cytokines in the plasma, namely Interleukins IL-1β, IL-10, IL-6, tumour necrosis factors alpha (TNF-α) and Chemokines (MCP-1). These inflammatory signals affect HSC biology. For example, Chronic exposure to TNF-α leads to necroptosis and myeloid lineage skew by up regulating p65-nuclear factor kB (NF-kB)-dependent gene program (Yamashita and Passegue 2019). IL-1β also enhances myeloid differentiation by activation of a PU.1-dependent gene program, it also transiently affects HSCs reconstitution capacity (Pietras et al. 2016). Monocyte chemoattractant protein-1 MCP-1/CCL2 play a crucial role in atherosclerosis progression by attracting circulating monocytes and to the site of oxLDL retention (McLaren et al. 2011). Studies on atherosclerotic mouse models lacking CCL2 showed reduced atherosclerotic lesion due to low monocyte recruitment (Combadiere et al. 2008). Nevertheless, some pro-inflammatory cytokines may have both pro- and anti-atherosclerotic functions, highlighting the complex roles of inflammatory cytokines in atherosclerosis. A case in point is IL-10; studies on *Ldlr*$^{-/-}$ mice showed that pro-inflammatory cytokines IL-10 exerts an anti-atherosclerotic function by attenuating cholesteryl ester build-up in atheroma loci (Han et al. 2010). On the contrary, employing a lentivirus to increase

pro-atherogenic IL-6 cytokine expression in ApoE$^{-/-}$ leads to the formation of unstable plaque (Zhang et al. 2012).

In addition, increased LDL accumulation in the plasma of *Ldlr*$^{-/-}$ mice may increase HSC growth factor receptor expression, triggering an expansion of their production including their progeny, ultimately increasing production of innate immune cells, that is monocytes and granulocytes (Feng et al. 2012). Partially in line with this, we observed total white blood cells increased *Ldlr*$^{-/-}$ mice, with monocytes differentially increased over granulocytes (Gomes et al. 2010; Feng et al. 2012). However, contrasting with these findings, a study by Feng *et al* study found increased granulocytes, but they built their research on 16 week wild-type mice fed chow diet versus *Ldlr*$^{-/-}$ fed chow diet, while our mouse cohort investigated 8-12 weeks *Ldlr*$^{-/-}$ mice fed chow diet, with results from the Feng *et al* study possibly reflecting ageing of the haematopoietic system in *Ldlr*$^{-/-}$ mice. Studies confirmed actual contribution of neutrophils in atherosclerotic plaques at various stages in atherosclerosis not constantly as other immune cells (Soehnlein 2012). Inflammatory cells, such as monocytes, and/or activated vascular cells generate inflammatory cytokines and likely account for the enhanced production of select chemokines/cytokines observed in *Ldlr*$^{-/-}$ mice here, which can further promote inflammation and recruit more innate and adaptive immune cells (Feng et al. 2012). Our findings confirm a heightened inflammatory status which leads to enhanced haematopoietic activity in *Ldlr*$^{-/-}$ mice, as evidenced by more HSC proliferation and augmented monocyte production.

Paradoxically, we detected reduced granulocyte-macrophage CFCs numbers from bone marrow of *Ldlr*$^{-/-}$ mice. This could be explained by absence of physiologic inflammatory signalling in the semi solid media *in vitro* compared to the *in vivo Ldlr*$^{-/-}$ bone marrow niche. Yet, several research groups have shown that HSPC cells cultured in LDL rich media differentiate into myeloid progeny compared to HSPC cells cultured in HDL, showing the differential sensitivity of haematopoietic progenitors to LDL and HDL, which is controlled by *Ldlr* (Ma and Feng 2016). Alternatively, the reduction on CFC-GM in *Ldlr*$^{-/-}$ mice could be explained by accelerated differentiation and expansion of the monocyte lineage observed. The conventional method for examining HSPC function and differentiation competence *in vivo* is the competitive bone marrow transplantation experiment (Aparicio-Vergara et al. 2010) (Herijgers et

al. 1997; Schiller et al. 2001; Rossi et al. 2012), which will need to be conducted in future experiments. More sophisticated serial transplantation – that tests HSC self-renewal - is also required to estimate the effect of increased proliferation activity on HSC self-renewal (Aparicio-Vergara et al. 2010). In addition, transcriptomic studies will be needed to identify genes that are differently expressed in HSCs from *Ldlr*$^{-/-}$ mice (Tie et al. 2014).

The spleen as a secondary haematopoietic organ showed increased myeloid cells with no difference in the prominent lymphoid population between the two genotypes. This is well explained by the limited size and ability of bone marrow to grow (Akinduro et al. 2018; Fernandez-Garcia et al. 2020) This finding correlates favourably with other previous studies that HSPCs start to cycle in the marrow and migrate to the spleen (Westerterp et al. 2012). HSPCs multiply and develop under the influence of increased growth factors dynamics which directly affect retention factor CXCL12 while also promotes proliferation into downstream myeloid cells such as monocytes in the spleen. Researchers have also categorised those monocytes as Ly6Chi monocytes which future contribute to the chronic inflammation circuit (Dutta et al. 2012; Robbins et al. 2012; Westerterp et al. 2012; Al-Sharea et al. 2019). A subsequent characterization of spleen myeloid cells and HSPCs in *Ldlr*$^{-/-}$ mice should be assessed to be evaluate this hypothesis.

Unexpectedly, steady-state *Ldlr* deficiency caused multiple defects in the erythroid pathway including a decrease in erythroid cells, increased mean corpuscular haemoglobin and a reduction of apoptosis in MEPs, though curiously no change in MEP abundance was noted. A recent study linked disturbed cholesterol metabolism to obstruction of erythroid differentiation. The article showed that cell cycle exit in the late stages of erythroid differentiation was regulated by cholesterol/mTORC1/ ribosome biosynthesis pathway (Lu et al. 2022).

The thymus, being a critical organ in the development of T lymphocytes, plays an important role in maintaining optimal immune system function throughout one's life. Immunophenotypic assessment of thymus from *Ldlr*$^{-/-}$ mice revealed a significant decrease in Thymic DN, CD4 and CD8 frequencies in comparison to control mice. On the contrary, DP thymic cells was drastically increased, suggesting that *Ldlr* deficiency

caused a T-cell maturation block during positive selection. Research shows that Low density lipoprotein (LDL) or cholesterol inhibits the production of the thymus transcription factor Foxn1 via low density lipoprotein receptors (LDLR) on the membrane surface and low-density lipoprotein receptor-related proteins on the cell surface, causing thymus function to deteriorate (Dai et al. 2018). Due to thymus failure, the imbalance of T cell subgroups and the decline of naïve T cells induce an increase or decrease in the release of numerous inflammatory mediators including cytokines, specifically CXCR4 (Gomes et al. 2010; Witsch et al. 2010; Love and Bhandoola 2011; Dai et al. 2018). In future studies, exploring the role of Foxn1 and CXCR4 in mediating the phenotype in these mice is warranted.

This chapter has explored the role of in steady state haematopoiesis in adult *Ldlr*$^{-/-}$ mice, as a basis to link perturbed haematopoiesis with cardiovascular disease and examine its association to myeloid leukaemia in the next thesis chapters. The data, in the setting of moderate hypercholesteremia in this chapter, has encouraged me to further explore the role of *Ldlr* deficiency on haematopoiesis and atherosclerosis in the context of high fat diet.

Chapter 4: Exploring the effects of high fat diet on haematopoiesis in a hypercholesteremic low-density lipoprotein receptor deficient mouse model

4.1 Introduction

Consumption of high-fat, high-cholesterol meals known as Western-type diets (WTDs) in industrialised societies can lead to hypercholesterolemia and atherosclerosis, particularly in genetically susceptible individuals (Gidding and Allen 2019). Low-density lipoprotein (LDL) is the most atherogenic lipoprotein in the blood, with high levels of LDL stimulating cholesterol accumulation and an inflammatory reaction in the arterial wall, leading to atherosclerosis (Tall and Yvan-Charvet 2015).

The process of atherosclerosis involves increased levels of LDL in the plasma, increasing serum sheer force and endothelial cells start expressing adhesion molecules (VCAM-1). Perturbed endothelial tissue recruits monocytes and T cells to site of endothelial injury (Crowther 2005). Monocytes in response to endothelial monocytes chemoattractant protein 1 (MCP-1) migrate into arterial intima and start generating proinflammatory signalling molecules (Mehu et al. 2022). In addition to MCP-1, activated endothelial cells release other cytokines and chemokines, such as interleukin-8 (IL-8), tumour necrosis factor-alpha (TNF-α), junctional adhesion molecules (JAMs), and macrophage colony-stimulating factor (M-CSF), aid further leukocyte recruitment and intimal migration (McLaren et al. 2011). Oxidised and aggregated (so-called modified LDL) act as a ligand for pattern recognition receptors on macrophages such as toll-like receptors (TLRs) to initiate proinflammatory signalling production. In a mutual manner, modified LDL engulfed by macrophages create foam cells which in turn amplifies TLRs signalling (Michelsen and Arditi 2006).Consequently, increased TLR activity from macrophages and myeloid differentiation primary response protein 88 (MYD88)-dependant pathways leads to boosted cytokine and chemokine production, amplifying the inflammatory process (Tall and Yvan-Charvet 2015). Ultimately, inflammatory cells are recruited into the site where atherosclerotic plaque builds (Tolani et al. 2013).

Research shows that in the setting of hypercholesterolaemia, the overproduction of myeloid inflammatory cells in the bone marrow and spleen plays a role in the atherogenic process (Glass and Witztum 2001). Knowing that haematopoietic and immunological cells, such as inflammatory cells, are derived from a single type of precursor cell – the haematopoietic stem/progenitor cell (HSPC) - researchers have studied and identified that WTDs influence both intrinsic and extrinsic pathways in the HSC differentiation hierarchy (Mihaylova et al. 2014; Singer et al. 2014; Mana et al. 2017). This sustained stimulation of the immune system is a stressor for HSPCs in the bone marrow niche, where overproduction of haematopoietic cells not only worsens hypercholesteraemic mediated inflammation at the cellular level, but it can also alter DNA methylation patterns causing epigenetic changes in HSCs and myeloid progenitors cells (van Kampen et al. 2014).

In atherogenic mice, increased LDL induces the production of inflammatory cells in the bone marrow and spleen; this was observed in chow-fed mice (previous chapter) and becomes more profound in the context of WTDs. Likewise, children with familial hypercholesteremia have an inverse monocyte level in relation with HDL (Tolani et al. 2013). In atherogenic mice, these myeloid cells are characterized by an immature phenotype called myeloid-derived suppressor cells (MDSC). MDSC are divided into two different categories according to their differences in phenotype and function: polymorphonuclear MDSC-PMN and monocytic MDSC-M. As can be surmised from its name, these cells facilitate tumour development by the suppression of the adaptive immune response, namely suppression of immunosurveillance in response to mutated cells, as well as the promotion of tumour cell viability, angiogenesis, and metastasis (Diaz-Montero et al. 2009) (Bronte et al. 2016; Foks et al. 2016).

Innate inflammatory cells such as macrophages and neutrophils can sense inflammation related necrosis and damaged tissue through damage-associate molecular patterns (DAMPs) (Takeuchi and Akira 2010). These immune cells influence malignant cells through production of cytokines, chemokines and prostaglandins (Takeuchi and Akira 2010). For example, these inflammatory products, like cytokines and chemokines, activate key transcription factors, mainly nuclear factor kappa-light-chain-enhancer of activated B cells (NF-kB) (Zhang et al. 2021b) and

Signal transducer and activator of transcription (STAT3) (Yu et al. 2009). NF-kB mediate the expression of adhesion molecules, cytokines, and chemokines to facilitate monocyte recruitment to injury site (Kempe et al. 2005). NF-kB also promotes IL-6 production from myeloid cells, which in turn activate STAT3 in MDSCs, to facilitate cancer initiation and progression through pro-cancer inflammatory mediators and angiogenic and growth factors (Wang et al. 2019). It is also believed that stimulated inflammatory cells generate reactive oxygen and nitrogen species, which induce DNA damage and genomic instability (Grivennikov et al. 2010). Thus, oxygen radicals such as hydroxyl (OH) cause structural alterations to DNA while hydrogen peroxide (H_2O_2) affects cytoplasmic and nuclear signal transduction signalling (Wiseman and Halliwell 1996).

To examine the impact of WTDs on HSPC function, bone marrow transplantation assays employing *Ldlr*$^{-/-}$ mice fed on HFD were compared to *Ldlr*$^{-/-}$ mice fed on normal chow. Previous reports on *Ldlr* $^{-/-}$ HFD transplanted into mice *Ldlr* $^{-/-}$ HFD showed increased leukocytes count mainly F4/80 and CD11c+ cells. This finding was indicated even after removal of WTD, suggesting that haematopoietic progenitors were epigenetically biased to produce myeloid progenies after receiving WTD (van Kampen et al. 2014). Another group investigated the impact of hypercholesteraemic BM microenvironment on HSPCs production and found increases in LSK HSCs, and myeloid CMP and GMP respectively (Seijkens et al. 2014). The same result was reported when equally split amounts of BM from *Apoe*$^{-/-}$ with WT BM cells were transplanted in *Ldlr*$^{-/-}$ recipients or WT recipients (Murphy et al. 2011). These data together suggest that hypocholesteraemia induces immunophenotypic and functional changes in HSPCs.

To understand the molecular basis of these processes and the possible link between them, we have investigated how hypercholesteremia related inflammation influences adult HSC function and alters the blood/immune system with view to understanding the implications for the development of haematologic malignancy.

4.2 Aims of chapter

In the new era of evolving links between clonal haematopoiesis, atherosclerosis (including chronic inflammation in this setting) and, ultimately, the development of

leukaemia, it remains unclear how hypercholesteremia affects HSC self-renewal and differentiation and perturbs other haematopoietic lineages. The main purpose of this chapter is, therefore, to use *Ldlr*$^{-/-}$ murine model in the context of HFD to create a chronic hypercholesteraemic milieu that evaluates the effect of atherosclerosis-driven chronic inflammation on HSPC function and haematopoiesis, with the following aims:

1. To characterise immunophenotypically defined haematopoietic stem and progenitor cells (HSPCs) and lineage-positive cells in the bone marrow.
2. To characterise lineage positive cells in the bone marrow, thymus, spleen, and peripheral blood.
3. To identify immune regulatory cells in peripheral blood that contribute to inflammation and perturbed haematopoiesis in the context of HFD.
4. To functionally test HFD primed HSCs using competitive haematopoietic transplantation assay.
5. To evaluate, by bulk RNA-sequencing, the transcriptional programming arising from long term exposure of HSCs to HFD.

Ldlr$^{-/-}$ mice, aged 8-12 weeks, were fed either a HFD or a ND for 12 weeks. Following this time, immunophenotypic examination of HSPC population in bone marrow, lineage differentiated cells in bone marrow, peripheral blood, spleen, and thymus was conducted. Competitive HSC transplantation were also performed to examine HSC functioning in producing multilineage haematopoiesis and repopulation capability. Finally, bulk RNA sequencing was performed on *Ldlr*$^{-/-}$ HSCs exposed to HFD to understand the transcriptional alterations that occur in this setting (Figure 4.1).

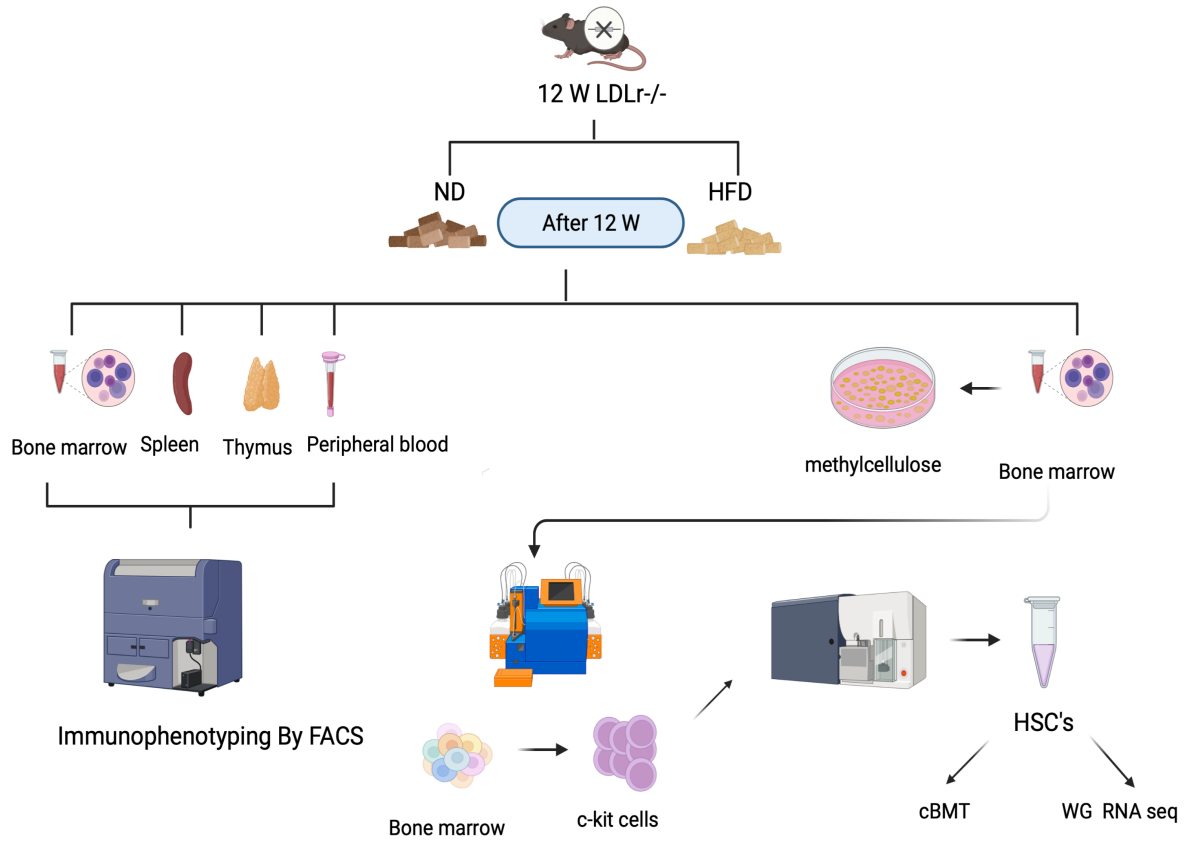

Figure 4.1 The experimental design used to investigate the effects of High-Fat Diet (HFD) on haematopoiesis in Ldlr-/- mice.

At 12 weeks of age, HFD was given to one cohort of *Ldlr*$^{-/-}$ mice, whereas another cohort of *Ldlr*$^{-/-}$ mice were given ND. Then, utilising flow cytometry bone marrow, peripheral blood, spleen, and thymus were extracted for immunophenotypic investigation. Bone marrow cells were processed to get c-kit enriched sample, which in turn were sorted to obtain highly purified HSCs for competitive bone marrow transplantation and whole genome RNA sequencing.

4.3 Results

4.3.1 *Ldlr* $^{-/-}$ mice on a HFD develop atherosclerosis plaques.

The *Ldlr*$^{-/-}$ mouse model is a well-established atherosclerotic mouse model, where a HFD leads to inflammation which causes atherosclerosis (Ma et al. 2012; Emini Veseli et al. 2017). Nonetheless, we re-validated the model in our experiments by assessing lipid content of atherosclerotic plaque from the arteries using Oil Red O staining. ORO is a fat-soluble, lipophilic dye that disperses in lipids and colours them red (Mohanta et al. 2016). ORO staining of frozen sections permits straightforward evaluation of the

lipid content and distribution in tissues using standard microscopy (Mehlem et al. 2013). Here, ORO staining was utilised to demonstrate the existence of atherosclerosis, which is characterised by lipid droplet accumulation and an increase in atherosclerotic plaque. Increased ORO staining indicated an increase in both atherosclerotic plaque and lipid droplets in aortic sinus of *Ldlr*$^{-/-}$ mice fed a HFD (Figure 4.2).

(A) *Ldlr*$^{-/-}$ ND (B) *Ldlr*$^{-/-}$ HFD

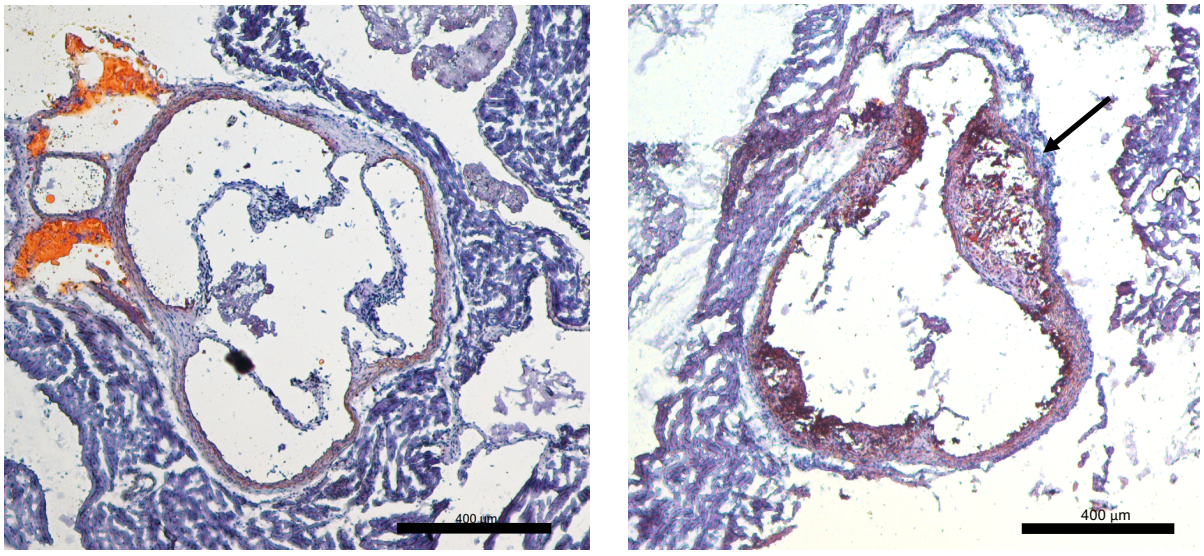

Figure 4.2 Oil Red O staining of aortic sinus in Ldlr-/- ND and Ldlr-/- HFD mice. *Ldlr*$^{-/-}$ mice were fed a normal diet (ND) (control) (A) or high fat diet (HFD) (B) for 12 weeks before being scarified, section B shows atherosclerotic thickening of HFD mice with atheroma. A cryostat was used to cut sections of the aortic root at the three valve cups, and Oil Red O staining was used to visualize the lipid within the plaques. The black arrow shows lesion with necrotic core and fibrous cap formed by vascular smooth muscle cells and macrophages (Ma et al. 2012). Representative images were taken from 8 extracted aortas from each cohort, at x5 magnification with scale bars of 400µm using a Leica DMRB microscope.

4.3.2 Hypercholesteremia Induces Expansion of Haematopoietic Stem and Progenitor Cells

Several studies have shown a direct correlation between increased plasma cholesterol levels and increased proliferation/frequency of HSPC in bone marrow, monocytosis, and neutrophilia in the peripheral blood (Papaemmanuil et al.) (Feng et al. 2012; Seijkens et al. 2014). This encouraged me to examine the role of severe hypercholesteremia in normal haematopoiesis and examine different haematopoietic and immune cell types contributing to the inflammatory process. To do this, we fed 8–12-week-old *Ldlr*$^{-/-}$ mice either a High Fat Diet (HFD) or a Normal Diet (ND) for 12 weeks. Bone marrow (BM) was harvested and HSPCs enumerated and mature differentiated progenies in BM, peripheral blood (Papaemmanuil et al.), spleen and thymus were quantified.

Initially, we measured the frequency of HSPC in BM of *Ldlr*$^{-/-}$ mice that either received normal diet or high fat diet for 12 weeks. Quantification of the HSPC containing **L**in- **S**ca-1+ c-**K**it+ (**LSK)** cells indicated significantly increased frequency and absolute number of LSK in *Ldlr*$^{-/-}$ mice fed HFD compared to *Ldlr*$^{-/-}$ mice fed ND (Figure 4.2), in agreement with other reports (Seijkens, T.et al., 2014) (Feng, Y.et al., 2012). Since the LSK HSPC compartment is a heterogenous mixture of stem and progenitor compartments and it is unclear whether an alteration in LSK also reflects changes in HSCs or other progenitor compartments, we further dissected the LSK into highly purified HSCs and progenitor subsets (HPC1, HPC2 and MPP) (Oguro et al. 2013) and found all 4 HSPC compartments in LSK cells, including HSCs, were significantly increased in frequency and absolute number in *Ldlr*$^{-/-}$ mice fed HFD. Thus, mice engineered to be deficient in in *Ldlr* display enhanced HSPC numbers when fed an HFD (Figure 4.3).

Next, we measured committed lineage restricted progenitors **L**in- c-**K**it+ **(LK)** cells within the in the same experimental animals, which showed significant increase in frequency in *Ldlr* $^{-/-}$ mice fed HFD compared to *Ldlr*$^{-/-}$ mice fed ND. The increase in frequency, but not absolute numbers, occurred in progenitors with both myeloid and lymphoid differentiation capability (CMP, LMPP and CLP) (Figure 4.4).

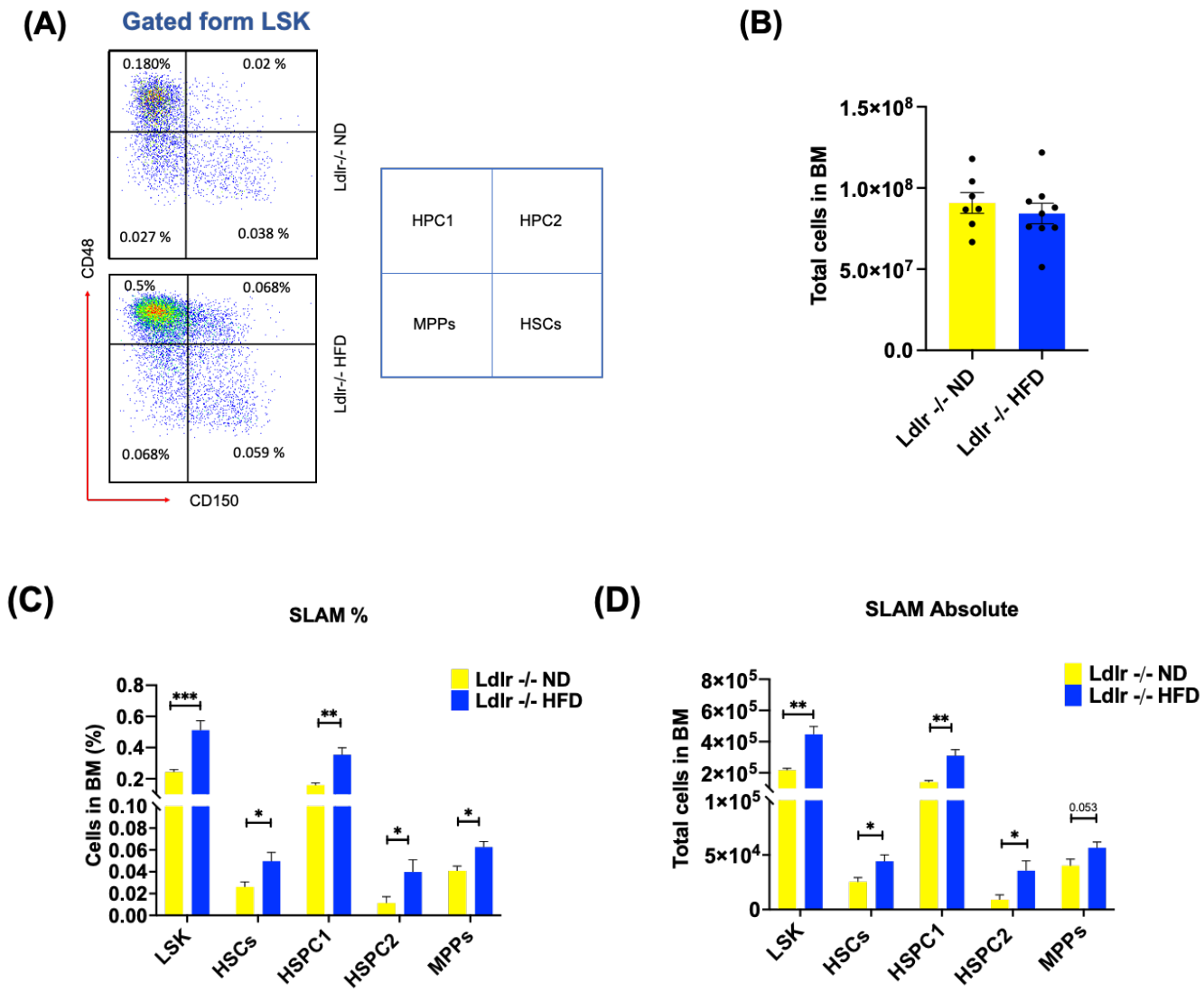

Figure 4.3 Ldlr-/- mice fed HFD exhibit enhanced HSPC frequency and absolute number.

(A) Representative immunophenotypic analysis, gating strategy (centre). (B) Total BM counts from in *Ldlr*$^{-/-}$ mice fed HFD and in *Ldlr*$^{-/-}$ mice fed ND. (C) Frequencies of primitive HSPC compartments in the BM of *Ldlr*$^{-/-}$ mice fed HFD and in *Ldlr*$^{-/-}$ mice fed ND (n=7 mice for each condition from four independent experiments in total). (D) Absolute numbers of primitive HSPC compartments in the BM of *Ldlr*$^{-/-}$ mice fed HFD and in *Ldlr*$^{-/-}$ mice fed ND (n=7 mice for each condition from four independent experiments in total). Data represents mean ± SEM. Statistical analysis: Mann-Whitney U test *, P ≤ 0.05; ** P ≤ 0.01; ***P ≤ 0.001.

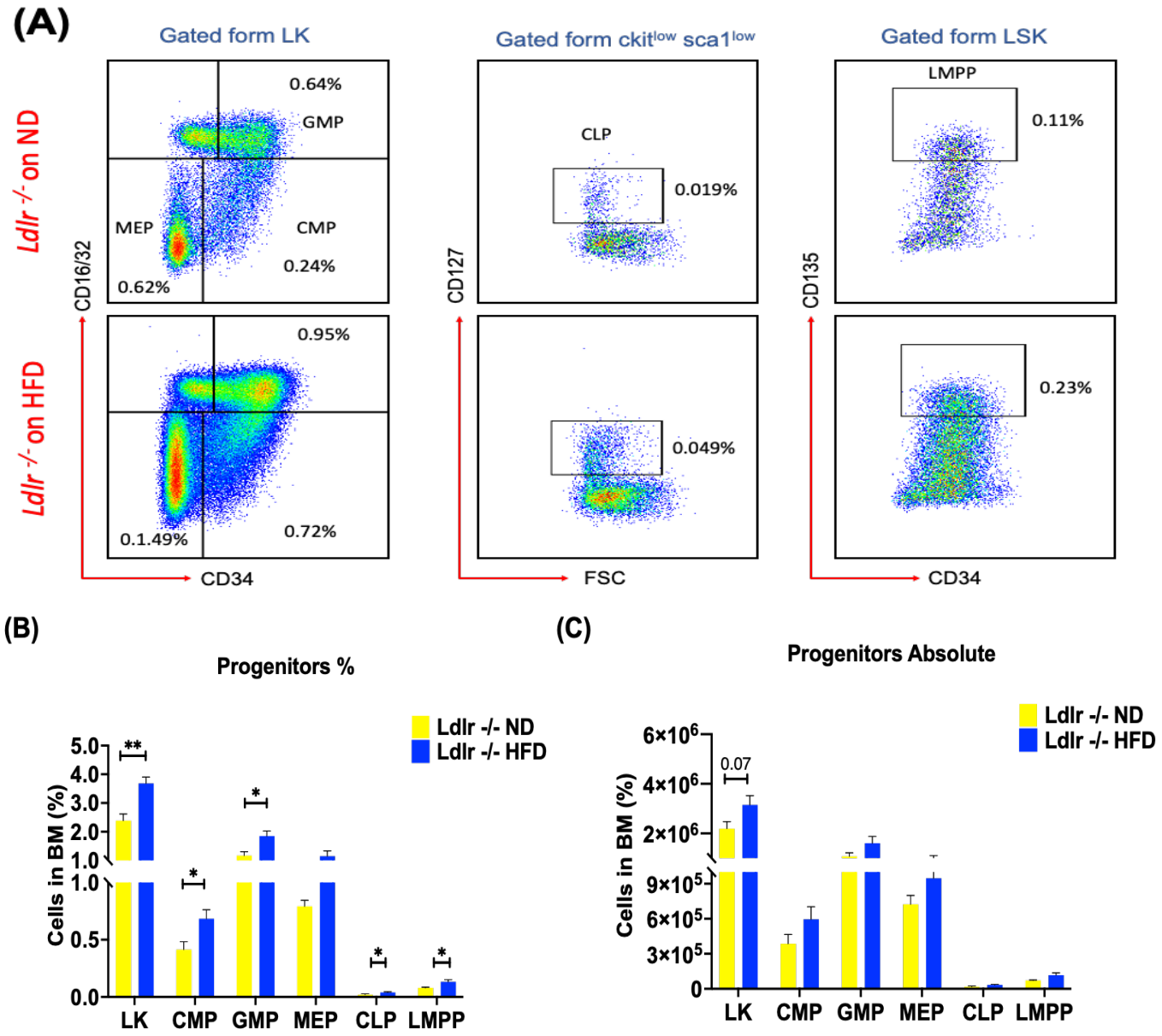

Figure 4.4 Flow cytometric analysis of committed haematopoietic progenitors in Ldlr-/- mice fed HFD.

(A) Representative immunophenotypic analysis of **L**ineage-c-**K**it+/committed myeloid progenitors/granulocytes monocytes progenitors/megakaryoblast erythroid progenitors/ commited lymphoid progenitors / Lymphomyeloid primed progenitors (LK, CMP, GMP, MEP, CLP and LMPP). (B) Frequencies and (C) Absolute committed progenitor compartments in *Ldlr*$^{-/-}$ mice fed HFD and in *Ldlr*$^{-/-}$ mice fed ND mice (from n=7 and n=9 mice respectively from four independent experiments). Data represents mean ± SEM. Statistical analysis: Mann-Whitney U test *P ≤ 0.05; **P ≤ 0.01.

4.3.3 Hypercholesteremia moderately enhances monocyte, platelet, and NK cell abundance in bone marrow of *Ldlr-/-* mice

As hypercholesteremia has impacts on myeloid differentiation, late differentiated myeloid effector cells in bone marrow were comprehensively evaluated in *Ldlr*$^{-/-}$ mice that ingested HFD. Our data showed a moderate increase in the frequency and absolute number monocytes in *Ldlr*$^{-/-}$ mice fed HFD, as expected from the literature (Feng et al. 2012), and platelet frequency, mirroring the myeloid committed progenitor expansion within the same experimental mice. Moreover, NK cells increased in frequency in *Ldlr*$^{-/-}$ mice fed HFD (Figure 4.5 and 4.6).

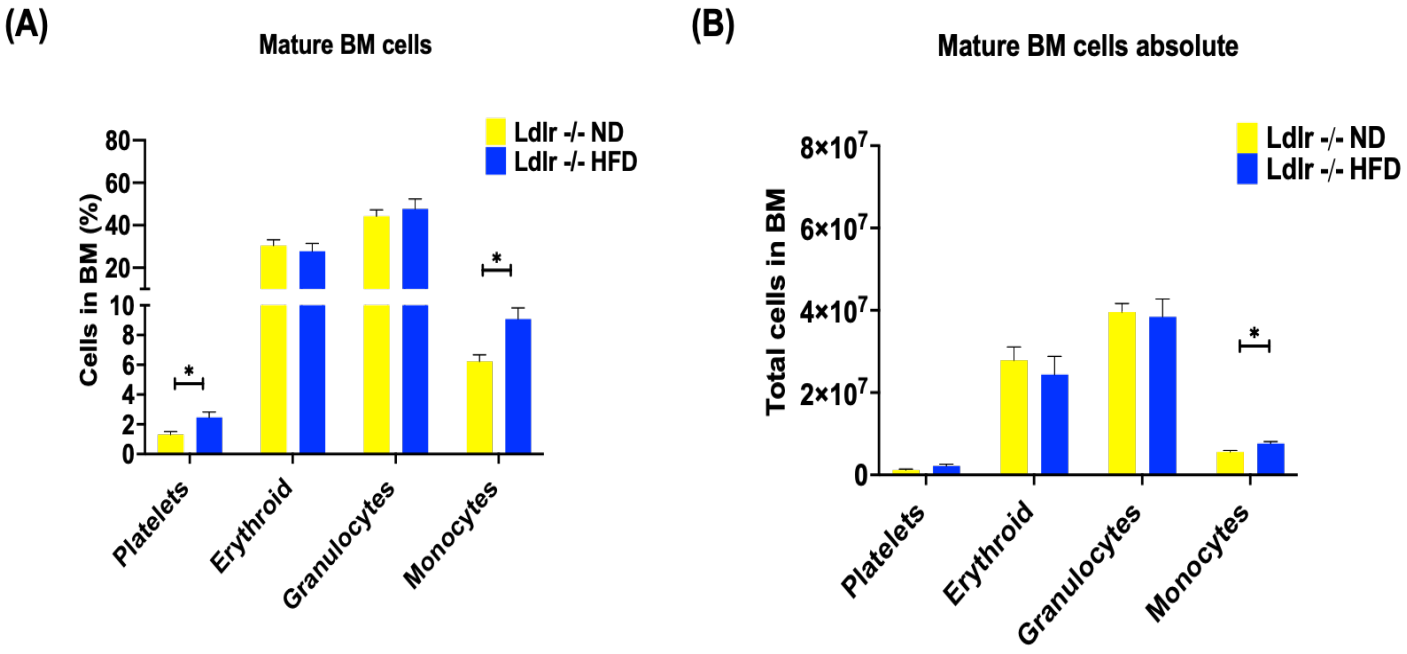

Figure 4.5 Increased platelets and monocytes in BM from Ldlr-/- mice on HFD.

(A) Fraction of BM cells: Platelets (CD41), Erythroid (CD117/Ter119), Monocytes (Ly6C+) and Granulocytes (LY6G+) from *Ldlr*$^{-/-}$ mice on ND (n=6) and *Ldlr*$^{-/-}$ mice on HFD (n=9) mice from four independent experiments. (B) Absolute cell counts of mature myeloid cells in BM from *Ldlr*$^{-/-}$ mice on ND (n=6) and *Ldlr*$^{-/-}$ mice on HFD (n=9) mice from four independent experiments. Data are mean ± SEM. Statistical analysis: Mann-Whitney U test, *P ≤ 0.05.

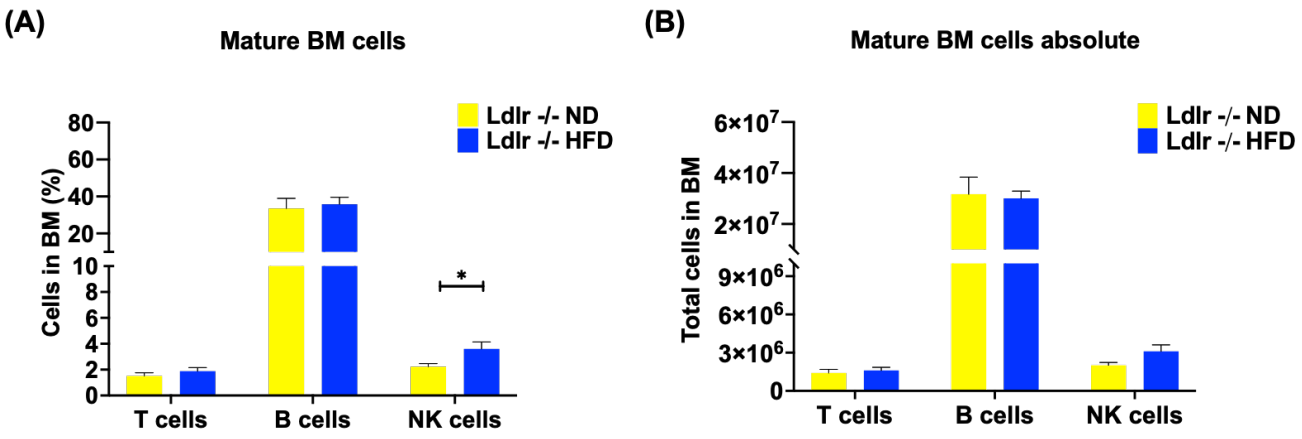

Figure 4.6 Increased NK cell frequency in BM from Ldlr-/- mice receiving a HFD.

(A) Proportion of Lymphoid cells: T cells (CD3), B cells (CD19) and NK cells (NK1.1) from *Ldlr*$^{-/-}$ mice on ND (n=6) and *Ldlr*$^{-/-}$ mice on HFD (n=9) mice from four independent experiments. (B) Absolute cell counts of mature lymphoid cells in BM from *Ldlr*$^{-/-}$ mice on ND (n=6) and *Ldlr*$^{-/-}$ mice on HFD (n=9) mice from four independent experiments. Data are mean ± SEM. Statistical analysis: Mann-Whitney U test *P ≤ 0.05.

4.3.4 Hypercholesteremia promotes specific inflammatory cell subsets in peripheral blood of *Ldlr*$^{-/-}$ mice

Given that hypercholesteremia imparts an inflammatory stimuli, as judged by increased monocytes in the bone marrow (Figure 4.5), we next evaluated how different inflammatory/myeloid cell subsets were involved in peripheral blood (Papaemmanuil et al.). Immunophenotypic analysis of PB displayed a significant increase in two main myeloid populations: monocytes or myeloid derived suppressor cells / Monocytes (MDSC-M) and Granulocytes or myeloid derived suppressor cells/granulocytes (MDSC-G). MDSC-M is defined immunophenotypically as CD11b+Ly6C and MDSC-G is defined by CD11b+Ly6G expression (Gabrilovich et al. 2007) (Figure 4.7). In *Ldlr*$^{-/-}$ mice on HFD compared to *Ldlr*$^{-/-}$ mice fed on ND respectively (Foks et al. 2016). Detailed analysis also reveals a trend, non-significant increase in CD115+/Ly6C^{High} monocytes population (pro-inflammatory with high chemokine receptor CCR2 expression) and trend, non-significant decrease in CD115/Ly6C$^{Moderate/low}$ (pro-inflammatory for moderate Ly6C and patrol / tissue repair for low Ly6C) (Yang et al. 2014) in *Ldlr*$^{-/-}$ mice on HFD, likely reflecting the inflammatory milieu created by high plasma LDL (Swirski et al. 2007) (Figure 4.7). Notably, the Tumour associated Macrophage (TAM), which is immunophenotypically defined by CD11b+CD115+F4/80+Ly6C- expression, was also significantly increased in *Ldlr*$^{-/-}$ mice on HFD; TAMs are found to be increased in the peripheral blood of tumour susceptible animals (Noy and Pollard 2014; Bronte et al. 2016) (Figure 4.7). TAMs produce a wide variety of effector substances such as cytokines, chemokines, surface proteins and enzymes involved in anti-tumour derived responses(Biswas et al. 2013). Recent research, however, has pointed to the Ly6C+ population of circulating mouse monocytes in transplanted tumours as the likely source of the vast majority of TAM subpopulations (Movahedi et al. 2010).

Morphological examination of peripheral blood smears was qualitatively evaluated in *Ldlr*$^{-/-}$ mice on HFD, revealing atypical, dysplastic features found in a chronic inflammatory reaction (Figure 4.8) (O'Connell et al. 2015). These data indicate that *Ldlr*$^{-/-}$ mice receiving a HFD display an aberrant pro-inflammatory state consistent with perturbed, deregulated haematopoiesis.

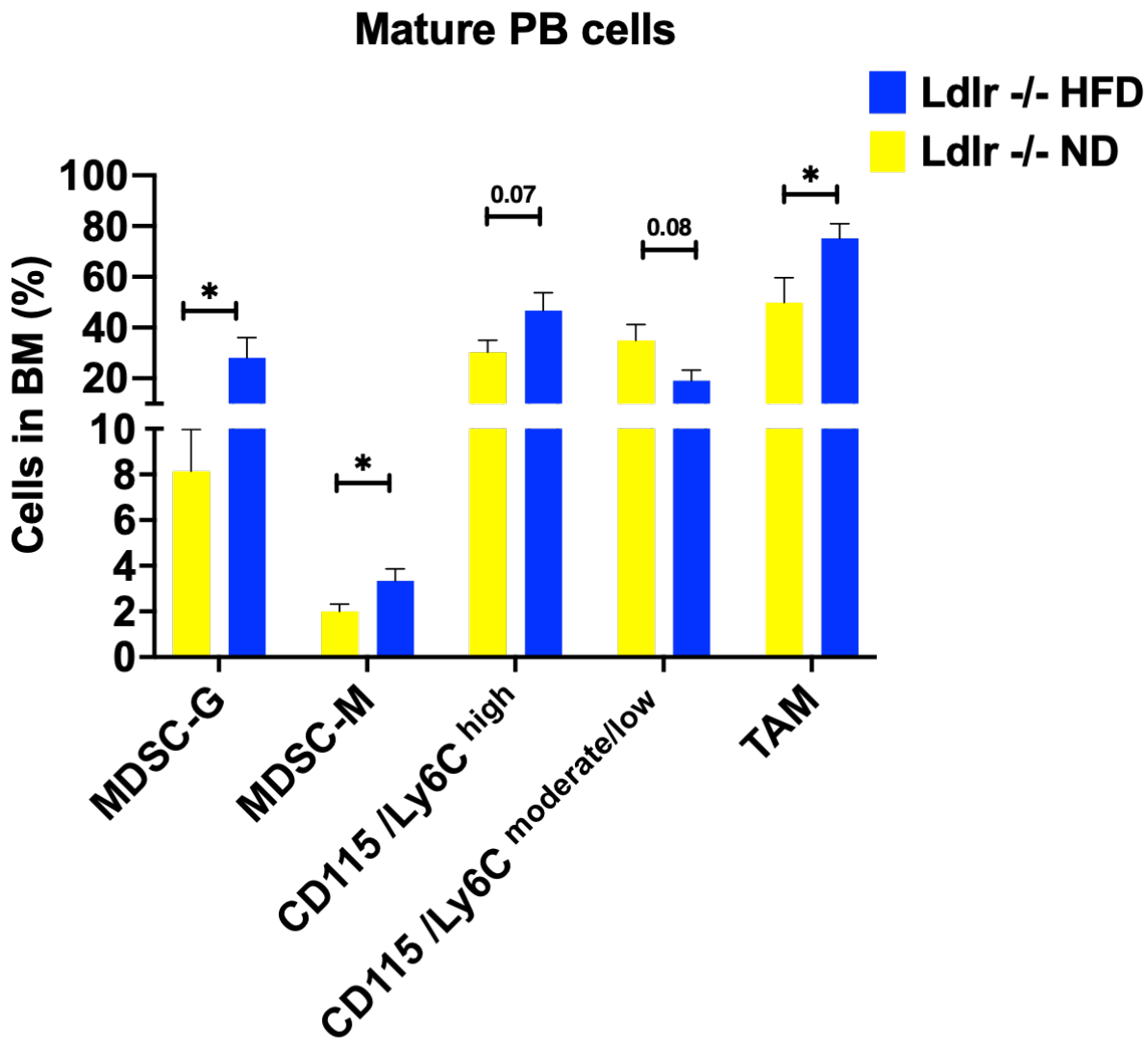

Figure 4.7 Prominent inflammatory cell subsets are deregulated in peripheral blood of Ldlr-/- mice receiving HFD.

Significant myeloid derived suppressor cells, MDSC-M or monocytes (CD11b+Ly6C+) and MDSC-G granulocytes (CD11b+Ly6G+) were observed. Also, inflammatory CD115/Ly6C^{high} monocytes were elevated in *Ldlr*$^{-/-}$ mice on HFD (n=10) in comparison to *Ldlr*$^{-/-}$ mice on ND (n=7). Tumour associated macrophages significantly increased due to hyperinflammation. These data are from four independent experiments. Data are mean ± SEM. Statistical analysis: Mann-Whitney U test, *P ≤ 0.05.

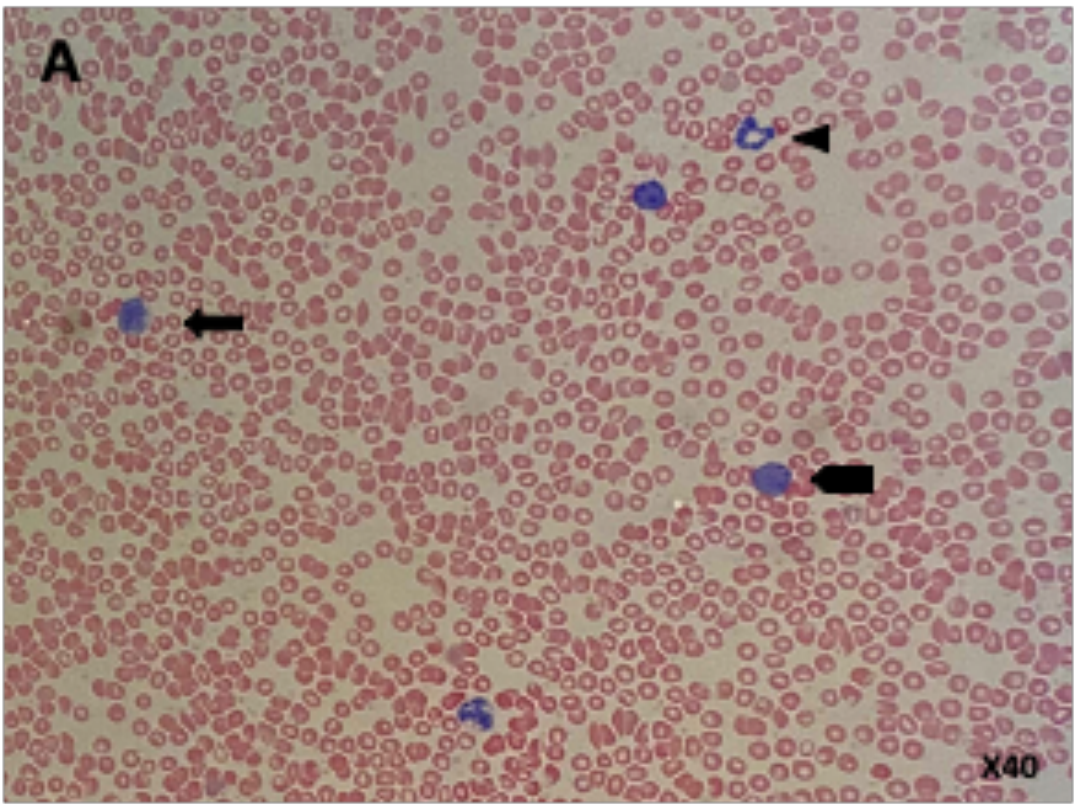
A
X40

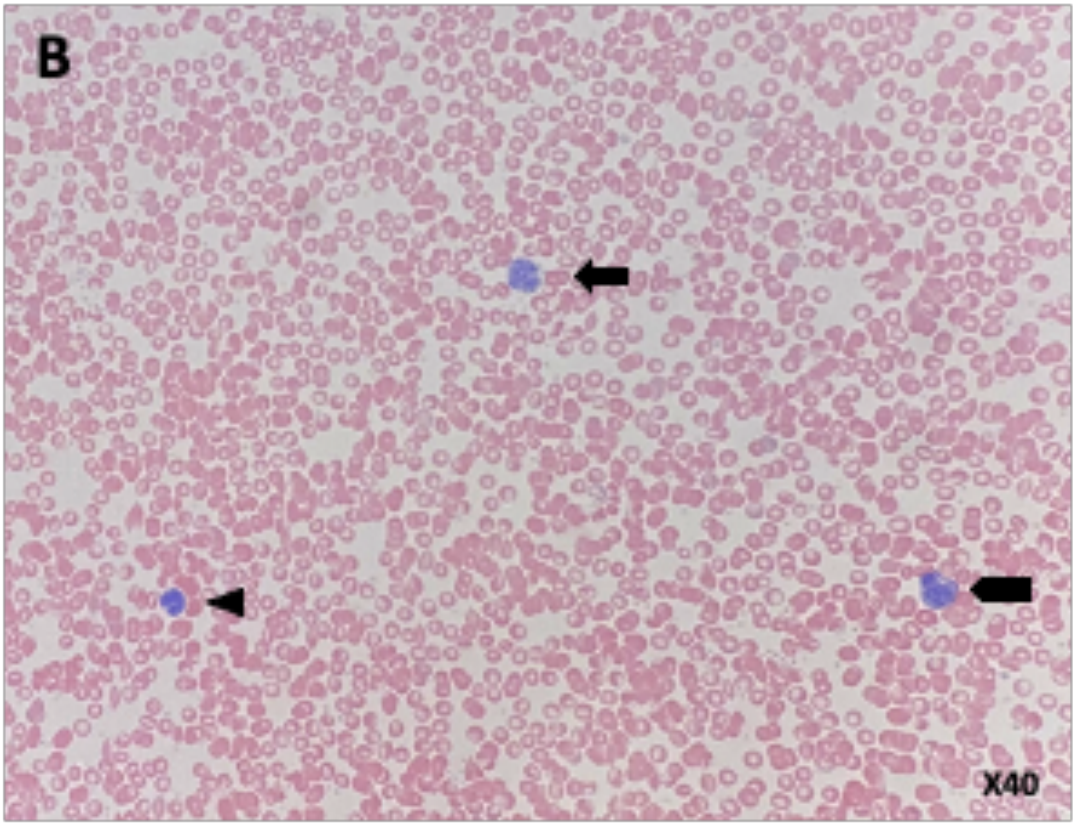
B
X40

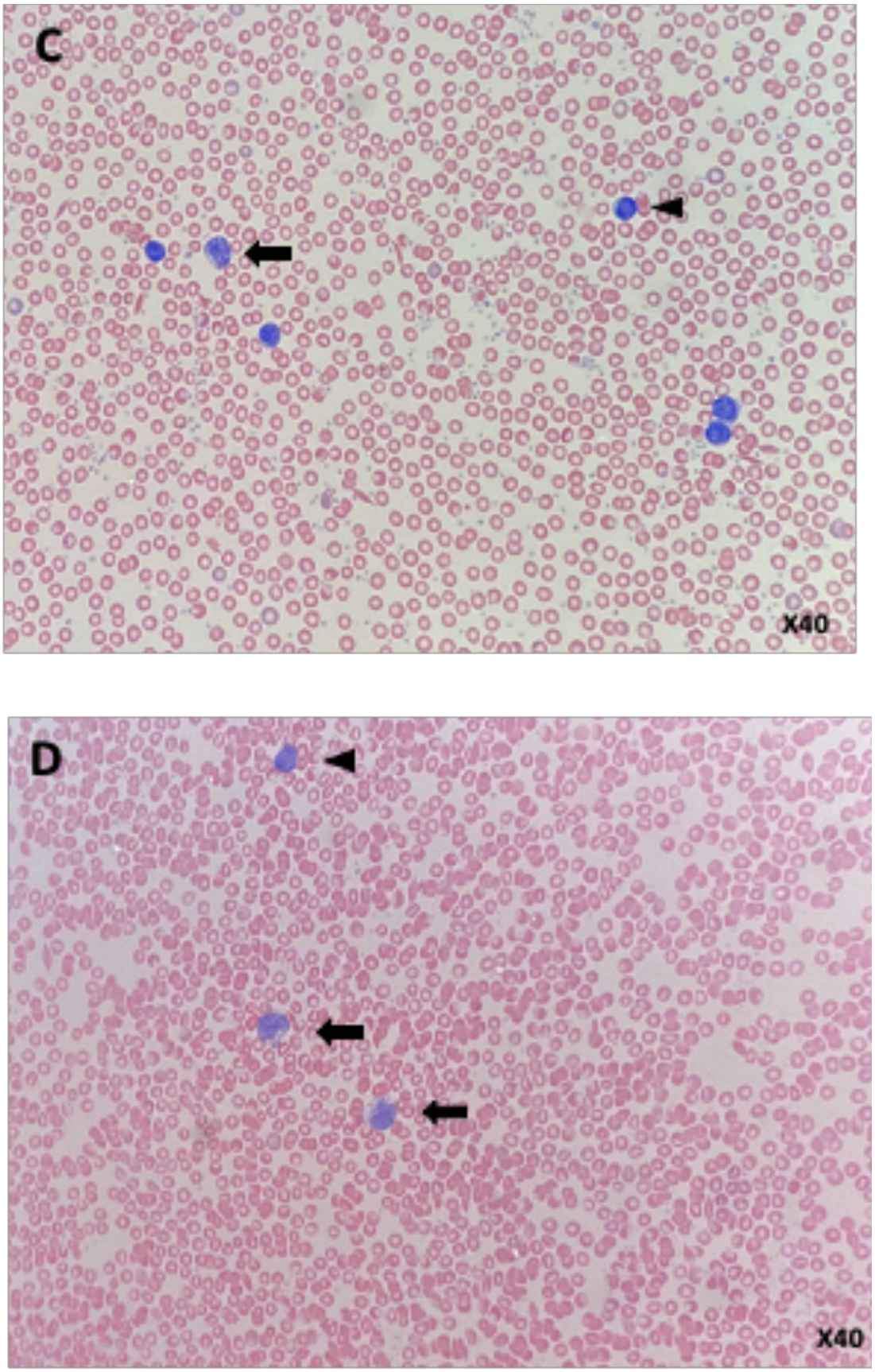

Figure 4.8 Morphological features of peripheral blood from Ldlr-/- mice receiving HFD.

(A) Normal mature neutrophils indicating left shift (arrowhead), characterized by faint, finely granular cytoplasm, and dense chromatin. activated lymphocytes (arrow) and (pentagon arrow). (B) 3 types of enlarged atypical lymphocytes, clefted lymphocytes (arrowhead), increased Nuclear/cytoplasm ratio (pentagon arrow), vacuolated lymphocytes (arrow). (C) Enlarged atypical lymphocytes (arrow) in comparison to normal lymphocytes (arrowhead). (D) two Atypical Monocytes (arrow) with heavy vacuolation, characterized by abundant pale gray-blue cytoplasm with vacuoles and some weakly eosinophilic granules; their nuclei have loose chromatin and are often bi- or trilobed, reniform, or horseshoe-shaped. Total of 6 *Ldlr*$^{-/-}$ on HFD blood film were reviewed and contrasted with 4 *Ldlr*$^{-/-}$ on ND. Wright–Giemsa staining; original magnification, X40, using Leica DM2500 microscope.

Key: → Arrow, ⬟ Pentagon arrow, ► Arrowhead.

4.3.5 High fat diet impacts peripheral blood lymphoid cells involved in immunosuppression.

Having shown a pro-inflammatory state in *Ldlr*$^{-/-}$ mice receiving a HFD, we next comprehensively analysed the peripheral blood lymphoid cell compartment of *Ldlr*$^{-/-}$ mice receiving HFD. This analysis included the three major lymphoid populations: T cells (including T helper and T cytotoxic), B cells and NK cells. Results of the main lymphoid cells largely reflect the findings in bone marrow, with a significant increase in NK cells and insignificant increase in NK/T cells in *Ldlr*$^{-/-}$ mice ingesting a HFD compared to their normal diet counterparts. Interestingly, a significant increase in CD3+CD4-CD8- cells (DN T cells) was observed which is considered to be a rare subsets of regulatory T cell (Treg) (Wu et al. 2022) (Figure 4.9).

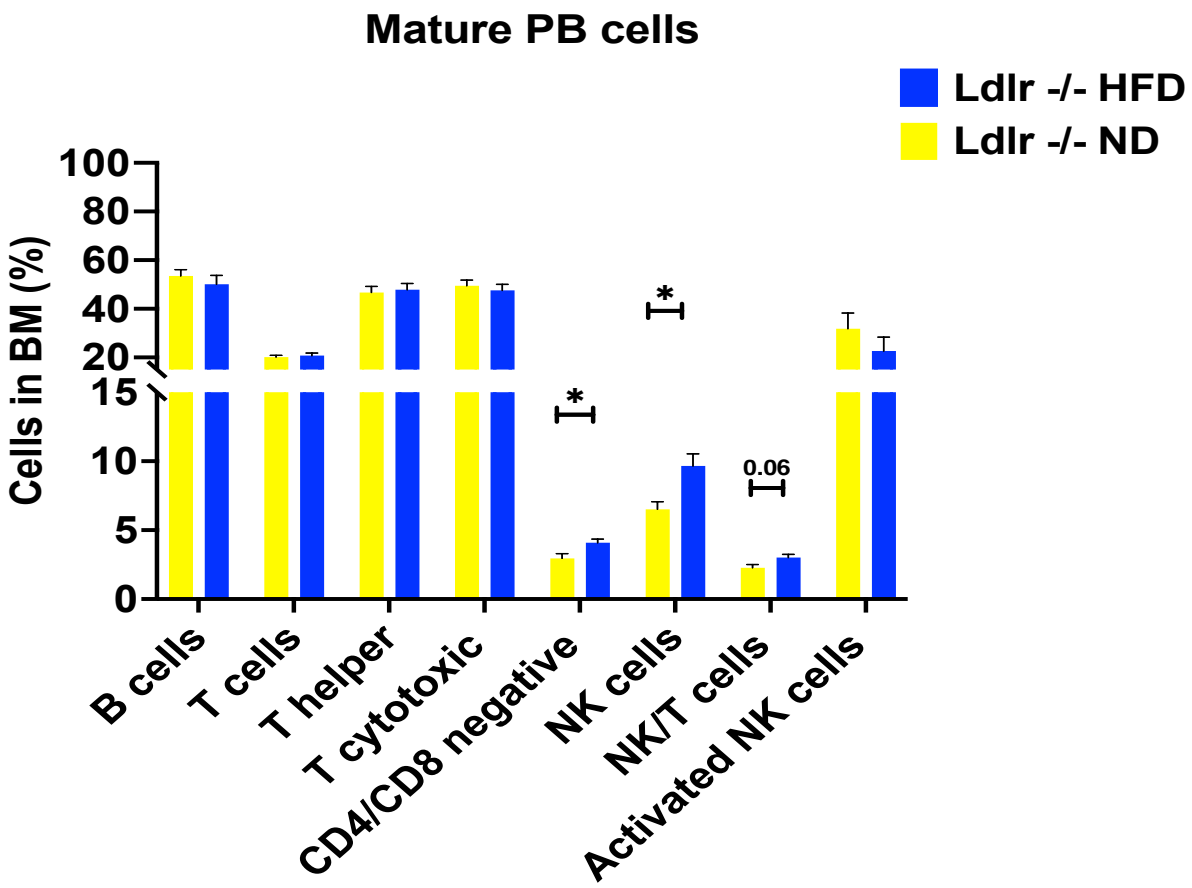

Figure 4.9 Enhanced lymphoid regulatory cells in Ldlr-/- mice receiving a HFD.

(A) Lymphoid cells B cells (CD19), T cells (CD3), T helper (CD4), T cytotoxic (CD8) and NK cells (NK1.1) were similar between *Ldlr*$^{-/-}$ mice receiving a ND (n=9) and *Ldlr*$^{-/-}$ mice receiving a HFD (n=10). (B) Regulatory Lymphoid cells NK/T cells (CD3/NK1.1) and double negative T cells (CD3+CD4-CD8-) were statistically increased in the HFD group, respectively. Activated NK cells (NK1.1/NKP46) was unchanged. Data was generated from four independent experiments. Data are mean ± SEM. Statistical analysis: Mann-Whitney U test, *P ≤ 0.05.

4.3.6 Hypercholesteremia stimulates myeloid haematopoiesis in the spleen of *Ldlr*$^{-/-}$ mice.

Given that hypercholesteremia affects the migratory capacity of HSPCs (Murphy et al. 2011), we next analysed the spleen of *Ldlr*$^{-/-}$ mice ingesting a HFD, a site of extramedullary haematopoiesis which can traffic and receive HSPCs and blood cells from the peripheral circulation and bone marrow (Fernandez-Garcia et al. 2020). Immunophenotypic analysis showed significant expansion in the frequency of Mac-1+Gr-1+ myeloid cells in *Ldlr*$^{-/-}$ mice receiving a HFD, mirroring our findings from BM and PB. Spleen weights and total cellular counts were unchanged between the two experimental settings (Figure 4.10). However, qualitative analysis of spleen sections showed intermingled red pulp (which acts as a blood filter, eliminating abnormal cells and debris while retaining healthy red cells, iron and platelets) and white pulp (which is responsible for the immune response) in *Ldlr*$^{-/-}$ mice receiving a HFD (Figure 4.11). These structural changes are likely to be inflammation related and therefore congruent with our findings in Section 3.3, with a recent reference correlating high cytokines production to pulp disorganization (Cesta 2006; Montes de Oca et al. 2020) (Figure 4.11).Thus, atherosclerosis driven chronic inflammation causes cellular immune response deregulation, which leads to displacement and destruction of splenic structural integrity (Montes de Oca et al. 2020).

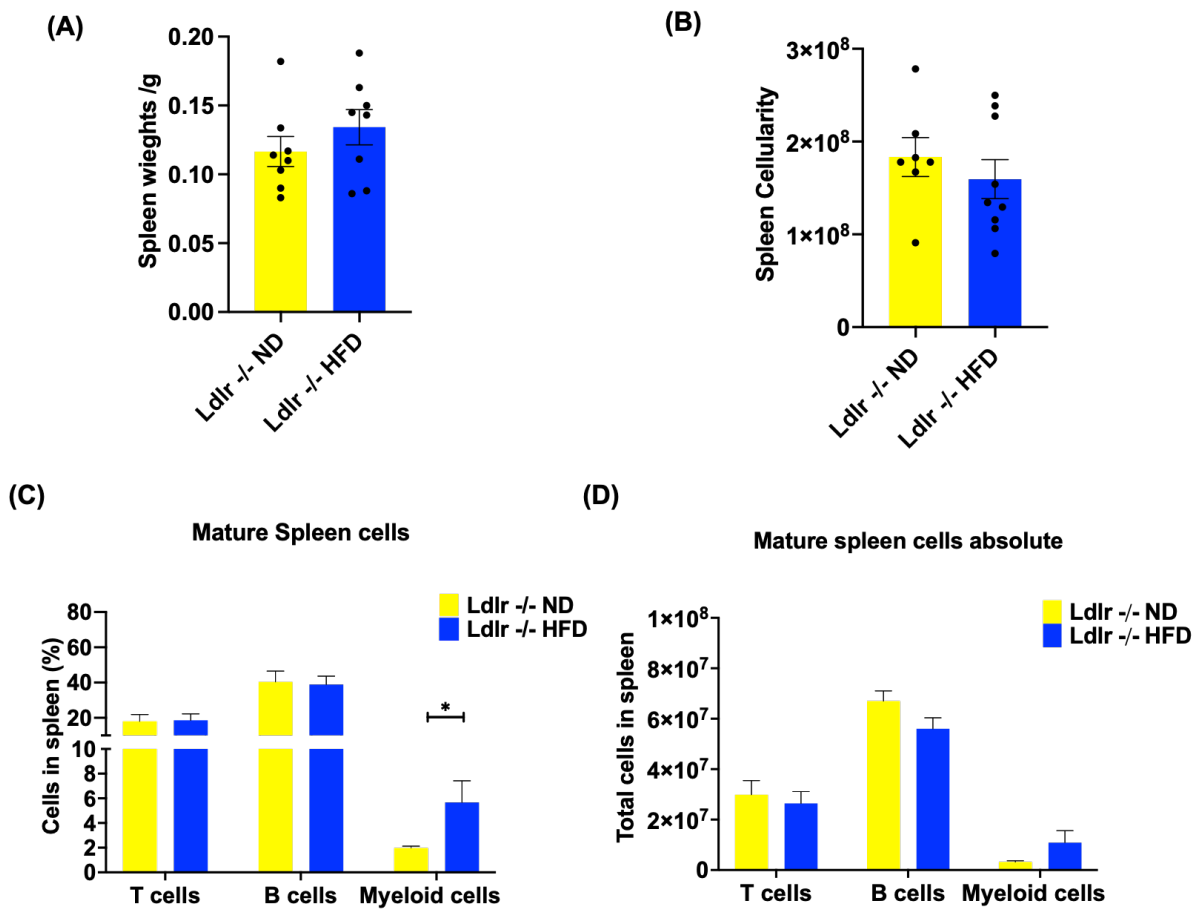

Figure 4.10 Extramedullary myelopoiesis in Ldlr-/- mice ingesting a HFD.

(A) Equivalent weight and (B) cellularity of spleens between *Ldlr*$^{-/-}$ on HFD (n=8) and *Ldlr*$^{-/-}$ mice on ND (n=6). (C) *Ldlr*$^{-/-}$ HFD exhibit increased frequencies of myeloid cells (Mac-1+/Gr-1+) cells in comparison to *Ldlr*$^{-/-}$ ND, However, T cells (CD3) and B cells (CD19) percentages were unchanged. (D) Absolute numbers in *Ldlr*$^{-/-}$ mice from both diets. Data generated from four mice from each condition. Data are mean ± SEM. Statistical analysis: Mann-Whitney U test, *P ≤ 0.05.

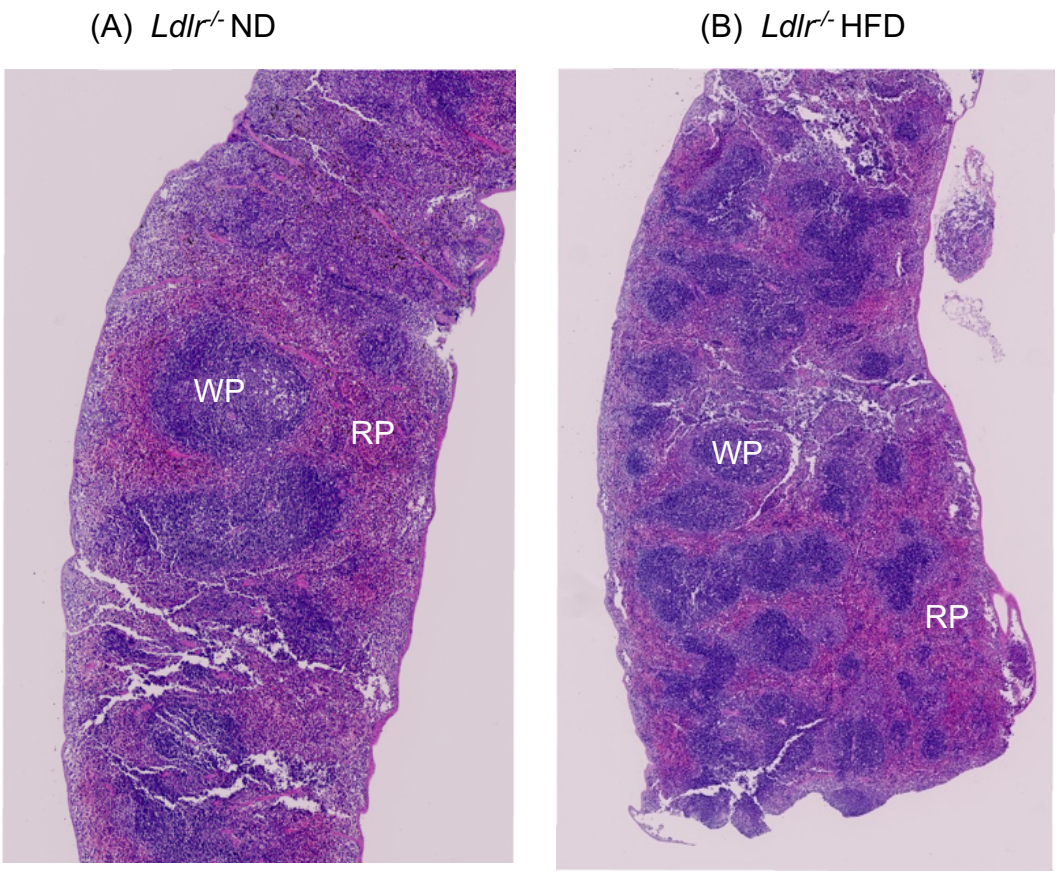

Figure 4.11 Hypercholesteremia induces structural changes in splenic architecture in Ldlr-/- mice on a HFD.

(A) H&E staining for spleen from *Ldlr*$^{-/-}$ ND (control) showing normal red pulp (RP) and white pulp (WP) distribution. (B) disrupted red pulp (RP) and white pulp (WP) in *Ldlr*$^{-/-}$ mice on a HFD. (RP) are three-dimensional meshwork of splenic cords and venous sinuses, Within the spaces between the cords are blood cells (erythrocytes, granulocytes, and mononuclear cells) thus, any extra medullary haematopoiesis should be shown. (WP) white pulp is subdivided into periarteriolar lymphoid sheaths, the follicles, and the marginal zone. It is composed of lymphocytes, macrophages, dendritic cells, plasma cells, arterioles, and capillaries in a reticular framework. Original magnification, X40 using an Olympus VS200 slide scanner.

4.3.7 Lymphoid cell development in the thymus were not affected by a high-fat diet in *Ldlr*$^{-/-}$ mice.

Having noted deregulated lymphoid progenitors and mature cells in *Ldlr*$^{-/-}$ mice that were fed a HFD, we thoroughly investigated T-cell development and in mature T-cell populations, which revealed that severe hypercholesteremia had no substantial influence on T-cell development in the thymus (Figure 4.12).

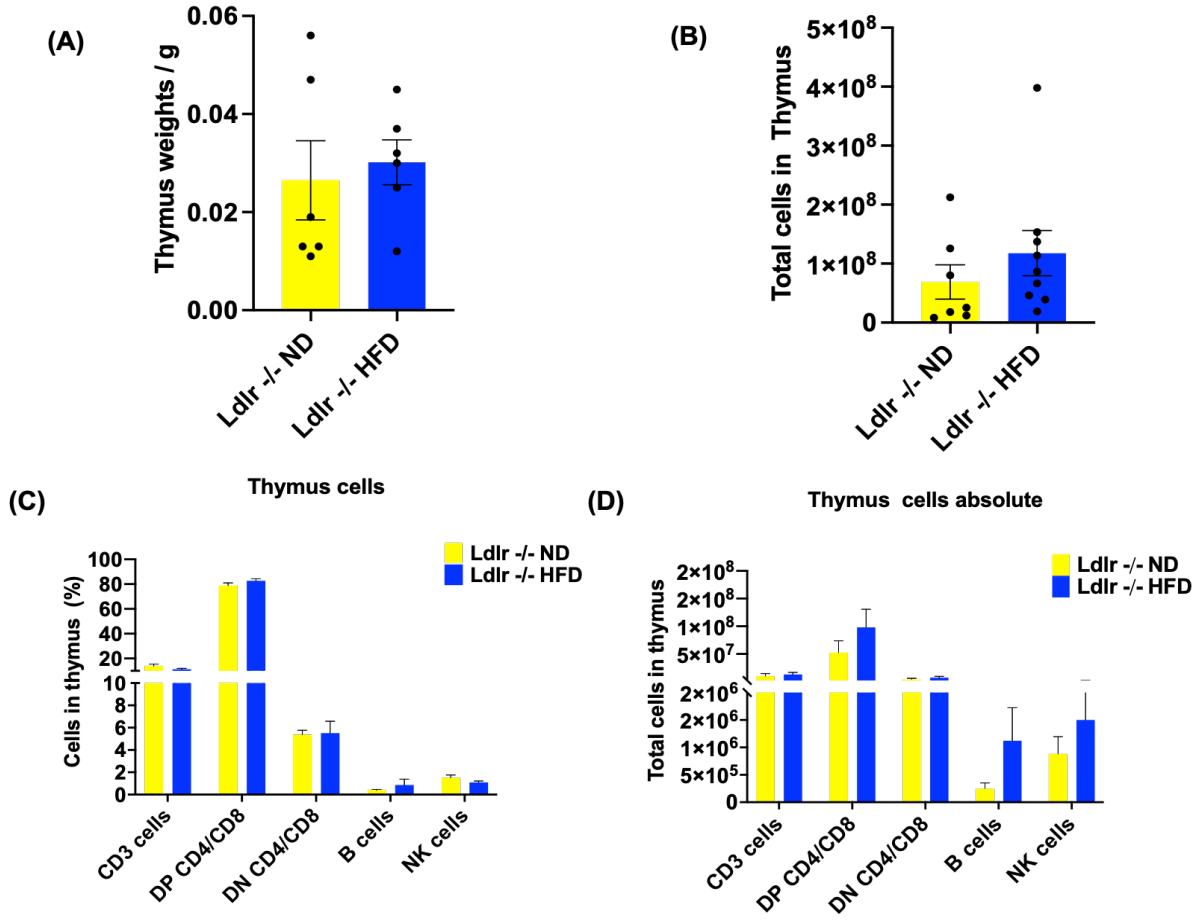

Figure 4.12 Hypercholesteremia has no impact on T cell development in the thymus.

(A) Thymus weight and cellularity in ND versus *Ldlr*$^{-/-}$ HFD were unchanged. (B) similar frequencies in T cells (CD3), double positive (CD4/CD8), double negative (CD4/CD8), B cells (CD19) and NK cells (NK1.1) between *Ldlr*$^{-/-}$ ND (n=7) and *Ldlr*$^{-/-}$ HFD (n=9). (C) absolute counts of different cell populations in thymuses of *Ldlr*$^{-/-}$ ND (n=7) and *Ldlr*$^{-/-}$ HFD (n=9) from four independent experiments. Data are mean ± SEM. Statistical analysis: Mann-Whitney U test.

4.3.8 HSCs from *Ldlr*$^{-/-}$ mice fed a HFD are functionally impaired in competitive bone marrow transplantation

To systematically assess the functional capabilities of HSCs of *Ldlr*$^{-/-}$ mice that ingested HFD, competitive transplantation studies were conducted to examine the ability of HSCs to repopulate haematopoietic lineages *in vivo* (Roy et al. 2012). FACS-isolated CD45.2 HSCs from *Ldlr*$^{-/-}$ mice on a HFD or *Ldlr*$^{-/-}$ mice on a ND were combined with wild-type competitor BM cells from CD45.1 mice and intravenously administered into irradiated recipient mice (CD45.1) (Figure 4.13 A).

To examine the donor contributions of HSCs to multi-lineage haematopoiesis, PB of recipient mice were evaluated at 4, 8, 12, and 16-weeks post-transplant, which, from week 8 onward, showed an overall decrease in donor contribution and decrease in T-cell, B-cell, and myeloid lineage specific contribution to recipients receiving HSCs from *Ldlr*$^{-/-}$ mice on a HFD (Figure 4.13 B and 4.13 C).

At week 16, recipient mice were sacrificed, and BM, spleen, and thymus were harvested and immunophenotyped for engraftment. Compared to control transplant cells, the chimerism of CD45.2 *Ldlr*$^{-/-}$ cells in myeloid, erythroid, T-cell, and B-cell lineages was considerably reduced in these haematopoietic organs, with myeloid lineages the most significantly altered (Figure 4.14 C,D,E and F). In addition, we analysed the donor contribution for primitive and committed haematopoietic compartments and found that the percentages of *Ldlr*$^{-/-}$ HFD HSCs donor cells for HSPCs (LSK, HSC, MPPs, HPC1, and HPC2), committed myeloid-progenitors (LK, CMPs, GMPs and MEPs), and committed lymphoid-progenitors (CLPs) in the bone marrow were significantly lower, especially myeloid primed stem/progenitor populations such as HSPC1, HSCP2, GMP and MEP (Figure 4.14 A and B). Together, these data show that exposure of *Ldlr*$^{-/-}$ HSCs to a HFD reduces their functional ability to engraft and their ability to contribute to multi-lineage haematopoiesis in transplantation.

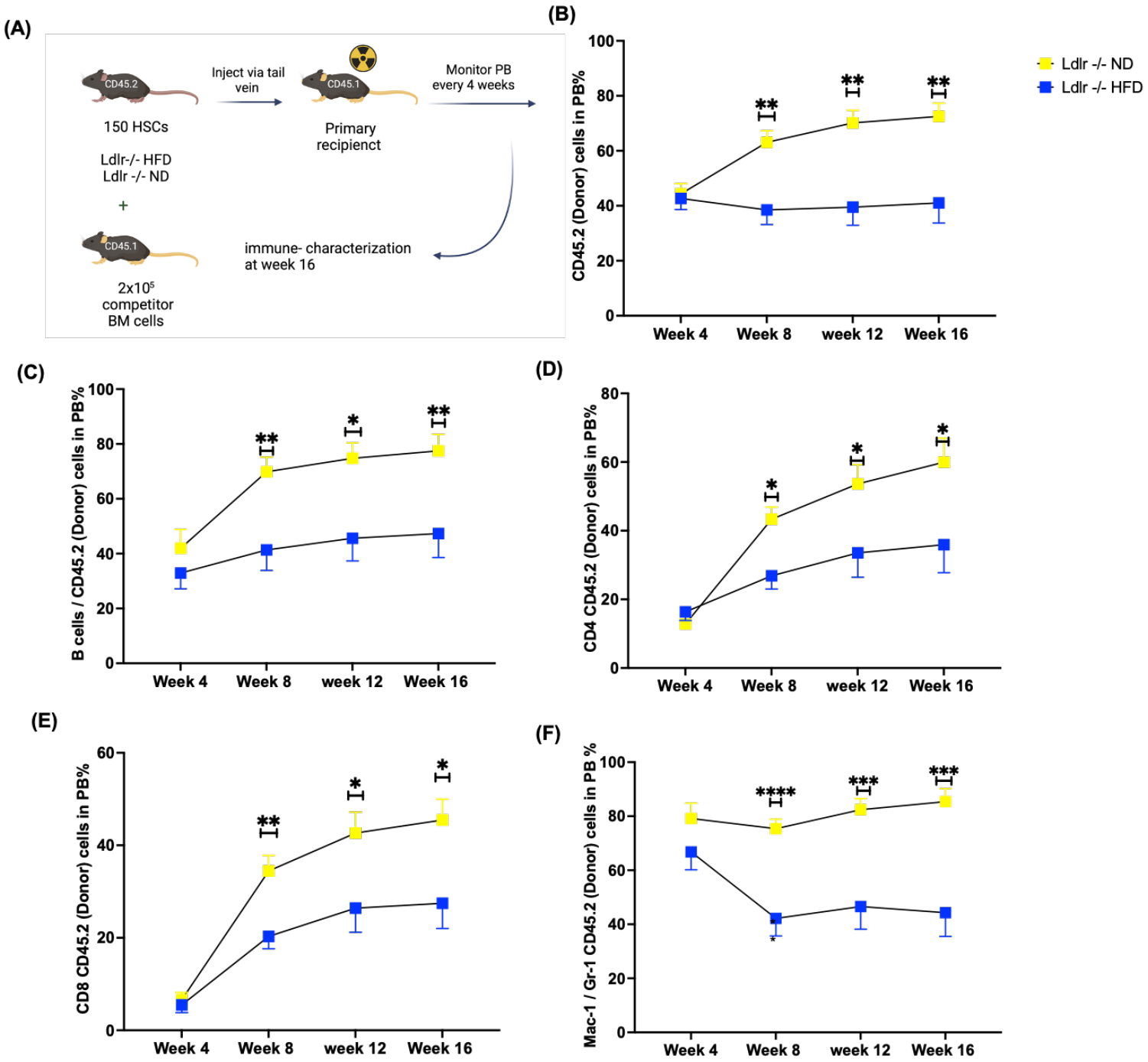

Figure 4.13 Purified HSCs from Ldlr-/- mice that received a HFD display a multilineage engraftment defect in competitive transplantation.

(A) Experimental design for primary HSCs transplantation. 150 HSCs from *Ldlr*$^{-/-}$ mice on a ND or *Ldlr*$^{-/-}$ mice on a HFD (Donor cells) were mixed with 2x10^5 CD45.1 support BM cells, which were injected via tail vain into lethally irradiated CD45.1 recipient mice. PB were extracted and analysed for donor cells chimerism assessment every 4 weeks. (B) Total CD45.2 donor engraftment from *Ldlr*$^{-/-}$ mice on a ND or *Ldlr*$^{-/-}$ mice on a HFD

(assessed every 4 weeks for 16 weeks total). (C-D-E-F) Donor CD45.2$^+$ B cells (B220$^+$), T cells (CD4$^+$, CD8$^+$) and Myeloid cells (MAC-1$^+$, GR-1$^+$) contribution in CD45.1$^+$ recipient mice peripheral blood for 16 weeks post-transplantation of *Ldlr*$^{-/-}$ mice on a ND and *Ldlr*$^{-/-}$ mice on a HFD. n= 11 mice for each group from three independent experiments and six independent biological donors were used for each condition. Data represents mean ± SEM. Statistical analysis: Mann-Whitney U test, *P ≤ 0.05; **P ≤ 0.01; ***P ≤ 0.001, ****P ≤ 0.0001.

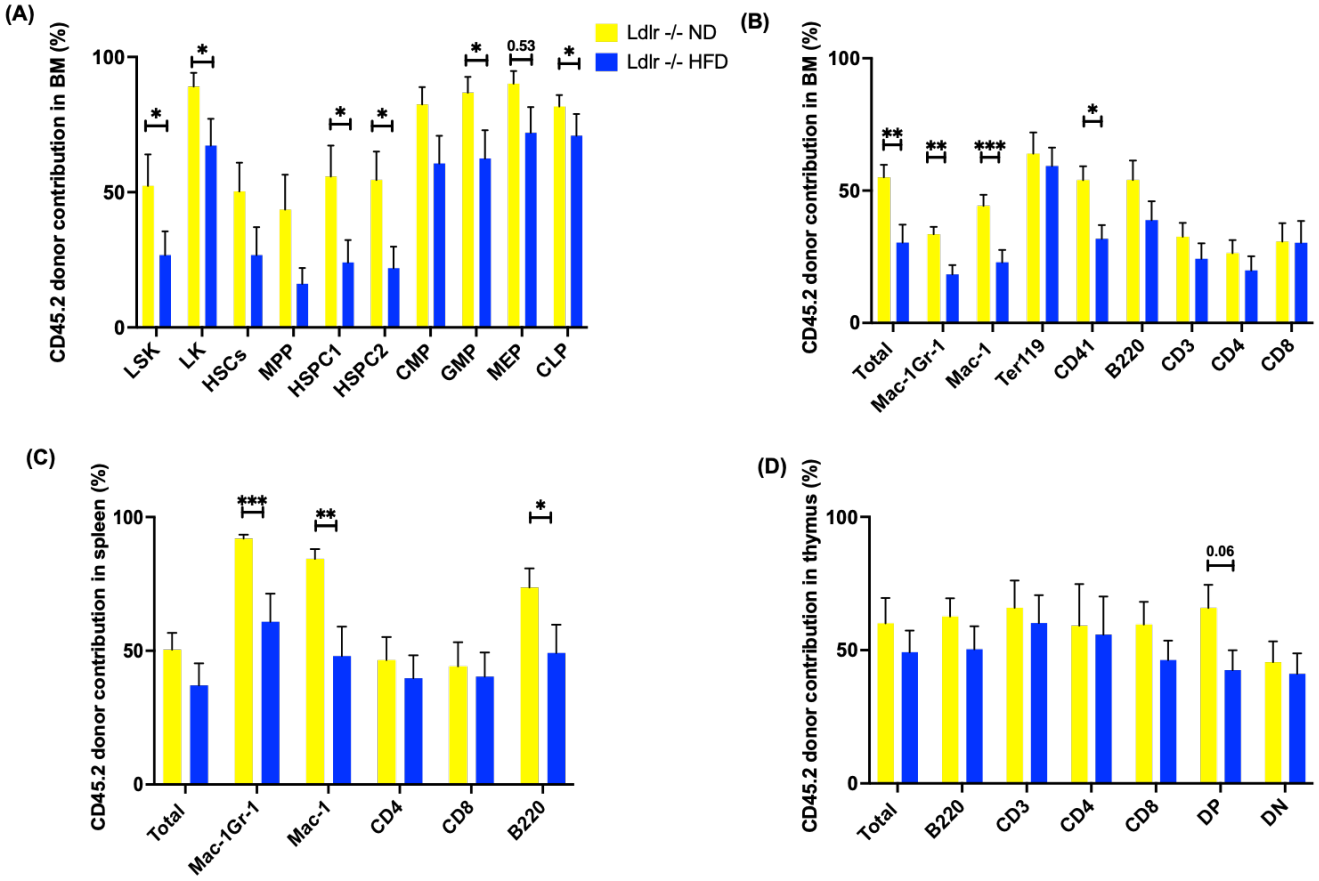

Figure 4.14 Purified HSCs from Ldlr-/- mice that received a HFD display a multilineage engraftment defect in competitive transplantation.

(A) Total CD45.2 percentages or donor contribution in bone marrow of CD45.1 recipient mice. *Ldlr*$^{-/-}$ HFD donor contribution cell frequencies to stem/ progenitor cells (LSK, HSCs, MPPs, HPC1 and HPC2) and committed/myeloid-lymphoid progenitors (LK, CMPs, GMPs, MEPs, and CLPs) in bone marrow. (B-C-D) Percentages of total CD45.2 cells donor contribution in bone marrow, spleen for Myeloid-cells (Mac1+Gr1+); Erythroid-cells (Ter119+); T-cells (CD4+ and CD8+); and B-cells (B220+) and thymus B-cells (B220+); T-cells (CD3) ; DP (CD3-CD4+CD8+); DN

(CD3-CD4-CD8-) at week 16 following transplantation of HSCs from *Ldlr*$^{-/-}$ mice on a HFD (n= 9) and *Ldlr*$^{-/-}$ mice on a ND (n=10) mice. Data were gathered from three separate experimental cohorts, with six donors employed for each condition. The results shown are the mean SEM. *P ≤0.05; ** P ≤0.01; *** P ≤ 0.001; statistical analysis: Mann-Whitney U test.

4.3.9 Differentially expressed transcriptional signatures relating to apoptosis, inflammation, RNA metabolism and deregulated haematopoiesis in HSCs from *Ldlr*$^{-/-}$ mice ingesting HFD

HSCs from *Ldlr*$^{-/-}$ mice on a HFD were functionally impaired, as judged by competitive transplantation experiments. To explore the transcriptional programme underpinning this defect, RNA-Seq was performed on purified HSCs (Lineage^{-} Sca-1^{+}ckit^{+}CD150^{+} CD48^{+}) from *Ldlr*$^{-/-}$ mice on a HFD and *Ldlr*$^{-/-}$ mice on a ND (Figure 4.15).

To fully assess the quality of our RNA-seq data, we used principal component analysis (PCA), which reduces the number of gene "dimensions" to a linearly modified set of dimensions that reflect the total variation in the dataset. A two-dimensional plot is used to display the results, with the data represented along axes that describe the variation in the dataset (Koch et al. 2018). Our PCA showed that replicates within samples and sample groups distributed over the two PCs clustered largely as predicted (Figure 4.16A). Another method to identify both intra and intergroup variability is correlation measurement between samples using Pearson's coefficient. This approach identifies the linear relationship between two variables accounting for differences in their mean and standard deviation (Koch et al. 2018). Our Pearson's correlation analysis showed minimal variation between samples giving all correlations value r > 0.9 (Figure 4.16B). After outlier assessment, expressed gene distribution analysis or clustering is required to determine relationship between groups of genes. We used hierarchical clustering in our study, which is Agglomerative or "bottom-up" type (Reeb et al. 2015) (Figure 4.16C). This method automatically builds a tree structure from a collection of input data points by treating each point as a cluster then integrating those clusters into bigger ones (called "clades"), without any human intervention (Koch et al. 2018). In total, 113 differentially expressed genes were identified in *Ldlr*$^{-/-}$ mice fed a HFD, with

58 out of 113 being downregulated (50.8%) and 56 out of 113 were upregulated (49.2%) (Figure 4.16D).

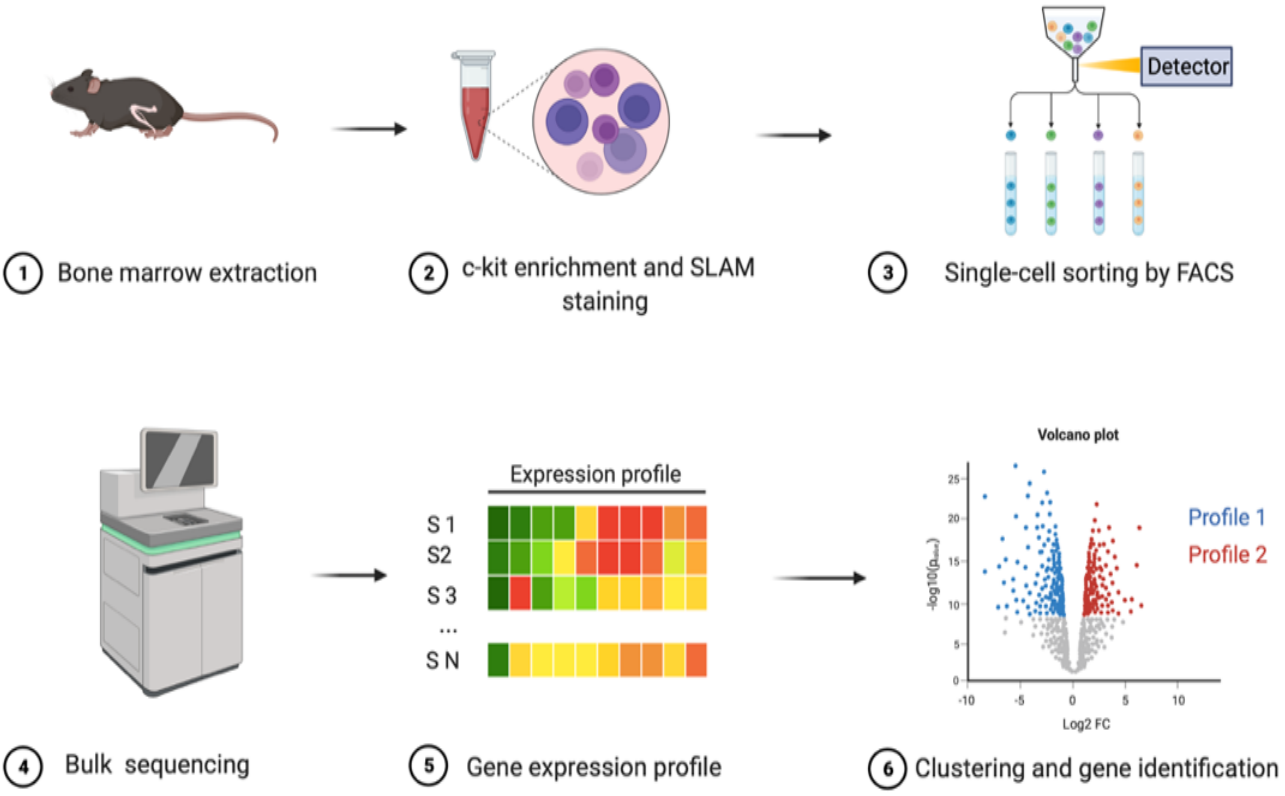

Figure 4.15 Experimental design for RNA sequencing of Ldlr-/- HFD primed HSCs.

HSCs are extracted from fresh bone marrow samples of *Ldlr*$^{-/-}$ that received HFD or ND. Lineage-ve , Sca-1, c-kit, CD150, CD48 stained sample are sorted by FACS to obtain 7000 (Lineage – Sca-1+ c-kit + CD150+) HSCs. After that 4 sample from each condition underwent gene expression profiling and then gene clustering and identification.

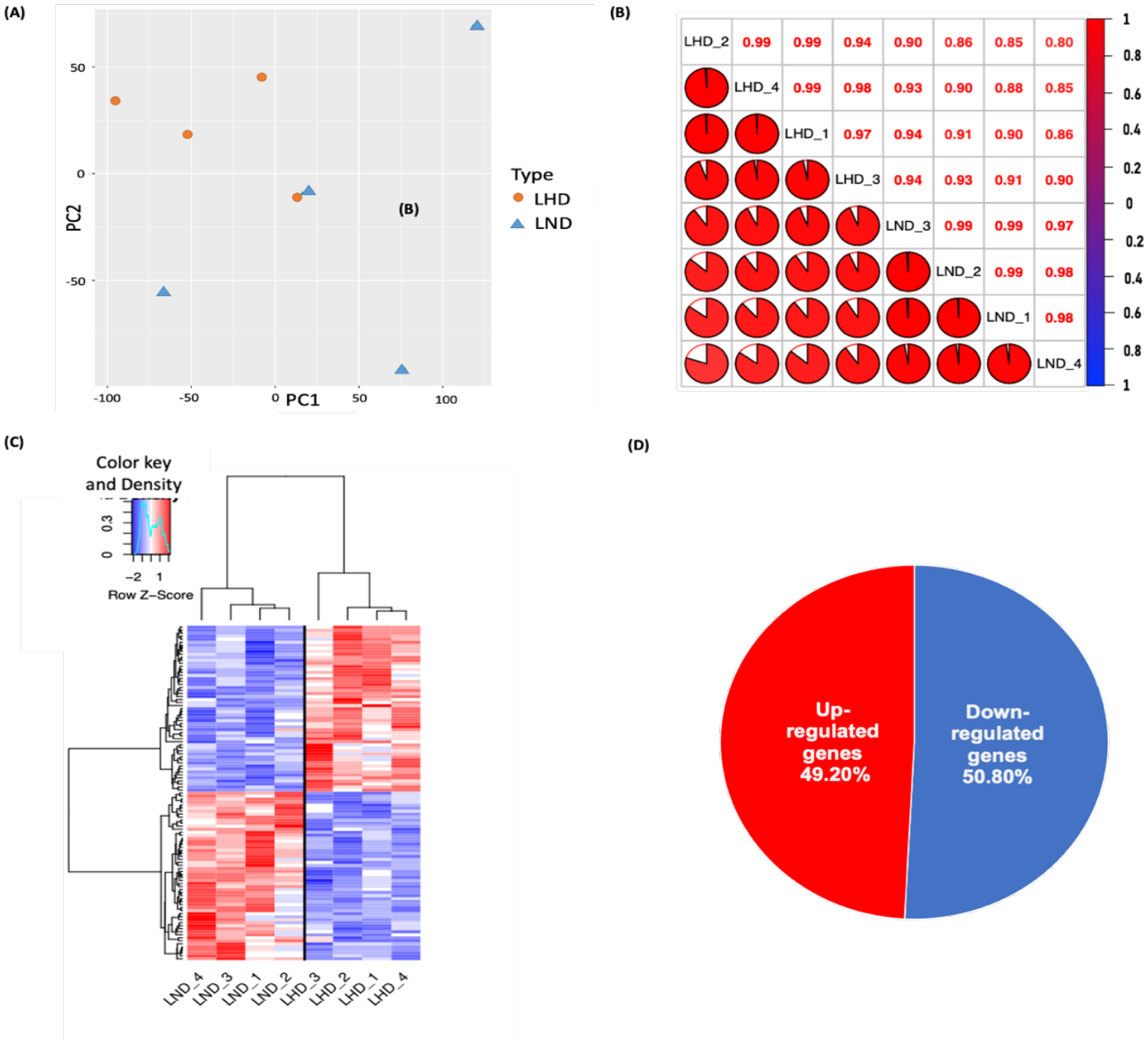

Figure 4.16 Assessing inter- and intragroup variability in transcriptome changes between Ldlr-/- ND and Ldlr-/- HFD HSCs.

(A) A principal component analysis (PCA) visualization to assess how replicates cluster together and for pointing out technical or biological outliers. (B) Pearson's correlation plot visualizing the correlation (r) values between 4 samples from each cohort (n=8). Scale bar represents the range of the correlation coefficients (r) displayed. The closer the R value is to 1, the more correlated the samples. (C) Hierarchical clustering performed on differentially expressed genes defined by ANOVA with a false discovery rate less than 0.05. Using all replicates per group, *Ldlr*$^{-/-}$ ND (n=4) and *Ldlr*$^{-/-}$ HFD (n=4) samples, 113 genes were clustered. The z-score

scale bar represents relative expression ± 2 SD from the mean. (D) The Venn diagram illustrates significant numbers of differentially dysregulated genes in purified HSCs from *Ldlr*$^{-/-}$ mice on a HFD (n=4) compared to control *Ldlr*$^{-/-}$ mice on a ND (n=4), affected 113 genes.

A robust signature of deregulated genes associated with perturbed haematopoiesis and AML was observed in HSCs from *Ldlr*$^{-/-}$ mice fed a HFD (Figure 4.17). Key downregulated genes included *Hmox1* (Heme Oxygenase 1), which under physiological conditions is involved in iron recycling and intracellular hemeostasis maintenance and is involved in AML cells apoptosis (Lin et al. 2015). *Matn4* (Matrilin 4), which is an extracellular matrix adaptor protein, has been correlated with increase proliferation/expansion of HSCs especially after the stress of chemotherapy and transplantation (Uckelmann et al. 2016). *C1qc* (Complement C1q C chain) is an immune cell receptor that is downregulated in AML (Huang et al. 2022b). *Hpgds* (Haematopoietic prostaglandin D synthase), which plays a role in the production of prostanoids in the immune system and mast cells (Kanaoka and Urade 2003), is downregulated in leukaemic stem cells after Ara-C chemotherapy in most AML patients (Farge et al. 2017) (Figure 4.17). Highly upregulated genes identified in HSCs from *Ldlr*$^{-/-}$ mice fed a HFD include *serpina3g* (Serine peptidase inhibitor, clade A, member 3G), which inhibit serine proteases released from neutrophils and mast cells such as elastase, cathepsin G and chymase (Wagsater et al. 2012), was recently found to be upregulated in fusion proteins MLL-AF9, MLL-AF10 and CALM-AF10 (Chen et al. 2021). Also upregulated was *Ifitm3* (Interferon induced transmembrane protein 3), that regulates adaptive immune cells signalling especially CD4 helper (Yanez et al. 2020), and found to correlated with poor prognosis in AML patients (Liu et al. 2020) and *Plac8* (Placenta Associated 8), a growth factor that can acts as an oncogene regulating apoptosis, proliferation, stemness, drug resistance, cell differentiation and others (Mao et al. 2021).

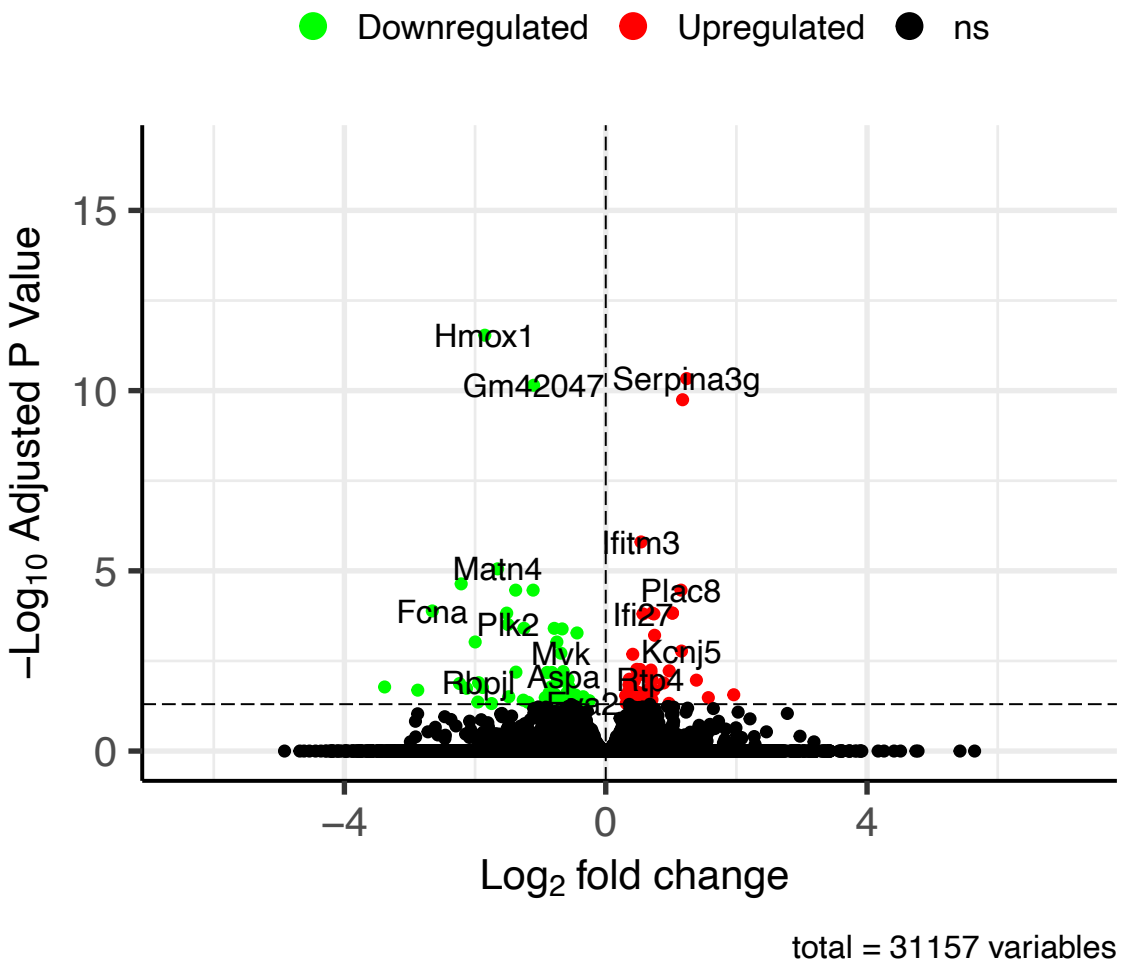

Figure 4. 17 Volcano plot showing highly up and downregulated genes in Ldlr-/- HSCs exposed to a HFD.

The y axis of a volcano plot is generated by graphing the negative logarithm of the p value (usually base 10). This causes data points with low p values (very significant) to display in the upper portion of the graphic. The x axis represents the logarithm of the change in fold between the two conditions.

Feeding our data into to the unbiased Ingenuity Pathway Analysis program IPA showed that most of deregulated genes sorted from HSCs *Ldlr*$^{-/-}$ mice ingesting a HFD BM were broadly associated with apoptosis, inflammation, and lipid metabolism pathways, with association of deregulated genes in diseases involved in cardiovascular disease, and, as alluded to above, haematological disease (Figure 4.18). The top 7 genes that were involved in all pathways are ABCG1, ITGB3, BCL3, HMOX1, C1QA, LGALS3 and TNF-α (Thorp 2010; Marchetti et al. 2015; Hardy et al. 2017; Suthahar et al. 2018; Sheikhvatan et al. 2019; Bellner et al. 2020; Rolski and Blyszczuk 2020), all of which are involved in AML disease initiation, progression, and prognosis (Marzac et al. 2011; Miller et al. 2013; Tian et al. 2014; Lin et al. 2015; Niu et al. 2019; Mer et al. 2021) in addition to nephrotoxicity, and hepatoxicity pathways, which shared 3 genes and 4 genes, respectively (Figure 4.18). Notably, differentially expressed genes in these categories intersected with each other (Figure 4.19), highlighting the close relationship that deregulated haematopoietic cells have in promoting cardiovascular and haematological disease in addition to novel associations with nephrotoxicity and hepatoxicity (Libby and Ebert 2018).

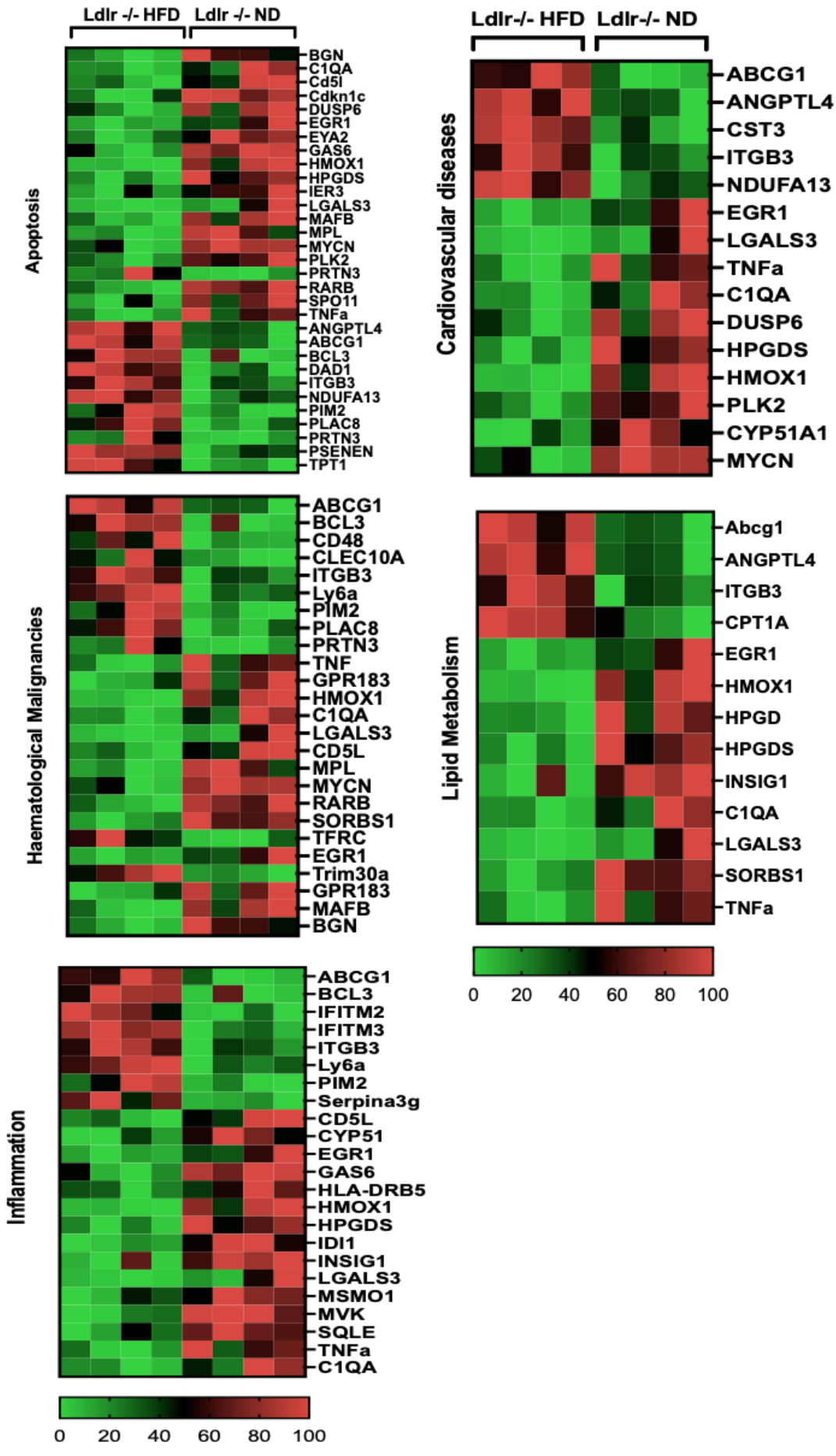
Ldlr -/- HFD
Ldlr -/- ND
Apoptosis
BGN
C1QA
Cd5l
Cdkn1c
DUSP6
EGR1
EYA2
GAS6
HMOX1
HPGDS
IER3
LGALS3
MAFB
MPL
MYCN
PLK2
PRTN3
RARB
SPO11
TNFa
ANGPTL4
ABCG1
BCL3
DAD1
ITGB3
NDUFA13
PIM2
PLAC8
PRTN3
PSENEN
TPT1
Ldlr-/- HFD
Ldlr-/- ND
Cardiovascular diseases
ABCG1
ANGPTL4
CST3
ITGB3
NDUFA13
EGR1
LGALS3
TNFa
C1QA
DUSP6
HPGDS
HMOX1
PLK2
CYP51A1
MYCN
Haematological Malignancies
ABCG1
BCL3
CD48
CLEC10A
ITGB3
Ly6a
PIM2
PLAC8
PRTN3
TNF
GPR183
HMOX1
C1QA
LGALS3
CD5L
MPL
MYCN
RARB
SORBS1
TFRC
EGR1
Trim30a
GPR183
MAFB
BGN
Lipid Metabolism
Abcg1
ANGPTL4
ITGB3
CPT1A
EGR1
HMOX1
HPGD
HPGDS
INSIG1
C1QA
LGALS3
SORBS1
TNFa
0 20 40 60 80 100
Inflammation
ABCG1
BCL3
IFITM2
IFITM3
ITGB3
Ly6a
PIM2
Serpina3g
CD5L
CYP51
EGR1
GAS6
HLA-DRB5
HMOX1
HPGDS
IDI1
INSIG1
LGALS3
MSMO1
MVK
SQLE
TNFa
C1QA
0 20 40 60 80 100

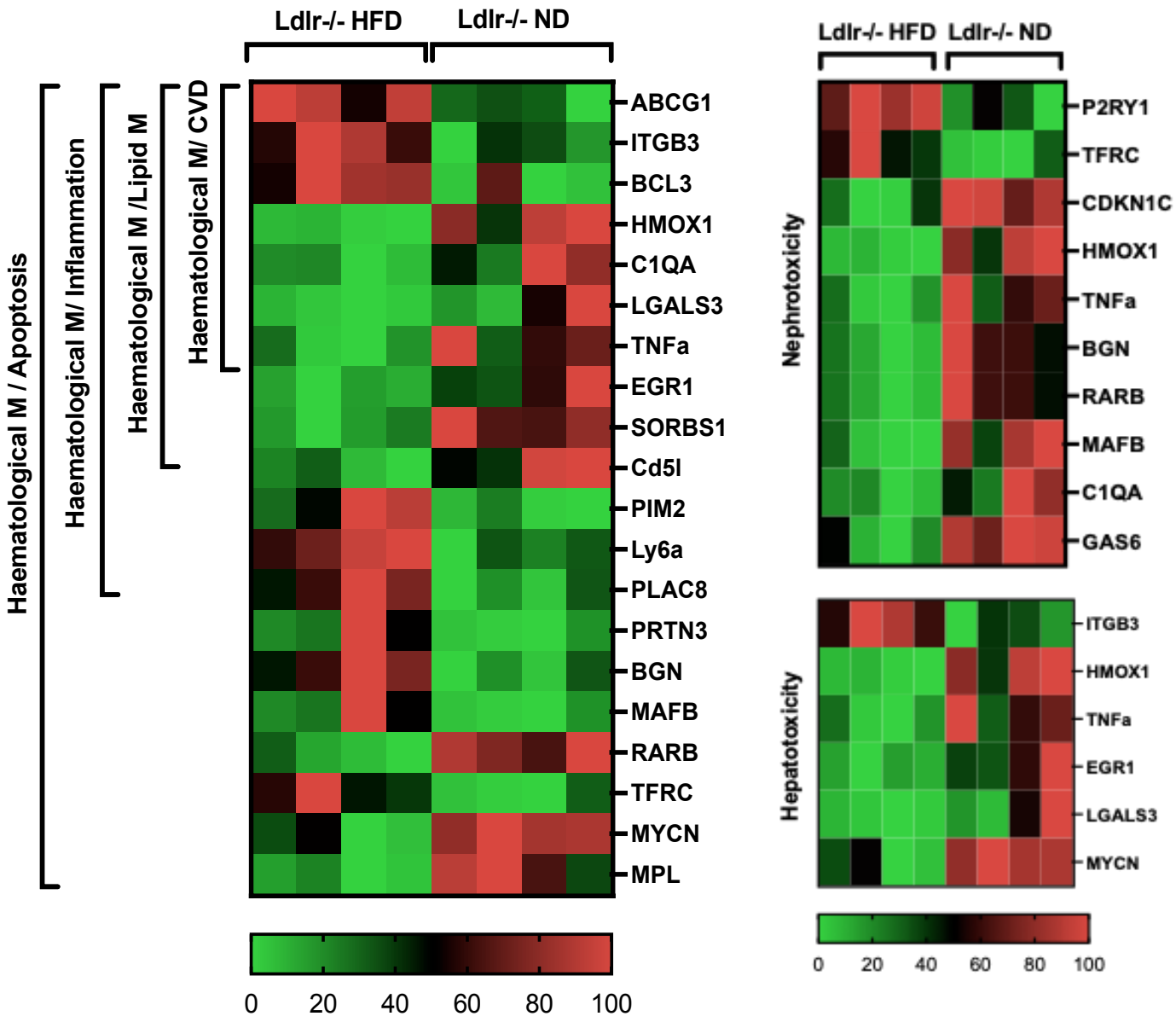

Figure 4.18 IPA of RNA-seq data from HSCs from Ldlr-/- mice fed a HFD reveals differentially deregulated genes in apoptosis, inflammation, and lipid metabolism pathways associated with cardiovascular disease, haematological disease, nephrotoxicity and hepatoxicity.

Heat maps of the differentially significant genes in *Ldlr*$^{-/-}$ HFD HSCs (n=4) compared to *Ldlr*$^{-/-}$ ND HSCs (n=4). Significant genes are mainly involved in apoptosis, inflammation, lipid metabolism (LM), cardiovascular diseases (CVD), and Haematological malignancies (HM). IPA analysis correlated apoptosis, inflammation and dysregulated lipid metabolism are responsible for development of several

diseases or conditions such as cardiovascular disease, haematological malignancies, nephrotoxicity and hepatotoxicity. Heat maps are drawn by Prism software after normalization. Red colour indicated up regulated genes; and green colour indicated down regulated genes. The colour gradient symbolises the intensity of gene expression.

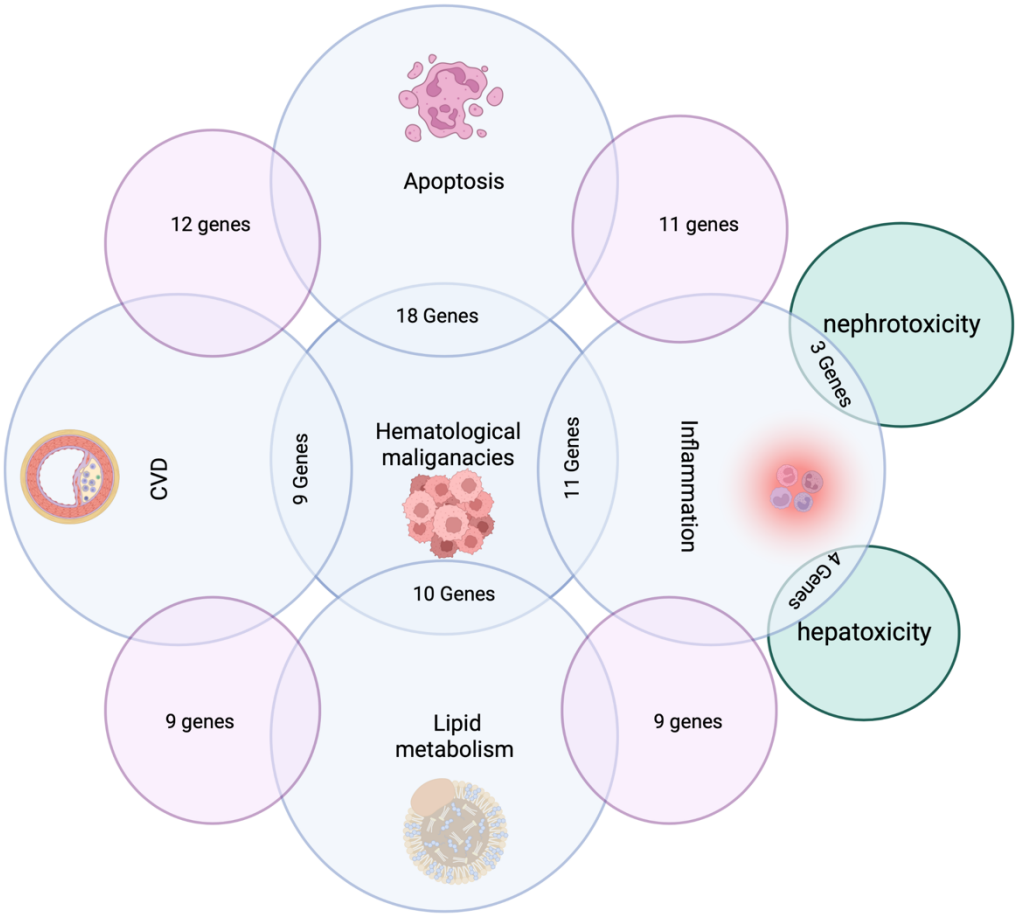

Figure 4.19 Interaction between differentially dysregulated genes in haematological diseases, lipid metabolism, inflammation, apoptosis, cardiovascular disease, nephrotoxicity and hepatoxicity.

Haematological disease shared dysregulated genes with other 4 different conditions, primarily apoptosis with 18 genes, then Inflammation 11 genes, then lipid metabolism 10 genes, and CVD 9 genes. Moreover, nephrotoxicity and hepatotoxicity are linked to inflammation. All conditions/ diseases share affected genes, showing significant link between mentioned disease.

Further unbiased analysis of our bulk-RNA data was performed using the g:Profiler analysis (Raudvere et al. 2019) which confirmed alteration of these pathways, including deregulated cholesterol/sterol pathways, a critical regulator of haematopoietic stem/progenitor cell integrity (Oguro 2019) (Figure 4.20). For example, increased cholesterol forces HSCs to enter cell cycle to self-renew and differentiate. It also aids in HSC/progenitor mobilization from BM to PB through CXCR4:SDF-1 axis reduction (Gomes et al. 2010). Moreover, cholesterol metabolites such as sex steroid hormones (mainly oestrogen), oxysterols, especially 27-hydroxycholesterol (27HC), bile acid and 25-hydroxycholesterol (25HC) (Oguro 2019) affect HSCs in steady state by binding to abundantly expressed oestrogen receptor-α, which increases their proliferation and differentiation capacity (Nakada et al. 2014). Increased 27HC modulates the endoplasmic reticulum of HSCs with the aid of oestrogen receptor (Oguro et al. 2017), whereas 25HC is an immune modulator that has pivotal roles in both infection and inflammation (Gold et al. 2014). Furthermore, cholesterol is the main precursor for bile acids and studies show that during foetal haematopoiesis bile acid relieves ER stress in HSCs to allow for adequate expansion (Sigurdsson et al. 2016).

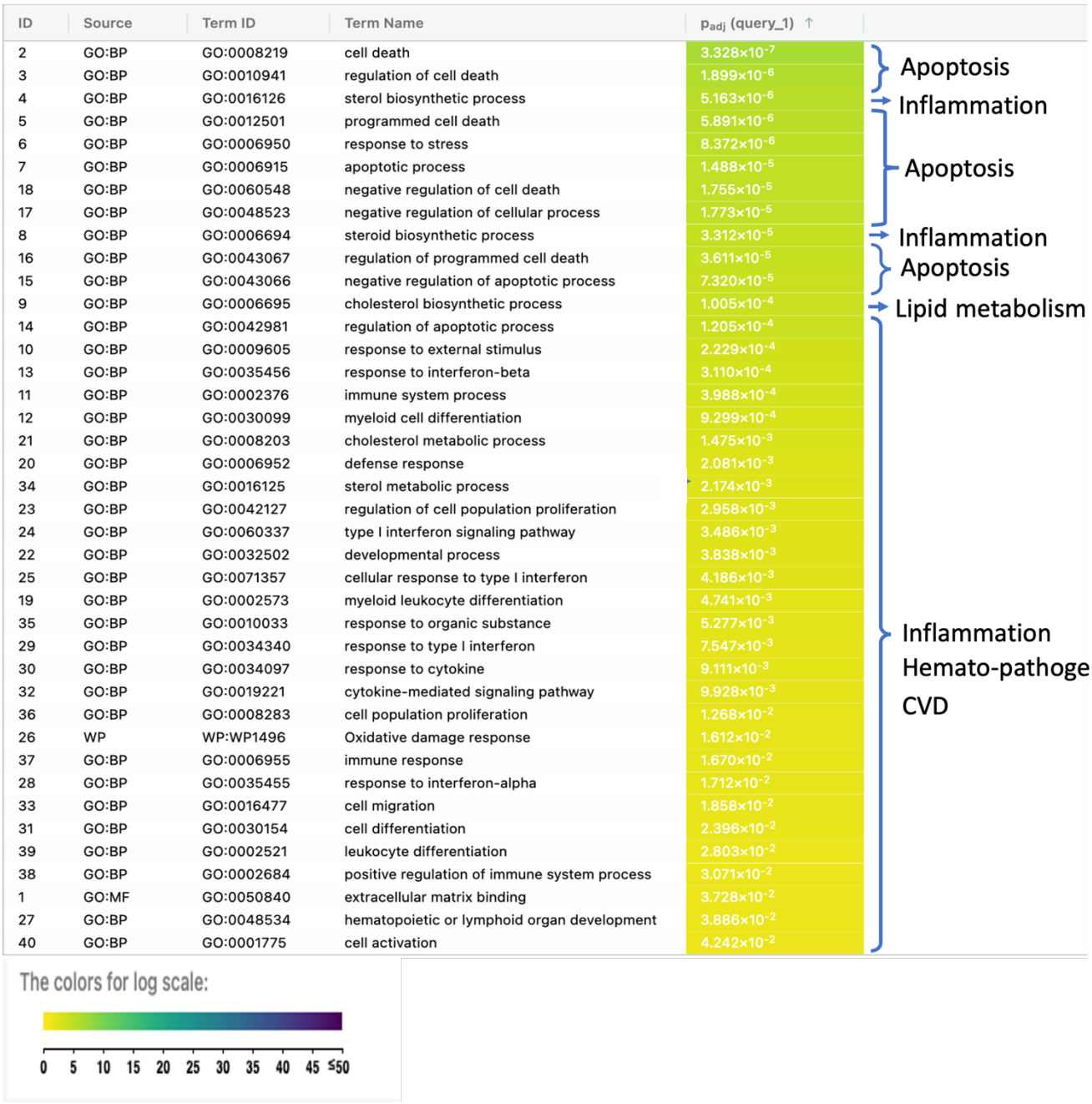

ID	Source	Term ID	Term Name	p_{adj} (query_1)
2	GO:BP	GO:0008219	cell death	3.328×10^{-7}
3	GO:BP	GO:0010941	regulation of cell death	1.899×10^{-6}
4	GO:BP	GO:0016126	sterol biosynthetic process	5.163×10^{-6}
5	GO:BP	GO:0012501	programmed cell death	5.891×10^{-6}
6	GO:BP	GO:0006950	response to stress	8.372×10^{-6}
7	GO:BP	GO:0006915	apoptotic process	1.488×10^{-5}
18	GO:BP	GO:0060548	negative regulation of cell death	1.755×10^{-5}
17	GO:BP	GO:0048523	negative regulation of cellular process	1.773×10^{-5}
8	GO:BP	GO:0006694	steroid biosynthetic process	3.312×10^{-5}
16	GO:BP	GO:0043067	regulation of programmed cell death	3.611×10^{-5}
15	GO:BP	GO:0043066	negative regulation of apoptotic process	7.320×10^{-5}
9	GO:BP	GO:0006695	cholesterol biosynthetic process	1.005×10^{-4}
14	GO:BP	GO:0042981	regulation of apoptotic process	1.205×10^{-4}
10	GO:BP	GO:0009605	response to external stimulus	2.229×10^{-4}
13	GO:BP	GO:0035456	response to interferon-beta	3.110×10^{-4}
11	GO:BP	GO:0002376	immune system process	3.988×10^{-4}
12	GO:BP	GO:0030099	myeloid cell differentiation	9.299×10^{-4}
21	GO:BP	GO:0008203	cholesterol metabolic process	1.475×10^{-3}
20	GO:BP	GO:0006952	defense response	2.081×10^{-3}
34	GO:BP	GO:0016125	sterol metabolic process	2.174×10^{-3}
23	GO:BP	GO:0042127	regulation of cell population proliferation	2.958×10^{-3}
24	GO:BP	GO:0060337	type I interferon signaling pathway	3.486×10^{-3}
22	GO:BP	GO:0032502	developmental process	3.838×10^{-3}
25	GO:BP	GO:0071357	cellular response to type I interferon	4.186×10^{-3}
19	GO:BP	GO:0002573	myeloid leukocyte differentiation	4.741×10^{-3}
35	GO:BP	GO:0010033	response to organic substance	5.277×10^{-3}
29	GO:BP	GO:0034340	response to type I interferon	7.547×10^{-3}
30	GO:BP	GO:0034097	response to cytokine	9.111×10^{-3}
32	GO:BP	GO:0019221	cytokine-mediated signaling pathway	9.928×10^{-3}
36	GO:BP	GO:0008283	cell population proliferation	1.268×10^{-2}
26	WP	WP:WP1496	Oxidative damage response	1.612×10^{-2}
37	GO:BP	GO:0006955	immune response	1.670×10^{-2}
28	GO:BP	GO:0035455	response to interferon-alpha	1.712×10^{-2}
33	GO:BP	GO:0016477	cell migration	1.858×10^{-2}
31	GO:BP	GO:0030154	cell differentiation	2.396×10^{-2}
39	GO:BP	GO:0002521	leukocyte differentiation	2.803×10^{-2}
38	GO:BP	GO:0002684	positive regulation of immune system process	3.071×10^{-2}
1	GO:MF	GO:0050840	extracellular matrix binding	3.728×10^{-2}
27	GO:BP	GO:0048534	hematopoietic or lymphoid organ development	3.886×10^{-2}
40	GO:BP	GO:0001775	cell activation	4.242×10^{-2}

Figure 4.20 g:Profiler pathway enrichment analysis of RNA-seq data from HSCs from Ldlr-/- mice fed a HFD reveals apoptosis, inflammation, and lipid metabolism pathways associated with cardiovascular and haematological

Listed are 40 of the most significantly altered biological pathways according to adjusted P value in *Ldlr*$^{-/-}$ HFD HSCs (n=4) compared to Ldlr-/- ND HSCs (n=4) in order of most statistical significance. Main pathways include apoptosis, inflammation and lipid metabolism relating to cardiovascular disease (CVD), and haematological malignancies.

Gene Set Enrichment Analysis software (GSEA) enrichment analysis additionally revealed dysregulated genes involved in multiple aspects of RNA biology, including RNA metabolism (Saha et al. 2019), RNA translation (Khanna-Gupta 2011), RNA processing, RNA methylation (Wu et al. 2020), which are emerging key regulators of normal and leukemic haematopoiesis (Wu et al. 2020)(Figure 4.21). In addition to GSEA revealing pathways, like CBFAT3, necessary for maintaining HSC integrity (Speck and Gilliland 2002) being deregulated in *Ldlr*$^{-/-}$ HSCs receiving a HFD, other targets relating to increased inflammation, such as c-myc (Wilson et al. 2004; Rodriguez et al. 2021) and oxidative phosphorylation, were established as differentially regulated *Ldlr*$^{-/-}$ HSCs receiving a HFD (Papa et al. 2019).

Analysis of canonical pathways was conducted using IPA which demonstrated that affected pathways (i.e. either up or down-regulated genes) were related to lipid metabolism (e.g. LXR/RXR activation), metabolic regulation in general (e.g. sirtuin signalling, mitochondrial dysfunction), inflammation (e.g. PPR receptors in innate immune system, interferon signalling, acute phase response signalling, IL-10 signalling), and apoptosis (e.g. ferropotosis) (Figure 4.22).

Notably, genes involved in the Inhibitor of DNA binding 1 (ID1) signalling pathway were activated overall, and genes involved in LPS/IL-1 mediated inhibition of RXR function were downregulated overall (Figure 4.22). ID1 is a common target for oncogenic kinases such as BCR-ABL, TEL-ABL, TEL-PDGFβR and FLT3-ITD, and when activated it is responsible for development and enhanced cycling of most tumours, including AML (Tam et al. 2008). Moreover, ID1 induces vascular endothelial cell/endothelial-mesenchymal transition, angiogenic reendothelialization, injury-induced reendothelialization, atherosclerotic plaque development and rupture, correlating with atherosclerosis, supporting the close relationship between deregulated haematopoiesis and cardiovascular disease (Qiu et al. 2022). LPS/IL-1 mediated inhibition of RXR function pathway is mainly required for lipid metabolism (Mucunguzi et al. 2017). Of relevance to our results, genome-wide expression analysis in the mouse liver following acute damage revealed that an upstream regulator inhibiting RXR activity caused increased inflammation and reduced metabolism (Campos et al. 2020). (Figure 4.22).

Collectively, parallel unbiased analysis of our RNA-seq data from HSCs in *Ldlr* deficient mice fed a HFD suggest that the defects observed in HSC function were related to transcriptional alterations in inflammation, lipid metabolism and other metabolic processes, RNA biology and apoptosis, with direct relevance not only to haematological disease and cardiovascular disease, but also nephrotoxicity and hepatoxicity.

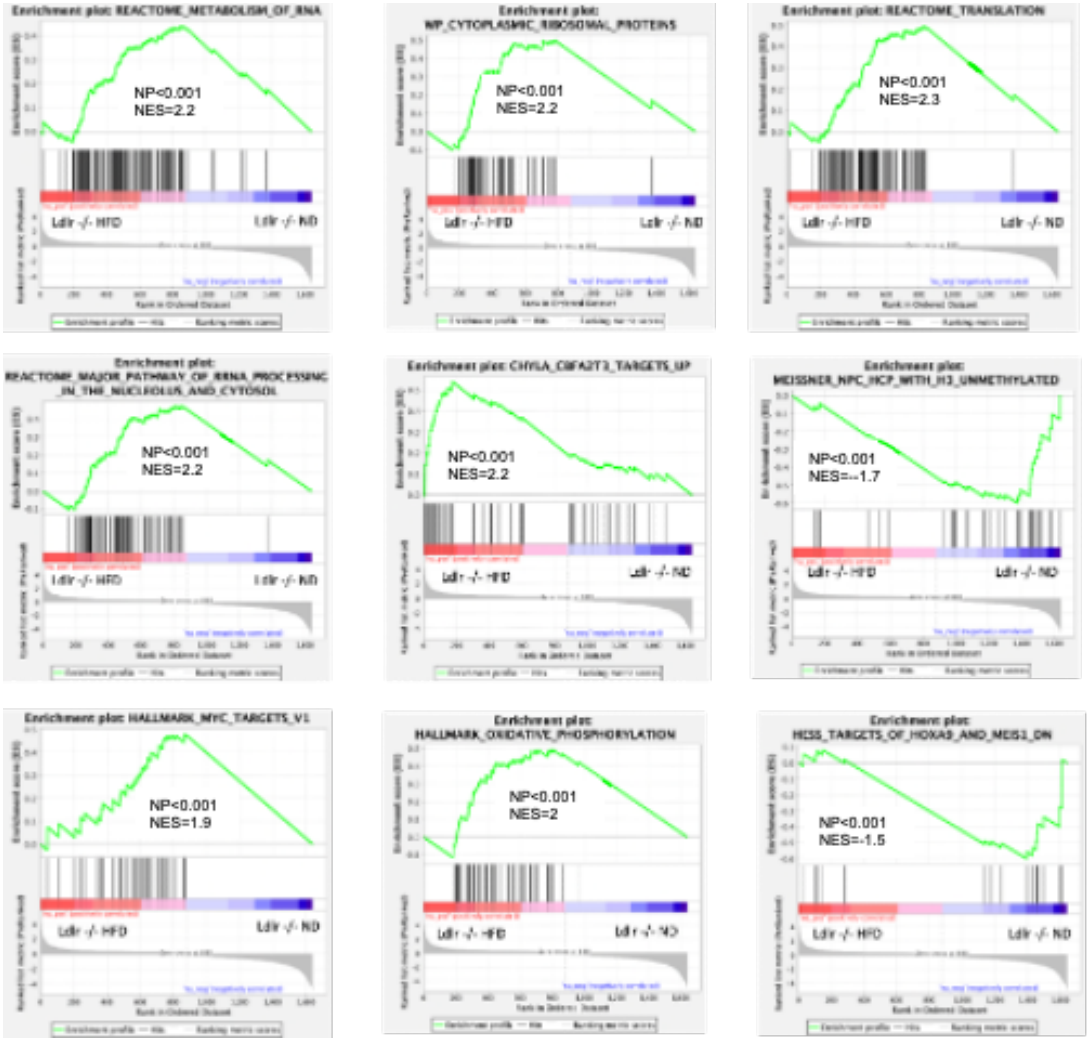

Figure 4.21 GSEA analysis of Ldlr-/- HSCs receiving a HFD reveals deregulated RNA biology, inflammation, and perturbed haematopoiesis.

GSEA plots showing enriched pathways for up-regulated genes and downregulated genes in Ldlr-/- HFD HSCs. Statistical significance is determined by Normalised p-values ≤ 0.05 and NES-values at between 0 and ± 2. NES indicates normalised enrichment score.

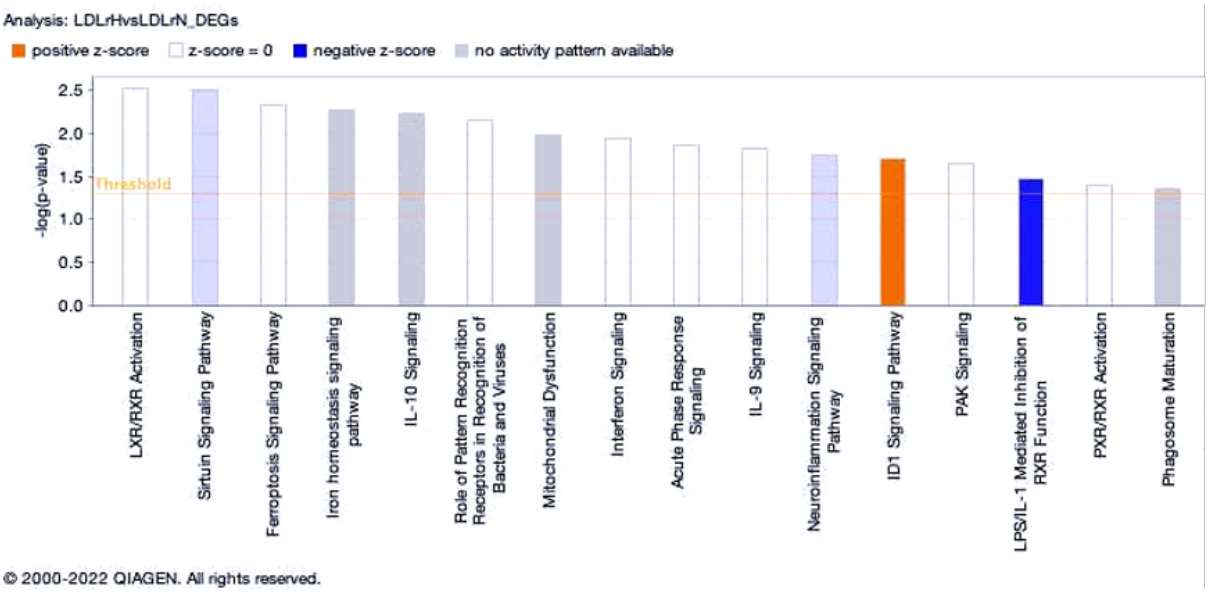

Figure 4.22 Canonical pathway analysis in IPA reveals ID1 signalling pathway genes are upregulated and LPS/IL-1 mediated inhibition of RXR pathway genes is downregulated in Ldlr-/- HSCs receiving a HFD.

ID1 signalling pathway is normally regulation of cell-cycle progression and cell differentiation, while LPS/IL-1 mediated inhibition of RXR is inflammatory related pathway. The significance values (p-value of overlap) for the canonical pathways are calculated by the right-tailed Fisher's Exact Test along the x-axis. The z-score represents the activated genes or inhibition of an individual canonical pathway. A z-score greater than 2.0 is considered significantly activated. A z-score smaller than −2.0 is considered significantly inhibited.

4.4 Discussion

Atherosclerosis is the most common cause of morbidity and mortality throughout the world. When it comes to the pathophysiology of atherosclerosis, inflammation plays a critical role. Inflammation is initiated when LDL increases, and HDL decrease in the context of hypercholesteremia. This makes the blood denser and causes injury to the inner lumen of the major arteries by sheer force, then the intima becomes excessively fibrotic, fatty plaques develop, and smooth muscle cells proliferate and migrate. Subsequently, cytokines and oxidised lipid activate endothelial cells. In addition, monocytes, T cells, and platelets are produced in response to the inflammatory signals and migrate into the site of injury respectively. In parallel, cytokines are then secreted to activate both cells and adhesion molecules, recruit and attract more cells to the site of injury and polarise monocytes into activated macrophages. Thus, production of key cells in atheroma progression, as it absorbs oxidised LDL, and ultimately foam cells produce. Foam cells start in plaque pathogenesis since the beginning where accumulates in arterial walls as lipid streaks, then some of them die through apoptosis in the developing lesion (Rafieian-Kopaei et al. 2014).

Hypercholesteremia is a chronic inflammation characterised by an increased production of inflammatory cells along with increased secretion of cytokines which has a role in immunosuppression, resulting in a milieu that is favourable for tumorigenesis (Multhoff et al. 2011; Wildes et al. 2019). Inflammatory cells act as tumour promoting agents by secreting cytokines/chemokines/growth factors which act to cause immunosuppression. This immunosuppression can be induced by activation of immunosuppressor cells which include but are not limited to macrophages, dendritic cells and myeloid-derived suppressor cells (MDSC) (Grivennikov et al. 2010). Thus, in the setting of chronic inflammation there is a distorted balance between pro-inflammatory and anti-inflammatory signals which cause immune imbalance and is one of the hallmarks of cancer initiation and progression (Gonzalez et al. 2018).

This motivated me to investigate the long-term effects of a high-fat diet on haematopoiesis in general, including inflammatory cells production in *Ldlr*$^{-/-}$ mice fed a HFD diet. Furthermore, haematopoietic tissues were harvested to examine the

function and features of HSCs under the conditions of stress of a high-fat diet and atherosclerosis and a possible relationship to the development of pre-leukaemia/leukaemia. This analysis is especially relevant given that clonal haematopoiesis of indeterminate potential CHIP, an HSC clonal disorder that increases the likelihood of leukaemia development, has also been associated with the development of atherosclerosis (Jaiswal et al. 2017).

In *Ldlr*$^{-/-}$ mice fed a HFD diet we found several features consistent with a heightened pro-inflammatory cellular milieu, including increased myeloid derived suppressor cells (MDSCs) and enhanced inflammatory monocytes. Studies on human and mice on MDSCs have shown that they promote tumour development by blocking antitumor immunity and overcoming this is considered to be critical in cancer immunotherapy treatments (Ostrand-Rosenberg and Fenselau 2018). MDSCs promote tumour progression through several mechanisms, most importantly, releasing ROS and Arg1 to prevent T cell activation, polarizing macrophages into tumour promoting phenotype and inhibiting NK cell killing activity (Ostrand-Rosenberg and Fenselau 2018) (Condamine and Gabrilovich 2011). This result complements our observation of increased MDSC cells in *Ldlr*$^{-/-}$ HFD mice.

On the other hand, inflammatory monocytes, identified by CD11b^{+}CD115^{+} and Ly6C^{+} expression level, can be subdivided into (inflammatory Ly6C^{high} and patrolling Ly6C $^{dim/negative}$) populations. The Ly6C^{high} / Ly6C $^{dim/negative}$ ratio in peripheral blood from *Ldlr* $^{-/-}$ mice on HFD was higher in comparison to *Ldlr*$^{-/-}$ mice on ND, confirming the heightened inflammatory context noted in other studies (Rahman et al. 2017). Classical monocytes (Ly6C ^{High}) leave the bone marrow as Ly6C^{++} and differentiate into LY6C^{-} or macrophages (Yang et al. 2014). In hypercholesteremia related chronic inflammation LY6C^{+} dominate the blood due to excessive recruitment (Geissmann et al. 2010) as observed in our results. These cells secrete ROS, TNF-α and IL-1β and can easily convert to inflammatory macrophages M1 and M2 to enhance inflammation (Yang et al. 2014). The heightened inflammatory environment in the setting of hypercholesteremia appears to be programmed at the HSC level as HPSCs are responsible for producing inflammatory cells and HSCs from *Ldlr*$^{-/-}$ mice fed a HFD displayed a robust inflammatory signature, as observed in our RNA-sequencing analysis. Furthermore, this inflammatory environment may feedback to alter HSPC

function (Caiado et al. 2021). For example, we found MYC-targets were overexpressed in HSCs from *Ldlr*$^{-/-}$ mice fed a HFD, consistent with another study where overexpression of MYC-targets in HSPC was found due to pro-inflammatory cytokine signalling, including TNF-a, IL-6, MCP-1, and Ilβ (Caiado et al. 2021). Further evidence at the cellular level for an impact of the pro-inflammatory environment of *Ldlr*$^{-/-}$ mice fed a HFD altering HSPC behaviour is provided by our immunophenotyping data. In mouse, MPP2 and MPP3 appear to act as an emergency route that grows during inflammation or regeneration, resulting in the production of myeloid-lineage cells, in these conditions (Cabezas-Wallscheid et al. 2014). On the other hand, the traditional lymphoid-primed MPP (designated MPP4/LMPP) is the most prevalent MPP subtype and is thought to be responsible for the majority of multilineage blood under homeostatic circumstances (Cabezas-Wallscheid et al. 2014). *Ldlr*$^{-/-}$ animals given a HFD showed expansion of HSPCs of MPPs (in particular HPC1, HPC2), where MPP2 overlaps with HPC2 and MPP3 resembles HPC1 (Pietras et al. 2015). While other HSPC populations were also expanded (e.g HSCs) MPPs responsible for inflammatory blood cell production were specifically enhanced in *Ldlr*$^{-/-}$ animals given a HFD, with the inflammatory milieu presumably feeding back on select MPP subsets to increase and sustain pro-inflammatory cell production in this model.

Chronic inflammation, if unresolved, as is the case in the setting of *Ldlr*$^{-/-}$ HFD, eventually leads to cross-talk with the adaptive immune response and an antigen-specific adaptive immunological responses activated and directed by T and B cells (Cronkite and Strutt 2018). In the adaptive immune response arm, the peripheral blood results showed dramatic NK frequency increase in *Ldlr*$^{-/-}$ HFD in comparison to *Ldlr*$^{-/-}$ ND. This finding is mirrored in bone marrow lineage specific cell populations, where NK cells were significantly high as well. Studies suggest that natural killer (NK) cells may play a role in atherogenesis through both their cytotoxic characteristics and their ability to create pro-atherogenic inflammatory cytokines, primarily IFN-γ (Bonaccorsi et al. 2015). (Schiller et al. 2002). However, NK activity marker assessment between the two cohorts were inconclusive. This agrees with previous studies on NK activity in atherosclerotic patients (Bruunsgaard et al. 2001). Nevertheless, earlier studies demonstrated that NK pro-atherogenic studies are independent of NK cell-mediated cytolysis (Schiller et al. 2002). In parallel, NK cells are important player in leukemic microenvironment (Yang et al. 2018). As indicated in Yang et al. 2018 study, where

they found increased splenic NK cell in Murine MLL-AF9 induced AML model. This result again argues for the strong relationship between chronic inflammation, immune dysregulation and acute myeloid leukaemia.

NKT cells also tended to increase in HFD fed *Ldlr*$^{-/-}$ mice. This confirms previous studies conducted on atherogenic mice on HFD (To et al. 2009). Studies on *Ldlr*$^{-/-}$ model correlated increased NKT to increased atherosclerosis burden (Aslanian et al. 2005). NKT cells are lymphocytes that share CD3/NK1.1 and CD4 markers and they are stimulated by lipid antigens. Most studies in atherosclerosis mouse models indicate that NKT cells have pro-atherogenic characteristics (To et al. 2009). NKT cells are activated directly by glycolipids taken up by antigen presented cells or indirectly via TLR activation , when activated they produce proinflammatory cytokines, such as IL-12, TNF- α and IFN-γ (Braun et al. 2010). Increased activation of NKT cells by effector cells such as T cells, even in normal numbers contributes to a variety of pathological disease such as multiple sclerosis, solid tumours and haematological malignancies (VanderLaan et al. 2007; Berzins et al. 2011; Getz et al. 2011; Getz and Reardon 2017; Goh and Huntington 2017).

Atherosclerotic fatty streaks are made up of not only monocytes derived macrophages but also T lymphocytes (Schiller et al. 2002). Our results showed T cells including CD4 T helper cells, or CD8 T cytotoxic cells and B cells frequencies were comparable between our two cohort groups, although its functional competencies were not evaluated in this thesis. Nevertheless, our peripheral blood morphological examination revealed analysis revealed clear lymphocyte reactive morphology. Several studies have highlighted the need to control cholesterol metabolism in T cells to sustain lipid raft homeostasis, which is required for appropriate T cell activity and communication (Guo et al. 2017b). As a result, alterations in T cell function, activation, and reprogramming are caused by impairments in cholesterol metabolic enzymes, cholesterol modulators, and transporters (Bietz et al. 2017) (Aguilar-Ballester et al. 2020). Hypercholesteremia induced T cell activation in *Ldlr* $^{-/-}$ mice, hence the need for hepatic T reg differentiation is required to mediate immune suppression and avoid autoimmune disease (Mailer et al. 2017b). Prolonged exposure to high levels of circulating lipids boosts CD4+ and CD8+ T cell proliferation and results in an increased fraction of CD4+ central memory T cells inside the draining lymph nodes of *Ldlr*$^{-/-}$ mice

(Pollock et al. 2016). Thus, increased number and/or activity of both anti-inflammatory Treg cells and pro-inflammatory effector T cells disrupts the immunological balance and raises the risk of compromised immune responses (Mailer et al. 2017a). Yet, (Wang et al. 2016) and (Swamy et al. 2016) showed that cholesterol or cholesterol derivative inhibit TCR signalling by disturbing TCR multimers or via binding to TCRβ transmembrane domain. Also, recent studies indicated that cholesterol induces CD8+ T cells activation of immune checkpoint that may lead to cell exhaustion (Ma, 2019 *148) Therefore, the involvement of cholesterol in T-cell activation remains controversial. It is also worthy of mention that LDL receptor was recently found to be essential in regulating CD8+ T cells antitumour potential. *Ldlr*$^{-/-}$ CD8+ T cells showed impaired effector function upon stimulation, such as reduced cytokine and granule secretion, as well as diminished clonal proliferation, upon stimulation in comparison to wild-type CD8+ T cells (Yuan et al. 2021).

CD3+ CD4-CD8- double negative T cells from *Ldlr*$^{-/-}$ fed a HFD were significantly increased. These rare peripheral T cell subsets have crucial role in immune disease, inflammation, and cancer as a subset of regulatory T (Treg) cells (Wu et al. 2022). DN T cells originate from a subset of thymocytes during specific phases in the thymus. DN T cells are involved in both innate and adaptive immune responses. Based on Ag-TCR-specific identification, DN T cells can inhibit or destroy adaptive immune cells, hence decreasing immunological-mediated illnesses, including autoimmunity (Martina et al. 2015). Additionally, DN T cells can release several cytokines to drive innate immune responses (Martina et al. 2015; Wu et al. 2022). CD3+CD4–CD8– double negative T cells can inhibit allogeneic immune responses by eliminating activated syngeneic CD8+ T cells. Also, the same study shows that DN T cells express significantly high Ly-6A (Zhang et al. 2002). These studies were consistent with our RNA expression results where Ly6A expression on *Ldlr* $^{-/-}$ HFD HSCs were increased as well. It is not entirely clear why immunosuppressive cells such as Tregs are enhanced in a pro-inflammatory environment, but explanations include the need for a controlling mechanism to regulate effector T cells to avoid autoimmune destruction (Li and Tsokos 2021). Further investigation should include αβ- DN T cells and other T reg subsets to be more specific about their impact of immune regulation in our model (Brandt and Hedrich 2018).

Platelets were considerably increased in *Ldlr*$^{-/-}$ HFD. Due to hypercholesteremia inflammatory stress, platelets are can be produced from HSCs directly (Sanjuan-Pla et al. 2013), as well MPP populations, specifically MPP3 (Pietras 2017). Thus, increased platelets may be caused by the expanded HSC and MPP compartments in our *Ldlr*$^{-/-}$ HFD group. Platelets in atherosclerosis may produce several inflammatory mediators, which further enrich and intensify the inflammatory environment by facilitating the recruitment of inflammatory cells to lesion sites (Lim 2020). This evidenced by a study showing that depleting platelets in *Ldlr*$^{-/-}$ mice fed a Western diet slowed macrophage recruitment in atherosclerotic plaques, leading to decreased plaque size and necrotic area mediated by loss of Platelet-induced myeloid Socs3 expression. (Barrett et al. 2019)

Competitive bone marrow transplantation of donor *Ldlr-/-* HFD HSCs was conducted to thoroughly analyse HSC functional ability for multilineage repopulation (Herbert et al. 2008; Sawen et al. 2018). Analysis of the chimerism in recipients from the *Ldlr-/-* HFD group revealed a significant decrease in reconstitution potential in various haematopoietic organs (peripheral blood, bone marrow, spleen, and thymus) when compared with the *Ldlr-/-* ND. Table 4.1 summarizes recent studies where hypercholesteremia primed bone marrow cells were competitively transplanted to test HSC function. Our data contrasts with some studies (Seijkens et al. 2014) (van den Berg et al. 2016), but agrees with most other studies. In Table 4.1 In our study, we isolated HSCs with better homogeneity utilising FACS with highly specific HSC cell surface markers. Part of the explanation for the discrepancies between studies may reflect differences in high-fat diet composition used, mouse model used, including genetic background, donor cell heterogeneity (e.g. if total BM was used or if purified HSCs were used in transplant) and cell dosage injected into transplant recipients. For instance, BM from *Ldlr-/-* mice given a HFD may have altered adipogenesis which impacts haematopoiesis and could affect donor cell engraftment if total unfractionated BM cells are used in transplantation experiments (Lee et al. 2018). We transplanted highly purified HSCs to exclude any auxiliary role of other haematopoietic or non-haematopoietic cells in testing HSC function. Thus, to our knowledge, for the first time we directly measured the intrinsic HSC potential from *Ldlr-/-* fed a HFD.

Table 4.1 Recent hypercholesteraemic primed Haematopoietic cells transplantation experiments summary

Model	HFD	Duration	Results	Transplantation	Donor cells dose	Reference
Ldlr -/-	16% fat and 0.15% cholesterol.	Not declared	High HSCs Proliferation and mobilization	Hypercholesteremic CD45.1-Ldlr$^{-/-}$ BMCs were transplanted into chow-fed CD45.2-Ldlr$^{-/-}$recipients increased reconstitution of CMPs and GMPs, compared with non-primed HSPCs. increased total leukocyte reconstitution potential	Donor 1x10^6 BM Competitor 5X10^5 BM	(Seijkens et al. 2014)
Ldlr-/-	15% cacao butter +0.25% cholesterol	45 weeks		WT-hypercholesteraemic were transplanted into normocholesterolemic Ldlr-/-. No difference in amounts of BM progenitor cells between LDLR KO recipients transplanted with WTD BM or Chow BM. Only increased circulated leukocytes in PB	Donor 3x10^6 BM	(van Kampen et al. 2014)
C57BL/6J /OB	45% kilocalories/ fat	From 1 d to 18 weeks	Increase pro-inflammatory immune cells in PB, increased differentiation potential of BM HSPC	CD45.1 BM from age-matched 10 wk HFD or 10 wk chow-fed donor mice was mixed with CD45.2 BM from chow donor mice and transplanted into chow CD45.2 recipients. Decreased HSPCs reconstitute capacity	Not declared	(van den Berg et al. 2016)

C57BL/6J	42% fat HFD	4 weeks		Lower haematopoietic reconstitution potential after transplantation.	200,000 cells	(Hermetet et al. 2019)
$ApoE^{-/-}$	20 g fat/100 g, 11.25 g cholesterol/ 100 g diet	8 weeks	Increased total LSK % in BM, with decrease in HSC's % within LSK	Lower haematopoietic reconstitution potential after transplantation.	Not declared	(Tie et al. 2014)
$ApoE^{-/-}$ Ldlr-/-	21% milk fat, 0.2% cholesterol	10 weeks	Increase pro-inflammatory immune cells in PB, increased differentiation potential of BM HSPC	Equal ratio bone marrow (BM) cells from WT CD45.1 and CD45.2 mice, or WT CD45.1 and Apoe-/- CD45 mice, were transplanted into either WT or Ldlr-/- recipients. Upon BM reconstitution, fed HFD	Not declared	(Murphy et al. 2011)
Ldlr-/-	21% (w/w) pork lard and 0.15 percent (w/w) cholesterol	12 weeks	Increased primitive and progenitors in BM with increased myeloid immune cells in PB	Lower haematopoietic reconstitution potential after transplantation.	150 HSC's + 200,000 cells	Our study 2022

To understand the molecular basis for functional deregulation when HSCs from *Ldlr*$^{-/-}$ mice on a HFD were transplanted, we undertook RNA-seq. GSEA analysis results reflected the impact of chronic inflammation on HSC integrity from *Ldlr*$^{-/-}$ mice that ingested a HFD. For example, GSEA analysis performed with gene signature showed increased expression of genes related to oxidative phosphorylation in *Ldlr*$^{-/-}$ HFD HSCs. Basically, the metabolic switch from glycolysis to mitochondrial energy generation is accompanied by HSC differentiation and lineage commitment (Papa et al. 2019). This can make HSCs more susceptible to oxidative stress and high ROS levels (Suda et al. 2011). Moreover, excessive ROS levels stimulate the exit of HSCs from quiescence, decrease their capacity for multilineage differentiation, and promote uncontrollable proliferation and sustained DNA damage, eventually leading to HSC exhaustion (Jang and Sharkis 2007). Supporting an enhanced proliferative signature in HSC of *Ldlr*$^{-/-}$ on HFD is the increased MYC target expression in this setting (Delgado and Leon 2010). However, to confirm accelerated cell cycle or the enhanced proliferation concept in HSC of *Ldlr*$^{-/-}$ on HFD, the Ki67 cell cycle assay should be evaluated in future experiments.

Our RNA-seq analysis also revealed an impact on HSC integrity in terms of general differentiation capability, apart from the excessive production of inflammatory cells. For example, a Histone methylation gene signature was downregulated in HSC of *Ldlr*$^{-/-}$ on HFD. Histone methylation is essential in binding regulatory protein to the chromatin (Hyun et al. 2017). Epigenetic changes in DNA are well known in the aetiology of atherosclerosis (Kandi and Vadakedath 2015), clonal haematopoiesis (Libby and Ebert 2018), and myeloid malignancies (Boila and Sengupta 2020). For example, EZH2, MLL, and DOT1L are genes involved in histone methylation and demethylation, and are mutated in both primary and secondary AML (Castelli et al. 2018). Moreover, epigenetic altering encoding genes DMT3A, ASXL1, TET2, IDH1, and IDH2 are the found in 50-80% of CHIP clones in CVD high risk patients (Haybar et al. 2019). Studies also found aberrant DNA methylation motifs in early stages of atherosclerosis in atherogenic mice, linking abnormal hyperlipidaemic lipoprotein profile to aberrant DNA methylation (Lund et al. 2004).

Further linked to altered HSC integrity we observed downregulation of a HOXA9 and MEIS1 signature in HSCs from *Ldlr*$^{-/-}$ mice on a HFD. Normally, in haematopoietic

differentiation phase, HOX expression is down-regulated (Slany 2009) and HOXA9 is specifically diminished during myeloid differentiation (Fujino et al. 2001; Ramos-Mejia et al. 2014). Thus, the enhanced myeloid differentiation potential in HSCs *Ldlr*$^{-/-}$ mice on a HFD may instigated by transcriptional downregulation in HSCs of HOXA9 expression and MEIS1, which is a co-factor for HOX genes. Furthermore, *HOXA9* deregulated expression can be a result of a different genetic mutation *NUP98*-fusions, *NPM1* mutations, *CDX* deregulation, and MOZ-fusions and *MLL*-translocations. Thus, *HOXA9/MEIS1* alliance are involved in many human acute leukaemias (Collins and Hess 2016) and may reflect pre-malignant potential in HSCs from *Ldlr*$^{-/-}$ mice on a HFD. Nevertheless, consistently, AMLs with good outcomes had downregulated HOX expression, with inv(16) AML as an example (Andreeff et al. 2008).

Reflecting pre-malignant potential in HSCs from *Ldlr*$^{-/-}$ mice, gene targets of CBFA2T3, a transcriptional co-repressor and well-known regulator in in haematopoiesis and AML (Steinauer et al. 2020), were upregulated. Normally, haematopoietic stem and progenitor cells (HSPCs) are regulated by CBFA2T3 which is co-expressed with E proteins (E2A, HEB); specifically E2A activates p21 (CDKN1A) gene transcription to induce cell quiescence (Cai et al. 2009). CBFA2T3 maintains HSPC proliferation and inhibits differentiation by repressing the E proteins (Goardon et al. 2006). A recent study showed that CBFA2T3 expressed in AML patient samples is required for maintaining LSC gene signatures and proliferation of AML cells. Of relevance to our study, reports proved that AML cells expressing high levels of CBFA2T3 are correlated with adverse outcome and AML cells expressing low CBFA2T3 do not have the mechanism to repress cell type– specific activation of CBFA2T3 by GCN5, making it associated with poor prognosis in AML as well (Steinauer et al. 2019).

Genes involved in upregulating RNA metabolism, ribosomal protein synthesis, RNA translation and RNA processing were also deregulated (all with NES = 2.2 except for RNA translation with NES = 2.3), which also has implications for normal and leukaemic haematopoiesis. For example, Saha et al., 2019 group studied RNA binding proteins (RBPs) as key players in enhancing post-transcriptional gene regulation to drive intracellular fate of individual transcripts, from their biogenesis to RNA metabolism. They found that RBPs regulate transcript levels within cells in numerous ways and functions related to RNA metabolism. Most known RBPs are TTP, AUF-1, KSRP, HuR,

TIA-1, and TIAR(Garcia-Maurino et al. 2017). Moreover, they observed that based on RBP expression, they can divide cells to normal and leukemic, which indicated their ability to decide cellular identity. They detected over expression of RBP genes such as CLK1, CLK4, TRIM71, and DYNLL1 in LSCs (Saha et al. 2019). Also, cap-binding protein eukaryotic initiation factor 4E (eIF4E) is a key regulator of RNA translation process as it recruits the 40S ribosomal subunit to the 5′ end of mRNA. Researchers found that up - regulation of eIF4E is adequate to transform cells, as they found eIF4E in bone marrow mononuclear cells in AML patients were overexpressed (Khanna-Gupta 2011). RNA methylation induces inflammatory conditions, metabolic disorders, and cancer by disrupting gene expression and functions, causing improper cell differentiation, and disturbing cellular homeostasis (Wu et al. 2020). Methylation in mRNA also plays a role in immune regulation (Zhang et al. 2021a). Moreover, mRNA methylation affects RNA fate by affecting splicing, nuclear export, translation, and degradation which has a clear influence on the development of haematological malignancies including MDS and CLL (Hodson et al. 2019). Cytoplasmic ribosomal protein pathway upregulation reflects increased proliferative processing in normal cells and are involved on an oncogenic signalling in cancer cells (Silvera et al. 2010).

In summary, inflammation caused by diet induced hypercholesteremia in the *Ldlr*$^{-/-}$ mouse model stimulates excessive production of immune cells and cytokines induction, impacting and directing HSC differentiation with skewing to the myeloid lineage. Inflammatory signalling in our model, in turn, feeding back to limit HSPC function and disturb normal haematopoietic differentiation, as judged by immunophenotyping and functional analysis during transplantation (Figure 4.23). Inflammation may have potential to drive HSCs to acquire oncogenic mutations by driving HSC proliferation. This could, in principle provide a selective advantage for the acquisition of mutations leading to the development of AML. Constant generation of proinflammatory signals associated with chronic inflammation and/or physiological aging can significantly shift HSC activity and output, in contrast to homeostat blood production in which HSCs create a balanced lineage output. For instance, in our model, lymphoid output and erythroid production (erythropoiesis) declines because of chronic overproduction of myeloid cells and platelets. Furthermore, chronic inflammation may lead to BM niche dysfunction, and exposure to stressors like reactive oxygen species (ROS) promoting genomic instability and providing a further

environment for the acquisition of somatic mutations, including those which are characteristic of clonal haematopoiesis of indeterminate potential. Therefore, persistent inflammation may serve as both a trigger and a driver of haematological malignancy. In addition to our RNA-seq data for HSCs from *Ldlr*$^{-/-}$ mice fed a HFD providing evidence to support this hypothesis, two other lines of our analysis suggest the development of a pre-malignant phenotype in the context of diet induced hypercholesteremia in the *Ldlr*$^{-/-}$ mouse model. First, peripheral blood films from diet induced hypercholesteremia in the *Ldlr*$^{-/-}$ mouse model were reviewed to investigate the presence of haematopoietic cells with atypical morphology, and this analysis revealed reactive lymphocytes, increased monocytes vacuolation, occasional band neutrophils and clefted lymphocytes. These morphological findings are correlated to chronic inflammation and some of the atypical morphology observed here are also seen in the peripheral blood of murine haematological malignancies (O'Connell et al. 2015). Second, the myeloid population (Gr-1/Mac-1) was significantly increased in the spleen of *Ldlr*$^{-/-}$ HFD. Further experimentation should focus broadly on characterising the basis for the expansion of myeloid cells to explore the possibility of predisposition to AML (Hey et al. 2015). In support of this possibility, H&E cross sections of *Ldlr*$^{-/-}$ HFD spleens showed characteristic features of perturbed

extramedullary haematopoiesis, where red pulp infiltrates the white pulp and separates them to smaller islets (Wang and Li 2019).

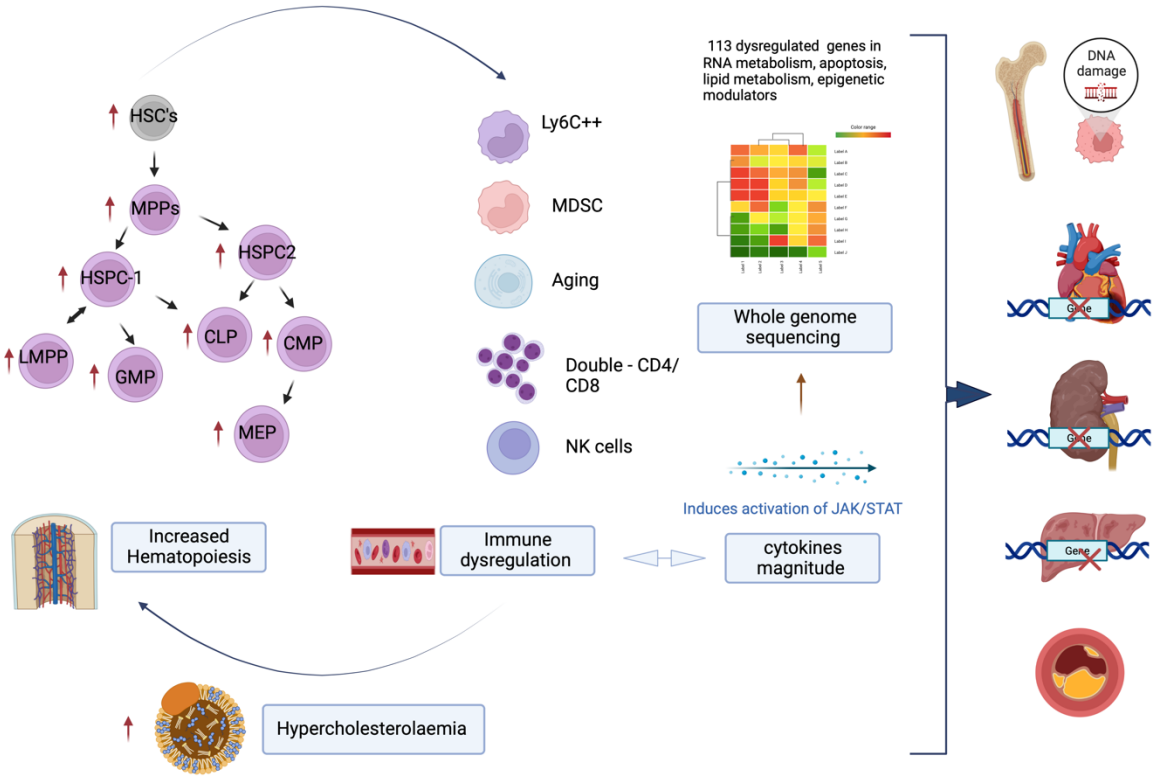

Figure 4.23 Deregulation of haematopoiesis in Ldlr-/- mice fed a HFD results in inflammation, general immune dysregulation and a potential tumour initiating microenvironment.

A proposed model of how continuous stimulation of the immune system along with atypical bone marrow niche signals damages haematopoiesis and potentially causes a pre-malignant haematopoietic environment as well as impacts on cardiovascular disease, nephrotoxicity and hepatoxicity.

Chapter 5: Exploring the role of high fat diet in MLL-AF9 driven acute myeloid leukaemia *in vitro* and *in vivo*

5.1 Introduction

Deregulation of the molecular mechanisms controlling haematopoiesis occur because of both genetic and epigenetic mutations in tumour suppressor genes and proto-oncogenes that can lead to the development of either chronic or acute haematological malignancies (Vogelstein and Kinzler 2004; Shin 2022). Genetic and epigenetic alteration driven causes of AML are an area of intense investigation. With respect to epigenetic alterations, researchers have identified lifestyle, including Western-type diet, as a possible risk factor in AML (Ma et al. 2010). In particular, Western-type diets encourage high cholesterol consumption. Moreover, growing research has linked increased cholesterol levels and its derivatives with dysregulated haematopoiesis and haematological malignancy (Oguro 2019). Cholesterol is essential part of cellular membrane, and its metabolites play a variety of cellular vital roles (Sato 2015). Thus, by adjusting cellular membrane homeostasis, cholesterol organizes the numerous cellular receptors and transporters that would otherwise be dispersed haphazardly across the plasma cell membrane. Finally, cholesterol can form rafts that partition the cell membrane, facilitating the orderly transport of signalling molecules, the sorting of membrane proteins, and the control of neurotransmission (Schade et al. 2020).

Cholesterol can be synthesised by nearly all cells. However, the liver accounts for about half of the total synthesised cholesterol amount in humans (Repa and Mangelsdorf 2000; Seijkens et al. 2014). Cholesterol synthesis requires acetyl-CoA, ATP, oxygen and reducing factors (Brown et al. 2021). The process is strictly regulated through four essential players: Two regulatory transcription factors: sterol regulatory element-binding protein 2 (SREBP2), liver X receptors (LXR-α and β iso- forms) (Janowski et al. 1996) and two main enzymes: 3-hydroxy-3-methyl- glutaryl coenzyme A reductase (HMGCR) and squalene monooxygenase (Luo et al. 2020) (Figure 5.1) When cholesterol level is low SREBP2 will be activated and bind to genes regulating *de novo* cholesterol synthesis. Also, it induces LDLR expression for LDL endocytosis (Luo et

al. 2020). However, when cholesterol levels are high, oxysterols bind to LXRs and activate expression of Cholesterol transporters ABCA1 and ABCG1 to export cholesterol to peripheral blood (Yvan-Charvet et al. 2010b). In parallel, they activate reverse cholesterol transport pathway by activating ABCG5 and ABCG8 through the bile duct and intestine (Brendolan and Russo 2022).

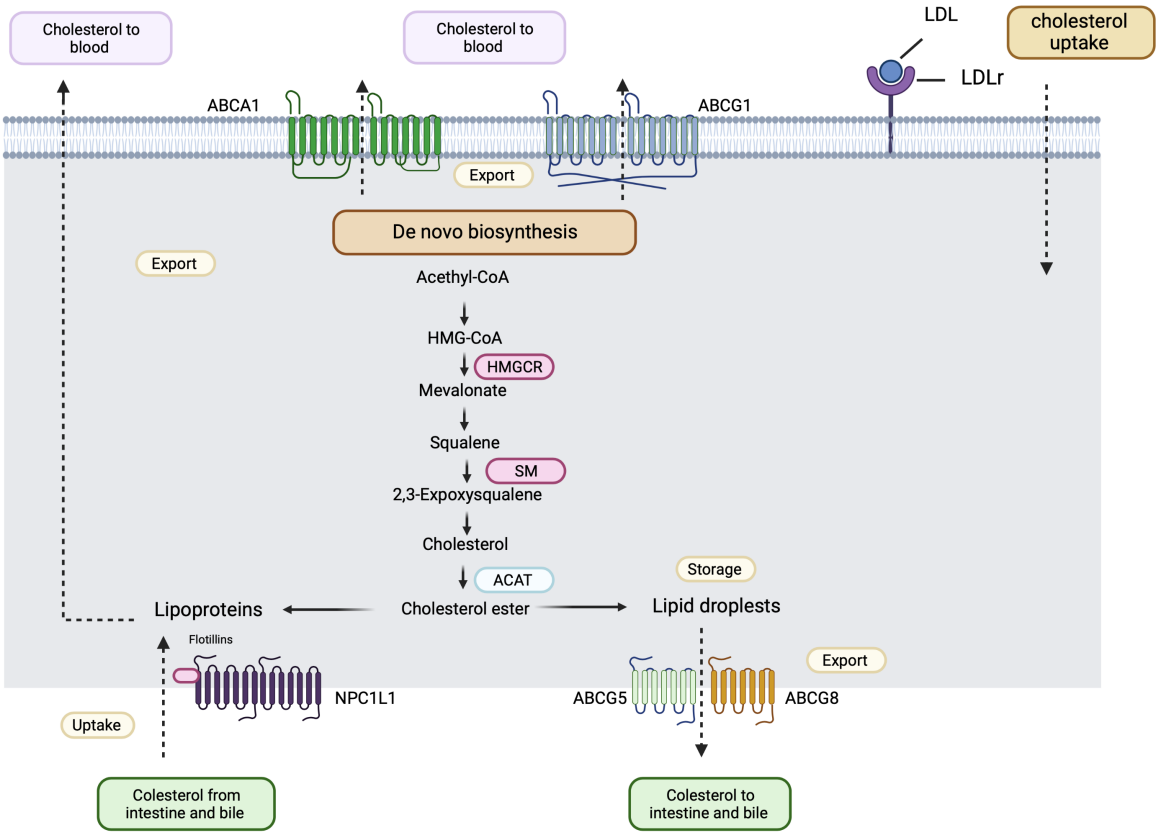

Figure 5.1 Major cholesterol signalling pathways.

Cholesterol is synthesized *de novo* starting from acetyl-CoA through a series of ~30 reactions using 3-hydroxy-3-methylglutaryl coenzyme A reductase (HMGCR) and squalene monooxygenase (SM) as the rate-limiting enzymes. In addition, cholesterol is carried by low-density lipoprotein (LDL) particles in the blood can be taken up by LDL receptor (LDLr). Also, free cholesterol can be absorbed from the intestines and bile by hepatocytes in the liver. Absorption is facilitated by Niemann–Pick type C1-like 1 (NPC1L1). Extra intra cellular cholesterol is extracted to the blood by ATP-binding cassette subfamily A member 1 (ABCA1) or the homodimer of ATP-binding cassette subfamily G member 1 (ABCG1) or to the intestinal lumen and bile by ABCG5 and

ABCG8 heterodimer. Cholesterol can also be converted to cholesteryl ester (CE) by the aid of acyl coenzyme A: cholesterol acyltransferase (Paracatu and Schuettpelz) then stored as lipid droplets or alternatively secreted as lipoproteins (Luo et al. 2020).

Imbalanced regulation of cholesterol uptake or uncontrollable metabolite production disturbs cellular and systemic functions. In cancer, intrinsic and extrinsic pathways control cholesterol metabolism to support tumour cells growth and invasion (Huang et al. 2020). For example, cholesterol biosynthesis plays a significant part in sustaining cancer stem cells (CSCs) by activating descending signalling pathways of sonic hedgehog, Notch and receptor tyrosine kinases (Kim 2019). Moreover, increased cholesterol metabolites play an essential role in tumour progression through producing immunosuppressive cells (MDSCs and TAM), preventing immune effector cells and inhibiting antigen presentation (Tannenbaum et al. 2019). MDSC and TAM cells are induced due to hypercholesteremia inflammatory environment activating signal transducers and activators of transcription family 3 (STAT3) and other inflammatory signals such as growth factors, chemokines and cytokines (Chalmin et al. 2010), including IL1β (Bunt et al. 2006).

It has been shown in preclinical and clinical studies that controlling cholesterol metabolism can slow tumour growth, alter the immunological landscape, and influence anti-tumour mechanisms (Huang et al. 2020). For example, even after tumour initiation, different types of CSCs such as ovarian, colorectal and breast cancers can support their growth and resist apoptosis by *de novo* cholesterol synthesis (Kim 2019). Researchers have also found that CSCs had higher levels of mono- unsaturated lipids in their lipidomic profile and that targeting cholesterol and unsaturated fatty acid synthesis pathways using small RNA (siRNA) interference selectively affected CSCs. They used small interfering RNA (siRNA) screening to identify 5 molecules that are essential for the self-renewal of cancer stem-like cells but not bulk cancer cell development. Two of these molecules are crucial for cholesterol synthesis (Kim 2019). Blocking HMG-CoA reductase inhibitors, atorvastatin, specifically eradicated glioblastoma multiforme GBM, colorectal, and lung cancer stem cells, and the effect was reversed by adding downstream metabolite products after pharmacologic blockade of this target pathway (Song et al. 2017). Thus, in general, proliferation,

invasion, and migration of cancerous cells are influenced by the metabolism of cholesterol (Xi et al. 2021).

Several studies on a subtype of AML, acute promyelomonocytic leukeamia (APL), revealed that total cholesterol, high-density lipoprotein cholesterol and low-density lipoprotein cholesterol were higher compared to control group, which suggests lipid dysregulation as an independent risk factor in APL (Sun et al. 2020). Also, it has been shown that leukaemia cells have an increased ability to synthesise and uptake cholesterol, as evidenced by increased HMGCR activity and expression, as well as enhanced LDL-R mediated degradation of LDL (Ho et al. 1978; Bhuiyan et al. 2017). Likewise, in AML mouse models and AML patient samples, the cholesterol-lowering drugs Lovastatin, Fluvastatin, and Simvastatin kill LSCs – which drive and maintain tumourogenesis in AML - by inhibiting HMG-CoA reductase activity (HMGRC) (Hartwell et al. 2013). Another cholesterol biosynthesis pathway is mevalonate pathway, which is known to be upregulated in AML (Ha and Lee 2020) and has essential role in cellular homeostasis. Consequently, the combination of statins with other anti-leukaemia treatments may be a promising strategy for targeting cholesterol signalling in AML (Chiarella et al. 2022).

One of the main regulators sensing cholesterol, as an element of LDLs, from the circulation into various cells is *Ldlr*. Familial hypercholesterolaemia, which is a genetic mutation that causes a decrease in Ldlr-mediated LDL uptake and results in an increase in plasma LDL, emphasising the role of *Ldlr* in maintaining healthy levels of total body cholesterol (Lara et al. 1997). Notably, 3 – 100-fold increases of LDL consumption have been observed in blood from AML patient samples, suggesting increased cellular LDL receptor expression. Moreover, studies showed that AML cells with monocytic differentiation had invariably elevated LDL degradation than other AML subtypes (Vitols et al. 1984; Rudling et al. 1998). This suggests that AML cells require LDL to proliferate and progress. Studies also show that low density lipoprotein receptor activity in leukemic cells from patients with AML are higher in comparison to normal white blood cells in peripheral blood and bone marrow (Tatidis et al. 1997). Moreover, AML cells shows reduced feedback control of LDL-receptor activity in response to sterol. These findings provide further evidence that higher LDL-receptor activity is linked to sterol resistance and cell proliferation in AML cells (Tatidis et al. 1997).More

recently, *Ldlr* has been considered as an independent risk factor for AML prognosis and is suggested as a promising targeted therapy approach for AML treatment to overcome the limitations of conventional chemotherapy which often fail to drive durable remission in AML (Floeth et al. 2021). This group studied primary AML samples LDLR expression and found it inversely correlated with patient outcome. Thus, increased LDLR expression is associated with decreasing overall survival. Lastly, Hermetet et al 2020, discovered that high fat diet consumption accelerates development of AML in MLL-AF9 knock-in mouse model via an increase in activation of the JAK-STAT pathways (Hermetet et al. 2020).

5.2 Aims of this chapter

Studies have already established a link between modern lifestyle including Western type diet and cancer development (Crysandt et al. 2016). Elevated plasma cholesterol levels trigger cholesterol metabolism dysregulation, and it is considered one of the main risk factors for inflammation and disordered haematopoiesis (Ma and Feng 2016). Also, cholesterol metabolism defects have been reported in haematological malignancies, which suggests that malignant haematopoietic cells and aberrant cholesterol metabolism may be linked (Oguro 2019). LDL receptor (*Ldlr*) is one of the main regulators of cholesterol metabolism and its deficiency causes impaired LDL clearance, resulting in high LDL levels in plasma, and as consequence, significant hypercholesteremia, as exemplified by familial hypercholesteremia. Our work in Chapter 3 and others has shown *Ldlr* is expressed abundantly on all cells including haematopoietic stem and progenitor cells (HSPCs) (Lara et al. 1997; Goldstein and Brown 2009). *Ldlr* deficiency can influence haematopoietic malignancy development directly by influencing CHIP that represents a risk factor for AML (Luis et al. 2019) as well as atherosclerosis. Notably, high cholesterol resulting from a *Ldlr* defect has been linked to inflammation and development of haematopoietic neoplasia (Banker et al. 2004). *Ldlr* deficiency leads LDL abundance in blood plasma or hypercholesteremia. Hypercholesteremia is a sort of chronic inflammation that induce perturbed haematopoiesis, epigenetic changes that lead to possible haematopoietic malignancies (Tall and Yvan-Charvet 2015).

However, the direct role of *Ldlr* in the onset, progression and maintenance of leukaemia has yet to be established. This chapter explores whether *Ldlr* plays a critical role in the onset, progression, and maintenance of AML pre-LSCs and LSCs in the setting of a high-fat diet (HFD) in MLL-AF9 driven mouse models. To ascertain the relevance of our findings to the human setting, we also explore the impact of cholesterol in human MLL-AF9 AML cells. With these goals in mind, this chapter aimed to investigate the role of *Ldlr* and cholesterol in leukemogenesis with the following objectives:

1. Use colony-forming assay to evaluate *in vitro* pre-LSC capacity of MLL-AF9 transduced HSPCs (c-kit+ cells) that were isolated from *Ldlr*$^{-/-}$ mice ingesting a HFD.
2. To characterise these pre-LSCs generated from *Ldlr*$^{-/-}$ mice fed a HFD immunophenotypically by flow cytometry.
3. To assess the *in vivo* role of *Ldlr* deficient HSPCs fed a HFD in the maintenance and progression of LSCs using the MLL-AF9 leukaemia murine model.
4. To evaluate biologic alterations in MLL-AF9 human AML cells in response to LDL and oxidative LDL exposure (that mimic the *in vivo* Ldlr mouse model in a *in vitro* human setting).

5.3 Results

5.3.1 In vivo experiment:

5.3.1.1 Assessing colony forming cells (CFC) capability of Ldlr -/- HFD BM c-kit cells selectively transduced with MLL-AF9 oncogene.

Acute myeloid leukaemia (AML) is a condition in which abnormal myeloid blasts in the bone marrow expand and spread clonally to the peripheral blood and/or other organs (Kantarjian et al. 2021). Unfortunately, the overall survival for this disease is poor, and treatment advances in the recent 30 years have not advanced survival prospects. One of the challenges is how to eradicate the LSCs, which are a subpopulation of AML cells that have proliferation and self-renewal ability, much like normal HSCs, but which drive disease initiation maintenance and relapse (Shin 2022). Cholesterol metabolism is one possible regulator of LSCs (Hartwell et al. 2013). To understand the role of *Ldlr* and cholesterol in AML LSCs, we utilised a retroviral murine model of AML driven by the MLL-AF9 oncogene (Chen et al. 2008). This model is used to develop pre-LSCs/LSCs *in vitro* and follow LSC progression *in vivo* (Almosailleakh and Schwaller 2019). In brief, normal bone marrow LK (Lin^- $cKit^+$) HSPCs were isolated from *Ldlr*$^{-/-}$ mice that were fed either a normal diet (ND) or a high fat diet (HFD). These HSPCs were efficiently transformed into pre-LSCs via retroviral transduction of the MLL-AF9 oncogene and were subsequently replated in methylcellulose medium containing IL-3, IL-6, SCF and GM-CSF for 5-days. Next, these cells bearing the MLL-AF9 oncogene were replated a further two times. At the third replating, generated pre-LSCs were collected and transplanted into lethally irradiated primary recipients. Transplanted pre-LSCs home to BM and produce LSCs, and then initiate AML leukaemia disease by producing immature differentiated leukemic blast cells which infiltrate the bone marrow and spleen, and which egress into the peripheral blood. Bone marrow and peripheral blood from moribund mice was collected for further immunophenotypic analysis (Thiel et al. 2010) (Figure 5.2).

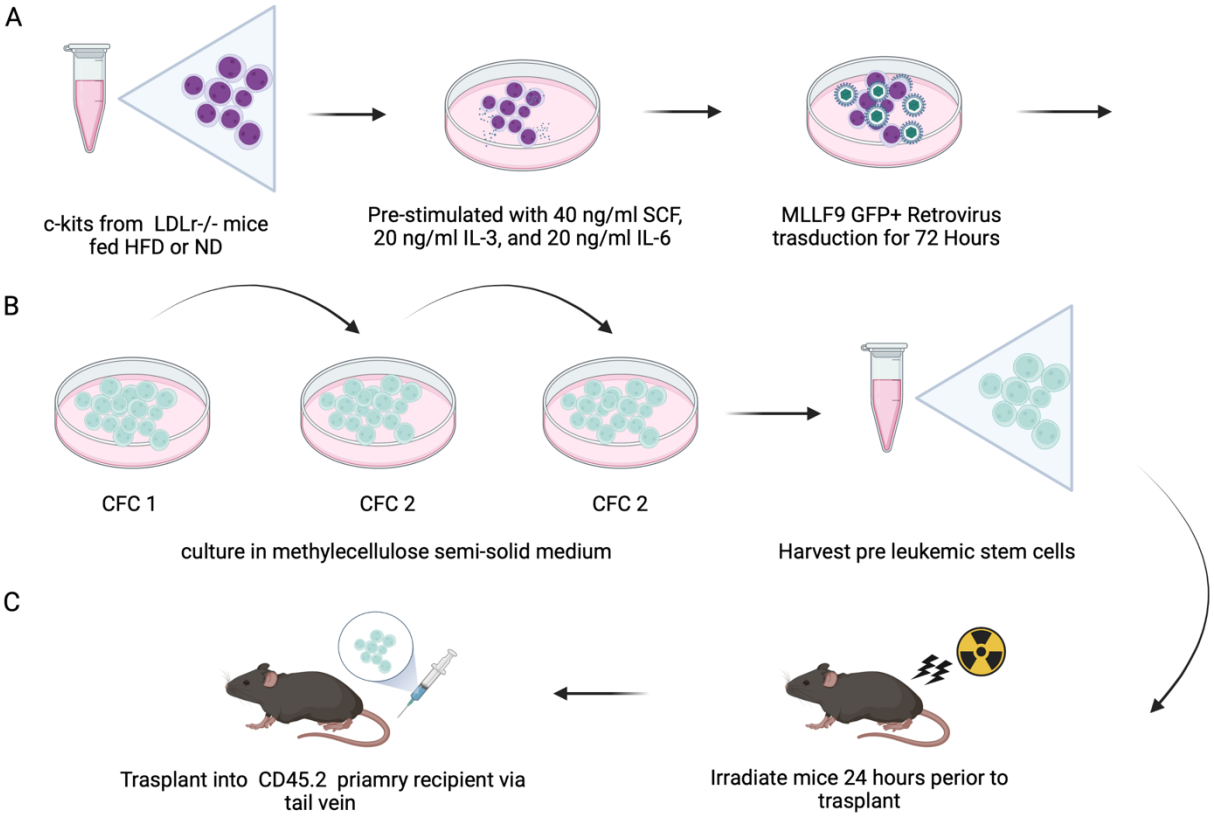

Figure 5.2 Schematic of MLL-AF9 leukemogenesis assay showing c-kit transformation of normal HSPCs into pre LSCs/LSCs.

A) HSPCs LK population from bone marrow were enriched from *Ldlr*$^{-/-}$ mice fed a ND or HFD. Then, c-kit+ cells were re-stimulated with a selective panel of growth factors and were transduced by MLL-AF9 oncogene bearing retroviruses. B) Transduced cells with retroviruses expressing MLL-AF9 were replated in methylcellulose three times, then pre-LSCs were collected. C) Generated pre-LSCs are transplanted into lethally irradiated primary recipients were transplanted pre-leukemic cells initiate AML disease.

Initially, we conducted a quantitative and qualitative microscopic examination of CFC transformed cells. In this approach, three types of CFC were generated: A) Compact colony, B) compact colonies with a corona of migrating cells, and C) small and diffuse colonies of large corona of migrating cells. Compact colonies and compact colonies with corona of migrating cells hold the strongest leukemic potency (Mi et al. 2010). Conversely, small, and diffuse colonies of large corona of migrating cells contains differentiated cells and might be less potent in transforming into leukemic cells (Mi et al. 2010). There were no significant differences in CFC subtypes between the two conditions (data not shown). Quantitation of MLL-AF9 transduced CFCs isolated from *Ldlr*$^{-/-}$ BM cells from mice that were fed either a HFD or ND showed a decrease in overall CFC potential at CFC1, but not at CFC2 and CFC3 (Figure 5.3) in two independent experiments. Further experiments will need to be performed to confirm these results.

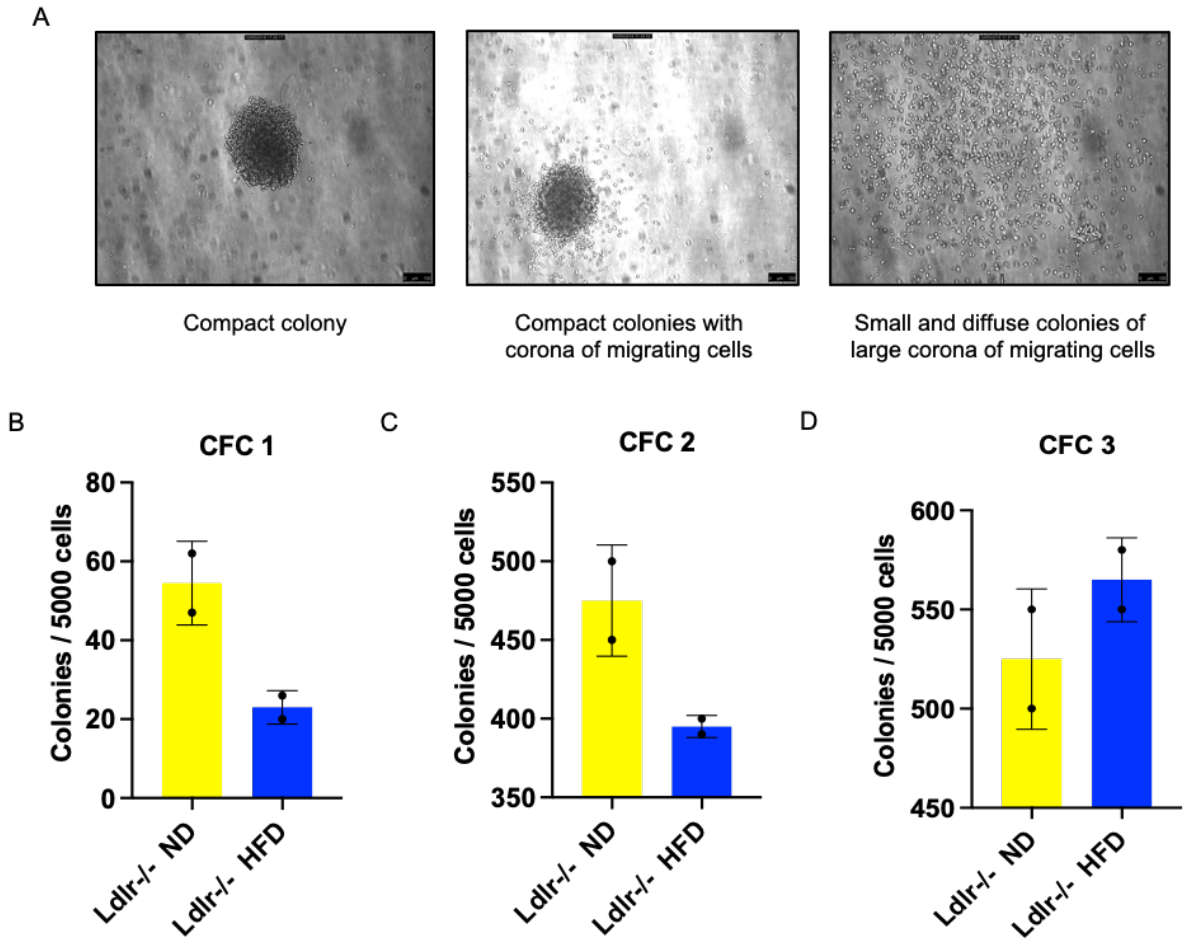

Figure 5.3 CFC potential of MLL-AF9 transformed pre-LSCs obtained from Ldlr-/- HSPCs fed on a HFD.

A) CFC colony appearance of pre-LSCs produced from *Ldlr* $^{-/-}$ HSPCs fed an HFD or ND. This image shows \10x magnification of CFC3 colonies. B) Number of total colonies in first plating incubated for 6 days. C) Number of total colonies in second plating incubated for 5 days. D) Number of total colonies in third plating incubated for 5 days. Statistical analysis was performed using Mann Whitney test (GraphPad prism). Error bars represent the mean ± SEM of 2 independent experimental cultures using 2 *Ldlr*$^{-/-}$ mice fed a ND and *Ldlr*$^{-/-}$ mice fed a HFD. ND: Normal diet, HFD: high fat diet.

5.3.1.2 Immunophenotyping of CFCs from MLL-AF9 transformed c-kit$^+$ cells from Ldlr$^{-/-}$ mice fed HFD

To assess the immunophenotypic status of pre-LSCs from the CFC assay, we evaluated the pre-LSC marker c-kit (CD117) and mature/late phase myeloid markers Mac-1 or (CD11b) and Gr-1 or (Ly6C, Ly6G) (Somervaille and Cleary 2006). In the single experiment performed, no notable changes in the percentage of c-kit+, Mac-1+ and Gr-1+ expression was observed between conditions (Figure 5.4A). We also analysed the mean fluorescence intensity (MFI) of these markers. For the *Ldlr$^{-/-}$* HFD group, c-kit+ MFI expression was lower than in the *Ldlr-/-* ND group in CFC1 and gradually increased during replating (CFC1 – CFC3), presumably reflecting the impact of *Ldlr* deficiency and HFD on the generation of pre-LSCs during re-plating (Figure 5.4B). In contrast, the MFI of late-stage myeloid differentiation markers Mac-1+ and Gr-1+ was significantly higher in the *Ldlr$^{-/-}$* HFD group than the *Ldlr$^{-/-}$* ND group at CFC1 but declined by CFC3, likely reflecting how *Ldlr* deficiency and HFD cause an intrinsic block in myeloid differentiation in this *in vitro* leukemogenesis assay (Figure 5.4B). As alluded to above, these results were obtained in the context of a single experiment and further experimentation will be required to confirm these initial provocative findings.

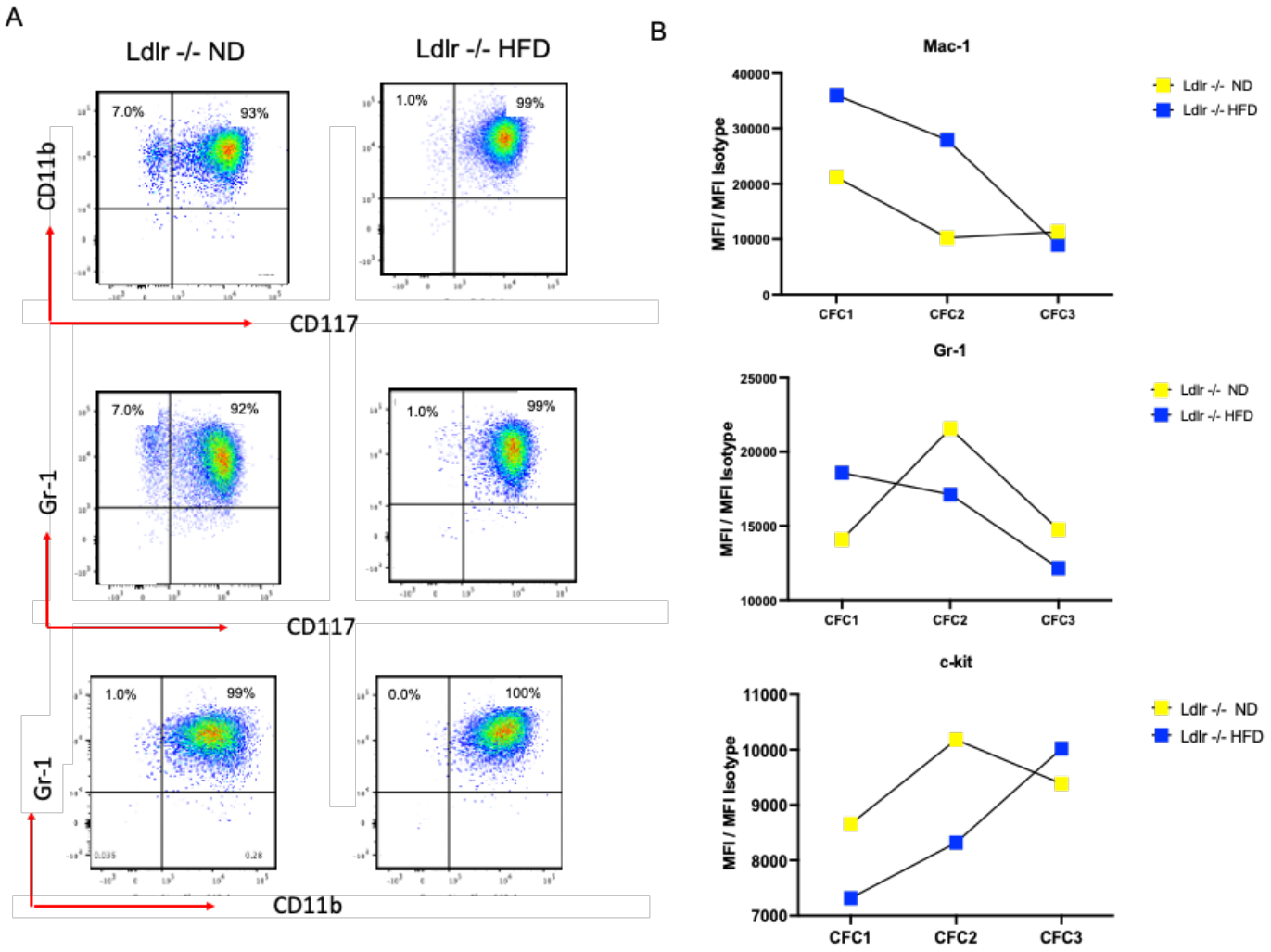

Figure 5.4 Flow cytometry characterization of Ldlr-/- of HFD of pre-LSCs from CFC replating assay

A) Mac-1, Gr-1 and c-kit markers percentages, CFC1, CFC2 and CFC3 showed the same expression pattern for both conditions. B) MFI for CFC1, CFC2 and CFC3 for pre-LSCs obtained form Ldlr-/- HSPCs fed on HFD and ND, no significant changes were detected. This is a single experiment performed with two samples for each condition.

5.3.1.3 Examining the impact of high-fat diet primed Ldlr$^{-/-}$ HSPCs on leukaemia induction and progression of MLL-AF9 driven AML in vivo

While the impact of HFD primed *Ldlr*$^{-/-}$ HSPCs on the generation of pre-LSCs *in vitro* is unclear, in Chapter 4, our RNA-seq experiments of *Ldlr*$^{-/-}$ HSPC fed a HFD revealed several deregulated genes involved in the AML setting. Therefore, to further explore the functional effect of deregulated transcriptional programming of *Ldlr*$^{-/-}$ HSPC fed a HFD in the setting of AML *in vivo*, we obtained pre-LSCs from each of the experimental conditions in CFC3 and transplanted them into sub-lethally irradiated congenic hosts, which clonally proliferate in the bone marrow niche, encouraging AML leukaemia development. Peripheral blood samples were drawn periodically to assess AML disease progression. Our results showed significant leukemic cell engraftment for the *Ldlr*$^{-/-}$ ND condition in the peripheral blood from week 4 post-transplant onwards. In striking and unexpected contrast there was little evidence of blast cell engraftment in the peripheral blood of recipients from the *Ldlr*$^{-/-}$ HFD group from 4 weeks post-transplant onwards and throughout the experiment until the mice became moribund (Figure 5.5A and B). Indeed, mice from the *Ldlr*$^{-/-}$ HFD group often became moribund and succumbed to AML without evidence of disease in the peripheral blood. While both groups eventually succumbed to AML with the expected blast cell burden in the bone marrow (Figure 5.5C), we found an approximately 3-fold higher bone marrow blast cell/peripheral blood blast cell ratio in the *Ldlr*$^{-/-}$ HFD group compared to the *Ldlr*$^{-/-}$ ND group (Figure 5.5C). This suggests delayed blast cell egress from the bone marrow to the peripheral blood in recipients of transformed HSPCs from *Ldlr*$^{-/-}$ mice fed a HFD. However, when Kaplan-Meier survival analysis was applied to assess the long-term survival of transplanted mice it unexpectedly revealed that the *Ldlr*$^{-/-}$ HFD group survived AML longer than their normal diet counterparts (Figure 5.6).

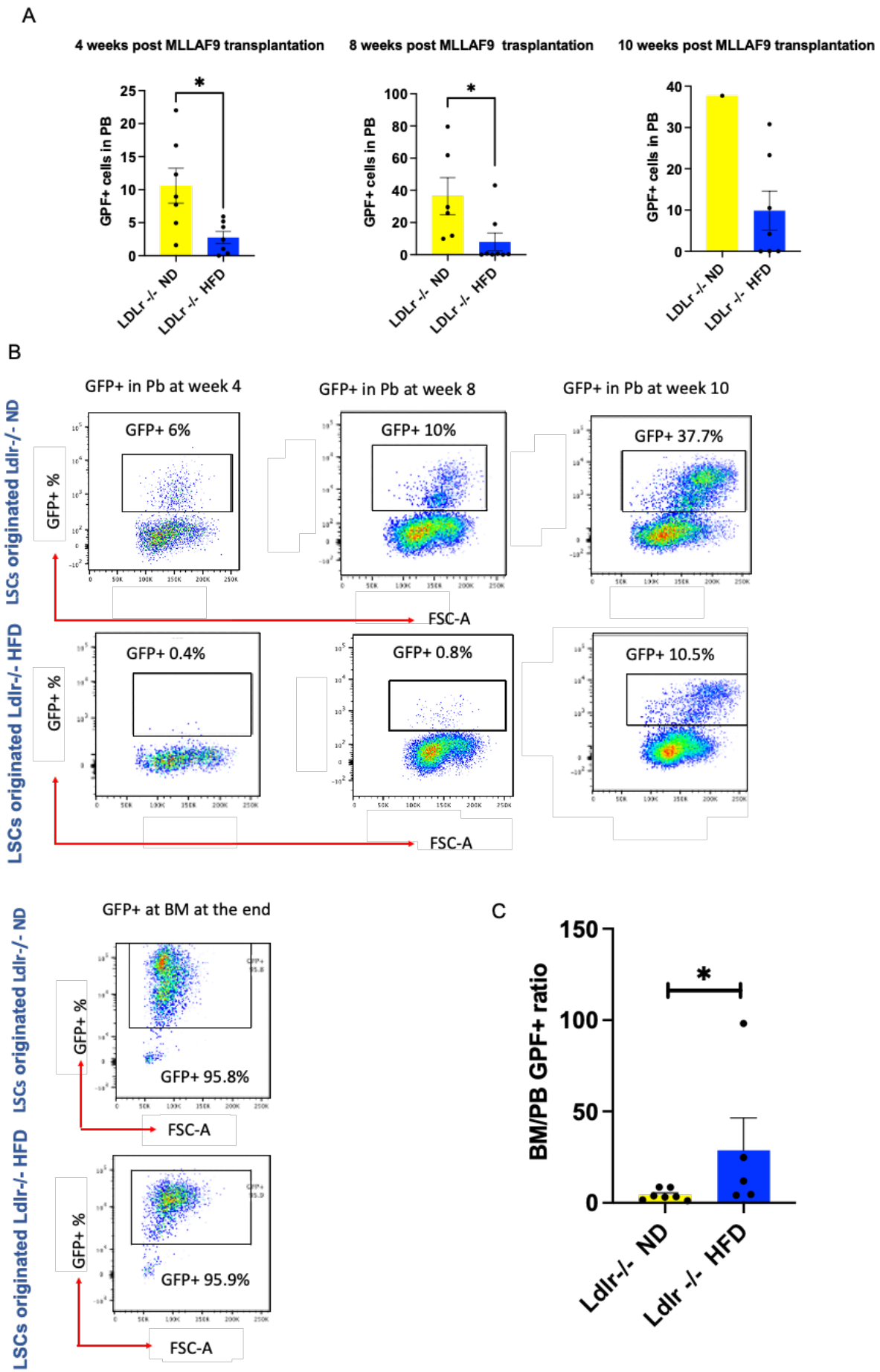
A
4 weeks post MLLAF9 transplantation
8 weeks post MLLAF9 trasplantation
10 weeks post MLLAF9 transplantation
GPF+ cells in PB
LDLr -/- ND
LDLr -/- HFD
B
GFP+ in Pb at week 4
GFP+ in Pb at week 8
GFP+ in Pb at week 10
LSCs originated Ldlr-/- ND
LSCs originated Ldlr-/- HFD
GFP+ %
FSC-A
GFP+ 6%
GFP+ 10%
GFP+ 37.7%
GFP+ 0.4%
GFP+ 0.8%
GFP+ 10.5%
GFP+ at BM at the end
GFP+ 95.8%
GFP+ 95.9%
C
BM/PB GPF+ ratio
Ldlr-/- ND
Ldlr -/- HFD

Figure 5.5 LSC transplant recipients of pre-LSCs from Ldlr-/- mice fed HFD showed delayed expulsion of leukaemic blasts to the peripheral blood.

A) Bar graph shows LSCs (GFP+) percentages in peripheral blood obtained periodically via tail vein bleed (week 4, week 8 and week 10). Results shows significant decrease in LSCs % in *Ldlr*$^{-/-}$ HFD group. B) representative dotplots of *Ldlr*$^{-/-}$ HFD peripheral blood are blast free, while BM is full of blasts. *Ldlr*$^{-/-}$ ND show similar blast content both in peripheral blood and bone marrow. C) *Ldlr*$^{-/-}$ HFD shows three-fold increase in BM/PB blast ratio, suggesting delayed blast cell migration to the peripheral blood. Statistical analysis was performed using Mann Whitney test (GraphPad prism). Error bars represent the mean ± SEM of the 1 independent experiment using *Ldlr*$^{-/-}$ ND 7 mice and *Ldlr*$^{-/-}$ HFD 8 mice. ND: Normal diet, HFD: high fat diet. *P≤ 0.05.

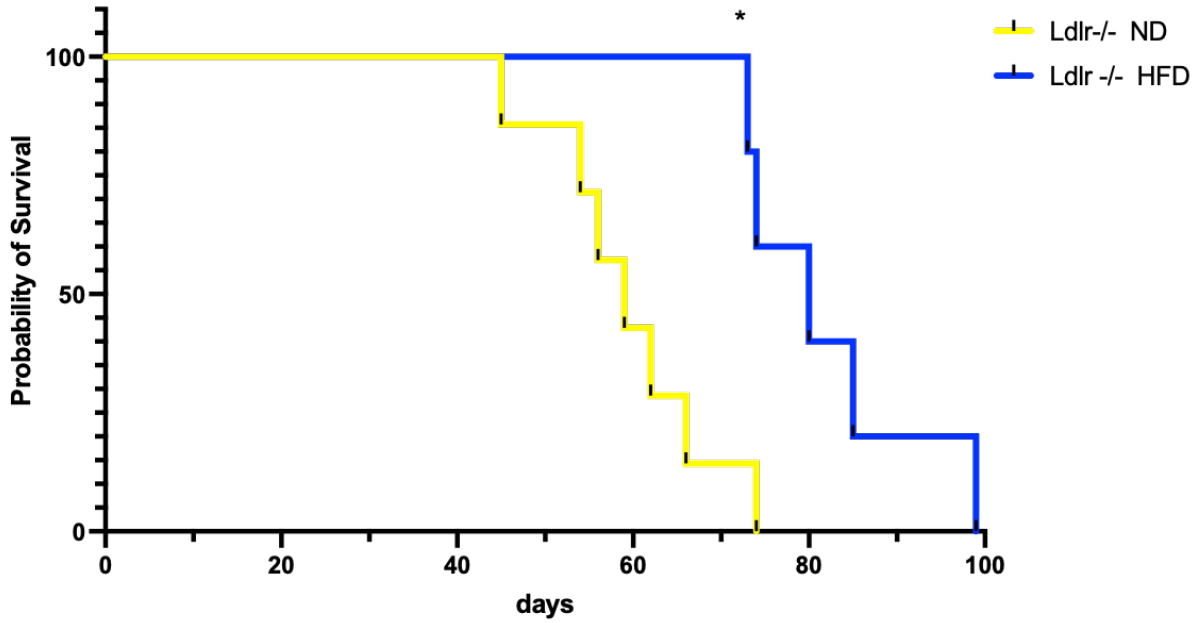

Figure 5.6 AML survival curve for recipients of MLL-AF9 transduced HSPCs from Ldlr-/- mice fed a high-fat diet.

Survival rates from recipients of transformed HSPCs (pre-LSCs) from *Ldlr*$^{-/-}$ HFD or *Ldlr*$^{-/-}$ ND. The median survival was 60 days for *Ldlr*$^{-/-}$ ND (n= 7) and 70 days for *Ldlr*$^{-/-}$ HFD (n= 5). *P* value measured by Mantel–Haenszel test after normalizing the data (GraphPad prism). P*≤ 0.05

5.3.2 In Vitro Experiments

5.3.2.1 The impact of LDL and oxLDL on human MLL-AF9 AML cells in vitro

Having shown altered retention of blasts in the bone marrow of AML mouse model derived from HSPCs exposed to HFD in the context of *Ldlr* deficiency, we next sought to mimic the impact of pro-atherogenic high-fat diet in a human AML setting using stimulation of MLL-AF9 cell lines (NOMO-1 and THP-1) by low density lipoprotein (LDL) and Oxidised low-density lipoprotein (OxLDL) *in vitro*. Notably, we used OxLDL as this form of LDL, which is formed through modification of lipids by lipid peroxidation, facilitating inflammation and the formation of atherosclerotic plaque (Yang et al. 2012) and it is main is toxic component arising from HFD (Holvoet et al. 2008). Previous reports showed pro-atherogenic lipoproteins induce global DNA hypermethylation when exposed to differentiated human THP-1 cells (Lund et al. 2004).

Our analysis was predominantly carried out in one AML cell line, NOMO-1, which is a cell line derived from the bone marrow of a 31-year-old woman with MLL-AF9 driven AML (sub-type AML-M5a) (Towatari et al. 1990). Select analysis was also carried out in THP-1 cells, which were established from the peripheral blood of a 1-year-old boy with MLL-AF9 driven acute monocytic leukaemia (AML-M5b) (Odero et al. 2000). The intention in our experiments was to use the highest but least toxic dose of LDL and OxLDL to mimic increased LDL and OxLDL in our *in vivo* model (Getz and Reardon 2006). To start with, LDL and OxLDL doses were selected according to published literature to avoid toxicity effect. Then, a series of preliminary experiments with selected doses were carried out to decipher the optimal dose that did not kill AML cells (data not shown). Based on these initial experiments, we decided to use a dose of 50ug/ml for LDL and 15ug/ml for oxLDL for all further experimentation in this chapter.

Our analysis focussed on adhesion molecules in human AML cells following LDL and OxLDL exposure given the potential epigenetic changes that occur on exposure of HSPCs to a HFD in the mouse AML model, presented earlier in this Chapter; in particular the potential retention of LSCs/blasts in bone marrow that may reflect

changes in adhesion molecules in the bone marrow niche. With the exception of CD44, significant downregulation of adhesion molecules tested, namely, CD11a, CD11c, CD56 and CD15 was observed after incubation with oxLDL in NOMO-1 for 22 hours (Figure 5.7A and 5.8A).

We also assessed myeloid related markers in AML cells which may be altered in response to OxLDL, which may the function of OxLDL as a pro-atherogenic agent that facilitates the myeloid driven inflammatory processes (Chistiakov et al. 2018). Myeloid/monocytic markers CD64 and Phagocytic Lipopolysaccharide receptor CD14 were significantly increased after exposure to OxLDL in NOMO-1; CD14 was also significantly increased in THP-1 (Figure 5.7B, 5.8B and 5.9B). Pan myeloid transmembrane receptor CD33 and membrane-bound metalloprotease CD13 were both significantly increased their expression when incubated with LDL in NOMO-1 (Figure 5.7C and 5.8C).

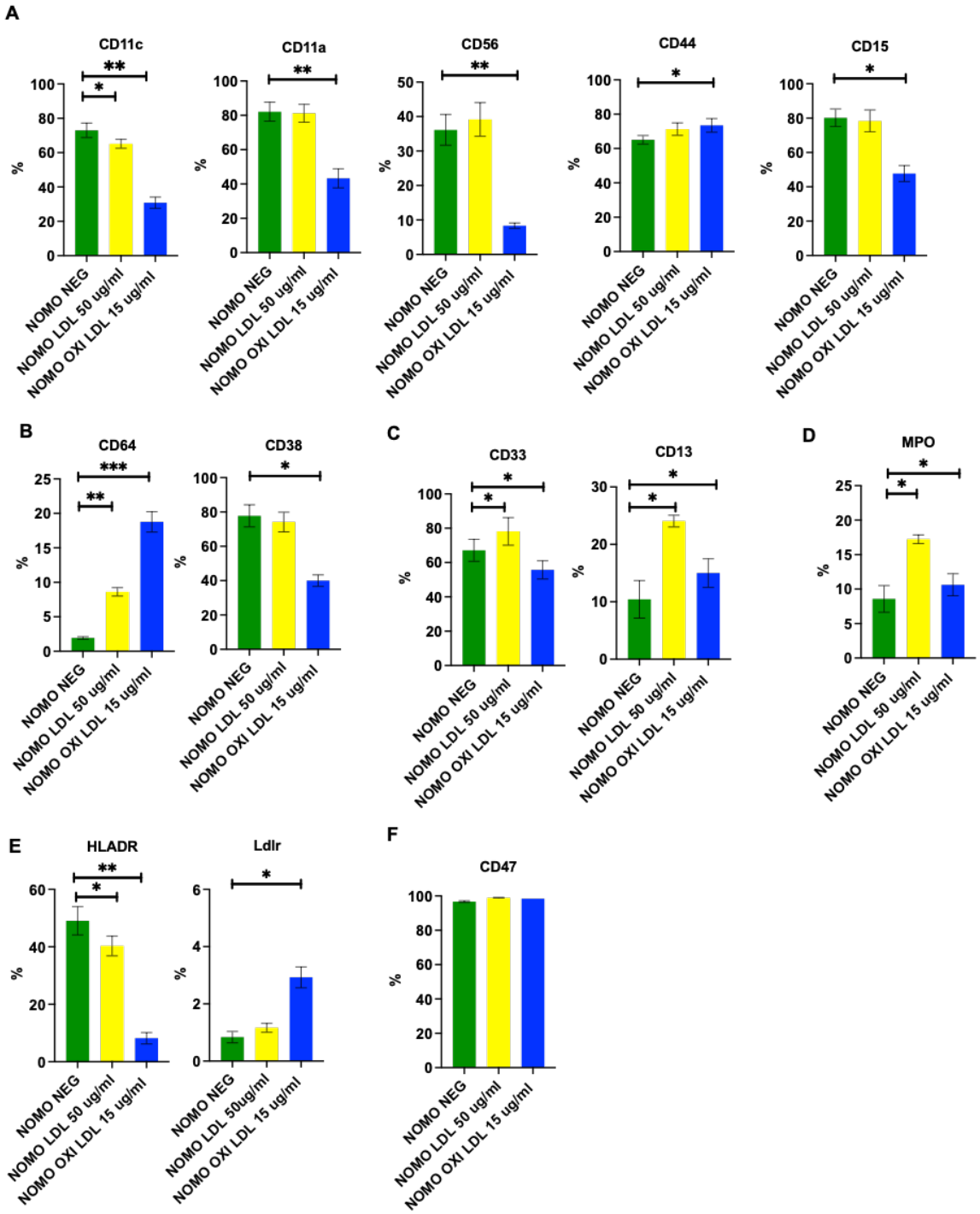

Figure 5.7 Alterations in expression (%) of adhesion and immunological markers in NOMO-1 following LDL and oxLDL exposure.

A) Adhesion molecules percentages were significantly decreased following LDL and oxLDL exposure, except for CD44. B) CD64 expression was increased when incubated with LDL and oxLDL whereas CD38 expression decreased when incubated with oxLDL C) Myeloid markers CD33, CD13 and MPO respectively were increased when incubated with LDL. Statistical analysis was performed using one-way ANOVA

nonparametric (3- groups for comparison) test (GraphPad prism). bars represent the mean ± SEM of the 3 independent experiments using 3 different passages. *P≤0.05, **P≤0.01

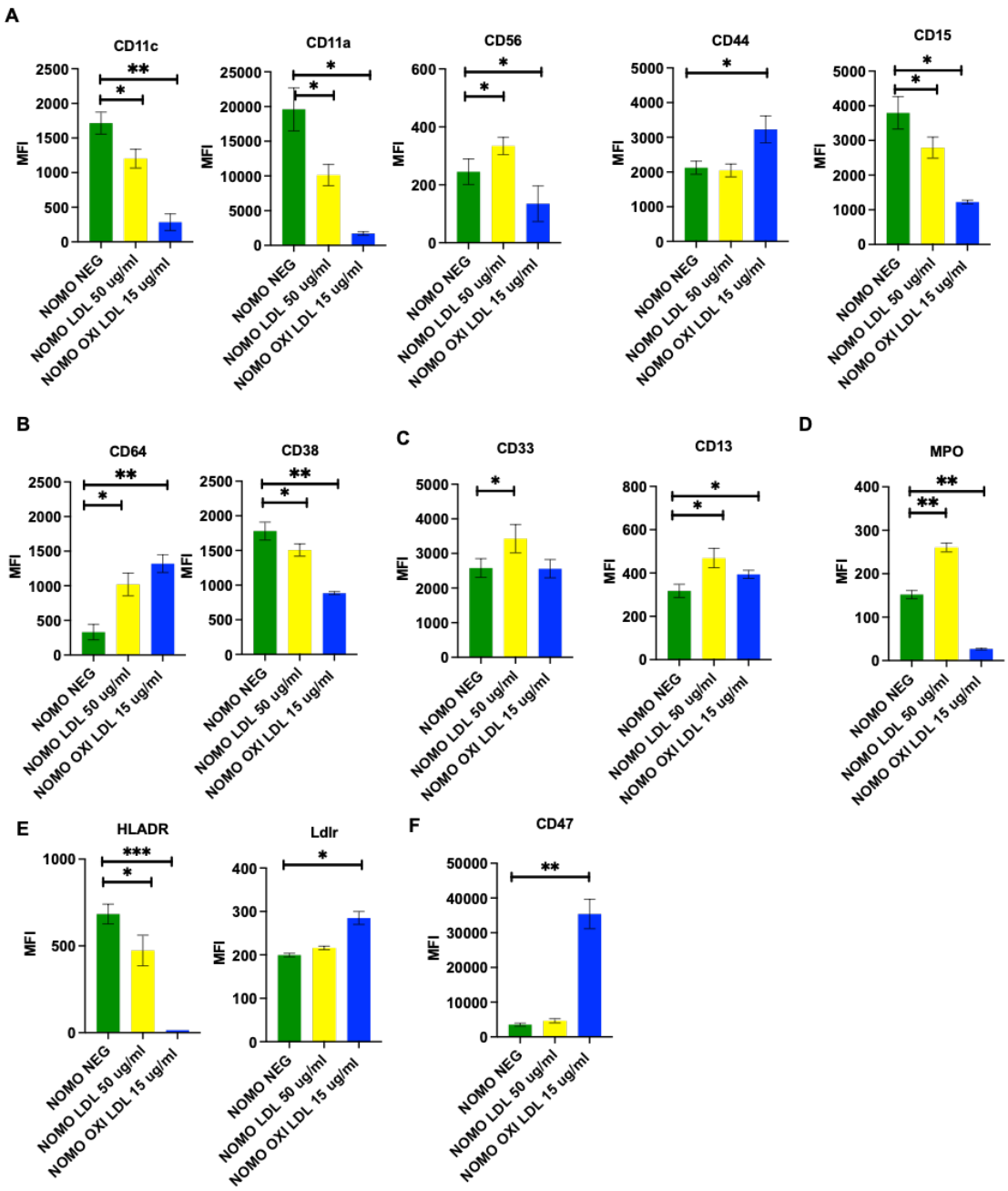

Figure 5.8 Alterations in expression of adhesion and immunological markers in NOMO-1 following LDL and OxLDL exposure

A) NOMO-1 adhesion molecules MFI were down regulated except for CD44. B) CD64 were showed two-fold increase when incubated with LDL and four-fold increase when incubated with oxidative LDL whereas CD38 showed two-fold decrease when incubated with oxLDL. C) myeloid surface antigens CD33, CD13 and intracellular MPO respectively were increased when incubated with LDL and decreased with OxLDL. Statistical analysis was performed using one-way ANOVA nonparametric (3-groups for comparison) test (GraphPad prism). Bars represent the mean ± SEM of the

3 independent experiments using 3 different passages. *P≤0.05, **P≤ 0.01, ***P≤ 0.001.

However, both myeloid antigens drastically decreased when incubated with oxidative LDL (Figure 5.7C and 5.8C). Multi-functional transmembrane protein CD38 was also significantly reduced in both LDL and OxLDL experiments (Figure 5.7B and 5.8B). These data highlight the complexity of myeloid cell marker expression following exposure of OxLDL to human AML cells.

We also analysed the impact of the 'pro-Inflammatory' cues and their potential impact on markers of how the immune system potentially recognizes leukaemia cells. Antigen presenting molecule human leukocyte antigen class II (HLADR) displayed reduced expression in NOMO-1 when incubated with oxLDL (Figure 5.7E and 5.8E) whereas inflammatory cytokine IL-1β was upregulated when incubated with LDL and OxLDL in both THP-1 and NOMO-1 (Figure 5.9A). CD47, an antigen that is a negative regulator of phagocytosis (Takimoto et al. 2019), massively increased its expression when incubated with OxLDL as judged by MFI only, suggesting that OxLDL exposure to AML cells may decrease their immune recognition by phagocytosis (Figure 5.7F and 5.8F).

We assessed the intracellular toxic effect of LDL and OxLDL on human AML cells, as judged by myeloperoxidase and reactive oxygen species (ROS) production. Oxidative stress, translated into ROS production, is an indicator of normal and neoplastic cell quiescence and differentiation status (Prieto-Bermejo et al. 2018). It has been known that ROS production is one of the main characters of cancer cells (Szatrowski and Nathan 1991) including AML cells (Hole et al. 2013). Studies shows that ROS increases oxidative DNA damage in leukaemia and hence may accelerate disease progression though mutagenesis (Aurelius et al. 2012). Exposure of both LDL and OxLDL in NOMO-1 and THP-1 cells induced ROS production (Figure 5.10). Intracellular myeloperoxidase MPO was significantly increased in both LDL and OxLDL (Figure 5.7D and 5.8D) mirroring the results found in analysis of ROS, which was significantly induced in both NOMO-1 and THP-1 cells (Figure 5.10). MPO plays a role in the destruction and removal of harmful microorganisms during infection, it is also implicated in the pathophysiology of autoimmune illnesses such granulomatosis with polyangiitis(Tallis et al. 2017).

These data collectively demonstrate increased intracellular toxicity of LDL and OxLDL exposure to AML cells.

Finally, we assessed modulation of *Ldlr* in response to OxLDL and LDL exposure on AML cells, which was significantly increased in response to only OxLDL in both THP-1 and NOMO-1 cells (Figure 5.7E and 5.8E).

A summary of the differential expression of markers assessed following exposure of NOMO-1 AML cells to atherogenic lipoproteins LDL and OxLDL *in vitro* is depicted in Figure 5.11.

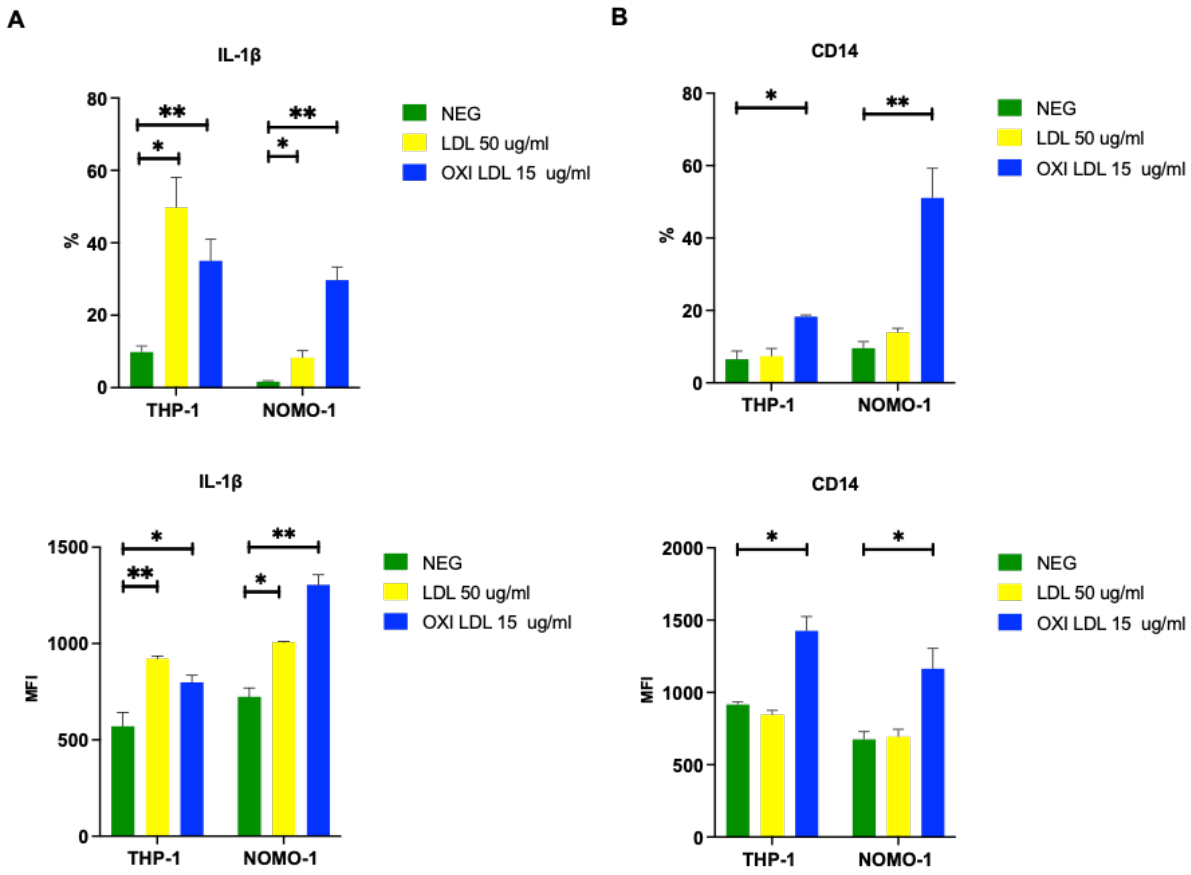

Figure 5.9 Alterations in expression (% and MFI) of IL-1□ and CD14 in NOMO-1 and THP1 following LDL and OxLDL exposure.

A) inflammatory receptor IL-1β where significantly induced in THP-1 or NOMO-1 when cultured with LDL or OxLDL for 22 days. B) Phagocytic Lipopolysaccharide receptor CD14 was upregulated in THP-1 and NOMO-1 cells line when exposed to LDL and OxLDL for 22 days. Statistical analysis was performed using one-way ANOVA non-parametric (3- groups for comparison) test (GraphPad prism). Bars represent the

mean ± SEM of the 3 independent experiments using 3 different passages. *P≤0.05, **P≤0.01, ***P≤0.001.

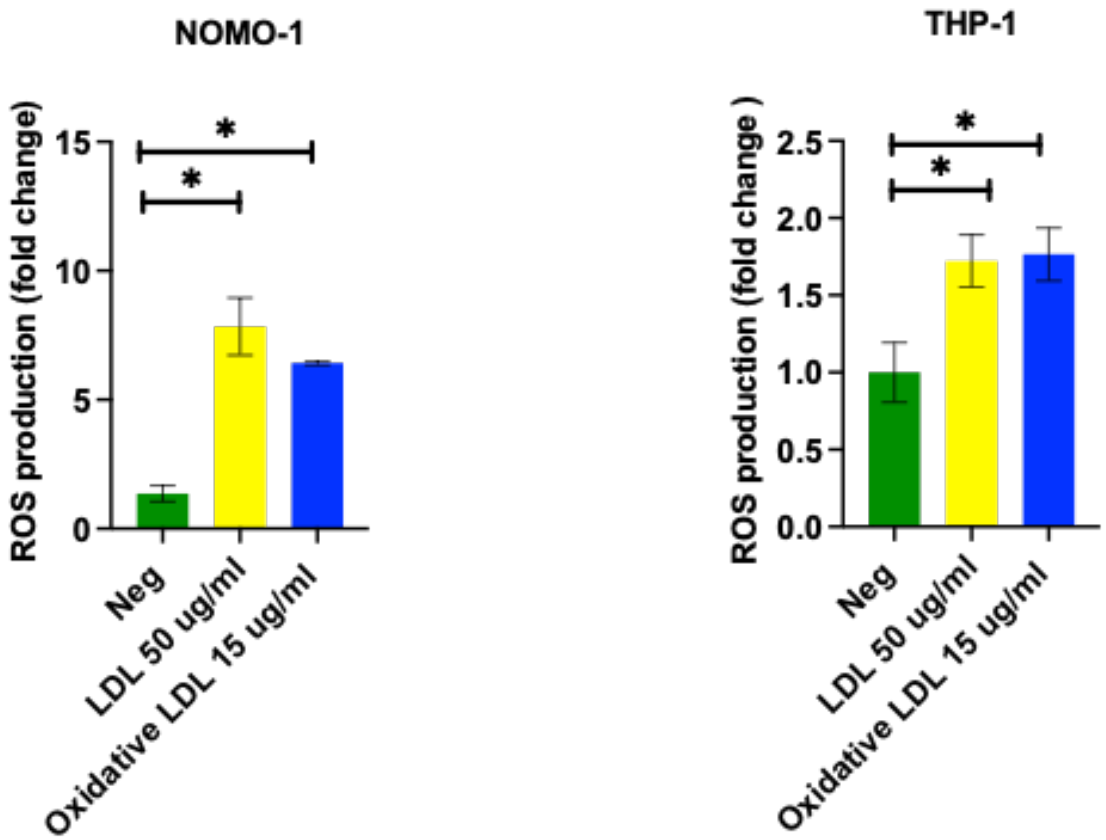

Figure 5.10 Exposure of LDL and OxLDL in THP-1 and NOMO-1 cells induced ROS production.

The effect of each on ROS production was assessed in a concentration dependent manner using the MitoSOX^{TM} Red mitochondrial superoxide indicator Assay Kit. Both THP-1 and NOMO-1 cells were treated with LDL and Oxi-LDL or vehicle (control). Cells treated with vehicle in the absence of cholesterol particles was used as a control. LDL used at concentration of 50 ug/ml and Oxidative LDL used at concentration 15 ug/ml incubated for 22 days. ROS production is displayed as fold-change to the Vehicle control which was normalised to 1. Data are presented as mean ± SEM from three independent experiments. Statistical analysis was performed using a One-way ANOVA nonparametric (3- groups for comparison) test (GraphPad prism) where *P ≤ 0.05

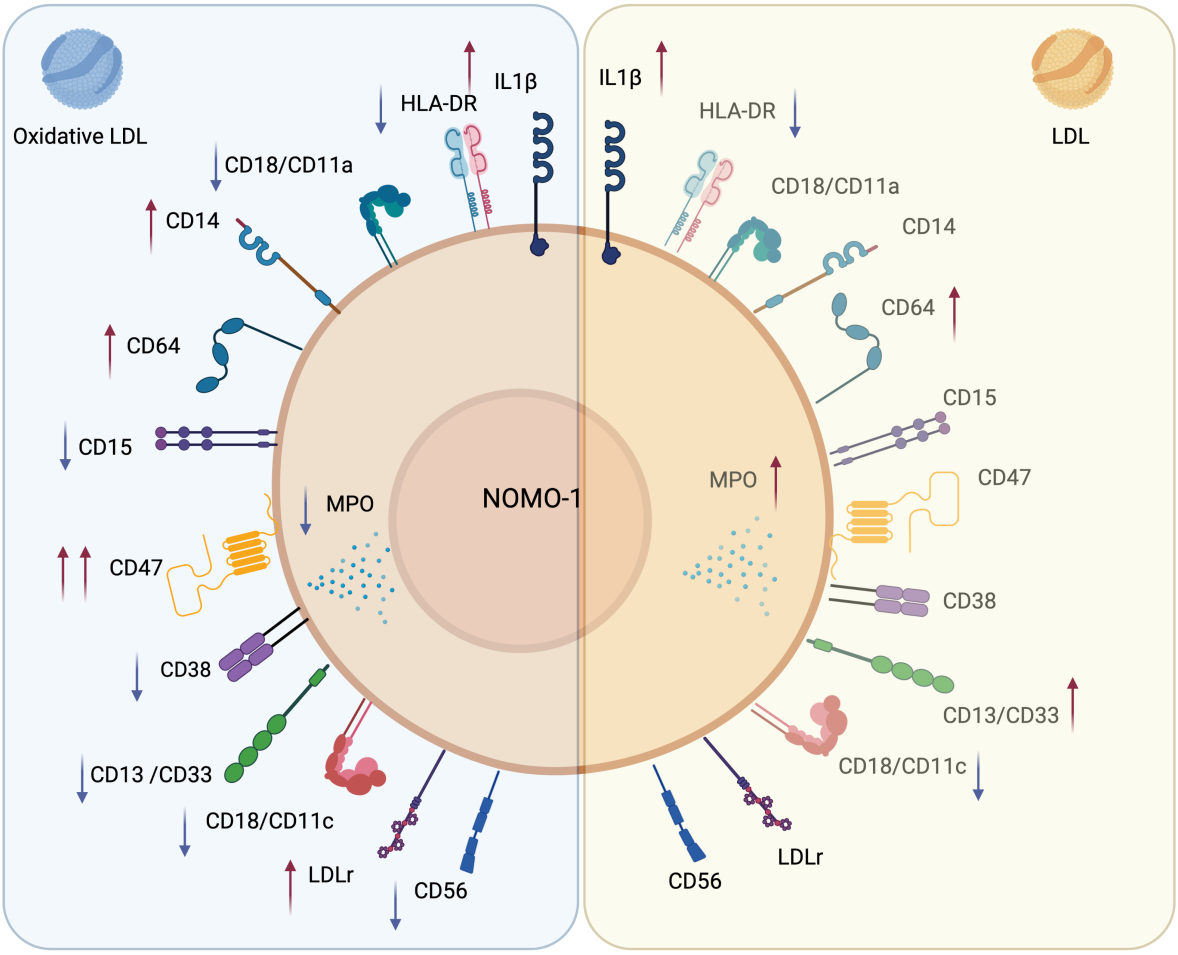

Figure 5.11 Summary of differential expression of select markers following exposure of NOMO-1 AML cells to atherogenic lipoproteins LDL and OxLDL in vitro.

5.4 Discussion

Several types of cancer have been linked to poor diet and nutritional deficiencies (Deschler and Lubbert 2006). High circulating cholesterol levels and high fat food consumption are also found to be correlated with cancer (Yang et al. 2020b). Low density lipoprotein receptor (*Ldlr*), the membrane receptor responsible for low-density lipoprotein endocytosis (LDL), is an integral component in cholesterol metabolism, and has been proven to be an independent adverse prognostic factor for AML outcome (Floeth et al. 2021). Furthermore, AML cells isolated from leukemic patients secrete factors to increase LDL uptake (Ho et al. 1978) (Bhuiyan et al. 2017). Research employing a MLL-AF9 knock-in mice model discovered that HFD regimen increased FLT3 signalling activation within the lipid raft of primitive haematopoiesis cells surface, increasing the chance of acquiring AML (Hermetet et al. 2020). Moreover, our RNA sequencing data in Chapter 4 revealed a strong correlation between abnormal cholesterol metabolism, cardiovascular disease, and haematological malignancies. For example, ID2 or Inhibitor if DNA Binding 2, an important transcriptional regulator for normal haematopoiesis, was downregulated in the *Ldlr*$^{-/-}$ HFD group. ID2 is responsible for initiation and maintenance of MLL-rearranged AML, where low endogenous Id2 expression is linked to LSC enrichment and Id2 overexpression hinders the onset and progression of MLL-AF9 leukaemia (Ghisi et al. 2016). Therefore, in this study, we employed *Ldlr*$^{-/-}$ mice to assess the effect of HFD on the development of leukaemia. This was done using a mouse MLL-AF9 induced AML *in vitro* and *in vivo* model and we extended our study to mimic HFD exposure in MLL-AF9 human leukaemia cells lines *in vitro*.

In the *Ldlr-/-* HFD murine model of AML driven by MLL-AF9, colony size and the immunophenotyping of myeloid markers linked to the AML differentiation blockage were initially evaluated during the production of pre-LSCs *in vitro*, but results were inconclusive due to the limited number of experiments performed. This caveat notwithstanding, our preliminary analysis appears to indicate that exposure of HFD to HSPCs in the context of Ldlr deficiency enhances their *in vitro* MLL-AF9 driven transformation capacity into pre-LSCs by increasing pre-LSC c-kit+ expression and decreasing Gr-1+ and Mac-1 expression i.e. markers of myeloid differentiation that are

blocked in AML. This interpretation is further supported by other preliminary data that shows that c-kit+ expression was increased, and Mac-1 expression was decreased in the bone marrow after transplantation of pre-LSCs in the *Ldlr*$^{-/-}$ HFD group (unpublished observations).

It was therefore surprising that upon transplantation of pre-LSCs *in vivo* the *Ldlr*$^{-/-}$ HFD group developed AML with the longest latency. This suggests that a HFD epigenetically programs *Ldlr*$^{-/-}$ HSPCs to alter their functional potential when transformed to LSCs. Part of the explanation for the longer latency in this setting was that LSCs/blasts were retained in the bone marrow and failed to do infiltrate and damage secondary haematopoietic organs and non-haematopoietic organs which could be affected by leukaemia (Yu and Scadden 2016). This could reflect alteration of intrinsic adhesion properties of transplanted *Ldlr*$^{-/-}$ HFD pre-LSCs. In support of this hypothesis, our RNA-sequencing of *Ldlr*$^{-/-}$ HSCs exposed to a HFD (Chapter 4) showed that ITGβ-3 (Integrin subunit Beta 3) was up-regulated. This adhesion molecule is an integral cell-surface protein composed of an alpha chain and a beta chain, participating in cell adhesion as well as cell-surface-mediated signalling (Johansen et al. 2018). Interestingly, a study identified ITGβ-3 as essential for murine MLL-AF9 driven AML, supporting an oncogenic role for ITGB-3 in AML (Zeisig and So 2013) (Miller et al. 2013). Moreover, overexpression of RasGEF1B circular RNA, a positive regulator of ICAM-1, one of the main adhesion molecules in immune cells trafficking (Ng et al. 2016), was also revealed in our RNA-seq data. Further investigations will be necessary to ascertain the precise role of adhesion molecules in our HFD model of AML. LSC/blast cell retention in the bone marrow may also be of clinical relevance; leukaemias are diagnosed when the peripheral blood sample (Papaemmanuil et al.) sample constitute 30% or more blast from total nucleated cells (Cheson et al. 1990). In this case BM aspirate may not be needed especially in vulnerable patients (Weinkauff et al. 1999). However, in clinical cases which mirror our mouse model, delayed or absent cell migration of blast cells from the bone marrow can lead to mis-diagnosis and disease progression; in this setting it will be important to determine the prognostic significance of estimating the PB/BM blast ratio.

In our *in vivo* MLL-AML leukemogenesis model we used a mixture of haematopoietic stem and progenitor cells (i.e. heterogenous HSPCs) as the cell of origin for

transduction with the MLL-AF9 vector (Cozzio et al. 2003). Studies have shown that the cell origin, whether it is a HSC or committed progenitors may influence gene expression, epigenetic programming, and drug resistance of the fully established leukaemias in MLL-AML patients, underscoring biological and clinical heterogeneity in molecularly defined leukaemias (Krivtsov et al. 2013). This raises the question of whether AML initiation and development would be differentially impacted if we used more homogenous haematopoietic cell types, such as more enriched primitive HSCs (Lin^- c-Kit^+ $Sca\text{-}1^+CD150^+CD48^-$) or specialised GMPs ($Lin^-$ c-Kit^+ $Sca\text{-}1^-$ $CD16/32^{high}$ $CD34^+$). This should be investigated in future. The self-renewal potential of LSCs in our HFD model of AML should also be explored; while HFD unexpectedly appears to promote a longer latency of AML, it is possible that these LSCs from the HFD group have potent self-renewal and will drive leukemogenesis more aggressively in secondary transplantation experiments that is used to assess LSC self-renewal.

Our results in the mouse model of MLL-AF9 encouraged us to examine the relevance of a pro-atherogenic HFD model in MLL-AF9 human AML cells. We developed an *in vitro* model to mimic HFD by exposing human AML cells to LDL and OxLDL. When AML cells were exposed to OxLDL more immunophenotypic changes occurred compared to when AML cells were cultured with LDL (see Figure 5.11). This is perhaps not unexpected given that OxLDL is the more potent form of LDL involved in atherosclerosis driven inflammation, which is a function of the degree of oxidation of LDL (Poznyak et al. 2020). Of relevance to the data presented in this Chapter and Chapter 4, other studies have shown that OxLDL induces epigenetic and metabolic resetting that might affect the proinflammatory function of monocytes and show sustained mechanistic target of rapamycin (mTOR) activation, increased reactive oxygen species (ROS) formation and accumulation of hypoxia-inducible factor 1α (HIF1α) with HIF1α target gene expression (Sohrabi et al. 2018).

We found that when AML cells were exposed to OxLDL this increased *Ldlr* expression, presumably due to enhanced LDL degradation in AML cells (Rudling et al. 1998). In hypercholesteremia conditions, increased LDL level induces monocytic and granulocytic proliferation and production (Tall and Yvan-Charvet 2015). Other studies have linked AML samples with monocytic differentiation to increased *Ldlr* expression (Rudling et al. 1998). Hypercholesteremia or increased LDL is considered a risk factor

for development of AML and prognostic risk factor for AML because it will increase the leukemic cell survival and enhance chemotherapy resistance by activating oncogenic signalling such as Hedgehog pathway. Also, it induces mTORC1 internal signalling and enhanced lipid raft components which play a crucial role in cancer signalling control (Ding et al. 2019). Moreover, AML cells shield themselves from the cytotoxicity of the drugs by rapidly increasing protective cholesterol levels, via an increase in *Hmgcr* and *Ldlr* mRNA level (Banker et al. 2004).

Consistent with decreased immune recognition and increased leukaemia cell survival, we noted substantial changes in the immunogenicity of human AML cells exposed to OxLDL. For example, we observed a decrease in HLA class II antigen (human homolog gene) in NOMO-1, mirroring our RNA sequencing data in Chapter 4, which revealed the mouse counterpart to HLA-Class II, the H2-Eb1 gene, was down regulated. The relevance of HLADR in AML pathogenesis remains unclear. A study suggest a correlation between negative HLADR expression and poor cytogenetics group association in AML, with M0, M1 and M2 FAB subtypes mostly affected (El-Meligui et al. 2021). On the contrary, other research based on 400 human samples concluded clinical outcomes in HLA-DR^{low} AML patients were not poorer to HLA-DR^{High} AML patients (Roerden et al. 2021). Nevertheless, HLADR expression reflects immune competence of antigen presenting cells, such as monocytes, in the setting of high cholesterol and this observation requires further detailed experimentation. For example, it has been known that Major histocompatibility complex (MHC) class-II antigen expression was reduced in lymphocytes and monocytes isolated from Type-II diabetes individuals with excessively high serum cholesterol and triglyceride levels (Romano-Carratelli et al. 1993).

CD47, as judged by MFI, was dramatically upregulated in NOMO-1 cells when incubated with OxLDL. CD47, also known as the “do not eat me” molecule, is expressed on all cells that are healthy, but importantly its expression is rapidly downregulated during apoptosis (Singla et al. 2021). This allows apoptotic cells to be ingested by phagocytes and removed from the body through a controlled efferocytic process (Singla et al. 2021). Interestingly, increased CD47 is also associated with atherosclerosis, and this may explain why efferocytosis of atheroma lesions by macrophages is impaired in advanced plaque (Kojima et al. 2016). To escape being

destroyed by macrophages, cancer cells use CD47 to evade recognition by the innate immune system, therefore decreasing immune recognition of cancer cells (Zhao et al. 2022). In AML, CD47 is overexpressed and is an independent poor prognostic indicator, and CD47 has been implicated many other solid tumours (Huang et al. 2022a) and other haematological malignancies (Eladl et al. 2020). This has encouraged researchers to target CD47 through monoclonal antibodies and test it clinically to treat cancer; it has been found a promising therapy in AML, where blocking the “don’t eat me” signals, improved innate immune system eradication of leukaemia cells more efficiently (Takimoto et al. 2019). Beyond cancer, CD47 may also be beneficial in treating cardiovascular disease, as alluded to above, and other co-morbidities involving deregulated efferocytosis, such as the autoimmune diseases rheumatoid arthritis and systemic lupus erythematosus (Boada-Romero et al. 2020).

CD38 was reduced when NOMO-1 cells was co-cultured with OxLDL. CD38 is a transmembrane glycoprotein expressed in a variety of cell types such as lymphocytes, myelocytes and myocytes with the main function of triggering T cell activation through CD31 (Zubiaur et al. 2002). Thus, reduced CD38 expression may indicate poor immune competence in hypercholesteraemic patients due to a defect in T cell activation required by CD38, and it may similarly cause poorer immune recognition of AML cells in CHIP driven AML. In support of this hypothesis, studies have shown higher CD38 expression were linked to better overall survival in patients with AML and ALL (Keyhani et al. 2000) and increased CD34+/CD38- expression in LSCs is a harbinger of poor prognosis (Plesa et al. 2017).

IL-1β is one of the major cytokines involved with chronic inflammation (Parting et al. 2020). To a large extent, atherosclerosis is influenced by modified LDLs since they are potent inflammatory inducers. By stimulating pattern recognition receptors such toll-like receptors (TLRs), they influence vascular physiology by setting off inflammatory signals, ROS, and matrix breakdown (Amiya 2016). If cholesterol is present, activation of IL-1β will occur due to these TLRs priming the Nod-like receptor protein 3 (NLRP3) inflammasome (Tunon et al. 2018). Our results showed increases in IL-1β receptor in response to OxLDL exposure. Importantly, studies shows that interleukin-1 (IL-1) induces a massive increase of abnormal myeloid progenitors while

suppressing the growth of normal progenitors in approximately 67% of AML patients. Additionally, clonogenicity and *in vivo* disease progression were significantly suppressed after IL-1 receptor silencing in AML patients, who had elevated levels of both IL-1β and IL-1 receptors (Carey et al. 2017). Thus, IL-1β may represent a novel therapeutic target in AML and atherosclerosis (Carey et al. 2017; Li et al. 2017).

Intracellular ROS content is also significantly increased in response to long term exposure to LDL and OxLDL in both leukemic cell lines. It is widely believed that over 60% of AML cells produce high level of NOX-derived ROS, facilitating cell proliferation and persistence (Hole et al. 2013). Nevertheless, ROS production is believed to be generated in response to differential metabolic activities pathways of carbohydrate, lipid and protein (Robinson et al. 2021). Studies have shown that lipid peroxidation products result in increased ROS, affecting genomic and mitochondrial DNA (mtDNA) (Wiseman and Halliwell 1996). This concurs with our finding of increased oxidative phosphorylation which cause mitochondrial damage in *Ldlr*$^{-/-}$ HFD HSCs RNA sequencing results in Chapter 4.

Supporting our hypothesis that a pro-atherogenic HFD model influences the behaviour of adhesion molecules in leukaemia cells, we observed a complex pattern of deregulation of adhesion molecules on exposure of LDL and OxLDL. Notably, CD44 was significantly upregulated when NOMO-1 cells when incubated with OxLDL. CD44 is a cell surface adhesion receptor upregulated in many cancers to regulate metastasis, and therefore aggressiveness of the cancer (Senbanjo and Chellaiah 2017) (Hidalgo et al. 2007). This marker has been reported to be overexpressed in AML which correlates with adverse disease prognosis (Legras et al. 1998). It is also known that upregulation of CD44 causes LSC retention in BM niches, which aid in survival and consequently resistance to chemotherapy (Pievani et al. 2020). Given our results in the MLL-AF9 mouse model suggesting increased LSC/blast retention in the bone marrow in the *Ldlr* HFD group, it will be of considerable interest to determine the role of CD44 in this process. Interestingly, CD44 is known to promote atherosclerosis by promoting macrophage cell recruitment (Cuff et al. 2001). Clinical trials using targeted therapy approach are using a monoclonal antibody directed to CD44 to

achieve better AML survival rates (Jin et al. 2006), but given its role in atherosclerosis, CD44 could also be applied to treat cardiovascular disease.

CD56, also known as neural cell adhesion molecule, is a member of immunoglobin superfamily (IgSF) group (Wai Wong et al. 2012). CD14+CD56+ monocytes have been identified in human peripheral blood, suggesting they may serve as a precursor to CD56+ DCs. Studies shows that number of CD14+/CD56+ monocytes in the peripheral blood was on average 3.70 times higher in cancer patients than in healthy controls (Papewalis et al. 2011), suggesting the role of monocytes expressing CD56 in cancer microenvironment and possibly in immune tolerance towards cancer cells (Van Acker et al. 2017). Moreover, flow cytometry investigation of monocytes different subpopulation in peripheral blood from obese humans showed increased occurrence of CD14+/CD56+, pointing to total cholesterol as one of the contributing factors (Friedrich et al. 2019). Nevertheless, CD56 expression on AML calls are associated with adverse outcome (Xu et al. 2015).

Our *in vitro* results showed significant increase in CD56 expression in NOMO-1 cells incubated with LDL and, contrastingly, a significant decrease when cultured with OxLDL. Our result concur with a recent publication confirming reduced IFN-γ, CD56, and NKG2D expression upon oxidized-desialylated LDL treatment of lymphokine activated killer cells (LAK) and, accordingly, their expression were amplified with incubated with native LDL (Aguilar Diaz de Leon et al. 2021). Yet, previous report confirmed that cellular deposition and elevated absorption of OxLDL lead to diminished immune cells properties against cancer development (Tapia-Vieyra et al. 2017). Collectively, this results underlines the effect of OxLDL on immune cell defects, which is a key hallmark of myeloid leukaemia development (Hanahan and Weinberg 2011).

LDL and OxLDL impacted the behaviour of myeloid markers of human AML cells, which may have implications for how a high cholesterol environment impacts the differentiation block in AML biologically and clinically. Some prominent expressed myeloid antigens on AML cells are CD33 and CD13. Both markers were significantly increased when incubated with LDL. CD33 monoclonal antibody is a widely accepted clinical target therapy because it is commonly expressed on LSCs but not on normal

primitive haematopoietic and progenitor cells, therefore decreasing the cytotoxic effect of normal haematopoietic cells (Wickstrom et al. 2011; Liu et al. 2022). The enzyme aminopeptidase N or CD13 is a Zn^{2+} membrane-bound ectopeptidase that metabolise proteins with neutral N-terminal amino acids (Wickstrom et al. 2011). Several human solid cancers, haematologic tumours and inflammation have been linked to aminopeptidase N, making it a potential therapeutic target for anti-cancer and anti-inflammatory drugs (Bauvois and Dauzonne 2006). Moreover, CD13 is expressed in lipid raft of monocytes and identified as a target for a cholesterol absorption inhibitor drug exetimib (Orso et al. 2006; Suchy et al. 2011).

We have used the human leukemic cells lines NOMO-1 and THP-1 to assess the effect of high atherogenic lipoproteins in AML cells. The most affected molecules are adhesion and immune recognition molecules, which likely reflects how cholesterol metabolites influence AML cell behaviour in an atherosclerosis-like model. Notably, some of the markers identified here have been implicated in both AML and atherosclerosis (e.g. CD44, CD47 and IL-1β). Our results therefore further highlight that these specific markers may be of prognostic and therapeutic significance in patients with CHIP driven atherosclerosis and haematological malignancies that will need to be investigated in the future. Broadly, our data highlights the interplay between inflammation (in this case driven by an atherosclerosis-like model) and human AML cell behaviour.

Chapter 6: General Discussion

Emerging evidence suggests a causal association between a high-fat diet (HFD) , atherosclerosis and the development of leukaemia (Vilchis-Ordoñez et al. 2021). In this project, we explored the currently ill-defined role of a HFD in an established mouse model of atherosclerosis and its impact on haematopoiesis and whether it promotes the development of acute myeloid leukaemia, a poor prognosis class of leukaemia. We showed that hypercholesterolemic atherosclerosis prone *Ldlr* knockout mice display largely normal steady-state haematopoietic potential but when fed a HFD develop atherosclerosis and display expanded haematopoietic stem cell populations in the bone marrow as well as alterations in myeloid and lymphoid cells and inferior HSC function, as assessed by competitive transplantation. Furthermore, reduced HSC function of *Ldlr* knockout mice fed a HFD was allied to a robust transcriptional signature of perturbed haematopoiesis, including gene signatures associated with inflammation, RNA biology, apoptosis, and, importantly, AML. To test whether HSPCs from *Ldlr* knockout mice fed a HFD had increased propensity to develop AML driven by the pro-inflammatory tone of these HSCs, we transduced HSPCs from *Ldlr* knockout mice fed a HFD with a retrovirus containing the AML driver MLL-AF9. In support of a pro-inflammatory role driving the development of leukaemia, multiple studies have shown that HFD driven obesity induces inflammatory cytokine IL-6 expression as part of an accelerated development of leukaemia (Camacho et al. 2021). In addition, a HFD and associated obesity accelerates development of another haematological malignancy, multiple myeloma (Lichtman 2010). Unexpectedly, we found that AML transformed HSPCs from *Ldlr* knockout mice fed a HFD had later disease manifestations than their ND counterparts. However, it appears that this may be driven by alterations in adhesion molecules retaining blasts in the bone marrow, perhaps delaying their egress from the bone marrow into the periphery and other organs. This contention is supported by other experiments in the thesis where human AML cells mimicking conditions of atherosclerosis *in vitro* were found to have altered adhesion molecule expression in addition to decreased immune recognition. Collectively, the data provided in this thesis provide mechanistic insights into how HFD epigenetically alters AML development, and they start to establish the relationship

between HFD, atherosclerosis and the development of perturbed haematopoiesis and AML (Figure 6.1).

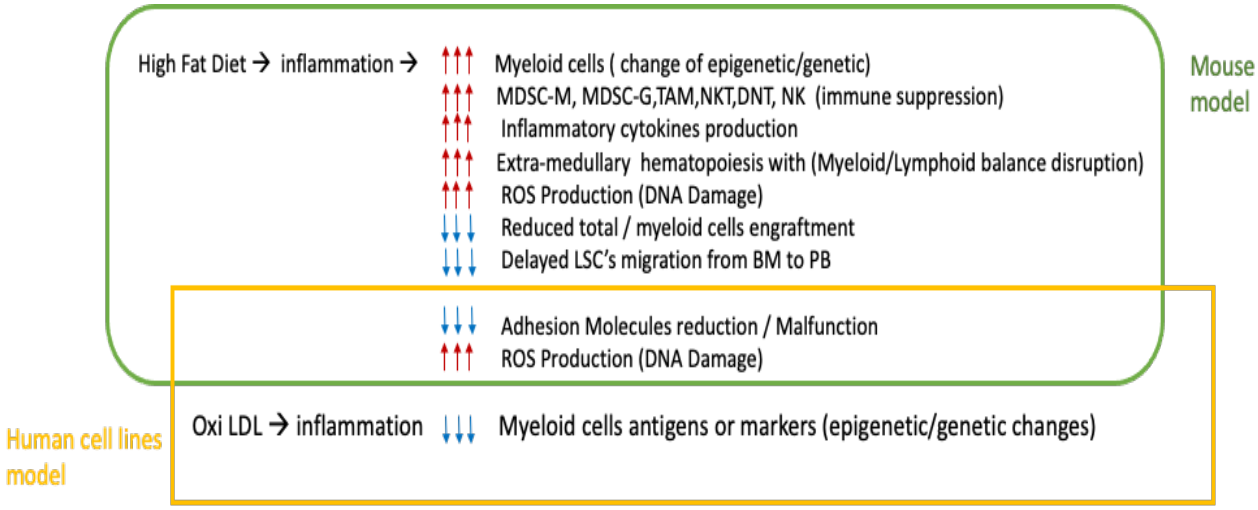

Figure 6.1 Overlap of mouse and human models used in this thesis to model haematopoietic response to atherogenic promoting lipoproteins.

In our mouse model, the final drive toward constant replacement of normal cells by their inflammatory counterpart, in this case increased production of epigenetically modified myeloid cells is proatherogenic lipoprotein OxiLDL. Also, in the context of HFD, immune suppressor cells are dominating the immune system, in addition proinflammatory cytokines and ROS are magnified. All the above facilitate the ongoing development of epigenetic bridges, which may encourage cell fate decisions such as hyperproliferation, metabolic stress, senescence, and/or malignant transformation. This is mirrored by observed reduced total/ myeloid cells engraftments in competitive BM transplantation, delayed MLLAF9 egress of leukaemic stem cells from BM to PB and genetically altered adhesion molecules. Human cells lines investigations overlapped with reduced or epigenetic / genetic of myeloid markers, adhesion molecule expression reduction and increased intracellular ROS production.

The two largest causes of mortality in the world are cancer and cardiovascular disease (CVD) (de Boer et al. 2019). CVD is caused by a group of risk factors that includes but is not limited to a cholesterol rich diet (western diet) and genetic factors. Accumulating evidence also suggests that metabolic syndromes are often linked together in disease settings. These include dyslipidaemia, type 2 diabetes, obesity and hypertension (Wilson et al. 2007). In support of this, a recent article investigated the blood glucose level on C3H strain *Ldlr*$^{-/-}$ mice model ingesting HFD and discovered that these mice not only developed severe hypercholesterolemia but also, they were hyperglycaemic with fasting glucose level above 250 mg/dL. Knowing that lipid, carbohydrate, amino acids and nucleotides are molecularly intertwined because they interact metabolically between glycolysis and the citric acid cycle pathways (Robinson et al. 2021), alteration in these metabolic pathways in proliferating cancer cells may be able to suppress metabolic signals that might limit tumour development or slow its spread (Hanahan and Weinberg 2011). This is supported by our RNA-seq data of HSCs from *Ldlr*$^{-/-}$ mice receiving HFD which displayed a metabolic signature consistent with an AML signature. For example, serine (or cysteine) peptidase inhibitor, clade A, member 3G (Serpina3g), ATP Binding Cassette Subfamily G Member 1 (Abcg1) and Mevalonate Kinase (Mvk).

Of relevance here, control of growing leukaemic cells can be attained by stopping its metabolic fuel, cholesterol, as evidenced by the impact of statins on LSCs (Pernes et al. 2019). Statin therapies have been demonstrated to reduce LSC function but not HSPCs. This conversely suggests that cholesterol production is beneficial to LSCs (Hartwell et al. 2013). Interestingly, statins can also modify oncogenic signalling in addition to their ability to inhibit dysregulated metabolic pathways. For example, statins restrict cholesterol production and RAS signalling via farnesylation inhibition (Nagarajan et al. 2016). Thus, targeting cholesterol metabolism may be a broadly applicable strategy to target cancer.

Ageing also increases the risk of both cardiovascular disease and cancer (Park and Bejar 2020). Why atherosclerosis occurs during ageing is multi-factorial and one recently identified contributing factor is the development of CHIP, which provides a heightened risk for leukaemia development and cardiovascular disease in the elderly, and where mutations arise in HSCs that are transmitted to their blood cell progeny,

which also harbour those mutations (Marnell et al. 2021). Interestingly, variations in clinical outcome are seen in individuals with solid tumours who exhibit CHIP (Park and Bejar 2020). However, it has been proved that tumours of the haematological system, such as leukaemia, may require fewer driver mutations than epithelial cancers like breast, colorectal, or prostate cancer (Miller 1980), so the basis for the variable association of solid tumours with CHIP is unclear. Our atherosclerosis prone *Ldlr* model provides a tractable model with which to explore the impact of CHIP in this context and the impact of CHIP on other non-haematopoietic tissues. It is perhaps not unexpected that mutated HSCs and their mutated blood progeny will impact other tissues in the body as blood is in circulation in all tissues in addition to haematopoietic organs. For example, in our study HSCs from *Ldlr* knockout mice receiving HFD displayed a nephrotoxic and hepatotoxic gene signature. This observation is consistent with the recent observation that CHIP is linked to chronic kidney disease in the general population, where chronic kidney disease is defined by tubulointerstitial fibrosis and the aggregation of clonal inflammatory cell infiltration and fibroblasts within the kidney interstitium (Kestenbaum et al. 2022). Also of relevance, CHIP appears to correlate with acceleration of pre-existing advanced chronic kidney disease (Vlasschaert et al. 2022). In future studies using the *Ldlr* knockout mice model in combination with mouse models for known CHIP mutations (e.g. TET2, ASXL1, DNM3TA) it will be of interest to explore the causality and reciprocity of CHIP with chronic kidney disease further and with hepatic diseases like non-alcoholic fatty liver disease and non-alcoholic steatohepatitis, which is also linked to heightened inflammation (Luci et al. 2020). In clinical studies, one could start investigating CHIP from onset (aged approx. 50), continuing to study ageing hypercholesteraemic individuals and understanding the haematopoietic characteristics in detail which may reveal hitherto unknown molecular characteristics of patients to produce a so called “hypercholesteraemic patient diagnostic profile”. In this type of study, we could pair flow cytometry along with next generation sequencing to identify additional molecular or matching molecular signatures associated with AML, kidney or hepatic disease, or indeed any inflammatory driven disorder in any tissue, as CHIP is known to enhance inflammation.

6.1 Further experiments

While the data in Chapter 5 has started to provide insights into the role of a HFD in promoting AML and the association between atherosclerosis and AML development, more detailed experimentation is needed to fully explore this association. HSCs from *Ldlr*$^{-/-}$ mice should undergo the leukaemogenic /LSC assay in Chapter 5 and further analysis should be performed at the CFC stage of the assay. In the CFC stage of the assay, leukaemic colony number can be enumerated at each plating, building on the preliminary result reported in this thesis, and further characterisation by flow cytometry for (i) induction of apoptosis using Annexin V, (ii) myeloid differentiation capacity and clonal analysis of leukaemic cell populations and (iii) proliferative capacity using the Ki67 assay. After transplantation of pre-LSCs from the CFC assay, mice that develop AML can be characterized in their LSC compartment for apoptosis, cell cycle and myeloid differentiation capacity, as described above, and further analysis of the bone marrow/peripheral blood ratio of leukaemic blasts can be performed as well as analysis of invasiveness to other organs (e.g. spleen and liver). Additionally, RNA-sequencing can be conducted on LSCs from to ascertain deregulated transcriptional mechanisms in LSCs. Independently of RNA-seq, proposed pathways we could study based on our preliminary data in human AML cells include adhesion molecules, reactive oxygen species and molecules involved in immune recognition like CD47. Finally, to specifically test the impact of HFD on the ability of AML LSCs to self-renew and therefore maintain leukaemia, LSCs from primary recipients can be injected secondary irradiated recipients; disease progression can be monitored and assayed as described in the primary transplant experiments above (mice develop AML in secondary transplantation between 3-6 weeks). These data will provide mechanistic insights into how HFD epigenetically alters AML development.

While these experiments provide an association between HFD and AML, *Ldlr*$^{-/-}$ mice provide a tractable model to **directly** assess whether HFD promotes AML in association with the development of atherosclerosis. To test this, **wild-type** HSCs could undergo the leukaemogenic assay described in above and Chapter 5 and pre-leukaemic CFCs will be transplanted into either *Ldlr*$^{-/-}$ mice or control mice and fed a HFD (or normal diet) for the duration of the experiment; this model will simultaneously

promote atherosclerosis and AML in *Ldlr*$^{-/-}$ mice. To assess the direct association between atherosclerosis and AML development, survival of mice and disease progression should be monitored as described in Chapter 5 and analysed as described in the preceding paragraph. The extent of aorta wall thickness, atherosclerotic plaque development and vascular calcification can also be assessed in recipients. An experiment should also be performed where leukaemic *Ldlr*$^{-/-}$ recipients are fed a HFD for half of the experiment, followed by a switch to a normal diet to allow for regression of atherosclerotic plaque; the impact on AML development will be monitored in this setting. To gain preliminary insights into the potential mechanistic role of atherosclerosis in promoting AML, recipients could be assessed for a selection of key markers of inflammation during atherosclerosis (e.g. MCP-1 and intercellular adhesion molecule-1) by qPCR and/or western blot analysis and/or ELISA or simply RNA-sequenced following by pathway validation. Together, these experiments will establish the direct relationship between HFD, AML and the development of atherosclerosis. Specifically they will have three broad implications for future analysis: (A) **Inflammation as a pathogenic driver of both atherosclerosis and AML and other cancers:** Building on data from these experiments, we could further explore inflammation in our model by focusing on (i) evaluating the inflammasome (responsible for the high levels of cytokines IL-1β during atherosclerosis, clonal haematopoiesis and AML) and (ii) assessing reactive oxygen species/anti-oxidant production (responsible for oxidative stress during atherosclerosis and AML pathogenesis). Further mechanistic insight regarding inflammation will also be provided by RNA-sequencing data generated in the above experiments and potential inflammatory pathways will be validated in our model by standard gain or loss of function approaches (e.g. lentiviral RNAi or overexpression). Finally, we could apply data generated here as proof of principle to support studies to better understand and potentially elucidate a link of atherosclerosis, as an inflammatory disorder, to solid cancers. (B) **Using existing cardiovascular drugs to target AML leukaemia stem cells and AML drugs to target cardiovascular disease**: The key to improving AML therapy will be to abolish LSC activity (Khaldoyanidi et al. 2022). In our mouse model, where LSCs can be prospectively isolated by flow cytometry, we can investigate the ability of existing cardiovascular drugs to target AML CSCs. To this end, in an independent project in the Rodrigues lab, where we performed a chemical screen for stem cell active drugs, we identified fluvastatin as a potential therapeutic target in AML

LSCs. Conversely, inhibitors of DNA methylation are used therapeutically in AML (e.g. 5-axa-2'deoxycytdine) and, since DNA methylation/histone acetylation has been implicated as a drug target in cardiovascular disease (Natarajan 2011) such AML drugs could also be assessed for their ability to alleviate atherosclerosis in our model. (C) **Clinical correlation between cardiovascular disease and AML prognosis**: If it was possible to access historical AML clinical samples/banks and information on individual patient's medical histories it may be possible to correlate how cardiovascular disease may influence AML prognosis.

References

Abbaspour Babaei, M. et al. 2016. Receptor tyrosine kinase (c-Kit) inhibitors: a potential therapeutic target in cancer cells. *Drug Des Devel Ther* 10, pp. 2443-2459. doi: 10.2147/DDDT.S89114

Abdelfattah, A. et al. 2021. Gata2 haploinsufficiency promotes proliferation and functional decline of hematopoietic stem cells with myeloid bias during aging. *Blood Adv* 5(20), pp. 4285-4290. doi: 10.1182/bloodadvances.2021004726

Adolfsson, J. et al. 2005. Identification of Flt3+ lympho-myeloid stem cells lacking erythro-megakaryocytic potential a revised road map for adult blood lineage commitment. *Cell* 121(2), pp. 295-306. doi: 10.1016/j.cell.2005.02.013

Aguilar Diaz de Leon, J. S. et al. 2021. Oxidized-Desialylated Low-Density Lipoprotein Inhibits the Antitumor Functions of Lymphokine Activated Killer Cells. *J Cancer* 12(16), pp. 4993-5004. doi: 10.7150/jca.55526

Aguilar-Ballester, M. et al. 2020. Impact of Cholesterol Metabolism in Immune Cell Function and Atherosclerosis. *Nutrients* 12(7), doi: 10.3390/nu12072021

Akashi, K. et al. 2000. A clonogenic common myeloid progenitor that gives rise to all myeloid lineages. *nature* 404(6774), pp. 193-197.

Akinduro, O. et al. 2018. Proliferation dynamics of acute myeloid leukaemia and haematopoietic progenitors competing for bone marrow space. *Nat Commun* 9(1), p. 519. doi: 10.1038/s41467-017-02376-5

Al-Ahmadi, W. et al. 2021. Pro-atherogenic actions of signal transducer and activator of transcription 1 serine 727 phosphorylation in LDL receptor deficient mice via modulation of plaque inflammation. *FASEB J* 35(10), p. e21892. doi: 10.1096/fj.202100571RR

Al-Sharea, A. et al. 2019. The haematopoietic stem cell niche: a new player in cardiovascular disease? *Cardiovasc Res* 115(2), pp. 277-291. doi: 10.1093/cvr/cvy308

Alharbi, R. A. et al. 2013. The role of HOX genes in normal hematopoiesis and acute leukemia. *Leukemia* 27(5), pp. 1000-1008. doi: 10.1038/leu.2012.356

Almosailleakh, M. and Schwaller, J. 2019. Murine Models of Acute Myeloid Leukaemia. *Int J Mol Sci* 20(2), doi: 10.3390/ijms20020453

Alomari, M. et al. 2019. Role of Lipid Rafts in Hematopoietic Stem Cells Homing, Mobilization, Hibernation, and Differentiation. *Cells* 8(6), doi: 10.3390/cells8060630

Amiya, E. 2016. Interaction of hyperlipidemia and reactive oxygen species: Insights from the lipid-raft platform. *World J Cardiol* 8(12), pp. 689-694. doi: 10.4330/wjc.v8.i12.689

Anders, S. and Huber, W. 2010. Differential expression analysis for sequence count data. *Nature Precedings*, doi: 10.1038/npre.2010.4282.1

Andreeff, M. et al. 2008. HOX expression patterns identify a common signature for favorable AML. *Leukemia* 22(11), pp. 2041-2047. doi: 10.1038/leu.2008.198

Aparicio-Vergara, M. et al. 2010. Bone marrow transplantation in mice as a tool for studying the role of hematopoietic cells in metabolic and cardiovascular diseases. *Atherosclerosis* 213(2), pp. 335-344. doi: 10.1016/j.atherosclerosis.2010.05.030

Arai, F. et al. 2004. Tie2/angiopoietin-1 signaling regulates hematopoietic stem cell quiescence in the bone marrow niche. *Cell* 118(2), pp. 149-161. doi: 10.1016/j.cell.2004.07.004

Argiropoulos, B. and Humphries, R. K. 2007. Hox genes in hematopoiesis and leukemogenesis. *Oncogene* 26(47), pp. 6766-6776. doi: 10.1038/sj.onc.1210760

Arinobu, Y. et al. 2007. Reciprocal activation of GATA-1 and PU.1 marks initial specification of hematopoietic stem cells into myeloerythroid and myelolymphoid lineages. *Cell Stem Cell* 1(4), pp. 416-427. doi: 10.1016/j.stem.2007.07.004

Aslanian, A. M. et al. 2005. Transient role for CD1d-restricted natural killer T cells in the formation of atherosclerotic lesions. *Arterioscler Thromb Vasc Biol* 25(3), pp. 628-632. doi: 10.1161/01.ATV.0000153046.59370.13

Aurelius, J. et al. 2012. Monocytic AML cells inactivate antileukemic lymphocytes: role of NADPH oxidase/gp91(phox) expression and the PARP-1/PAR pathway of apoptosis. *Blood* 119(24), pp. 5832-5837. doi: 10.1182/blood-2011-11-391722

Azzoni, E. et al. 2018. Kit ligand has a critical role in mouse yolk sac and aorta-gonad-mesonephros hematopoiesis. *EMBO Rep* 19(10), doi: 10.15252/embr.201745477

Bagger, F. O. et al. 2019. BloodSpot: a database of healthy and malignant haematopoiesis updated with purified and single cell mRNA sequencing profiles. *Nucleic Acids Res* 47(D1), pp. D881-D885. doi: 10.1093/nar/gky1076

Bain, B. J. and Estcourt, L. 2013. FAB Classification of Leukemia.*Brenner's Encyclopedia of Genetics*. pp. 5-7.

Baldridge, M. T. et al. 2010. Quiescent haematopoietic stem cells are activated by IFN-gamma in response to chronic infection. *nature* 465(7299), pp. 793-797. doi: 10.1038/nature09135

Banker, D. E. et al. 2004. Cholesterol synthesis and import contribute to protective cholesterol increments in acute myeloid leukemia cells. *Blood* 104(6), pp. 1816-1824. doi: 10.1182/blood-2004-01-0395

Barrett, T. J. et al. 2019. Platelet regulation of myeloid suppressor of cytokine signaling 3 accelerates atherosclerosis. *Sci Transl Med* 11(517), doi: 10.1126/scitranslmed.aax0481

Bauvois, B. and Dauzonne, D. 2006. Aminopeptidase-N/CD13 (EC 3.4.11.2) inhibitors: chemistry, biological evaluations, and therapeutic prospects. *Med Res Rev* 26(1), pp. 88-130. doi: 10.1002/med.20044

Bawazir, A. et al. 2019. The burden of leukemia in the Kingdom of Saudi Arabia: 15 years period (1999-2013). *BMC Cancer* 19(1), p. 703. doi: 10.1186/s12885-019-5897-5

Beerman, I. et al. 2010. Functionally distinct hematopoietic stem cells modulate hematopoietic lineage potential during aging by a mechanism of clonal expansion. *Proc Natl Acad Sci U S A* 107(12), pp. 5465-5470. doi: 10.1073/pnas.1000834107

Beerman, I. et al. 2014. Quiescent hematopoietic stem cells accumulate DNA damage during aging that is repaired upon entry into cell cycle. *Cell Stem Cell* 15(1), pp. 37-50. doi: 10.1016/j.stem.2014.04.016

Bekkering, S. et al. 2014. Oxidized low-density lipoprotein induces long-term proinflammatory cytokine production and foam cell formation via epigenetic reprogramming of monocytes. *Arterioscler Thromb Vasc Biol* 34(8), pp. 1731-1738. doi: 10.1161/ATVBAHA.114.303887

Bellner, L. et al. 2020. Heme Oxygenase-1 Upregulation: A Novel Approach in the Treatment of Cardiovascular Disease. *Antioxidants & Redox Signaling* 32(14), pp. 1045-1060. doi: 10.1089/ars.2019.7970

Bernitz, J. M. et al. 2016. Hematopoietic Stem Cells Count and Remember Self-Renewal Divisions. *Cell* 167(5), pp. 1296-1309 e1210. doi: 10.1016/j.cell.2016.10.022

Bertrand, J. Y. et al. 2007. Definitive hematopoiesis initiates through a committed erythromyeloid progenitor in the zebrafish embryo. *Development* 134(23), pp. 4147-4156. doi: 10.1242/dev.012385

Berzins, S. P. et al. 2011. Presumed guilty: natural killer T cell defects and human disease. *Nat Rev Immunol* 11(2), pp. 131-142. doi: 10.1038/nri2904

Bhuiyan, H. et al. 2017. Acute Myelogenous Leukemia Cells Secrete Factors that Stimulate Cellular LDL Uptake via Autocrine and Paracrine Mechanisms. *Lipids* 52(6), pp. 523-534. doi: 10.1007/s11745-017-4256-z

Bietz, A. et al. 2017. Cholesterol Metabolism in T Cells. *Front Immunol* 8, p. 1664. doi: 10.3389/fimmu.2017.01664

Bigas, A. and Espinosa, L. 2012. Hematopoietic stem cells: to be or Notch to be. *Blood* 119(14), pp. 3226-3235. doi: 10.1182/blood-2011-10-355826

Bilheimer, D. W. et al. 1984. Liver transplantation to provide low-density-lipoprotein receptors and lower plasma cholesterol in a child with homozygous familial hypercholesterolemia. *New England journal of medicine* 311(26), pp. 1658-1664.

Biswas, S. K. et al. 2013. Tumor-associated macrophages: functional diversity, clinical significance, and open questions. *Semin Immunopathol* 35(5), pp. 585-600. doi: 10.1007/s00281-013-0367-7

Boada-Romero, E. et al. 2020. The clearance of dead cells by efferocytosis. *Nat Rev Mol Cell Biol* 21(7), pp. 398-414. doi: 10.1038/s41580-020-0232-1

Boila, L. D. and Sengupta, A. 2020. Evolving insights on histone methylome regulation in human acute myeloid leukemia pathogenesis and targeted therapy. *Exp Hematol* 92, pp. 19-31. doi: 10.1016/j.exphem.2020.09.189

Bonaccorsi, I. et al. 2015. Natural killer cells in the innate immunity network of atherosclerosis. *Immunol Lett* 168(1), pp. 51-57. doi: 10.1016/j.imlet.2015.09.006

Bowie, M. B. et al. 2007. Identification of a new intrinsically timed developmental checkpoint that reprograms key hematopoietic stem cell properties. *Proc Natl Acad Sci U S A* 104(14), pp. 5878-5882. doi: 10.1073/pnas.0700460104

Bowman, R. L. et al. 2018. Clonal Hematopoiesis and Evolution to Hematopoietic Malignancies. *Cell Stem Cell* 22(2), pp. 157-170. doi: 10.1016/j.stem.2018.01.011

Bradley, J. E. et al. 2013. Effect of the GPI anchor of human Thy-1 on antibody recognition and function. *Lab Invest* 93(3), pp. 365-374. doi: 10.1038/labinvest.2012.178

Brandt, D. and Hedrich, C. M. 2018. TCRalphabeta(+)CD3(+)CD4(-)CD8(-) (double negative) T cells in autoimmunity. *Autoimmun Rev* 17(4), pp. 422-430. doi: 10.1016/j.autrev.2018.02.001

Braun, N. A. et al. 2010. Natural killer T cells and atherosclerosis: form and function meet pathogenesis. *J Innate Immun* 2(4), pp. 316-324. doi: 10.1159/000296915

Brendolan, A. and Russo, V. 2022. Targeting cholesterol homeostasis in hematopoietic malignancies. *Blood, The Journal of the American Society of Hematology* 139(2), pp. 165-176.

Bronte, V. et al. 2016. Recommendations for myeloid-derived suppressor cell nomenclature and characterization standards. *Nat Commun* 7, p. 12150. doi: 10.1038/ncomms12150

Brown, A. J. et al. 2021. Cholesterol synthesis.*Biochemistry of Lipids, Lipoproteins and Membranes*. pp. 317-355.

Brown, G. et al. 2018. The changing face of hematopoiesis: a spectrum of options is available to stem cells. *Immunol Cell Biol* 96(9), pp. 898-911. doi: 10.1111/imcb.12055

Brown, M. S. and Goldstein, J. L. 1997. The SREBP pathway: regulation of cholesterol metabolism by proteolysis of a membrane-bound transcription factor. *Cell* 89(3), pp. 331-340.

Bruunsgaard, H. et al. 2001. Decreased natural killer cell activity is associated with atherosclerosis in elderly humans. *Experimental gerontology* 37(1), pp. 127-136.

Buchwald, H. 1992. Cholesterol inhibition, cancer, and chemotherapy. *The Lancet* 339(8802), pp. 1154-1156.

Buckley, M. L. and Ramji, D. P. 2015. The influence of dysfunctional signaling and lipid homeostasis in mediating the inflammatory responses during atherosclerosis. *Biochim Biophys Acta* 1852(7), pp. 1498-1510. doi: 10.1016/j.bbadis.2015.04.011

Bunt, S. K. et al. 2006. Inflammation induces myeloid-derived suppressor cells that facilitate tumor progression. *J Immunol* 176(1), pp. 284-290. doi: 10.4049/jimmunol.176.1.284

Burke, L. P. and Kukoly, C. A. 2008. Statins induce lethal effects in acute myeloblastic leukemia [corrected] cells within 72 hours. *Leuk Lymphoma* 49(2), pp. 322-330. doi: 10.1080/10428190701760011

Cabezas-Wallscheid, N. et al. 2014. Identification of regulatory networks in HSCs and their immediate progeny via integrated proteome, transcriptome, and DNA methylome analysis. *Cell Stem Cell* 15(4), pp. 507-522. doi: 10.1016/j.stem.2014.07.005

Cai, Y. et al. 2009. Eto2/MTG16 and MTGR1 are heteromeric corepressors of the TAL1/SCL transcription factor in murine erythroid progenitors. *Biochem Biophys Res Commun* 390(2), pp. 295-301. doi: 10.1016/j.bbrc.2009.09.111

Caiado, F. et al. 2021. Inflammation as a regulator of hematopoietic stem cell function in disease, aging, and clonal selection. *Journal of Experimental Medicine* 218(7), doi: 10.1084/jem.20201541

Cain, D. W. et al. 2011. Inflammation triggers emergency granulopoiesis through a density-dependent feedback mechanism. *PLoS One* 6(5), p. e19957. doi: 10.1371/journal.pone.0019957

Calvi, L. M. and Link, D. C. 2014. Cellular complexity of the bone marrow hematopoietic stem cell niche. *Calcif Tissue Int* 94(1), pp. 112-124. doi: 10.1007/s00223-013-9805-8

Camacho, V. et al. 2021. Inflammatory Cytokines Shape an Altered Immune Response During Myeloid Malignancies. *Front Immunol* 12, p. 772408. doi: 10.3389/fimmu.2021.772408

Campos, G. et al. 2020. Inflammation-associated suppression of metabolic gene networks in acute and chronic liver disease. *Arch Toxicol* 94(1), pp. 205-217. doi: 10.1007/s00204-019-02630-3

Carey, A. et al. 2017. Identification of Interleukin-1 by Functional Screening as a Key Mediator of Cellular Expansion and Disease Progression in Acute Myeloid Leukemia. *Cell Rep* 18(13), pp. 3204-3218. doi: 10.1016/j.celrep.2017.03.018

Carrelha, J. et al. 2018. Hierarchically related lineage-restricted fates of multipotent haematopoietic stem cells. *nature* 554(7690), pp. 106-111. doi: 10.1038/nature25455

Castelli, G. et al. 2018. Targeting histone methyltransferase and demethylase in acute myeloid leukemia therapy. *Onco Targets Ther* 11, pp. 131-155. doi: 10.2147/OTT.S145971

Cenariu, D. et al. 2021. Extramedullary Hematopoiesis of the Liver and Spleen. *J Clin Med* 10(24), doi: 10.3390/jcm10245831

Cesta, M. F. 2006. Normal structure, function, and histology of the spleen. *Toxicol Pathol* 34(5), pp. 455-465. doi: 10.1080/01926230600867743

Challen, G. A. et al. 2009. Mouse hematopoietic stem cell identification and analysis. *Cytometry A* 75(1), pp. 14-24. doi: 10.1002/cyto.a.20674

Chalmin, F. et al. 2010. Membrane-associated Hsp72 from tumor-derived exosomes mediates STAT3-dependent immunosuppressive function of mouse and human myeloid-derived suppressor cells. *J Clin Invest* 120(2), pp. 457-471. doi: 10.1172/JCI40483

Chan, W.-I. et al. 2011. The Transcriptional Coactivator Cbp Regulates Self-Renewal and Differentiation in Adult Hematopoietic Stem Cells. *Molecular and Cellular Biology* 31(24), pp. 5046-5060. doi: 10.1128/mcb.05830-11

Chao, M. et al. eds. 2008. *Establishment of a normal hematopoietic and leukemia stem cell hierarchy*. *Cold Spring Harbor symposia on quantitative biology.* Cold Spring Harbor Laboratory Press.

Chen, B.-R. et al. 2021. A JAK/STAT-mediated inflammatory signaling cascade drives oncogenesis in AF10-rearranged AML. *Blood* 137(24), pp. 3403-3415.

Chen, F. et al. 2017. Oxidative Stress in Stem Cell Aging. *Cell Transplant* 26(9), pp. 1483-1495. doi: 10.1177/0963689717735407

Chen, M. J. et al. 2009. Runx1 is required for the endothelial to haematopoietic cell transition but not thereafter. *nature* 457(7231), pp. 887-891. doi: 10.1038/nature07619

Chen, W. et al. 2008. Malignant transformation initiated by Mll-AF9: gene dosage and critical target cells. *Cancer Cell* 13(5), pp. 432-440.

Cheng, T. et al. 2000a. Stem cell repopulation efficiency but not pool size is governed by p27kip1. *Nature medicine* 6(11), pp. 1235-1240.

Cheng, T. et al. 2000b. Hematopoietic stem cell quiescence maintained by p21cip1/waf1. *Science* 287(5459), pp. 1804-1808.

Cheshier, S. H. et al. 1999. In vivo proliferation and cell cycle kinetics of long-term self-renewing hematopoietic stem cells. *Proceedings of the National Academy of Sciences* 96(6), pp. 3120-3125.

Cheson, B. D. et al. 1990. Report of the National Cancer Institute-sponsored workshop on definitions of diagnosis and response in acute myeloid leukemia. *Journal of Clinical Oncology* 8(5), pp. 813-819.

Chiarella, E. et al. 2022. Targeting of Mevalonate-Isoprenoid Pathway in Acute Myeloid Leukemia Cells by Bisphosphonate Drugs. *Biomedicines* 10(5), doi: 10.3390/biomedicines10051146

Chistiakov, D. A. et al. 2018. The role of monocytosis and neutrophilia in atherosclerosis. *J Cell Mol Med* 22(3), pp. 1366-1382. doi: 10.1111/jcmm.13462

Christ, A. et al. 2018. Western Diet Triggers NLRP3-Dependent Innate Immune Reprogramming. *Cell* 172(1-2), pp. 162-175 e114. doi: 10.1016/j.cell.2017.12.013

Christensen, J. L. et al. 2004. Circulation and chemotaxis of fetal hematopoietic stem cells. *PLoS Biol* 2(3), p. E75. doi: 10.1371/journal.pbio.0020075

Clements, W. K. and Traver, D. 2013. Signalling pathways that control vertebrate haematopoietic stem cell specification. *Nat Rev Immunol* 13(5), pp. 336-348. doi: 10.1038/nri3443

Collins, C. T. and Hess, J. L. 2016. Deregulation of the HOXA9/MEIS1 axis in acute leukemia. *Curr Opin Hematol* 23(4), pp. 354-361. doi: 10.1097/MOH.0000000000000245

Collins, S. J. 2008. Retinoic acid receptors, hematopoiesis and leukemogenesis. *Current opinion in hematology* 15(4), pp. 346-351.

Combadiere, C. et al. 2008. Combined inhibition of CCL2, CX3CR1, and CCR5 abrogates Ly6C(hi) and Ly6C(lo) monocytosis and almost abolishes atherosclerosis in hypercholesterolemic mice. *Circulation* 117(13), pp. 1649-1657. doi: 10.1161/CIRCULATIONAHA.107.745091

Condamine, T. and Gabrilovich, D. I. 2011. Molecular mechanisms regulating myeloid-derived suppressor cell differentiation and function. *Trends Immunol* 32(1), pp. 19-25. doi: 10.1016/j.it.2010.10.002

Copley, M. R. et al. 2012. Hematopoietic stem cell heterogeneity takes center stage. *Cell Stem Cell* 10(6), pp. 690-697. doi: 10.1016/j.stem.2012.05.006

Cozzio, A. et al. 2003. Similar MLL-associated leukemias arising from self-renewing stem cells and short-lived myeloid progenitors. *Genes Dev* 17(24), pp. 3029-3035. doi: 10.1101/gad.1143403

Cronkite, D. A. and Strutt, T. M. 2018. The Regulation of Inflammation by Innate and Adaptive Lymphocytes. *J Immunol Res* 2018, p. 1467538. doi: 10.1155/2018/1467538

Crowther, M. A. 2005. Pathogenesis of atherosclerosis. *ASH Education Program Book* 2005(1), pp. 436-441.

Crysandt, M. et al. 2016. A high BMI is a risk factor in younger patients with de novo acute myelogenous leukemia. *Eur J Haematol* 97(1), pp. 17-24. doi: 10.1111/ejh.12675

Cuff, C. A. et al. 2001. The adhesion receptor CD44 promotes atherosclerosis by mediating inflammatory cell recruitment and vascular cell activation. *Journal of Clinical Investigation* 108(7), pp. 1031-1040. doi: 10.1172/jci200112455

Dai, X. et al. 2018. The Pivotal Role of Thymus in Atherosclerosis Mediated by Immune and Inflammatory Response. *Int J Med Sci* 15(13), pp. 1555-1563. doi: 10.7150/ijms.27238

Davidson, E. H. 2010. Emerging properties of animal gene regulatory networks. *nature* 468(7326), pp. 911-920. doi: 10.1038/nature09645

de Boer, R. A. et al. 2019. Cancer and heart disease: associations and relations. *Eur J Heart Fail* 21(12), pp. 1515-1525. doi: 10.1002/ejhf.1539

Delgado, M. D. and Leon, J. 2010. Myc roles in hematopoiesis and leukemia. *Genes Cancer* 1(6), pp. 605-616. doi: 10.1177/1947601910377495

Delogu, A. et al. 2006. Gene repression by Pax5 in B cells is essential for blood cell homeostasis and is reversed in plasma cells. *Immunity* 24(3), pp. 269-281. doi: 10.1016/j.immuni.2006.01.012

Deschler, B. and Lubbert, M. 2006. Acute myeloid leukemia: epidemiology and etiology. *Cancer* 107(9), pp. 2099-2107. doi: 10.1002/cncr.22233

Diaz-Montero, C. M. et al. 2009. Increased circulating myeloid-derived suppressor cells correlate with clinical cancer stage, metastatic tumor burden, and doxorubicin-cyclophosphamide chemotherapy. *Cancer Immunol Immunother* 58(1), pp. 49-59. doi: 10.1007/s00262-008-0523-4

Ding, L. and Morrison, S. J. 2013. Haematopoietic stem cells and early lymphoid progenitors occupy distinct bone marrow niches. *nature* 495(7440), pp. 231-235. doi: 10.1038/nature11885

Ding, L. et al. 2012. Endothelial and perivascular cells maintain haematopoietic stem cells. *nature* 481(7382), pp. 457-462. doi: 10.1038/nature10783

Ding, X. et al. 2019. The role of cholesterol metabolism in cancer. *American journal of cancer research* 9(2), p. 219.

Doulatov, S. et al. 2010. Revised map of the human progenitor hierarchy shows the origin of macrophages and dendritic cells in early lymphoid development. *Nat Immunol* 11(7), pp. 585-593. doi: 10.1038/ni.1889

Drechsler, M. et al. 2010. Hyperlipidemia-triggered neutrophilia promotes early atherosclerosis. *Circulation* 122(18), pp. 1837-1845. doi: 10.1161/CIRCULATIONAHA.110.961714

Drexler, H. G. et al. 2004. Malignant hematopoietic cell lines: in vitro models for the study of MLL gene alterations. *Leukemia* 18(2), pp. 227-232. doi: 10.1038/sj.leu.2403236

Dunn, G. P. et al. 2004. The three Es of cancer immunoediting. *Annu Rev Immunol* 22, pp. 329-360. doi: 10.1146/annurev.immunol.22.012703.104803

Dutko, J. A. and Mullins, M. C. 2011. SnapShot: BMP signaling in development. *Cell* 145(4), pp. 636-636. e632.

Dutta, P. et al. 2012. Myocardial infarction accelerates atherosclerosis. *nature* 487(7407), pp. 325-329. doi: 10.1038/nature11260

Dutta, P. et al. 2015. Myocardial Infarction Activates CCR2(+) Hematopoietic Stem and Progenitor Cells. *Cell Stem Cell* 16(5), pp. 477-487. doi: 10.1016/j.stem.2015.04.008

Dykstra, B. et al. 2011. Clonal analysis reveals multiple functional defects of aged murine hematopoietic stem cells. *J Exp Med* 208(13), pp. 2691-2703. doi: 10.1084/jem.20111490

Ehninger, A. and Trumpp, A. 2011. The bone marrow stem cell niche grows up: mesenchymal stem cells and macrophages move in. *J Exp Med* 208(3), pp. 421-428. doi: 10.1084/jem.20110132

Eich, M. et al. 2019. OMIP-059: Identification of Mouse Hematopoietic Stem and Progenitor Cells with Simultaneous Detection of CD45.1/2 and Controllable Green Fluorescent Protein Expression by a Single Staining Panel. *Cytometry A* 95(10), pp. 1049-1052. doi: 10.1002/cyto.a.23845

El-Meligui, Y. M. et al. 2021. Correlation Study on HLA-DR and CD117 (c-Kit) Expressions: Its Prognosis and Treatment Response in Acute Myeloid Leukemia Patients. *Pharmgenomics Pers Med* 14, pp. 381-393. doi: 10.2147/PGPM.S268986

Eladl, E. et al. 2020. Role of CD47 in Hematological Malignancies. *J Hematol Oncol* 13(1), p. 96. doi: 10.1186/s13045-020-00930-1

Emini Veseli, B. et al. 2017. Animal models of atherosclerosis. *Eur J Pharmacol* 816, pp. 3-13. doi: 10.1016/j.ejphar.2017.05.010

Esser, V. et al. 1988. Mutational analysis of the ligand binding domain of the low density lipoprotein receptor. *Journal of Biological Chemistry* 263(26), pp. 13282-13290.

Estefa, J. et al. 2021. New light shed on the early evolution of limb-bone growth plate and bone marrow. *Elife* 10, doi: 10.7554/eLife.51581

Estey, E. and Dohner, H. 2006. Acute myeloid leukaemia. *Lancet* 368(9550), pp. 1894-1907. doi: 10.1016/S0140-6736(06)69780-8

Ezoe, S. et al. 2014. Cell Cycle Regulation in Hematopoietic Stem/Progenitor Cells. *Cell Cycle* 3(3), pp. 312-316. doi: 10.4161/cc.3.3.710

Farge, T. et al. 2017. Chemotherapy-Resistant Human Acute Myeloid Leukemia Cells Are Not Enriched for Leukemic Stem Cells but Require Oxidative Metabolism. *Cancer Discov* 7(7), pp. 716-735. doi: 10.1158/2159-8290.CD-16-0441

Fazio, S. et al. 1997. Leukocyte low density lipoprotein receptor (LDL-R) does not contribute to LDL clearance in vivo: bone marrow transplantation studies in the mouse. *Journal of lipid research* 38(2), pp. 391-400.

Feng, Y. et al. 2012. Hematopoietic stem/progenitor cell proliferation and differentiation is differentially regulated by high-density and low-density lipoproteins in mice. *PLoS One* 7(11), p. e47286. doi: 10.1371/journal.pone.0047286

Fernandez, C. et al. 2004. Cholesterol is essential for mitosis progression and its deficiency induces polyploid cell formation. *Exp Cell Res* 300(1), pp. 109-120. doi: 10.1016/j.yexcr.2004.06.029

Fernandez-Garcia, V. et al. 2020. Contribution of Extramedullary Hematopoiesis to Atherosclerosis. The Spleen as a Neglected Hub of Inflammatory Cells. *Front Immunol* 11, p. 586527. doi: 10.3389/fimmu.2020.586527

Ferrara, F. and Schiffer, C. A. 2013. Acute myeloid leukaemia in adults. *Lancet* 381(9865), pp. 484-495. doi: 10.1016/S0140-6736(12)61727-9

Floeth, M. et al. 2021. Low-density lipoprotein receptor (LDLR) is an independent adverse prognostic factor in acute myeloid leukaemia. *Br J Haematol* 192(3), pp. 494-503. doi: 10.1111/bjh.16853

Foks, A. C. et al. 2016. CD11b+Gr-1+ myeloid-derived suppressor cells reduce atherosclerotic lesion development in LDLr deficient mice. *Cardiovasc Res* 111(3), pp. 252-261. doi: 10.1093/cvr/cvw114

Fraser, S. T. et al. 2007. Maturation and enucleation of primitive erythroblasts during mouse embryogenesis is accompanied by changes in cell-surface antigen expression. *Blood* 109(1), pp. 343-352. doi: 10.1182/blood-2006-03-006569

Friedrich, K. et al. 2019. Perturbation of the Monocyte Compartment in Human Obesity. *Front Immunol* 10, p. 1874. doi: 10.3389/fimmu.2019.01874

Friesen, J. A. and Rodwell, V. W. 2004. The 3-hydroxy-3-methylglutaryl coenzyme-A (HMG-CoA) reductases. *Genome biology* 5(11), pp. 1-7.

Fujino, T. et al. 2001. Inhibition of myeloid differentiation by Hoxa9, Hoxb8, and Meis homeobox genes. *Experimental hematology* 29(7), pp. 856-863.

Fujiwara, Y. et al. 1996. Arrested development of embryonic red cell precursors in mouse embryos lacking transcription factor GATA-1. *Proceedings of the National Academy of Sciences* 93(22), pp. 12355-12358.

Gabrilovich, D. I. et al. 2007. The terminology issue for myeloid-derived suppressor cells. *Cancer Res* 67(1), p. 425; author reply 426. doi: 10.1158/0008-5472.CAN-06-3037

Galan-Caridad, J. M. et al. 2007. Zfx controls the self-renewal of embryonic and hematopoietic stem cells. *Cell* 129(2), pp. 345-357. doi: 10.1016/j.cell.2007.03.014

Galy, A. et al. 1995. Human T, B, natural killer, and dendritic cells arise from a common bone marrow progenitor cell subset. *Immunity* 3(4), pp. 459-473.

Garcia-Maurino, S. M. et al. 2017. RNA Binding Protein Regulation and Cross-Talk in the Control of AU-rich mRNA Fate. *Front Mol Biosci* 4, p. 71. doi: 10.3389/fmolb.2017.00071

Geiger, H. et al. 2013. The ageing haematopoietic stem cell compartment. *Nat Rev Immunol* 13(5), pp. 376-389. doi: 10.1038/nri3433

Geissmann, F. et al. 2010. Development of monocytes, macrophages, and dendritic cells. *Science* 327(5966), pp. 656-661. doi: 10.1126/science.1178331

Gekas, C. et al. 2005. The placenta is a niche for hematopoietic stem cells. *Dev Cell* 8(3), pp. 365-375. doi: 10.1016/j.devcel.2004.12.016

Gencer, S. et al. 2021. Inflammatory Chemokines in Atherosclerosis. *Cells* 10(2), doi: 10.3390/cells10020226

Gent, J. and Braakman, I. 2004. Low-density lipoprotein receptor structure and folding. *Cell Mol Life Sci* 61(19-20), pp. 2461-2470. doi: 10.1007/s00018-004-4090-3

Georgopoulos, K. et al. 1994. The Ikaros gene is required for the development of all lymphoid lineages. *Cell* 79(1), pp. 143-156.

Getz, G. S. and Reardon, C. A. 2006. Diet and murine atherosclerosis. *Arterioscler Thromb Vasc Biol* 26(2), pp. 242-249. doi: 10.1161/01.ATV.0000201071.49029.17

Getz, G. S. and Reardon, C. A. 2017. Natural killer T cells in atherosclerosis. *Nat Rev Cardiol* 14(5), pp. 304-314. doi: 10.1038/nrcardio.2017.2

Getz, G. S. et al. 2011. Natural killer T cells in lipoprotein metabolism and atherosclerosis. *Thromb Haemost* 106(5), pp. 814-819. doi: 10.1160/TH11-05-0336

Ghisi, M. et al. 2016. Id2 and E Proteins Orchestrate the Initiation and Maintenance of MLL-Rearranged Acute Myeloid Leukemia. *Cancer Cell* 30(1), pp. 59-74. doi: 10.1016/j.ccell.2016.05.019

Giacinti, C. and Giordano, A. 2006. RB and cell cycle progression. *Oncogene* 25(38), pp. 5220-5227. doi: 10.1038/sj.onc.1209615

Gidding, S. S. and Allen, N. B. 2019. Cholesterol and Atherosclerotic Cardiovascular Disease: A Lifelong Problem. *J Am Heart Assoc* 8(11), p. e012924. doi: 10.1161/JAHA.119.012924

Glass, C. K. and Witztum, J. L. 2001. Atherosclerosis: the road ahead. *Cell* 104(4), pp. 503-516.

Goardon, N. et al. 2006. ETO2 coordinates cellular proliferation and differentiation during erythropoiesis. *EMBO J* 25(2), pp. 357-366. doi: 10.1038/sj.emboj.7600934

Goh, W. and Huntington, N. D. 2017. Regulation of Murine Natural Killer Cell Development. *Front Immunol* 8, p. 130. doi: 10.3389/fimmu.2017.00130

Gold, E. S. et al. 2014. 25-Hydroxycholesterol acts as an amplifier of inflammatory signaling. *Proc Natl Acad Sci U S A* 111(29), pp. 10666-10671. doi: 10.1073/pnas.1404271111

Goldstein, J. L. and Brown, M. S. 1985. The LDL receptor and the regulation of cellular cholesterol metabolism. *Journal of cell science* 1985(Supplement_3), pp. 131-137.

Goldstein, J. L. and Brown, M. S. 2009. The LDL receptor. *Arterioscler Thromb Vasc Biol* 29(4), pp. 431-438. doi: 10.1161/ATVBAHA.108.179564

Goldstein, J. L. and Brown, M. S. 2015. A century of cholesterol and coronaries: from plaques to genes to statins. *Cell* 161(1), pp. 161-172. doi: 10.1016/j.cell.2015.01.036

Golub, R. and Cumano, A. 2013. Embryonic hematopoiesis. *Blood Cells Mol Dis* 51(4), pp. 226-231. doi: 10.1016/j.bcmd.2013.08.004

Gomes, A. L. et al. 2010. Hypercholesterolemia promotes bone marrow cell mobilization by perturbing the SDF-1:CXCR4 axis. *Blood* 115(19), pp. 3886-3894. doi: 10.1182/blood-2009-08-240580

Gonzalez, H. et al. 2018. Roles of the immune system in cancer: from tumor initiation to metastatic progression. *Genes & development* 32(19-20), pp. 1267-1284.

Grivennikov, S. I. et al. 2010. Immunity, inflammation, and cancer. *Cell* 140(6), pp. 883-899. doi: 10.1016/j.cell.2010.01.025

Guo, L. et al. 2017a. Optimizing conditions for calcium phosphate mediated transient transfection. *Saudi J Biol Sci* 24(3), pp. 622-629. doi: 10.1016/j.sjbs.2017.01.034

Guo, X. et al. 2017b. Lipid-dependent conformational dynamics underlie the functional versatility of T-cell receptor. *Cell Res* 27(4), pp. 505-525. doi: 10.1038/cr.2017.42

Ha, N. T. and Lee, C. H. 2020. Roles of Farnesyl-Diphosphate Farnesyltransferase 1 in Tumour and Tumour Microenvironments. *Cells* 9(11), doi: 10.3390/cells9112352

Haeckel, E. 1868. *Natürliche Schöpfungsgeschichte: Gemeinverständliche wissenschaftliche Vorträge über die Entwickelungslehre im Allgemeinen und diejenige von Darwin, Göthe und Lamarck im Besonderen, über die Anwendung derselben auf den Ursprung des Menschen und andern damit zusammenhängende Gründfragen der Natur-Wissenschaft. Mit Tafeln, Holzschnitten, systematischen und genealogischen Tabellen*. Reimer.

Han, X. et al. 2010. Interleukin-10 overexpression in macrophages suppresses atherosclerosis in hyperlipidemic mice. *FASEB J* 24(8), pp. 2869-2880. doi: 10.1096/fj.09-148155

Han, Z. et al. 2021. Relative Quantification of NaV1. 1 Protein in Mouse Brains Using a Meso Scale Discovery-Electrochemiluminescence (MSD-ECL) Method. *Bio-protocol* 11(3), pp. e3910-e3910.

Hanahan, D. and Weinberg, R. A. 2011. Hallmarks of cancer: the next generation. *Cell* 144(5), pp. 646-674. doi: 10.1016/j.cell.2011.02.013

Hardy, L. M. et al. 2017. Critical Role of the Human ATP-Binding Cassette G1 Transporter in Cardiometabolic Diseases. *Int J Mol Sci* 18(9), doi: 10.3390/ijms18091892

Harslof, M. et al. 2021. Low High-Density Lipoprotein Cholesterol and High White Blood Cell Counts: A Mendelian Randomization Study. *Arterioscler Thromb Vasc Biol* 41(2), pp. 976-987. doi: 10.1161/ATVBAHA.120.314983

Hartwell, K. A. et al. 2013. Niche-based screening identifies small-molecule inhibitors of leukemia stem cells. *Nat Chem Biol* 9(12), pp. 840-848. doi: 10.1038/nchembio.1367

Hasegawa, K. et al. 2015. An Immunocompetent Mouse Model for MLL/AF9 Leukemia Reveals the Potential of Spontaneous Cytotoxic T-Cell Response to an Antigen Expressed in Leukemia Cells. *PLoS One* 10(12), p. e0144594. doi: 10.1371/journal.pone.0144594

Haybar, H. et al. 2019. Clonal hematopoiesis: Genes and underlying mechanisms in cardiovascular disease development. *J Cell Physiol* 234(6), pp. 8396-8401. doi: 10.1002/jcp.27752

Heidt, T. et al. 2014. Chronic variable stress activates hematopoietic stem cells. *Nat Med* 20(7), pp. 754-758. doi: 10.1038/nm.3589

Herbert, K. E. et al. 2008. The use of experimental murine models to assess novel agents of hematopoietic stem and progenitor cell mobilization. *Biol Blood Marrow Transplant* 14(6), pp. 603-621. doi: 10.1016/j.bbmt.2008.02.003

Herijgers, N. et al. 1997. Effect of bone marrow transplantation on lipoprotein metabolism and atherosclerosis in LDL receptor–knockout mice. *Arteriosclerosis, Thrombosis, and Vascular Biology* 17(10), pp. 1995-2003.

Hermetet, F. et al. 2019. High-fat diet disturbs lipid raft/TGF-beta signaling-mediated maintenance of hematopoietic stem cells in mouse bone marrow. *Nat Commun* 10(1), p. 523. doi: 10.1038/s41467-018-08228-0

Hermetet, F. et al. 2020. High-fat diet intensifies MLL-AF9-induced acute myeloid leukemia through activation of the FLT3 signaling in mouse primitive hematopoietic cells. *Sci Rep* 10(1), p. 16187. doi: 10.1038/s41598-020-73020-4

Herviou, L. et al. 2016. EZH2 in normal hematopoiesis and hematological malignancies. *Oncotarget* 7(3), p. 2284.

Hey, Y. Y. et al. 2015. Redefining Myeloid Cell Subsets in Murine Spleen. *Front Immunol* 6, p. 652. doi: 10.3389/fimmu.2015.00652

Heyde, A. et al. 2021. Increased stem cell proliferation in atherosclerosis accelerates clonal hematopoiesis. *Cell* 184(5), pp. 1348-1361 e1322. doi: 10.1016/j.cell.2021.01.049

Hidalgo, A. et al. 2007. Complete identification of E-selectin ligands on neutrophils reveals distinct functions of PSGL-1, ESL-1, and CD44. *Immunity* 26(4), pp. 477-489. doi: 10.1016/j.immuni.2007.03.011

Hindler, K. et al. 2006. The role of statins in cancer therapy. *The oncologist* 11(3), pp. 306-315.

Ho, A. and Dowdy, S. F. 2002. Regulation of G1 cell-cycle progression by oncogenes and tumor suppressor genes. *Current opinion in genetics & development* 12(1), pp. 47-52.

Ho, Y. et al. 1978. Low-density lipoprotein (LDL) receptor activity in human acute myelogenous leukemia cells. *Blood* 52(6), pp. 1099-1112.

Hock, H. and Shimamura, A. 2017. ETV6 in hematopoiesis and leukemia predisposition. *Semin Hematol* 54(2), pp. 98-104. doi: 10.1053/j.seminhematol.2017.04.005

Hodson, D. J. et al. 2019. RNA-binding proteins in hematopoiesis and hematological malignancy. *Blood, The Journal of the American Society of Hematology* 133(22), pp. 2365-2373.

Hoeffel, G. and Ginhoux, F. 2018. Fetal monocytes and the origins of tissue-resident macrophages. *Cell Immunol* 330, pp. 5-15. doi: 10.1016/j.cellimm.2018.01.001

Hoffbrand, A. V. and Moss, P. A. 2011. *Essential haematology*. John Wiley & Sons.

Hoffman, B. et al. 2002. The proto-oncogene c-myc in hematopoietic development and leukemogenesis. *Oncogene* 21(21), pp. 3414-3421.

Hole, P. S. et al. 2013. Overproduction of NOX-derived ROS in AML promotes proliferation and is associated with defective oxidative stress signaling. *Blood* 122(19), pp. 3322-3330. doi: 10.1182/blood-2013-04-491944

Holmes, C. and Stanford, W. L. 2007. Concise review: stem cell antigen-1: expression, function, and enigma. *Stem Cells* 25(6), pp. 1339-1347.

Holvoet, P. et al. 2008. Oxidized LDL and the metabolic syndrome. *Future Lipidol* 3(6), pp. 637-649. doi: 10.2217/17460875.3.6.637

Huang, B. et al. 2020. Cholesterol metabolism in cancer: mechanisms and therapeutic opportunities. *Nat Metab* 2(2), pp. 132-141. doi: 10.1038/s42255-020-0174-0

Huang, H. and Cantor, A. B. 2009. Common features of megakaryocytes and hematopoietic stem cells: what's the connection? *J Cell Biochem* 107(5), pp. 857-864. doi: 10.1002/jcb.22184

Huang, J. et al. 2022a. Role of CD47 in tumor immunity: a potential target for combination therapy. *Sci Rep* 12(1), p. 9803. doi: 10.1038/s41598-022-13764-3

Huang, S. et al. 2010. Mechanism of LDL binding and release probed by structure-based mutagenesis of the LDL receptor. *J Lipid Res* 51(2), pp. 297-308. doi: 10.1194/jlr.M000422

Huang, X. et al. 2022b. A novel ferroptosis-related gene signature can predict prognosis and influence immune microenvironment in acute myeloid leukemia. *Bosn J Basic Med Sci* 22(4), pp. 608-628. doi: 10.17305/bjbms.2021.6274

Huilgol, D. et al. 2019. Transcription Factors That Govern Development and Disease: An Achilles Heel in Cancer. *Genes (Basel)* 10(10), doi: 10.3390/genes10100794

Huszar, D. et al. 2000. Increased LDL Cholesterol and Atherosclerosis in LDL Receptor–Deficient Mice With Attenuated Expression of Scavenger Receptor B1. *Arteriosclerosis, Thrombosis, and Vascular Biology* 20, pp. 1068-1073.

Hyun, K. et al. 2017. Writing, erasing and reading histone lysine methylations. *Exp Mol Med* 49(4), p. e324. doi: 10.1038/emm.2017.11

Ishibashi, S. et al. 1993. Hypercholesterolemia in low density lipoprotein receptor knockout mice and its reversal by adenovirus-mediated gene delivery. *The Journal of clinical investigation* 92(2), pp. 883-893.

Ishibashi, S. et al. 1994. Massive Xanthomatosis and Atherosclerosis in Cholesterol-fed Low Density Lipoprotein Receptor-negative Mice. *the amirican society for clinical investigation* 93, pp. 1885-1893.

Iwasaki, H. and Akashi, K. 2007. Myeloid lineage commitment from the hematopoietic stem cell. *Immunity* 26(6), pp. 726-740. doi: 10.1016/j.immuni.2007.06.004

Iwasaki, H. et al. 2005. Distinctive and indispensable roles of PU.1 in maintenance of hematopoietic stem cells and their differentiation. *Blood* 106(5), pp. 1590-1600. doi: 10.1182/blood-2005-03-0860

Jagannathan-Bogdan, M. and Zon, L. I. 2013. Hematopoiesis. *Development* 140(12), pp. 2463-2467. doi: 10.1242/dev.083147

Jaiswal, S. and Ebert, B. L. 2019. Clonal hematopoiesis in human aging and disease. *Science* 366(6465), doi: 10.1126/science.aan4673

Jaiswal, S. et al. 2017. Clonal Hematopoiesis and Risk of Atherosclerotic Cardiovascular Disease. *N Engl J Med* 377(2), pp. 111-121. doi: 10.1056/NEJMoa1701719

Jang, Y. Y. and Sharkis, S. J. 2007. A low level of reactive oxygen species selects for primitive hematopoietic stem cells that may reside in the low-oxygenic niche. *Blood* 110(8), pp. 3056-3063. doi: 10.1182/blood-2007-05-087759

Janowski, B. A. et al. 1996. An oxysterol signalling pathway mediated by the nuclear receptor LXRα. *nature* 383(6602), pp. 728-731.

Jin, L. et al. 2006. Targeting of CD44 eradicates human acute myeloid leukemic stem cells. *Nat Med* 12(10), pp. 1167-1174. doi: 10.1038/nm1483

Johansen, S. et al. 2018. The Possible Importance of beta3 Integrins for Leukemogenesis and Chemoresistance in Acute Myeloid Leukemia. *Int J Mol Sci* 19(1), doi: 10.3390/ijms19010251

Jordan, C. T. 2007. The leukemic stem cell. *Best practice & research Clinical haematology* 20(1), pp. 13-18.

Jude, C. D. et al. 2007. Unique and independent roles for MLL in adult hematopoietic stem cells and progenitors. *Cell Stem Cell* 1(3), pp. 324-337. doi: 10.1016/j.stem.2007.05.019

Kadomatsu, T. and Oike, Y. 2019. Roles of angiopoietin-like proteins in regulation of stem cell activity. *J Biochem* 165(4), pp. 309-315. doi: 10.1093/jb/mvz005

Kanaoka, Y. and Urade, Y. 2003. Hematopoietic prostaglandin D synthase. *Prostaglandins Leukot Essent Fatty Acids* 69(2-3), pp. 163-167. doi: 10.1016/s0952-3278(03)00077-2

Kandi, V. and Vadakedath, S. 2015. Effect of DNA Methylation in Various Diseases and the Probable Protective Role of Nutrition: A Mini-Review. *Cureus* 7(8), p. e309. doi: 10.7759/cureus.309

Kansal, R. 2016. Acute myeloid leukemia in the era of precision medicine: recent advances in diagnostic classification and risk stratification. *Cancer Biol Med* 13(1), pp. 41-54. doi: 10.28092/j.issn.2095-3941.2016.0001

Kantarjian, H. et al. 2021. Acute myeloid leukemia: current progress and future directions. *Blood Cancer J* 11(2), p. 41. doi: 10.1038/s41408-021-00425-3

Kaperonis, E. A. et al. 2006. Inflammation and atherosclerosis. *Eur J Vasc Endovasc Surg* 31(4), pp. 386-393. doi: 10.1016/j.ejvs.2005.11.001

Karsunky, H. et al. 2008. Flk2+ common lymphoid progenitors possess equivalent differentiation potential for the B and T lineages. *Blood* 111(12), pp. 5562-5570. doi: 10.1182/blood-2007-11-126219

Kato, Y. et al. 1986. Establishment of peroxidase positive, human monocytic leukemia cell line (NOMO-1) and its characteristics. *Acta Haematol Jpn* 49, p. 277.

Kempe, S. et al. 2005. NF-kappaB controls the global pro-inflammatory response in endothelial cells: evidence for the regulation of a pro-atherogenic program. *Nucleic Acids Res* 33(16), pp. 5308-5319. doi: 10.1093/nar/gki836

Kestenbaum, B. et al. 2022. Clonal Hematopoiesis of Indeterminate Potential and Kidney Function Decline in the General Population. *Am J Kidney Dis*, doi: 10.1053/j.ajkd.2022.08.014

Keyhani, A. et al. 2000. Increased CD38 expression is associated with favorable prognosis in adult acute leukemia. *Leukemia research* 24(2), pp. 153-159.

Khaldoyanidi, S. K. et al. 2022. Leukemic stem cells as a target for eliminating acute myeloid leukemia: Gaps in translational research. *Crit Rev Oncol Hematol* 175, p. 103710. doi: 10.1016/j.critrevonc.2022.103710

Khaled, S. et al. 2016. Acute myeloid leukemia: biologic, prognostic, and therapeutic insights. *Oncology* 30(4), pp. 318-318.

Khanna-Gupta, A. 2011. Regulation and deregulation of mRNA translation during myeloid maturation. *Exp Hematol* 39(2), pp. 133-141. doi: 10.1016/j.exphem.2010.10.011

Khatri, R. et al. 2016. Reactive Oxygen Species Limit the Ability of Bone Marrow Stromal Cells to Support Hematopoietic Reconstitution in Aging Mice. *Stem Cells Dev* 25(12), pp. 948-958. doi: 10.1089/scd.2015.0391

Khoury, J. D. et al. 2022. The 5th edition of the World Health Organization Classification of Haematolymphoid Tumours: Myeloid and Histiocytic/Dendritic Neoplasms. *Leukemia* 36(7), pp. 1703-1719. doi: 10.1038/s41375-022-01613-1

Kiel, M. J. et al. 2005. SLAM family receptors distinguish hematopoietic stem and progenitor cells and reveal endothelial niches for stem cells. *Cell* 121(7), pp. 1109-1121.

Kieusseian, A. et al. 2012. Immature hematopoietic stem cells undergo maturation in the fetal liver. *Development* 139(19), pp. 3521-3530. doi: 10.1242/dev.079210

Kim, W. Y. 2019. Therapeutic targeting of lipid synthesis metabolism for selective elimination of cancer stem cells. *Arch Pharm Res* 42(1), pp. 25-39. doi: 10.1007/s12272-018-1098-z

Kimura, S. et al. 1998. Hematopoietic stem cell deficiencies in mice lacking c-Mpl, the receptor for thrombopoietin. *Proceedings of the National Academy of Sciences* 95(3), pp. 1195-1200.

Koch, C. M. et al. 2018. A Beginner's Guide to Analysis of RNA Sequencing Data. *Am J Respir Cell Mol Biol* 59(2), pp. 145-157. doi: 10.1165/rcmb.2017-0430TR

Kondo, M. et al. 1997. Identification of clonogenic common lymphoid progenitors in mouse bone marrow. *Cell* 91(5), pp. 661-672.

Konoplev, S. and Bueso-Ramos, C. E. 2006. Advances in the pathologic diagnosis and biology of acute myeloid leukemia. *Ann Diagn Pathol* 10(1), pp. 39-65. doi: 10.1016/j.anndiagpath.2005.10.001

Kopan, R. and Ilagan, M. X. 2009. The canonical Notch signaling pathway: unfolding the activation mechanism. *Cell* 137(2), pp. 216-233. doi: 10.1016/j.cell.2009.03.045

Kovtonyuk, L. V. et al. 2016. Enhanced thrombopoietin but not G-CSF receptor stimulation induces self-renewing hematopoietic stem cell divisions in vivo. *Blood* 127(25), pp. 3175-3179. doi: 10.1182/blood-2015-09-669929

Krivtsov, A. V. et al. 2013. Cell of origin determines clinically relevant subtypes of MLL-rearranged AML. *Leukemia* 27(4), pp. 852-860. doi: 10.1038/leu.2012.363

Kumaravelu, P. et al. 2002. Quantitative developmental anatomy of definitive haematopoietic stem cells/long-term repopulating units (HSC/RUs): role of the aorta-gonad-mesonephros (AGM) region and the yolk sac in colonisation of the mouse embryonic liver.

Kunisaki, Y. et al. 2013. Arteriolar niches maintain haematopoietic stem cell quiescence. *nature* 502(7473), pp. 637-643. doi: 10.1038/nature12612

Lagunas-Rangel, F. A. et al. 2017. Acute myeloid leukemia—genetic alterations and their clinical prognosis. *International journal of hematology-oncology and stem cell research* 11(4), p. 328.

Lakshmi, S. V. et al. 2009. Oxidative stress in cardiovascular disease.

Lam, K. and Zhang, D.-E. 2012. RUNX1 and RUNX1-ETO: roles in hematopoiesis and leukemogenesis. *Frontiers in bioscience: a journal and virtual library* 17, p. 1120.

Lampreia, F. P. et al. 2017. Notch Signaling in the Regulation of Hematopoietic Stem Cell. *Curr Stem Cell Rep* 3(3), pp. 202-209. doi: 10.1007/s40778-017-0090-8

Lander, A. D. et al. 2012. What does the concept of the stem cell niche really mean today? *BMC biology* 10(1), pp. 1-15.

Lane, S. W. et al. 2009. The leukemic stem cell niche: current concepts and therapeutic opportunities. *Blood* 114(6), pp. 1150-1157. doi: 10.1182/blood-2009-01-202606

Lara, L. et al. 1997. Low density lipoprotein receptor expression and function in human polymorphonuclear leucocytes. *Clinical & Experimental Immunology* 107(1), pp. 205-212.

Larochelle, A. et al. 1996. Identification of primitive human hematopoietic cells capable of repopulating NOD/SCID mouse bone marrow: implications for gene therapy. *Nature medicine* 2(12), pp. 1329-1337.

Lee, J. M. et al. 2018. Obesity alters the long-term fitness of the hematopoietic stem cell compartment through modulation of Gfi1 expression. *J Exp Med* 215(2), pp. 627-644. doi: 10.1084/jem.20170690

Legras, S. et al. 1998. A Strong Expression of CD44-6v Correlates With Shorter Survival of Patients With Acute Myeloid Leukemia. *Blood* 91(9), pp. 3401-3413. doi: 10.1182/blood.V91.9.3401

Li, A. C. and Glass, C. K. 2002. The macrophage foam cell as a target for therapeutic intervention. *Nature medicine* 8(11), pp. 1235-1242.

Li, B. et al. 2017. Inflammation: A Novel Therapeutic Target/Direction in Atherosclerosis. *Curr Pharm Des* 23(8), pp. 1216-1227. doi: 10.2174/1381612822666161230142931

Li, H. and Tsokos, G. C. 2021. Double-negative T cells in autoimmune diseases. *Curr Opin Rheumatol* 33(2), pp. 163-172. doi: 10.1097/BOR.0000000000000778

Li, J. et al. 2016. Hematopoietic Stem Cell Activity Is Regulated by Pten Phosphorylation Through a Niche-Dependent Mechanism. *Stem Cells* 34(8), pp. 2130-2144. doi: 10.1002/stem.2382

Libby, P. 2002. Inflammation in atherosclerosis. *nature* 420(19/26), pp. 868-874.

Libby, P. 2012. Inflammation in atherosclerosis. *Arterioscler Thromb Vasc Biol* 32(9), pp. 2045-2051. doi: 10.1161/ATVBAHA.108.179705

Libby, P. and Ebert, B. L. 2018. CHIP (Clonal Hematopoiesis of Indeterminate Potential): Potent and Newly Recognized Contributor to Cardiovascular Risk. *Circulation* 138(7), pp. 666-668. doi: 10.1161/CIRCULATIONAHA.118.034392

Lichtman, M. A. 2010. Obesity and the risk for a hematological malignancy: leukemia, lymphoma, or myeloma. *Oncologist* 15(10), pp. 1083-1101. doi: 10.1634/theoncologist.2010-0206

Liersch, R. et al. 2014. Prognostic factors for acute myeloid leukaemia in adults--biological significance and clinical use. *Br J Haematol* 165(1), pp. 17-38. doi: 10.1111/bjh.12750

Lim, G. B. 2020. Pro-inflammatory atherogenic role of platelets. *Nature Reviews Cardiology* 17(1), pp. 6-7.

Lin, X. et al. 2015. Heme oxygenase-1 suppresses the apoptosis of acute myeloid leukemia cells via the JNK/c-JUN signaling pathway. *Leuk Res* 39(5), pp. 544-552. doi: 10.1016/j.leukres.2015.02.009

Linton, M. F. and Fazio, S. 2001. Class A scavenger receptors, macrophages, and atherosclerosis. *Current opinion in lipidology* 12(5), pp. 489-495.

Liu, J. et al. 2022. Targeting CD33 for acute myeloid leukemia therapy. *BMC Cancer* 22(1), p. 24. doi: 10.1186/s12885-021-09116-5

Liu, Y. et al. 2020. High IFITM3 expression predicts adverse prognosis in acute myeloid leukemia. *Cancer Gene Ther* 27(1-2), pp. 38-44. doi: 10.1038/s41417-019-0093-y

Loaeza-Reyes, K. J. et al. 2021. An Overview of Glycosylation and its Impact on Cardiovascular Health and Disease. *Front Mol Biosci* 8, p. 751637. doi: 10.3389/fmolb.2021.751637

Long, N. A. et al. 2022. Acute Myeloid Leukemia Stem Cells: Origin, Characteristics, and Clinical Implications. *Stem Cell Rev Rep* 18(4), pp. 1211-1226. doi: 10.1007/s12015-021-10308-6

Love, P. E. and Bhandoola, A. 2011. Signal integration and crosstalk during thymocyte migration and emigration. *Nat Rev Immunol* 11(7), pp. 469-477. doi: 10.1038/nri2989

Lu, Z. et al. 2022. Fine-Tuning of Cholesterol Homeostasis Controls Erythroid Differentiation. *Adv Sci (Weinh)* 9(2), p. e2102669. doi: 10.1002/advs.202102669

Luci, C. et al. 2020. Chronic Inflammation in Non-Alcoholic Steatohepatitis: Molecular Mechanisms and Therapeutic Strategies. *Front Endocrinol (Lausanne)* 11, p. 597648. doi: 10.3389/fendo.2020.597648

Luis, T. C. et al. 2019. Biological implications of clonal hematopoiesis. *Exp Hematol* 77, pp. 1-5. doi: 10.1016/j.exphem.2019.08.004

Lund, G. et al. 2004. DNA methylation polymorphisms precede any histological sign of atherosclerosis in mice lacking apolipoprotein E. *J Biol Chem* 279(28), pp. 29147-29154. doi: 10.1074/jbc.M403618200

Luo, J. et al. 2020. Mechanisms and regulation of cholesterol homeostasis. *Nat Rev Mol Cell Biol* 21(4), pp. 225-245. doi: 10.1038/s41580-019-0190-7

Ma, X. and Feng, Y. 2016. Hypercholesterolemia Tunes Hematopoietic Stem/Progenitor Cells for Inflammation and Atherosclerosis. *Int J Mol Sci* 17(7), doi: 10.3390/ijms17071162

Ma, X. et al. 2010. Diet, lifestyle, and acute myeloid leukemia in the NIH-AARP cohort. *Am J Epidemiol* 171(3), pp. 312-322. doi: 10.1093/aje/kwp371

Ma, Y. et al. 2012. Hyperlipidemia and atherosclerotic lesion development in Ldlr-deficient mice on a long-term high-fat diet. *PLoS One* 7(4), p. e35835. doi: 10.1371/journal.pone.0035835

Mailer, R. K. W. et al. 2017a. Hypercholesterolemia Enhances T Cell Receptor Signaling and Increases the Regulatory T Cell Population. *Sci Rep* 7(1), p. 15655. doi: 10.1038/s41598-017-15546-8

Mailer, R. K. W. et al. 2017b. Hypercholesterolemia Induces Differentiation of Regulatory T Cells in the Liver. *Circ Res* 120(11), pp. 1740-1753. doi: 10.1161/CIRCRESAHA.116.310054

Mana, M. D. et al. 2017. Dietary Regulation of Adult Stem Cells. *Curr Stem Cell Rep* 3(1), pp. 1-8. doi: 10.1007/s40778-017-0072-x

Mantovani, A. and Sica, A. 2010. Macrophages, innate immunity and cancer: balance, tolerance, and diversity. *Curr Opin Immunol* 22(2), pp. 231-237. doi: 10.1016/j.coi.2010.01.009

Manz, M. G. et al. 2002. Prospective isolation of human clonogenic common myeloid progenitors. *Proc Natl Acad Sci U S A* 99(18), pp. 11872-11877. doi: 10.1073/pnas.172384399

Mao, M. et al. 2021. Multifaced roles of PLAC8 in cancer. *Biomark Res* 9(1), p. 73. doi: 10.1186/s40364-021-00329-1

Marchetti, G. et al. 2015. An integrated genomic-transcriptomic approach supports a role for the proto-oncogene BCL3 in atherosclerosis. *Thromb Haemost* 113(3), pp. 655-663. doi: 10.1160/TH14-05-0466

Marnell, C. S. et al. 2021. Clonal hematopoiesis of indeterminate potential (CHIP): Linking somatic mutations, hematopoiesis, chronic inflammation and cardiovascular disease. *J Mol Cell Cardiol* 161, pp. 98-105. doi: 10.1016/j.yjmcc.2021.07.004

Martin, L. A. et al. 2014. Mitochondrial cholesterol: mechanisms of import and effects on mitochondrial function. *Journal of Bioenergetics and Biomembranes* 48(2), pp. 137-151. doi: 10.1007/s10863-014-9592-6

Martina, M. N. et al. 2015. Double negative (DN) alphabeta T cells: misperception and overdue recognition. *Immunol Cell Biol* 93(3), pp. 305-310. doi: 10.1038/icb.2014.99

Marzac, C. et al. 2011. ATP Binding Cassette transporters associated with chemoresistance: transcriptional profiling in extreme cohorts and their prognostic impact in a cohort of 281 acute myeloid leukemia patients. *Haematologica* 96(9), pp. 1293-1301. doi: 10.3324/haematol.2010.031823

Matsumoto, A. et al. 2011. p57 is required for quiescence and maintenance of adult hematopoietic stem cells. *Cell Stem Cell* 9(3), pp. 262-271. doi: 10.1016/j.stem.2011.06.014

Mayle, A. et al. 2013. Flow cytometry analysis of murine hematopoietic stem cells. *Cytometry A* 83(1), pp. 27-37. doi: 10.1002/cyto.a.22093

McGrath, K. E. et al. 2011. A transient definitive erythroid lineage with unique regulation of the beta-globin locus in the mammalian embryo. *Blood* 117(17), pp. 4600-4608. doi: 10.1182/blood-2010-12-325357

McLaren, J. E. et al. 2011. Cytokines, macrophage lipid metabolism and foam cells: implications for cardiovascular disease therapy. *Prog Lipid Res* 50(4), pp. 331-347. doi: 10.1016/j.plipres.2011.04.002

Medzhitov, R. 2008. Origin and physiological roles of inflammation. *nature* 454(7203), pp. 428-435. doi: 10.1038/nature07201

Mehlem, A. et al. 2013. Imaging of neutral lipids by oil red O for analyzing the metabolic status in health and disease. *Nat Protoc* 8(6), pp. 1149-1154. doi: 10.1038/nprot.2013.055

Mehu, M. et al. 2022. Inflammatory Cells in Atherosclerosis. *Antioxidants (Basel)* 11(2), doi: 10.3390/antiox11020233

Mendelson, A. and Frenette, P. S. 2014. Hematopoietic stem cell niche maintenance during homeostasis and regeneration. *Nat Med* 20(8), pp. 833-846. doi: 10.1038/nm.3647

Mendes, S. C. et al. 2005. Mesenchymal progenitor cells localize within hematopoietic sites throughout ontogeny. *Development* 132(5), pp. 1127-1136. doi: 10.1242/dev.01615

Menendez-Gonzalez, J. B. et al. 2019. Gata2 as a Crucial Regulator of Stem Cells in Adult Hematopoiesis and Acute Myeloid Leukemia. *Stem Cell Reports* 13(2), pp. 291-306. doi: 10.1016/j.stemcr.2019.07.005

Mer, A. S. et al. 2021. Biological and therapeutic implications of a unique subtype of NPM1 mutated AML. *Nat Commun* 12(1), p. 1054. doi: 10.1038/s41467-021-21233-0

Mi, S. et al. 2010. Aberrant overexpression and function of the miR-17-92 cluster in MLL-rearranged acute leukemia. *Proc Natl Acad Sci U S A* 107(8), pp. 3710-3715. doi: 10.1073/pnas.0914900107

Michelsen, K. S. and Arditi, M. 2006. Toll-like receptor signaling and atherosclerosis. *Current opinion in hematology* 13(3), pp. 163-168.

Mihaylova, M. M. et al. 2014. Dietary and metabolic control of stem cell function in physiology and cancer. *Cell Stem Cell* 14(3), pp. 292-305. doi: 10.1016/j.stem.2014.02.008

Mikkola, H. K. et al. 2003. Haematopoietic stem cells retain long-term repopulating activity and multipotency in the absence of stem-cell leukaemia SCL/tal-1 gene. *nature* 421(6922), pp. 547-551.

Miller, D. G. 1980. On the nature of susceptibility to cancer. The presidential address. *Cancer* 46(6), pp. 1307-1318.

Miller, M. E. et al. 2016. Meis1 Is Required for Adult Mouse Erythropoiesis, Megakaryopoiesis and Hematopoietic Stem Cell Expansion. *PLoS One* 11(3), p. e0151584. doi: 10.1371/journal.pone.0151584

Miller, P. G. et al. 2013. In Vivo RNAi screening identifies a leukemia-specific dependence on integrin beta 3 signaling. *Cancer Cell* 24(1), pp. 45-58. doi: 10.1016/j.ccr.2013.05.004

Miyawaki, K. et al. 2015. CD41 marks the initial myelo-erythroid lineage specification in adult mouse hematopoiesis: redefinition of murine common myeloid progenitor. *Stem Cells* 33(3), pp. 976-987. doi: 10.1002/stem.1906

Mohanta, S. et al. 2016. Aorta atherosclerosis lesion analysis in hyperlipidemic mice. *Bio-protocol* 6(11), pp. e1833-e1833.

Montes de Oca, M. et al. 2020. Cytokines and splenic remodelling during Leishmania donovani infection. *Cytokine X* 2(4), p. 100036. doi: 10.1016/j.cytox.2020.100036

Mooney, C. J. et al. 2017. Selective Expression of Flt3 within the Mouse Hematopoietic Stem Cell Compartment. *Int J Mol Sci* 18(5), doi: 10.3390/ijms18051037

Moore, R. E. et al. 2003. Apolipoprotein A-I deficiency results in markedly increased atherosclerosis in mice lacking the LDL receptor. *Arterioscler Thromb Vasc Biol* 23(10), pp. 1914-1920. doi: 10.1161/01.ATV.0000092328.66882.F5

Morgan, D. O. 1997. Cyclin-dependent kinases: engines, clocks, and microprocessors. *Annual review of cell and developmental biology* 13, p. 261.

Morita, Y. et al. 2010. Heterogeneity and hierarchy within the most primitive hematopoietic stem cell compartment. *J Exp Med* 207(6), pp. 1173-1182. doi: 10.1084/jem.20091318

Morrison, S. J. and Scadden, D. T. 2014. The bone marrow niche for haematopoietic stem cells. *nature* 505(7483), pp. 327-334. doi: 10.1038/nature12984

Morrison, S. J. et al. 1996. The aging of hematopoietic stem cells. *Nature medicine* 2(9), pp. 1011-1016.

Morrison, S. J. and Weissman, I. L. 1994. The long-term repopulating subset of hematopoietic stem cells is deterministic and isolatable by phenotype. *Immunity* 1(8), pp. 661-673.

Mosig, S. et al. 2008. Monocytes of patients with familial hypercholesterolemia show alterations in cholesterol metabolism. *BMC Med Genomics* 1, p. 60. doi: 10.1186/1755-8794-1-60

Mosquera Orgueira, A. et al. 2021. Personalized Survival Prediction of Patients With Acute Myeloblastic Leukemia Using Gene Expression Profiling. *Front Oncol* 11, p. 657191. doi: 10.3389/fonc.2021.657191

Moss, J. W. and Ramji, D. P. 2016. Cytokines: roles in atherosclerosis disease progression and potential therapeutic targets. *Future medicinal chemistry* 8(11), pp. 1317-1330.

Movahedi, K. et al. 2010. Different tumor microenvironments contain functionally distinct subsets of macrophages derived from Ly6C(high) monocytes. *Cancer Res* 70(14), pp. 5728-5739. doi: 10.1158/0008-5472.CAN-09-4672

Mucunguzi, O. et al. 2017. Identification of the principal transcriptional regulators for low-fat and high-fat meal responsive genes in small intestine. *Nutr Metab (Lond)* 14, p. 66. doi: 10.1186/s12986-017-0221-3

Mukhopadhyay, R. 2013. Mouse models of atherosclerosis: explaining critical roles of lipid metabolism and inflammation. *J Appl Genet* 54(2), pp. 185-192. doi: 10.1007/s13353-013-0134-4

Multhoff, G. et al. 2011. Chronic inflammation in cancer development. *Front Immunol* 2, p. 98. doi: 10.3389/fimmu.2011.00098

Murphy, A. J. et al. 2011. ApoE regulates hematopoietic stem cell proliferation, monocytosis, and monocyte accumulation in atherosclerotic lesions in mice. *J Clin Invest* 121(10), pp. 4138-4149. doi: 10.1172/JCI57559

Murphy, A. J. et al. 2014. Cholesterol efflux pathways regulate myelopoiesis: a potential link to altered macrophage function in atherosclerosis. *Front Immunol* 5, p. 490. doi: 10.3389/fimmu.2014.00490

Murphy, A. J. and Tall, A. R. 2016. Disordered haematopoiesis and athero-thrombosis. *Eur Heart J* 37(14), pp. 1113-1121. doi: 10.1093/eurheartj/ehv718

Murphy, A. J. et al. 2008. High-density lipoprotein reduces the human monocyte inflammatory response. *Arterioscler Thromb Vasc Biol* 28(11), pp. 2071-2077. doi: 10.1161/ATVBAHA.108.168690

Naik, S. et al. 2018. Two to Tango: Dialog between Immunity and Stem Cells in Health and Disease. *Cell* 175(4), pp. 908-920. doi: 10.1016/j.cell.2018.08.071

Nakada, D. et al. 2014. Oestrogen increases haematopoietic stem-cell self-renewal in females and during pregnancy. *nature* 505(7484), pp. 555-558. doi: 10.1038/nature12932

Nakajima-Takagi, Y. et al. 2013. Role of SOX17 in hematopoietic development from human embryonic stem cells. *Blood* 121(3), pp. 447-458. doi: 10.1182/blood-2012-05-431403

Nakamura-Ishizu, A. et al. 2014. The analysis, roles and regulation of quiescence in hematopoietic stem cells. *Development* 141(24), pp. 4656-4666. doi: 10.1242/dev.106575

Natarajan, R. 2011. Drugs targeting epigenetic histone acetylation in vascular smooth muscle cells for restenosis and atherosclerosis. *Arterioscler Thromb Vasc Biol* 31(4), pp. 725-727. doi: 10.1161/ATVBAHA.111.222976

Nerlov, C. et al. 2000. GATA-1 interacts with the myeloid PU.1 transcription factor and represses PU.1-dependent transcription. *Blood* 95(8), pp. 2543-2551. doi: 10.1182/blood.V95.8.2543

Ng, W. L. et al. 2016. Inducible RasGEF1B circular RNA is a positive regulator of ICAM-1 in the TLR4/LPS pathway. *RNA Biol* 13(9), pp. 861-871. doi: 10.1080/15476286.2016.1207036

Nijnik, A. et al. 2007. DNA repair is limiting for haematopoietic stem cells during ageing. *nature* 447(7145), pp. 686-690.

Niu, Y. et al. 2019. BCL3 Expression Is a Potential Prognostic and Predictive Biomarker in Acute Myeloid Leukemia of FAB Subtype M2. *Pathol Oncol Res* 25(2), pp. 541-548. doi: 10.1007/s12253-018-0476-7

Nordestgaard, B. G. et al. 2013. Familial hypercholesterolaemia is underdiagnosed and undertreated in the general population: guidance for clinicians to prevent coronary heart disease: consensus statement of the European Atherosclerosis Society. *Eur Heart J* 34(45), pp. 3478-3490a. doi: 10.1093/eurheartj/eht273

North, T. et al. 1999. Cbfa2 is required for the formation of intra-aortic hematopoietic clusters. *Development* 126(11), pp. 2563-2575.

Notta, F. et al. 2011. Isolation of single human hematopoietic stem cells capable of long-term multilineage engraftment. *Science* 333(6039), pp. 218-221.

Notta, F. et al. 2016. Distinct routes of lineage development reshape the human blood hierarchy across ontogeny. *Science* 351(6269), p. aab2116. doi: 10.1126/science.aab2116

Noy, R. and Pollard, J. W. 2014. Tumor-associated macrophages: from mechanisms to therapy. *Immunity* 41(1), pp. 49-61. doi: 10.1016/j.immuni.2014.06.010

Nygren, J. M. et al. 2006. Prolonged cell cycle transit is a defining and developmentally conserved hemopoietic stem cell property. *J Immunol* 177(1), pp. 201-208. doi: 10.4049/jimmunol.177.1.201

O'Connell, K. E. et al. 2015. Practical murine hematopathology: a comparative review and implications for research. *Comparative medicine* 65(2), pp. 96-113.

Odero, M. D. et al. 2000. Cytogenetic and molecular analysis of the acute monocytic leukemia cell line THP-1 with an MLL-AF9 translocation. *Genes, chromosomes and cancer* 29(4), pp. 333-338.

Oguro, H. 2019. The Roles of Cholesterol and Its Metabolites in Normal and Malignant Hematopoiesis. *Front Endocrinol (Lausanne)* 10, p. 204. doi: 10.3389/fendo.2019.00204

Oguro, H. et al. 2013. SLAM family markers resolve functionally distinct subpopulations of hematopoietic stem cells and multipotent progenitors. *Cell Stem Cell* 13(1), pp. 102-116. doi: 10.1016/j.stem.2013.05.014

Oguro, H. et al. 2017. 27-Hydroxycholesterol induces hematopoietic stem cell mobilization and extramedullary hematopoiesis during pregnancy. *J Clin Invest* 127(9), pp. 3392-3401. doi: 10.1172/JCI94027

Ohta, H. et al. 2002. Polycomb group gene rae28 is required for sustaining activity of hematopoietic stem cells. *The Journal of experimental medicine* 195(6), pp. 759-770.

Organization, W. H. 2011. *Global status report on noncommunicable diseases 2010*. World Health Organization.

Orkin, S. H. 2000. Diversification of haematopoietic stem cells to specific lineages *Nature* 1, pp. 57-64.

Orkin, S. H. and Zon, L. I. 2008. Hematopoiesis: an evolving paradigm for stem cell biology. *Cell* 132(4), pp. 631-644. doi: 10.1016/j.cell.2008.01.025

Orso, E. et al. 2006. Ezetimib influences the expression of raft-associated antigens in human monocytes. *Cytometry A* 69(3), pp. 206-208. doi: 10.1002/cyto.a.20229

Osawa, M. et al. 1996. Long-term lymphohematopoietic reconstitution by a single CD34-low/negative hematopoietic stem cell. *Science* 273(5272), pp. 242-245.

Ostrand-Rosenberg, S. and Fenselau, C. 2018. Myeloid-Derived Suppressor Cells: Immune-Suppressive Cells That Impair Antitumor Immunity and Are Sculpted by Their Environment. *J Immunol* 200(2), pp. 422-431. doi: 10.4049/jimmunol.1701019

Ottersbach, K. et al. 2010. Ontogeny of haematopoiesis: recent advances and open questions. *Br J Haematol* 148(3), pp. 343-355. doi: 10.1111/j.1365-2141.2009.07953.x

Palis, J. 2016. Hematopoietic stem cell-independent hematopoiesis: emergence of erythroid, megakaryocyte, and myeloid potential in the mammalian embryo. *FEBS Lett* 590(22), pp. 3965-3974. doi: 10.1002/1873-3468.12459

Palis, J. et al. 1999. Development of erythroid and myeloid progenitors in the yolk sac and embryo proper of the mouse. *Development* 126(22), pp. 5073-5084.

Pant, V. et al. 2012. The p53 pathway in hematopoiesis: lessons from mouse models, implications for humans. *Blood* 120(26), pp. 5118-5127. doi: 10.1182/blood-2012-05-356014

Papa, L. et al. 2019. Mitochondrial Role in Stemness and Differentiation of Hematopoietic Stem Cells. *Stem Cells Int* 2019, p. 4067162. doi: 10.1155/2019/4067162

Papa, V. et al. 2020. Translating Evidence from Clonal Hematopoiesis to Cardiovascular Disease: A Systematic Review. *J Clin Med* 9(8), doi: 10.3390/jcm9082480

Papaemmanuil, E. et al. 2016. Genomic Classification and Prognosis in Acute Myeloid Leukemia. *N Engl J Med* 374(23), pp. 2209-2221. doi: 10.1056/NEJMoa1516192

Papewalis, C. et al. 2011. Increased numbers of tumor-lysing monocytes in cancer patients. *Mol Cell Endocrinol* 337(1-2), pp. 52-61. doi: 10.1016/j.mce.2011.01.020

Paracatu, L. C. and Schuettpelz, L. G. 2020. Contribution of Aberrant Toll Like Receptor Signaling to the Pathogenesis of Myelodysplastic Syndromes. *Front Immunol* 11, p. 1236. doi: 10.3389/fimmu.2020.01236

Pardee, A. B. 1974. A restriction point for control of normal animal cell proliferation. *Proceedings of the National Academy of Sciences* 71(4), pp. 1286-1290.

Parekh, C. and Crooks, G. M. 2013. Critical differences in hematopoiesis and lymphoid development between humans and mice. *J Clin Immunol* 33(4), pp. 711-715. doi: 10.1007/s10875-012-9844-3

Park, I.-k. et al. 2003. Bmi-1 is required for maintenance of adult self-renewing haematopoietic stem cells. *nature* 423(6937), pp. 302-305.

Park, S. J. and Bejar, R. 2020. Clonal hematopoiesis in cancer. *Exp Hematol* 83, pp. 105-112. doi: 10.1016/j.exphem.2020.02.001

Parting, O. et al. 2020. Therapeutic inhibition of FcgammaRIIb signaling targets leukemic stem cells in chronic myeloid leukemia. *Leukemia* 34(10), pp. 2635-2647. doi: 10.1038/s41375-020-0977-8

Peluso, I. et al. 2012. Oxidative stress in atherosclerosis development: the central role of LDL and oxidative burst. *Endocrine, Metabolic & Immune Disorders-Drug Targets (Formerly Current Drug Targets-Immune, Endocrine & Metabolic Disorders)* 12(4), pp. 351-360.

Perales-Clemente, E. et al. 2014. Metabolic regulation of redox status in stem cells. *Antioxid Redox Signal* 21(11), pp. 1648-1659. doi: 10.1089/ars.2014.6000

Perez-Campo, F. M. et al. 2014. MOZ-mediated repression of p16(INK) (4) (a) is critical for the self-renewal of neural and hematopoietic stem cells. *Stem Cells* 32(6), pp. 1591-1601. doi: 10.1002/stem.1606

Pernes, G. et al. 2019. Fat for fuel: lipid metabolism in haematopoiesis. *Clin Transl Immunology* 8(12), p. e1098. doi: 10.1002/cti2.1098

Perry, S. et al. 1959. Lymphocyte production and turnover. *AMA Archives of Internal Medicine* 103(2), pp. 224-230.

Pfaller, W. et al. 2001. Novel advanced in vitro methods for long-term toxicity testing. *Alternatives to Laboratory Animals* 29(4), pp. 393-426.

Pietras, E. M. 2017. Inflammation: a key regulator of hematopoietic stem cell fate in health and disease. *Blood* 130(15), pp. 1693-1698. doi: 10.1182/blood-2017-06-780882

Pietras, E. M. et al. 2016. Chronic interleukin-1 exposure drives haematopoietic stem cells towards precocious myeloid differentiation at the expense of self-renewal. *Nat Cell Biol* 18(6), pp. 607-618. doi: 10.1038/ncb3346

Pietras, E. M. et al. 2015. Functionally Distinct Subsets of Lineage-Biased Multipotent Progenitors Control Blood Production in Normal and Regenerative Conditions. *Cell Stem Cell* 17(1), pp. 35-46. doi: 10.1016/j.stem.2015.05.003

Pievani, A. et al. 2020. Location First: Targeting Acute Myeloid Leukemia Within Its Niche. *J Clin Med* 9(5), doi: 10.3390/jcm9051513

Pike, L. J. 2009. The challenge of lipid rafts. *J Lipid Res* 50 Suppl(Suppl), pp. S323-328. doi: 10.1194/jlr.R800040-JLR200

Pimanda, J. E. et al. 2007. Gata2, Fli1, and Scl form a recursively wired gene-regulatory circuit during early hematopoietic development. *Proc Natl Acad Sci U S A* 104(45), pp. 17692-17697. doi: 10.1073/pnas.0707045104

Pinho, S. et al. 2013. PDGFRalpha and CD51 mark human nestin+ sphere-forming mesenchymal stem cells capable of hematopoietic progenitor cell expansion. *J Exp Med* 210(7), pp. 1351-1367. doi: 10.1084/jem.20122252

Plesa, A. et al. 2017. High frequency of CD34+CD38-/low immature leukemia cells is correlated with unfavorable prognosis in acute myeloid leukemia. *World J Stem Cells* 9(12), pp. 227-234. doi: 10.4252/wjsc.v9.i12.227

Poller, W. C. et al. 2020. Hematopoiesis and Cardiovascular Disease. *Circ Res* 126(8), pp. 1061-1085. doi: 10.1161/CIRCRESAHA.120.315895

Pollock, A. H. et al. 2016. Prolonged Intake of Dietary Lipids Alters Membrane Structure and T Cell Responses in LDLr-/- Mice. *J Immunol* 196(10), pp. 3993-4002. doi: 10.4049/jimmunol.1501261

Porter, R. L. et al. 2013. Prostaglandin E2 increases hematopoietic stem cell survival and accelerates hematopoietic recovery after radiation injury. *Stem Cells* 31(2), pp. 372-383. doi: 10.1002/stem.1286

Poznyak, A. V. et al. 2020. Overview of OxLDL and Its Impact on Cardiovascular Health: Focus on Atherosclerosis. *Front Pharmacol* 11, p. 613780. doi: 10.3389/fphar.2020.613780

Prajitha, N. and Mohanan, P. V. 2021. Cellular and Immunological Response of THP-1 Cells in Response to Lipopolysaccharides and Lipoteichoic Acid Exposure. *Biomedical Research and Therapy* 8(9), pp. 4562-4582.

Prieto-Bermejo, R. et al. 2018. Reactive oxygen species in haematopoiesis: leukaemic cells take a walk on the wild side. *J Exp Clin Cancer Res* 37(1), p. 125. doi: 10.1186/s13046-018-0797-0

Pronk, C. J. et al. 2007. Elucidation of the phenotypic, functional, and molecular topography of a myeloerythroid progenitor cell hierarchy. *Cell Stem Cell* 1(4), pp. 428-442. doi: 10.1016/j.stem.2007.07.005

Pui, J. C. et al. 1999. Notch1 expression in early lymphopoiesis influences B versus T lineage determination. *Immunity* 11(3), pp. 299-308.

Qin, P. et al. 2021. Integrated decoding hematopoiesis and leukemogenesis using single-cell sequencing and its medical implication. *Cell Discov* 7(1), p. 2. doi: 10.1038/s41421-020-00223-4

Qiu, J. et al. 2022. The Role and Research Progress of Inhibitor of Differentiation 1 in Atherosclerosis. *DNA Cell Biol* 41(2), pp. 71-79. doi: 10.1089/dna.2021.0745

Quentmeier, H. et al. 2004. Expression of HOX genes in acute leukemia cell lines with and without MLL translocations. *Leuk Lymphoma* 45(3), pp. 567-574. doi: 10.1080/10428190310001609942

Radomska, H. S. et al. 1998. CCAAT/enhancer binding protein α is a regulatory switch sufficient for induction of granulocytic development from bipotential myeloid progenitors. *Molecular and Cellular Biology* 18(7), pp. 4301-4314.

Rafieian-Kopaei, M. et al. 2014. Atherosclerosis: process, indicators, risk factors and new hopes. *International journal of preventive medicine* 5(8), p. 927.

Rahman, K. et al. 2017. Inflammatory Ly6Chi monocytes and their conversion to M2 macrophages drive atherosclerosis regression. *J Clin Invest* 127(8), pp. 2904-2915. doi: 10.1172/JCI75005

Ramalho-Santos, M. and Willenbring, H. 2007. On the origin of the term "stem cell". *Cell Stem Cell* 1(1), pp. 35-38. doi: 10.1016/j.stem.2007.05.013

Ramos-Mejia, V. et al. 2014. HOXA9 promotes hematopoietic commitment of human embryonic stem cells. *Blood* 124(20), pp. 3065-3075. doi: 10.1182/blood-2014-03-558825

Raudvere, U. et al. 2019. g:Profiler: a web server for functional enrichment analysis and conversions of gene lists (2019 update). *Nucleic Acids Res* 47(W1), pp. W191-W198. doi: 10.1093/nar/gkz369

Reeb, P. D. et al. 2015. Assessing Dissimilarity Measures for Sample-Based Hierarchical Clustering of RNA Sequencing Data Using Plasmode Datasets. *PLoS One* 10(7), p. e0132310. doi: 10.1371/journal.pone.0132310

Rekers, P. E. et al. 1950. Effect of transplantation of bone marrow into irradiated animals. *Archives of Surgery* 60(4), pp. 635-667.

Repa, J. J. and Mangelsdorf, D. J. 2000. The role of orphan nuclear receptors in the regulation of cholesterol homeostasis. *Annual review of cell and developmental biology* 16(1), pp. 459-481.

Reta, C. et al. eds. 2010. *Segmentation of bone marrow cell images for morphological classification of acute leukemia*. *Twenty-Third International FLAIRS Conference.*

Richter, J. et al. 2017. The role of Wnt signaling in hematopoietic stem cell development. *Crit Rev Biochem Mol Biol* 52(4), pp. 414-424. doi: 10.1080/10409238.2017.1325828

Rieger, M. A. and Schroeder, T. 2012. Hematopoiesis. *Cold Spring Harb Perspect Biol* 4(12), doi: 10.1101/cshperspect.a008250

Rieger, M. A. et al. 2009. Improved prospective identification of megakaryocyte–erythrocyte progenitor cells. *British journal of haematology* 144(3), pp. 448-451.

Robb, L. et al. 1995. Absence of yolk sac hematopoiesis from mice with a targeted disruption of the scl gene. *Proceedings of the National Academy of Sciences* 92(15), pp. 7075-7079.

Robbins, C. S. et al. 2012. Extramedullary hematopoiesis generates Ly-6C(high) monocytes that infiltrate atherosclerotic lesions. *Circulation* 125(2), pp. 364-374. doi: 10.1161/CIRCULATIONAHA.111.061986

Robinson, A. J. et al. 2021. Reactive Oxygen Species Rewires Metabolic Activity in Acute Myeloid Leukemia. *Front Oncol* 11, p. 632623. doi: 10.3389/fonc.2021.632623

Rodriguez, A. et al. 2021. MYC Promotes Bone Marrow Stem Cell Dysfunction in Fanconi Anemia. *Cell Stem Cell* 28(1), pp. 33-47 e38. doi: 10.1016/j.stem.2020.09.004

Rodriguez-Fraticelli, A. E. et al. 2018. Clonal analysis of lineage fate in native haematopoiesis. *nature* 553(7687), pp. 212-216. doi: 10.1038/nature25168

Roerden, M. et al. 2021. Expression levels of HLA-DR in acute myeloid leukemia: implications for antigenicity and clinical outcome. *Leuk Lymphoma* 62(8), pp. 1907-1919. doi: 10.1080/10428194.2021.1885659

Rolski, F. and Blyszczuk, P. 2020. Complexity of TNF-alpha Signaling in Heart Disease. *J Clin Med* 9(10), doi: 10.3390/jcm9103267

Romano-Carratelli, C. et al. 1993. HLA class II antigens and interleukin-1 in patients affected by type-II diabetes mellitus and hyperlipemia. *Journal of medicine* 24(1), pp. 28-34.

Ross, R. 1986. The pathogenesis of atherosclerosis—an update. *New England journal of medicine* 314(8), pp. 488-500.

Rossi, L. et al. 2012. Less is more: unveiling the functional core of hematopoietic stem cells through knockout mice. *Cell Stem Cell* 11(3), pp. 302-317. doi: 10.1016/j.stem.2012.08.006

Rothenberg, E. V. et al. 2019. Mechanisms of Action of Hematopoietic Transcription Factor PU.1 in Initiation of T-Cell Development. *Front Immunol* 10, p. 228. doi: 10.3389/fimmu.2019.00228

Roy, S. et al. 2012. Donor hematopoietic stem cells confer long-term marrow reconstitution by self-renewal divisions exceeding to that of host cells. *PLoS One* 7(12), p. e50693. doi: 10.1371/journal.pone.0050693

Rudling, M. et al. 1998. Lipoprotein Receptors in Acute Myelogenous Leukemia: Failure to Detect Increased Low-Density Lipoprotein (LDL) Receptor Numbers in Cell Membranes despite Increased Cellular LDL Degradation. *The American Journal of Pathology* 153(6), p. 1923.

Rybtsov, S. et al. 2014. Tracing the origin of the HSC hierarchy reveals an SCF-dependent, IL-3-independent CD43(-) embryonic precursor. *Stem Cell Reports* 3(3), pp. 489-501. doi: 10.1016/j.stemcr.2014.07.009

Rybtsov, S. et al. 2011. Hierarchical organization and early hematopoietic specification of the developing HSC lineage in the AGM region. *J Exp Med* 208(6), pp. 1305-1315. doi: 10.1084/jem.20102419

Saha, S. et al. 2019. Transcriptomic Analysis Identifies RNA Binding Proteins as Putative Regulators of Myelopoiesis and Leukemia. *Front Oncol* 9, p. 692. doi: 10.3389/fonc.2019.00692

Saher, G. et al. 2005. High cholesterol level is essential for myelin membrane growth. *Nat Neurosci* 8(4), pp. 468-475. doi: 10.1038/nn1426

Sanjuan-Pla, A. et al. 2013. Platelet-biased stem cells reside at the apex of the haematopoietic stem-cell hierarchy. *nature* 502(7470), pp. 232-236. doi: 10.1038/nature12495

Santaguida, M. et al. 2009. JunB protects against myeloid malignancies by limiting hematopoietic stem cell proliferation and differentiation without affecting self-renewal. *Cancer Cell* 15(4), pp. 341-352. doi: 10.1016/j.ccr.2009.02.016

Sato, R. 2015. Functions of cholesterol metabolites. *Journal of nutritional science and vitaminology* 61(Supplement), pp. S151-S153.

Sawen, P. et al. 2018. Murine HSCs contribute actively to native hematopoiesis but with reduced differentiation capacity upon aging. *Elife* 7, doi: 10.7554/eLife.41258

Schade, D. S. et al. 2020. Cholesterol Review: A Metabolically Important Molecule. *Endocr Pract* 26(12), pp. 1514-1523. doi: 10.4158/EP-2020-0347

Schiller, N. K. et al. 2002. Inflammation in atherosclerosis: lesion formation in LDL receptor-deficient mice with perforin and Lyst(beige) mutations. *Arterioscler Thromb Vasc Biol* 22(8), pp. 1341-1346. doi: 10.1161/01.atv.0000024082.46387.38

Schiller, N. K. et al. 2001. Effect of γ-irradiation and bone marrow transplantation on atherosclerosis in LDL receptor-deficient mice. *Arteriosclerosis, Thrombosis, and Vascular Biology* 21(10), pp. 1674-1680.

Schonewille, M. et al. 2016. Statins increase hepatic cholesterol synthesis and stimulate fecal cholesterol elimination in mice. *J Lipid Res* 57(8), pp. 1455-1464. doi: 10.1194/jlr.M067488

Schwanbeck, R. and Just, U. 2011. The Notch signaling pathway in hematopoiesis and hematologic malignancies. *Haematologica* 96(12), pp. 1735-1737. doi: 10.3324/haematol.2011.055954

Seijkens, T. et al. 2014. Hypercholesterolemia-induced priming of hematopoietic stem and progenitor cells aggravates atherosclerosis. *FASEB J* 28(5), pp. 2202-2213. doi: 10.1096/fj.13-243105

Seita, J. and Weissman, I. L. 2010. Hematopoietic stem cell: self-renewal versus differentiation. *Wiley Interdiscip Rev Syst Biol Med* 2(6), pp. 640-653. doi: 10.1002/wsbm.86

Senbanjo, L. T. and Chellaiah, M. A. 2017. CD44: A Multifunctional Cell Surface Adhesion Receptor Is a Regulator of Progression and Metastasis of Cancer Cells. *Front Cell Dev Biol* 5, p. 18. doi: 10.3389/fcell.2017.00018

Sever, R. and Brugge, J. S. 2015. Signal transduction in cancer. *Cold Spring Harb Perspect Med* 5(4), doi: 10.1101/cshperspect.a006098

Sheikhvatan, M. et al. 2019. Integrin Beta-3 Gene Polymorphism and Risk for Myocardial Infarction in Premature Coronary Disease. *Iran J Biotechnol* 17(2), p. e1921. doi: 10.21859/ijb.1921

Shin, D. Y. 2022. Human acute myeloid leukemia stem cells: evolution of concept. *Blood Res* 57(S1), pp. 67-74. doi: 10.5045/br.2022.2021221

Sigurdsson, V. and Miharada, K. 2018. Regulation of unfolded protein response in hematopoietic stem cells. *Int J Hematol* 107(6), pp. 627-633. doi: 10.1007/s12185-018-2458-7

Sigurdsson, V. et al. 2016. Bile Acids Protect Expanding Hematopoietic Stem Cells from Unfolded Protein Stress in Fetal Liver. *Cell Stem Cell* 18(4), pp. 522-532. doi: 10.1016/j.stem.2016.01.002

Silva, G. M. and Vogel, C. 2016. Quantifying gene expression: the importance of being subtle. *Mol Syst Biol* 12(10), p. 885. doi: 10.15252/msb.20167325

Silvera, D. et al. 2010. Translational control in cancer. *Nat Rev Cancer* 10(4), pp. 254-266. doi: 10.1038/nrc2824

Singer, K. et al. 2014. Diet-induced obesity promotes myelopoiesis in hematopoietic stem cells. *Mol Metab* 3(6), pp. 664-675. doi: 10.1016/j.molmet.2014.06.005

Singh, P. et al. 2013. Cholesterol biosynthesis and homeostasis in regulation of the cell cycle. *PLoS One* 8(3), p. e58833. doi: 10.1371/journal.pone.0058833

Singla, B. et al. 2021. Loss of myeloid cell-specific SIRPalpha, but not CD47, attenuates inflammation and suppresses atherosclerosis. *Cardiovasc Res*, doi: 10.1093/cvr/cvab369

Skrtic, M. et al. 2011. Inhibition of mitochondrial translation as a therapeutic strategy for human acute myeloid leukemia. *Cancer Cell* 20(5), pp. 674-688. doi: 10.1016/j.ccr.2011.10.015

Slany, R. K. 2009. The molecular biology of mixed lineage leukemia. *Haematologica* 94(7), pp. 984-993. doi: 10.3324/haematol.2008.002436

Soehnlein, O. 2012. Multiple roles for neutrophils in atherosclerosis. *Circulation research* 110(6), pp. 875-888.

Soehnlein, O. and Swirski, F. K. 2013. Hypercholesterolemia links hematopoiesis with atherosclerosis. *Trends Endocrinol Metab* 24(3), pp. 129-136. doi: 10.1016/j.tem.2012.10.008

Sohrabi, Y. et al. 2018. mTOR-Dependent Oxidative Stress Regulates oxLDL-Induced Trained Innate Immunity in Human Monocytes. *Front Immunol* 9, p. 3155. doi: 10.3389/fimmu.2018.03155

Somervaille, T. C. and Cleary, M. L. 2006. Identification and characterization of leukemia stem cells in murine MLL-AF9 acute myeloid leukemia. *Cancer Cell* 10(4), pp. 257-268. doi: 10.1016/j.ccr.2006.08.020

Song, M. et al. 2017. Loss-of-function screens of druggable targetome against cancer stem-like cells. *FASEB J* 31(2), pp. 625-635. doi: 10.1096/fj.201600953

Spangrude, G. J. et al. 1988. Purification and characterization of mouse hematopoietic stem cells. *Science* 241(4861), pp. 58-62.

Speck, N. A. and Gilliland, D. G. 2002. Core-binding factors in haematopoiesis and leukaemia. *Nat Rev Cancer* 2(7), pp. 502-513. doi: 10.1038/nrc840

Spyropoulos, D. D. et al. 2000. Hemorrhage, impaired hematopoiesis, and lethality in mouse embryos carrying a targeted disruption of the Fli1 transcription factor. *Molecular and Cellular Biology* 20(15), pp. 5643-5652.

Steinauer, N. et al. 2019. Myeloid translocation gene CBFA2T3 directs a relapse gene program and determines patient-specific outcomes in AML. *Blood Adv* 3(9), pp. 1379-1393. doi: 10.1182/bloodadvances.2018028514

Steinauer, N. et al. 2020. The transcriptional corepressor CBFA2T3 inhibits all-trans-retinoic acid-induced myeloid gene expression and differentiation in acute myeloid leukemia. *J Biol Chem* 295(27), pp. 8887-8900. doi: 10.1074/jbc.RA120.013042

Steinberg, D. 2002. Atherogenesis in perspective: hypercholesterolemia and inflammation as partners in crime. *Nature medicine* 8(11), pp. 1211-1217.

Suchy, D. et al. 2011. Ezetimibe--a new approach in hypercholesterolemia management. *Pharmacol Rep* 63(6), pp. 1335-1348. doi: 10.1016/s1734-1140(11)70698-3

Suda, T. et al. 2011. Metabolic regulation of hematopoietic stem cells in the hypoxic niche. *Cell Stem Cell* 9(4), pp. 298-310. doi: 10.1016/j.stem.2011.09.010

Südhof, T. C. et al. 1985. The LDL receptor gene: a mosaic of exons shared with different proteins. *Science* 228(4701), pp. 815-822.

Sugiyama, T. et al. 2006. Maintenance of the hematopoietic stem cell pool by CXCL12-CXCR4 chemokine signaling in bone marrow stromal cell niches. *Immunity* 25(6), pp. 977-988. doi: 10.1016/j.immuni.2006.10.016

Sun, J. et al. 2020. Hypertriglyceridemia in Newly Diagnosed Acute Promyelocytic Leukemia. *Front Oncol* 10, p. 577796. doi: 10.3389/fonc.2020.577796

Sun, J. et al. 2014. Clonal dynamics of native haematopoiesis. *nature* 514(7522), pp. 322-327. doi: 10.1038/nature13824

Suthahar, N. et al. 2018. Galectin-3 Activation and Inhibition in Heart Failure and Cardiovascular Disease: An Update. *Theranostics* 8(3), pp. 593-609. doi: 10.7150/thno.22196

Swamy, M. et al. 2016. A Cholesterol-Based Allostery Model of T Cell Receptor Phosphorylation. *Immunity* 44(5), pp. 1091-1101. doi: 10.1016/j.immuni.2016.04.011

Swirski, F. K. et al. 2007. Ly-6Chi monocytes dominate hypercholesterolemia-associated monocytosis and give rise to macrophages in atheromata. *J Clin Invest* 117(1), pp. 195-205. doi: 10.1172/JCI29950

Szatrowski, T. P. and Nathan, C. F. 1991. Production of large amounts of hydrogen peroxide by human tumor cells. *Cancer research* 51(3), pp. 794-798.

Tabas, I. and Lichtman, A. H. 2017. Monocyte-Macrophages and T Cells in Atherosclerosis. *Immunity* 47(4), pp. 621-634. doi: 10.1016/j.immuni.2017.09.008

Takeuchi, O. and Akira, S. 2010. Pattern Recognition Receptors and Inflammation. *Cell* 140(6), pp. 805-820. doi: 10.1016/j.cell.2010.01.022

Takimoto, C. H. et al. 2019. The Macrophage 'Do not eat me' signal, CD47, is a clinically validated cancer immunotherapy target. *Ann Oncol* 30(3), pp. 486-489. doi: 10.1093/annonc/mdz006

Tall, A. R. and Yvan-Charvet, L. 2015. Cholesterol, inflammation and innate immunity. *Nat Rev Immunol* 15(2), pp. 104-116. doi: 10.1038/nri3793

Tallis, E. et al. 2017. Identification of Myeloperoxidase As a Leukemia-Associated Antigen and Therapeutic Target for Acute Myeloid Leukemia. *Blood* 130, p. 4460.

Tam, W. F. et al. 2008. Id1 is a common downstream target of oncogenic tyrosine kinases in leukemic cells. *Blood* 112(5), pp. 1981-1992. doi: 10.1182/blood-2007-07-103010

Tannenbaum, C. S. et al. 2019. Mediators of Inflammation-Driven Expansion, Trafficking, and Function of Tumor-Infiltrating MDSCs. *Cancer Immunol Res* 7(10), pp. 1687-1699. doi: 10.1158/2326-6066.CIR-18-0578

Tapia-Vieyra, J. V. et al. 2017. Atherosclerosis and Cancer; A Resemblance with Far-reaching Implications. *Arch Med Res* 48(1), pp. 12-26. doi: 10.1016/j.arcmed.2017.03.005

Tatidis, L. et al. 1997. Decreased feedback regulation of low density lipoprotein receptor activity by sterols in leukemic cells from patients with acute myelogenous leukemia. *Journal of lipid research* 38(12), pp. 2436-2445. doi: 10.1016/s0022-2275(20)30028-6

Testa, U. et al. 2019. CD123 as a Therapeutic Target in the Treatment of Hematological Malignancies. *Cancers (Basel)* 11(9), doi: 10.3390/cancers11091358

Thiel, A. T. et al. 2010. MLL-AF9-induced leukemogenesis requires coexpression of the wild-type Mll allele. *Cancer Cell* 17(2), pp. 148-159. doi: 10.1016/j.ccr.2009.12.034

Thorp, E. B. 2010. Mechanisms of failed apoptotic cell clearance by phagocyte subsets in cardiovascular disease. *Apoptosis* 15(9), pp. 1124-1136. doi: 10.1007/s10495-010-0516-6

Tian, T. et al. 2014. TNF-alpha, a good or bad factor in hematological diseases? *Stem Cell Investig* 1, p. 12. doi: 10.3978/j.issn.2306-9759.2014.04.02

Tie, G. et al. 2014. Hypercholesterolemia induces oxidant stress that accelerates the ageing of hematopoietic stem cells. *J Am Heart Assoc* 3(1), p. e000241. doi: 10.1161/JAHA.113.000241

Till, J. E. and McCulloch, E. A. 1961. A direct measurement of the radiation sensitivity of normal mouse bone marrow cells. *Radiation research* 14(2), pp. 213-222.

Ting, C.-N. et al. 1996. Transcription factor GATA-3 is required for development of the T-cell lineage. *nature* 384(6608), pp. 474-478.

To, K. et al. 2009. NKT cell subsets mediate differential proatherogenic effects in ApoE-/- mice. *Arterioscler Thromb Vasc Biol* 29(5), pp. 671-677. doi: 10.1161/ATVBAHA.108.182592

Tolani, S. et al. 2013. Hypercholesterolemia and reduced HDL-C promote hematopoietic stem cell proliferation and monocytosis: studies in mice and FH children. *Atherosclerosis* 229(1), pp. 79-85. doi: 10.1016/j.atherosclerosis.2013.03.031

Towatari, M. et al. 1990. Enhanced expression of DNA topoisomerase II by recombinant human granulocyte colony-stimulating factor in human leukemia cells. *Cancer research* 50(22), pp. 7198-7202.

Traore, K. et al. 2005. Signal transduction of phorbol 12-myristate 13-acetate (PMA)-induced growth inhibition of human monocytic leukemia THP-1 cells is reactive oxygen dependent. *Leuk Res* 29(8), pp. 863-879. doi: 10.1016/j.leukres.2004.12.011

Trapnell, C. et al. 2010. Transcript assembly and quantification by RNA-Seq reveals unannotated transcripts and isoform switching during cell differentiation. *Nat Biotechnol* 28(5), pp. 511-515. doi: 10.1038/nbt.1621

Trumpp, A. et al. 2010. Awakening dormant haematopoietic stem cells. *Nat Rev Immunol* 10(3), pp. 201-209. doi: 10.1038/nri2726

Tsuchiya, S. et al. 1980. Establishment and characterization of a human acute monocytic leukemia cell line (THP-1). *International journal of cancer* 26(2), pp. 171-176.

Tunon, J. et al. 2018. Interplay between hypercholesterolaemia and inflammation in atherosclerosis: Translating experimental targets into clinical practice. *Eur J Prev Cardiol* 25(9), pp. 948-955. doi: 10.1177/2047487318773384

Turner, N. and Grose, R. 2010. Fibroblast growth factor signalling: from development to cancer. *Nat Rev Cancer* 10(2), pp. 116-129. doi: 10.1038/nrc2780

Uckelmann, H. et al. 2016. Extracellular matrix protein Matrilin-4 regulates stress-induced HSC proliferation via CXCR4. *J Exp Med* 213(10), pp. 1961-1971. doi: 10.1084/jem.20151713

Vagapova, E. et al. 2018. The role of TAL1 in hematopoiesis and leukemogenesis. *Acta Naturae (англоязычная версия)* 10(1 (36)), pp. 15-23.

Van Acker, H. H. et al. 2017. CD56 in the Immune System: More Than a Marker for Cytotoxicity? *Front Immunol* 8, p. 892. doi: 10.3389/fimmu.2017.00892

van den Berg, S. M. et al. 2016. Diet-induced obesity in mice diminishes hematopoietic stem and progenitor cells in the bone marrow. *FASEB J* 30(5), pp. 1779-1788. doi: 10.1096/fj.201500175

van der Meer, L. T. et al. 2010. Gfi1 and Gfi1b: key regulators of hematopoiesis. *Leukemia* 24(11), pp. 1834-1843. doi: 10.1038/leu.2010.195

van der Valk, F. M. et al. 2017. Increased haematopoietic activity in patients with atherosclerosis. *European heart journal* 38(6), pp. 425-432.

van Kampen, E. et al. 2014. Diet-induced (epigenetic) changes in bone marrow augment atherosclerosis. *J Leukoc Biol* 96(5), pp. 833-841. doi: 10.1189/jlb.1A0114-017R

van Velthoven, C. T. J. and Rando, T. A. 2019. Stem Cell Quiescence: Dynamism, Restraint, and Cellular Idling. *Cell Stem Cell* 24(2), pp. 213-225. doi: 10.1016/j.stem.2019.01.001

VanderLaan, P. A. et al. 2007. Characterization of the natural killer T-cell response in an adoptive transfer model of atherosclerosis. *Am J Pathol* 170(3), pp. 1100-1107. doi: 10.2353/ajpath.2007.060188

Varret, M. et al. 2008. Genetic heterogeneity of autosomal dominant hypercholesterolemia. *Clin Genet* 73(1), pp. 1-13. doi: 10.1111/j.1399-0004.2007.00915.x

Venegas-Pino, D. E. et al. 2013. Quantitative analysis and characterization of atherosclerotic lesions in the murine aortic sinus. *J Vis Exp* (82), p. 50933. doi: 10.3791/50933

Viatour, P. et al. 2008. Hematopoietic stem cell quiescence is maintained by compound contributions of the retinoblastoma gene family. *Cell Stem Cell* 3(4), pp. 416-428. doi: 10.1016/j.stem.2008.07.009

Vignon, C. et al. 2013. Flow cytometric quantification of all phases of the cell cycle and apoptosis in a two-color fluorescence plot. *PLoS One* 8(7), p. e68425. doi: 10.1371/journal.pone.0068425

Vilchis-Ordoñez, A. et al. 2021. The triad inflammation-microenvironment-tumor initiating cells in leukemia progression. *Current Opinion in Physiology* 19, pp. 211-218. doi: 10.1016/j.cophys.2020.10.010

Virtaneva, K. et al. 2001. Expression profiling reveals fundamental biological differences in acute myeloid leukemia with isolated trisomy 8 and normal cytogenetics. *Proceedings of the National Academy of Sciences* 98(3), pp. 1124-1129.

Vitols, S. et al. 1984. Elevated low density lipoprotein receptor activity in leukemic cells with monocytic differentiation.

Vlasschaert, C. et al. 2022. Association of Clonal Hematopoiesis of Indeterminate Potential with Worse Kidney Function and Anemia in Two Cohorts of Patients with Advanced Chronic Kidney Disease. *J Am Soc Nephrol* 33(5), pp. 985-995. doi: 10.1681/ASN.2021060774

Vogelstein, B. and Kinzler, K. W. 2004. Cancer genes and the pathways they control. *Nat Med* 10(8), pp. 789-799. doi: 10.1038/nm1087

Vu, T. et al. 2020. Hematopoietic stem and progenitor cell-restricted Cdx2 expression induces transformation to myelodysplasia and acute leukemia. *Nat Commun* 11(1), p. 3021. doi: 10.1038/s41467-020-16840-2

Wadman, I. A. et al. 1997. The LIM-only protein Lmo2 is a bridging molecule assembling an erythroid, DNA-binding complex which includes the TAL1, E47, GATA-1 and Ldb1/NLI proteins. *The EMBO journal* 16(11), pp. 3145-3157.

Wagsater, D. et al. 2012. Serine protease inhibitor A3 in atherosclerosis and aneurysm disease. *Int J Mol Med* 30(2), pp. 288-294. doi: 10.3892/ijmm.2012.994

Wai Wong, C. et al. 2012. The role of immunoglobulin superfamily cell adhesion molecules in cancer metastasis. *Int J Cell Biol* 2012, p. 340296. doi: 10.1155/2012/340296

Walter, P. and Ron, D. 2011. The unfolded protein response: from stress pathway to homeostatic regulation. *Science* 334(6059), pp. 1081-1086.

Wang, F. et al. 2016. Inhibition of T cell receptor signaling by cholesterol sulfate, a naturally occurring derivative of membrane cholesterol. *Nat Immunol* 17(7), pp. 844-850. doi: 10.1038/ni.3462

Wang, J. et al. 2019. Crosstalk between cancer and immune cells: Role of tumor-associated macrophages in the tumor microenvironment. *Cancer Med* 8(10), pp. 4709-4721. doi: 10.1002/cam4.2327

Wang, L. D. and Wagers, A. J. 2011. Dynamic niches in the origination and differentiation of haematopoietic stem cells. *Nat Rev Mol Cell Biol* 12(10), pp. 643-655. doi: 10.1038/nrm3184

Wang, Q. et al. 1996. Disruption of the Cbfa2 gene causes necrosis and hemorrhaging in the central nervous system and blocks definitive hematopoiesis. *Proceedings of the National Academy of Sciences* 93(8), pp. 3444-3449.

Wang, W. et al. 2018a. Macrophage Inflammation, Erythrophagocytosis, and Accelerated Atherosclerosis in Jak2 (V617F) Mice. *Circ Res* 123(11), pp. e35-e47. doi: 10.1161/CIRCRESAHA.118.313283

Wang, X. et al. 2018b. MYB - A regulatory factor in hematopoiesis. *Gene* 665, pp. 6-17. doi: 10.1016/j.gene.2018.04.065

Wang, X. and Li, Y. 2019. The disruption of hematopoiesis in tumor progression. *Blood Sci* 1(1), pp. 88-91. doi: 10.1097/BS9.0000000000000001

Warren, A. J. et al. 1994. The oncogenic cysteine-rich LIM domain protein rbtn2 is essential for erythroid development. *Cell* 78(1), pp. 45-57.

Weinkauff, R. et al. 1999. Use of peripheral blood blasts vs bone marrow blasts for diagnosis of acute leukemia. *American journal of clinical pathology* 111(6), pp. 733-740.

Westerterp, M. et al. 2012. Regulation of hematopoietic stem and progenitor cell mobilization by cholesterol efflux pathways. *Cell Stem Cell* 11(2), pp. 195-206. doi: 10.1016/j.stem.2012.04.024

Wickstrom, M. et al. 2011. Aminopeptidase N (CD13) as a target for cancer chemotherapy. *Cancer Sci* 102(3), pp. 501-508. doi: 10.1111/j.1349-7006.2010.01826.x

Wildes, T. J. et al. 2019. Concise Review: Modulating Cancer Immunity with Hematopoietic Stem and Progenitor Cells. *Stem Cells* 37(2), pp. 166-175. doi: 10.1002/stem.2933

Will, B. and Steidl, U. 2010. Multi-parameter fluorescence-activated cell sorting and analysis of stem and progenitor cells in myeloid malignancies. *Best Pract Res Clin Haematol* 23(3), pp. 391-401. doi: 10.1016/j.beha.2010.06.006

Wilson, A. et al. 2008. Hematopoietic stem cells reversibly switch from dormancy to self-renewal during homeostasis and repair. *Cell* 135(6), pp. 1118-1129. doi: 10.1016/j.cell.2008.10.048

Wilson, A. et al. 2004. c-Myc controls the balance between hematopoietic stem cell self-renewal and differentiation. *Genes Dev* 18(22), pp. 2747-2763. doi: 10.1101/gad.313104

Wilson, N. K. et al. 2010. Combinatorial transcriptional control in blood stem/progenitor cells: genome-wide analysis of ten major transcriptional regulators. *Cell Stem Cell* 7(4), pp. 532-544. doi: 10.1016/j.stem.2010.07.016

Wilson, P. W. et al. 2007. Prediction of incident diabetes mellitus in middle-aged adults: the Framingham Offspring Study. *Archives of internal medicine* 167(10), pp. 1068-1074.

Wiseman, H. and Halliwell, B. 1996. Damage to DNA by reactive oxygen and nitrogen species: role in inflammatory disease and progression to cancer. *Biochemical Journal* 313(Pt 1), p. 17.

Witsch, E. et al. 2010. Roles for growth factors in cancer progression. *Physiology (Bethesda)* 25(2), pp. 85-101. doi: 10.1152/physiol.00045.2009

Wu, A. M. et al. 1968. Cytological evidence for a relationship between normal hematopoietic colony-forming cells and cells of the lymphoid system. *The Journal of experimental medicine* 127(3), pp. 455-464.

Wu, J. et al. 2020. Emerging role of m(6) A RNA methylation in nutritional physiology and metabolism. *Obes Rev* 21(1), p. e12942. doi: 10.1111/obr.12942

Wu, Z. et al. 2022. CD3(+)CD4(-)CD8(-) (Double-Negative) T Cells in Inflammation, Immune Disorders and Cancer. *Front Immunol* 13, p. 816005. doi: 10.3389/fimmu.2022.816005

Xi, Y. et al. 2021. Mechanisms of induction of tumors by cholesterol and potential therapeutic prospects. *Biomed Pharmacother* 144, p. 112277. doi: 10.1016/j.biopha.2021.112277

Xu, M.-j. et al. 2001. Evidence for the presence of murine primitive megakarycytopoiesis in the early yolk sac. *Blood, The Journal of the American Society of Hematology* 97(7), pp. 2016-2022.

Xu, S. et al. 2015. Prognostic value of CD56 in patients with acute myeloid leukemia: a meta-analysis. *J Cancer Res Clin Oncol* 141(10), pp. 1859-1870. doi: 10.1007/s00432-015-1977-3

Yamashita, M. and Passegue, E. 2019. TNF-alpha Coordinates Hematopoietic Stem Cell Survival and Myeloid Regeneration. *Cell Stem Cell* 25(3), pp. 357-372 e357. doi: 10.1016/j.stem.2019.05.019

Yanez, D. C. et al. 2020. The IFITM protein family in adaptive immunity. *Immunology* 159(4), pp. 365-372. doi: 10.1111/imm.13163

Yang, F. et al. 2018. Characteristics of NK cells from leukemic microenvironment in MLL-AF9 induced acute myeloid leukemia. *Mol Immunol* 93, pp. 68-78. doi: 10.1016/j.molimm.2017.11.003

Yang, H. et al. 2012. Oxidized low density lipoprotein, stem cells, and atherosclerosis. *Lipids in health and disease* 11(1), pp. 1-9.

Yang, H. X. et al. 2020a. Cholesterol in LDL receptor recycling and degradation. *Clin Chim Acta* 500, pp. 81-86. doi: 10.1016/j.cca.2019.09.022

Yang, J. et al. 2020b. Role of de novo cholesterol synthesis enzymes in cancer. *J Cancer* 11(7), pp. 1761-1767. doi: 10.7150/jca.38598

Yang, J. et al. 2014. Monocyte and macrophage differentiation: circulation inflammatory monocyte as biomarker for inflammatory diseases. *Biomarker research* 2(1), pp. 1-9.

Yang, L. et al. 2005. Identification of Lin–Sca1+ kit+ CD34+ Flt3–short-term hematopoietic stem cells capable of rapidly reconstituting and rescuing myeloablated transplant recipients. *Blood* 105(7), pp. 2717-2723.

Yoshida, T. and Georgopoulos, K. 2014. Ikaros fingers on lymphocyte differentiation. *Int J Hematol* 100(3), pp. 220-229. doi: 10.1007/s12185-014-1644-5

Yoshida, T. et al. 2006. Early hematopoietic lineage restrictions directed by Ikaros. *Nat Immunol* 7(4), pp. 382-391. doi: 10.1038/ni1314

Yoshihara, H. et al. 2007. Thrombopoietin/MPL signaling regulates hematopoietic stem cell quiescence and interaction with the osteoblastic niche. *Cell Stem Cell* 1(6), pp. 685-697. doi: 10.1016/j.stem.2007.10.020

Yu, H. et al. 2009. STATs in cancer inflammation and immunity: a leading role for STAT3. *Nat Rev Cancer* 9(11), pp. 798-809. doi: 10.1038/nrc2734

Yu, V. W. and Scadden, D. T. 2016. Hematopoietic Stem Cell and Its Bone Marrow Niche. *Curr Top Dev Biol* 118, pp. 21-44. doi: 10.1016/bs.ctdb.2016.01.009

Yuan, J. et al. 2021. Potentiating CD8(+) T cell antitumor activity by inhibiting PCSK9 to promote LDLR-mediated TCR recycling and signaling. *Protein Cell* 12(4), pp. 240-260. doi: 10.1007/s13238-021-00821-2

Yuan, Y. et al. 2004. In vivo self-renewing divisions of haematopoietic stem cells are increased in the absence of the early G1-phase inhibitor, p18INK4C. *Nat Cell Biol* 6(5), pp. 436-442. doi: 10.1038/ncb1126

Yvan-Charvet, L. et al. 2010a. ATP-binding cassette transporters and HDL suppress hematopoietic stem cell proliferation. *Science* 328(5986), pp. 1689-1693. doi: 10.1126/science.1189731

Yvan-Charvet, L. et al. 2010b. Role of HDL, ABCA1, and ABCG1 transporters in cholesterol efflux and immune responses. *Arterioscler Thromb Vasc Biol* 30(2), pp. 139-143. doi: 10.1161/ATVBAHA.108.179283

Zeisig, B. B. and So, C. W. 2013. Linking MLL Leukemia with Integrin Signaling. *Cancer Cell* 24(1), pp. 5-7. doi: 10.1016/j.ccr.2013.06.011

Zhang, D. X. and Gutterman, D. D. 2007. Mitochondrial reactive oxygen species-mediated signaling in endothelial cells. *Am J Physiol Heart Circ Physiol* 292(5), pp. H2023-2031. doi: 10.1152/ajpheart.01283.2006

Zhang, K. et al. 2012. Interleukin 6 destabilizes atherosclerotic plaques by downregulating prolyl-4-hydroxylase alpha1 via a mitogen-activated protein kinase and c-Jun pathway. *Arch Biochem Biophys* 528(2), pp. 127-133. doi: 10.1016/j.abb.2012.09.007

Zhang, M. et al. 2021a. Roles of RNA Methylation on Tumor Immunity and Clinical Implications. *Front Immunol* 12, p. 641507. doi: 10.3389/fimmu.2021.641507

Zhang, P. et al. 2004. Enhancement of hematopoietic stem cell repopulating capacity and self-renewal in the absence of the transcription factor C/EBP alpha. *Immunity* 21(6), pp. 853-863. doi: 10.1016/j.immuni.2004.11.006

Zhang, T. et al. 2021b. NF-kappaB signaling in inflammation and cancer. *MedComm (2020)* 2(4), pp. 618-653. doi: 10.1002/mco2.104

Zhang, Z. X. et al. 2002. Ly-6A is critical for the function of double negative regulatory T cells. *European journal of immunology* 32(6), pp. 1584-1592.

Zhao, H. et al. 2022. CD47 as a promising therapeutic target in oncology. *Front Immunol* 13, p. 757480. doi: 10.3389/fimmu.2022.757480

Zhou, J. et al. 2014. Shear stress-initiated signaling and its regulation of endothelial function. *Arterioscler Thromb Vasc Biol* 34(10), pp. 2191-2198. doi: 10.1161/ATVBAHA.114.303422

Zhou, J. D. et al. 2019. BCL2 overexpression: clinical implication and biological insights in acute myeloid leukemia. *Diagn Pathol* 14(1), p. 68. doi: 10.1186/s13000-019-0841-1

Zjablovskaja, P. and Florian, M. C. 2019. Acute Myeloid Leukemia: Aging and Epigenetics. *Cancers (Basel)* 12(1), doi: 10.3390/cancers12010103

Zubiaur, M. et al. 2002. CD38 is associated with lipid rafts and upon receptor stimulation leads to Akt/protein kinase B and Erk activation in the absence of the CD3-zeta immune receptor tyrosine-based activation motifs. *J Biol Chem* 277(1), pp. 13-22. doi: 10.1074/jbc.M107474200